

## Influence of existing scenery in an on-site forest environment in terms of Subjective Appraisal, Restorativeness, Affect

TAKAYAMA, Norimasa<sup>1\*</sup> ; FUJIWARA, Aki<sup>2</sup> ; SAITO, Haruo<sup>2</sup> ; HORIUCHI, Masahiro<sup>3</sup>

<sup>1</sup>Forestry and Forest Products Research Institute, <sup>2</sup>The University of Tokyo Forests, <sup>3</sup>Yamanashi Institute of Environmental Sciences

### INTRODUCTION

Many stressors of urban life are increasingly driving humans to seek some form of stress relief (Frumkin, 2001). Natural environments, including typical urban parks and natural, secondary or artificial man-made forests are generally associated with stronger positive health effects compared with urban environments (Velarde, Fry & Tveit, 2007). For instance, natural scenes bring higher tranquility and a reduced feeling of danger compared to urban scenes (Herzog & Chernick, 2000), while outdoor recreation in a green environment has been shown to relieve stress among urban inhabitants (Li et al., 2008), hence the evidence to date seems to indicate the positive health effect of a natural setting. However, the question of how the existence of scenery as a sight stimulus produces a psychological effect in an on-site forest environment and to what extent remain unclear.

Therefore, during this research conducted in an on-site forest environment (a mixed forest including Larch, Giant dogwood), we set out our research purpose, namely to clarify the psychological healing effect of forest scenery as visual stimuli on respondents.

### METHOD

With eleven male and four female adult respondents respectively, we conducted a viewing experiment to investigate the appraisal (Semantic differential method; abbreviated to SDM; 25-paired adjectives), the affect (Positive And Negative Affect Schedule; abbreviated to PANAS; 16-queries), subjective restorative quality (Restorative Outcome Scale; abbreviated to ROS; 6-queries) and degree of attention restoration (Perceived Restorativeness Scale; abbreviated to PRS; 26-queries) using four types of research questionnaires. The viewing experiment was conducted in the forest inside the Forest Therapeutic Research Institute (Fuji Iyashi-no-mori Institute) and managed by the University of Tokyo Forests in early May 2013. The experiments were conducted one-by-one during fine weather throughout the experimental period (four days). Each respondent was given respectively from the opening session (with well-managed forest scenery) to the closing session (forest scenery covered by tarpaulin) or vice versa to eliminate any order effect.

### RESULT AND CONSIDERATION

Consequently, in terms of the comparison of appraisal, the opening session saw scores higher than the closing session for many measurement indexes and the degrees of score difference were cleared. Conversely, it became clear that a difference would emerge in both the opening and closing sessions, even if it was a measurement index not corresponding to visual senses but directly to other senses. Finally, based on the result of multiple regression analysis, it emerged that the basic links between them included aspects of difference and commonality for the integrated index appraisal such as likableness, comfort, beauty and sense of security when comparing the opening and closing of the forest landscape respectively, and this was an appraisal of concrete environmental factors which resulted in such differences and commonality. Furthermore, in terms of affect, even though neither a positive nor negative affect could be confirmed from statistical interaction when comparing the opening and closing sessions, there was a statistical decline (reduction) in the before (pre-viewing experiment) compared to after (post-viewing experiment). As for the quality of subjective restorative, the interaction between the opening-closing and before - after sessions was confirmed as well as individual statistical differences when comparing before and after in the opening session and opening and closing sessions in the after session sequentially. Regarding the degree of attention restoration, subsequent results of the opening-closing comparison clarified that the criteria of run away, fascination, scope and compatibility were statistically higher in the opening rather than closing session.

Keywords: Attention restoration theory, Positive affect, Negative affect, Subjective restorative outcome, Appraisal, Forest therapy

## Evaluation of Landscape Conservation at Green Space on Campus Based on the Level of Willingness to Work

TAKASE, Yui<sup>1\*</sup> ; FURUYA, Katsunori<sup>1</sup>

<sup>1</sup>Graduate School of Horticulture, Chiba University

### 1. Introduction

A university campus with a large-scale green space is precious access to green for the residents in the surrounding vicinity. However, very often only a very low budget is granted for management of green space on university campuses in Japan. Volunteer activities among students are expected for management of the landscape and maintenance of those green spaces on campus. In this study, landscape conservation of green space on campus has been evaluated, based on the level of students' willingness to work.

### 2. Study Methods

Matsudo Campus of Chiba University in Japan has been selected as a subject. The total area of this campus is 15 hectares, and 13.7 of which counts for green space. A survey was conducted in July, 2013, with students who belong to the Faculty of Horticulture at Chiba University. The number of respondents was 77. The following four items were surveyed: 1) Attribute of respondents (gender, participation experience in green space conservation activities, and willingness to participate), 2) future vision of green space on campus from nature experiences, 3) ecosystem services expected from green space on campus, and 4) desired participation hours to spare for green space conservation activities.

### 3. Results and Considerations

Regarding respondents' attributes, the number of valid responses was 59, with 35 males (59%) and 24 females (41%). The number of people who have participation experience in green space conservation activities counted 27 (46%). The number of those who are willing to participate in those activities was 48 (81%).

With regard to the future vision of green space on campus, an free answer question was provided and 65 valid responses were obtained. The two most common opinions were as following: 1) " Increasing of nature experience events " (19 respondents, 29%), and 2) " Increasing of facilities such as restrooms, benches, gathering area, and lighting " (19 respondents, 29%). The next most significant answer was " Better management of gardens and woods " (15 respondents, 23%).

The next topic about ecosystem services expected from green space on campus was captured from 59 valid responses. Approximately 90% of them had certain expectations from ecological services related to green space on campus: examples, " to create beautiful landscape in the area " and " space where people can enjoy nature " .

Finally, as for the number of participation days to spare for conservation activities on Matsudo campus, 59 students provided valid answers. The average number of days that they are willing to participate is 14.2. Since the participation hours per day had been specified and presented as four hours, the average hours figure is 56.8, converted from the number of days. The grand total of days willing to spare among all valid respondents counted 841 days. Next, the number of desired days to spare was computed for each activity location within the campus. " Ohisama Garden " , which is a flower garden managed mainly by students' initiatives earned the highest number of days among all the campus locations. Thirty-five respondents (59%) are willing to spare time here with an average of 6.4 days, which totals 225 days. On the other hand, traditional garden is the most popular in terms of the number of respondents who are willing to spare time. Forty respondents (68%) indicated their interest in sparing time in the traditional garden. The average counted 4.8 days, which totals 191 days. While the main reason of the location choice for Ohisama Garden was " interest in the activities " (14 respondents), the one for the traditional garden was " to acquire knowledge and know-how " (12 respondents).

### 4. Conclusion

In this study, students' willingness to participate in landscape conservation was clarified by gauging their willingness to work. In doing so, the specific number of days and the available labor in scenery maintenance have been drawn.

Keywords: Willingness to Work, Landscape Conservation, Green Space on Campus

HGG01-02

Room:424

Time:April 29 14:30-14:45

Table. Result of the number of participation days to spare for conservation activities on Matsudo campus

Traditional Garden	Ohisama Garden	Bamboo Grove	Around School Grounds	Sloping Forest	Other
					
Average of days 4.7 days	Average of days 6.4 days	Average of days 3.4 days	Average of days 3.2 days	Average of days 4.9 days	Average of days 4.8 days
Number of Respondents 40 (68%)	Number of Respondents 35 (59%)	Number of Respondents 36 (61%)	Number of Respondents 20 (34%)	Number of Respondents 32 (54%)	Number of Respondents 16 (27%)

## Landscape Evaluation Method by Visitor-Employed Photography with Usage of Cell-phones - Case Study of Mount Gwanak, Korea

MIZUUCHI, Yusuke<sup>1\*</sup> ; SON, Yonghoon<sup>2</sup> ; KANG, Moonseok<sup>2</sup> ; FURUYA, Katsunori<sup>1</sup>

<sup>1</sup>Graduate School of Horticulture, Chiba University, <sup>2</sup>Graduate School of Environmental Studies, Seoul National University

### 1. Introduction

For spatial planning and designing such as natural parks, it is important to understand how users percept and evaluate landscapes. The relationship between viewpoints and a viewing object has been regarded important in the landscape perception model which has been studied in Landscape architecture, Geography and some sciences. One of the study methods to understand such landscape perception uses a camera called Visitor-Employed Photography (VEP), and this method is considered effective in extracting visual images of a space. However, while existing VEP is effective in understanding viewing objects, it still has shortcomings. It requires interviews and descriptions separately in order to extract viewpoints. Therefore, in order to develop a study method of landscape perception to overcome these limitations, we conducted experiments to get viewpoints by using the GPS function of cellphones which visitors to the sites possess for their daily usage.

### 2. Outline of the experiment

A research was conducted with 60 subjects, and the trail of Mount Gwanak in the suburbs of Seoul, Korea, was selected as a site. This location is designated as Urban Eco-Park. The subjects were instructed to use their own cellphones and take photos of landscapes which subjects evaluate. They were also instructed that Geotag must be attached to the photos. In addition, geographic information of the subject's action was simultaneously collected by GPS logging application of their cellphones. Following this activity, a questionnaire survey about subject's profile was conducted. From the collected photos and spatial characteristics of Mount Gwanak, we analyzed landscape objects which are appreciated by the visitors.

### 3. Results

1,119 photos were collected from 60 respondents. Among these, the redundant photos of the same composition taken by the same subject (121 photos) were eliminated. In addition, geographic information were not available from 6 subjects, hence theirs (99 photos) were also eliminated. Further eliminated were the other photos with geographic information errors (45 photos), and the remaining 842 photos were used for analysis. These photos were categorized based on the viewing objects and viewing distance. As a result, based on the trail as a viewpoint, the photos of landscapes within the woods counted most with 120 photos. Panoramic views (105 photos) and closer shots of the space with a river as a main subject were also common. We analyzed the collected geographic information with the Kernel density estimation, and identified the viewpoints of visitor's preference (Fig. 1). This result was combined with the categorized viewing subjects for further analysis, and it was found that photo shooting density tends to be high at the following locations: 1) panoramic view, and the rock and the building at the mountain top in the surrounding area of the mountain top (Fig. 1.1), 2) the touching points of the trail and the river (Fig. 1.2 and 1.3), and 3) locations with a temple (Fig. 1.4)

### 4. Conclusion

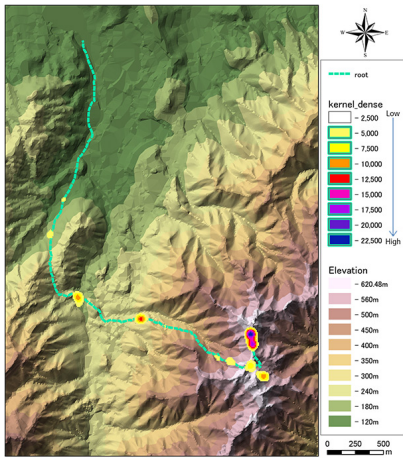
In this research, landscapes within the woods, panoramic views, and river views from the trail are highly appreciated at Mount Gwanak. While panoramic views and river landscapes were concentrated in certain locations, there was no spatial tendency detected with the landscapes within the woods. From the questionnaire survey, 42 respondents (70%) responded comfortable. Eighteen (30%) responded not comfortable; and among those, two (3.3%) were about GPS and others were about the course. Thus, the load of study method itself can be considered light. As described above, this study method can be useful as a future development of a landscape perception research method. It enables visual extraction of viewpoints and viewing objects as shown in this research. Furthermore, this method can be applicable to international comparative studies to identify cultural differences in landscape recognition.

Keywords: landscape evaluation, GPS, GIS, Visitor Employed Photography

HGG01-03

Room:424

Time:April 29 14:45-15:00



## Comparison of natural landscape appreciation between Russia and Japan: landscape exoticism evaluation

PETROVA, Elena<sup>1\*</sup>; MIRONOV, Yury<sup>2</sup>; AOKI, Yoji<sup>3</sup>; MATSUSHIMA, Hajime<sup>4</sup>; EBINE, Satoshi<sup>4</sup>; FURUYA, Katsunori<sup>5</sup>; PETROVA, Anastasia<sup>6</sup>; TAKAYAMA, Norimasa<sup>7</sup>; UEDA, Hirofumi<sup>8</sup>

<sup>1</sup>Lomonosov Moscow State University, Faculty of Geography, <sup>2</sup>Vernadsky State Geological Museum of the Russian Academy of Sciences, <sup>3</sup>Haiku International Association, <sup>4</sup>Research Faculty of Agriculture, Hokkaido University, <sup>5</sup>Graduate School of Horticulture, <sup>6</sup>Institute for Oriental Studies of the Russian Academy of Sciences, <sup>7</sup>Forestry and Forest Products Research Institute in Japan, <sup>8</sup>School of Design, Sapporo City University

People belonging to different cultures differ by their landscape preferences due to a number of ethno-cultural features as well as historical, social, and environmental factors. It is very important to reveal and consider these differences. The purpose of this study is to compare perception, visual and emotional evaluation of natural landscapes in Russia and Japan, that are situated so close to each other and share a common border, but differ so greatly in cultural aspects, while both have deep-rooted traditions of landscape appreciation. We have interviewed respondents in university centres of Russia (Moscow in Central Russia, Irkutsk in East Siberia, and Petropavlovsk-Kamchatsky in Far East) and Japan (Sapporo, Chiba, and Miyazaki); metropolitan areas of both countries and two outermost areas, which differ most strongly in their natural environment, were represented. Young respondents (17 to 30 years old men and women) have taken part in the survey. During the interview, each respondent received the same set of 70 photos of natural landscape. For evaluating the exoticism, we asked respondents to use the 3-point scale, on which exotic landscape got a mark "+1" and usual landscape - "-1". When respondents could not decide between these categories, they were suggested to use an average value "0". Data obtained were analyzed using elementary and multivariate statistical methods.

Exoticism is very important parameter in landscape appreciation and evaluation. As we have learned during the interview, respondents consider attractive landscape as beautiful and comfortable not only for a long-term stay, but for living in. Exotic landscape is "unfamiliar" to respondents; even if it were unsightly, it would be interesting to look at, at least once. Therefore, when assessing attractiveness of landscape, respondents focus primarily on their aesthetic feelings, but in the evaluation of exoticism dominates their educational interest to an unknown. As we revealed, practically no correlation exists between Russian and Japanese respondents to evaluate exotic landscapes ( $R = 0.26$ ). The majority of Russian respondents evaluate mountain landscapes, waterfalls, and sea coasts as the most exotic, but forests, rivers, and treeless plains as the most usual. At the same time, coastal areas are usual and treeless plains are exotic for the Japanese. All the other types of landscapes vary considerably in their exoticism degree for Japanese respondents. All groups of Japanese respondents assess the exoticism of landscapes virtually identical (the correlation coefficients between their scores are:  $R = 0.90-0.96$ ), while the groups of Russian respondents show some differences.

To discover the ethno-cultural aspect, we compare the survey data from Kamchatka to that from Hokkaido, which are similar in terms of natural conditions. In their assessments of the exotic landscapes residents of Kamchatka are closer to the representatives of their culture, living in fundamentally different environmental conditions, than to the representatives of the Japanese culture, living in a similar environment. At the same time, Kamchatka respondents evaluate some of exotic landscapes virtually identical to the estimates of Japanese respondents and very different to those of Russian respondents from other regions. This applies to seacoasts and mountain landscapes that are both the most remarkable and most similar elements of natural environment of Kamchatka and Japan. Thus, if all respondents evaluate the attractiveness of landscapes almost equally, which may indicate the existence of universal human concepts of their aesthetics, then when assessing the exoticism, important role play both ethno-cultural differences and features of natural environment where the respondents live or that they have experience to communicate with. For Russian respondents the most exotic landscapes are also the most attractive, although we cannot see such a tendency for Japanese respondents.

**Keywords:** landscape appreciation comparison between Russia and Japan, visual and emotional evaluation of natural landscapes, exotic landscape, attractive landscape, ethno-cultural differences, features of natural environment

## Exploring reasons for residents use and appreciation of informal urban greenspace in Sapporo and Brisbane

RUPPRECHT, Christoph<sup>1\*</sup>

<sup>1</sup>Environmental Futures Research Institute, <sup>2</sup>School of Environment, Griffith Univ.

Informal urban greenspaces (IGS), such as vacant lots, street verges and river banks are an important new topic in urban recreation and landscape studies. At last year's JpGU 2013 I showed that residents in Sapporo (Japan) and Brisbane (Australia) use and appreciated IGS as adults and during their childhood. But two important questions remained: (1) What role does IGS play for residents in comparison to formal green space, such as parks?, and (2) Why do residents in Brisbane evaluate IGS more positively than in Sapporo? This presentation reports preliminary answers to these questions.

To examine the first question, I used a GIS analysis to compare the amount of formal greenspace within 500m of the sites where the questionnaire on IGS use and perception was distributed to Sapporo and Brisbane residents. A negative correlation between formal greenspace area and IGS use would imply residents indeed use IGS as a substitute for parks. But the results showed no correlation. This suggests residents deliberately choose to use IGS. IGS therefore plays a unique role in residents' recreation - different from formal greenspace.

But why did residents in Sapporo feel IGS made their daily life both better and worse, while residents in Brisbane felt IGS had a mostly positive impact on their daily life? Looking for potential reasons for this difference in IGS appreciation, I measured IGS quantity, accessibility and vegetation structure in both cities. The type of IGS (e.g. lot, street verge, brownfield, railway, gap space, powerline, waterside etc.) was determined using a IGS typology. Accessibility of IGS was categorized in three levels: accessible, partially accessible and not accessible. Vegetation structure was recorded by measuring coverage of four strata: tree, bush, herb and ground cover.

The results show IGS makes up a surprisingly large percentage of city land use in both cities (~5% of total surveyed land use), but there were differences in the amount of IGS types and vegetation structure. We analysed the questionnaire data and field survey data, and found these different IGS types and vegetation structure could explain why residents evaluate IGS differently. Understanding how residents appreciate IGS may in turn help us to unlock the potential of IGS for recreation.

Keywords: urban geography, recreation, wildscape, urban planning, naturalness, spontaneous vegetation

## A review of English papers on psychological evaluation of landscape from 2009 to 2013

AOKI, Yoji<sup>1\*</sup>

<sup>1</sup>Open University of Japan

This paper reviews interesting studies on landscape evaluation in terms of psychological tests referred in Landscape and Urban Planning, Landscape Research, J. of Environmental Psychology, Environment and Behavior, J. of Environmental Management and some other scientific journal from 2009 to 2013. Until 2005, I reviewed various experiments of landscape evaluation in the papers of Review Articles (Aoki 1999, Aoki 2006, and Aoki 2007). During recent 5 years, more works were published compared to the decade of last report. So I tried to summaries them according to the key subjects of the former papers, i.e. (1) clarifications of landscape phenomena, (2) respondents' attributes, (3) landscape appreciation, (4) sampling of landscapes and presentation, and (5) predictive models of psychological response and applications in physical planning.

### (1) Clarifications of landscape phenomena (Table1)

The first proposal of the explanation of the landscape appreciation was proposed by J. Appleton (1975). The detail mechanisms of the appreciations were not explained because of the complicated reaction system of human brain (Thiel 1997). This hard situation was discussed by the advanced brain system endowed to human being (Bourassa 1991). We already got the tool to measure the activities in the brain, but the clarification of the landscape phenomena will take more time because of the complicity of the landscape appreciation (Aoki 2008).

In recent 5 years, the childhood and adolescence to feel at home was examined (Adevi and Grahn 2012).

### (2) Respondents' attributes (Table 2, 3)

Two kinds of attributes e.g. identities of human group and personality were reported.

For the former, mountain tribe Sherpa (Beza 2010) and Nigeria children (Falk and Balling 2010) were investigated.

For the latter, the attribute of tourists was increased and sibling was newly investigated (Howley et al. 2012).

The meaning of sampling through internet was yet under consideration.

### (3) Landscape appreciation (Table 4)

Preference has popularly used in recent years. Willingness to pay became popular in this field. SD method was yet used in the appreciation.

Other appraisals, e.g. feeling at home (Adevi and Grahn 2012), familiarity (Dobbe 2013) and photo location (Sugimoto 2013) were used.

### (4) Landscape sampling and presentation (Table 5, 6)

In the landscape sampled, new ideas; transportation (Bernasconi et al. 2009), Mt Everest (Beza 2010), fire prone (Islas and Vergara 2012), seasonal change (Eroglu et al. 2012) were tried.

As for the presentation method, on-site visits was increasing and use of GPS (Sugimoto 2013) became popular by the development of mobile phone.

### (5) Predictive model and planning (Table 7, 8)

As for the predictive model, biodiversity (Jungels et al. 2013) and flow of stream (Pflueger et al. 2010) were tried.

Proposal for planning were offered in terms of mapping (Ribeiro et al 2013, Schirpke et al. 2013).

### Reference

Aoki, Y. 1999 Review Article: trends in the study of the psychological evaluation of landscape, Landscape Research 24(1), 85-94.

Aoki, Y. A. 2006 Historical review on landscape studies in term of psychological evaluation, Landscape planning for Russia: results and prospects 37-46.

Aoki, Y. 2007 Recent trends of English papers on the psychological evaluation of landscape, J. of Environmental Information Science 35(5), 181-188.

Aoki, Y. 2008 Scientific evaluation of landscape, Seasonal publication Environmental Research 148, 120-126.

Appleton, J. 1975 The Experience of Landscape, London. Wiley.

Bourassa, S.C. 1991 The Aesthetics of Landscape, London: Belhaven Press.

Thiel, P. 1997 People, Paths and Purposes, Seattle, WA: University of Washington Press.

Keywords: landscape appreciation, English papers, 200-2013, review

## Comparison of Races in Terms of Images of Landscapes in Fiji Using Image Sketches

KOSUGE, Takashi<sup>1\*</sup> ; FURUYA, Katsunori<sup>1</sup> ; VERMA, Mukesh<sup>2</sup>

<sup>1</sup>Graduate School of Horticulture, Chiba University, <sup>2</sup>Hard, Social Sciences, Fiji National

### Methods

This research was intended to clarify the difference in imaging of forests between Fijian and Indian residents based on the SKETCH SURVEY. We administered the sketch survey to Fijian residents during our stay in the Republic of Fiji from August to December, 2013. The survey was carried out through interviews, and 158 respondents gave their answers. In the survey, the respondents were asked to describe forests in keywords, sentences or sketches. 1) Firstly, the respondents entered several keywords related to FORESTS in Fiji based on their own idea. 2) Secondly, they described the image of FORESTS in sentences consisting of about 100 words. 3) Lastly, they drew simple sketches of the image of FORESTS. In the process of analysis, the number of elements depicted in the sketches was counted in order to review their imaging of forests. Furthermore, the space structures of the sketches drawn by the respondents were divided into four categories in total: the near view, intermediate view and distant view based on the distance between the landscapes and the drawers, and the downward view depicted from high view points. For analysis of the differences in the races, Mann Whitney U test was used.

### Considerations and Research results

1,504 elements were sampled from the sketches drawn by all the 158 respondents, and that is to say 9.5 elements were sampled from one sketch on an average. These 1,504 elements were classified into 73 categories. When the appearance rate of the elements in the 158 respondents sketches was calculated, the appearance rate of mountains was highest (82%), followed by trees (69%), the sun (63%), palm trees(58%), houses (51%), oceans (47%), rivers (44%), woods (42%), birds (35%), villages (34%) and clouds (32%). In many of their sketches, not only nature elements such as mountains, trees and the sun but also familiar elements such as palm trees, houses and oceans were depicted. In some of the Fijian residents sketches, palm trees extending in the tropical zone with a background of mountains were depicted. Furthermore, houses, villages and other elements were simultaneously depicted in the natural landscapes, and it seems that nature is closely linked to their daily lives. Concerning space structures of the sketches, the rate of the distant view was highest (59%), followed by the downward view (18%), near view (13%) and intermediate view (8%).

Regarding the differences in the percentage of the answers between the races, 76% of Fijian respondents and 54% of Indian respondents associated forests with nature, and here a significant difference was found ( $p < .05$ ). Furthermore, 24% of Fijians and 44% of Indians associated forests with farming villages, and here a significant difference was also found ( $p < .05$ ). It may be possible that Fijians regard forests as a factor of nature, while on the other hand Indians consider forests as a factor of not only nature but also farming villages.

Differences between the races were checked in each of the 73 categories, and significant differences were detected with only six categories of them. The categories in which significant differences in the percentage of the answers between the races were detected were palm trees (50%, 74%), the sun with expression (19%, 34%), grass fields (34%, 12%), sugar canes (7%, 20%), plains (1% of Fijians, 10% of Indians) and hotels (0%, 8%). The analysis of the depictions in the sketches showed that Fijians tend to depict nature-related objects elaborately and Indians tend to depict plants and other similar objects more elaborately than Fijians.

Concerning space structures of the sketches, 55% of Fijians and 68% of Indians drew distant-view sketches, and there was a tendency that both races preferred the distant view. In some of the sketches, there was a range of mountains from which waterfalls and rivers flew into the sea, and in some of the sketches trees, tropical palm trees and artifacts such as houses and villages were depicted.

Keywords: Image Sketches, Landscape, Comparison of Races, Republic of Fiji

## A Comparative Study on Landscape Cognition Between Japanese who have been in New Zealand(NZ) and who have not been to NZ

HORIUCHI, Kana<sup>1\*</sup> ; FURUYA, Katsunori<sup>1</sup>

<sup>1</sup>Graduate School of Horticulture, Chiba University

### Introduction

NZ is almost same size and has same climate, temperate zone and subtropical zone, with Japan. Though a lot of Japanese have immigrated to or lived on long term in NZ, few Japanese knows NZ well because the long distance between both countries might be bottleneck for flow of people. Thus, the objective of this study is to clarify differences of landscape recognition of Japanese who have been in NZ and Japanese who have never been to NZ.

### Methods

69 landscape photos taken in both countries (35photos from Japan, 34photos from NZ) were categorized to the group of coast, waterfall, river, forest, wetland, mountain, and lake. Respondents were asked to select three photos each for characteristic landscape image of NZ and Japan. Then, they were asked to write down the three keywords each about the landscape image of both countries. Respondents were the group of 25 Japanese people who have been in NZ (NJG), the group of 42 Japanese people who have never been to NZ (JPG), and the group of 12 New Zealander people (NZG).

### Result

Firstly, the most selected photo as the characteristic landscape image of Japan among all groups was the photo of Mt.Fuji with Ashinoko lake and shrine gate (NJG76.0%, JPG74.0%, NZG50.0%). Also, second top photo was Mt.Fuji's one. The different result was shown on third top photo. NJG chose the photo of Mt.Fuji with forest (32.0%), JPG chose the photo of creek (28.7%), NZG chose the photo of waterfall with autumn leaves (16.7%), and the photo of forest with lingering snow (16.7%).The creek's photo selected by JPG was recognized as Japanese landscape though taken in NZ.

For the characteristic landscape image of NZ, there was not the photo selected intensively such as Mt. Fuji one. However, the most selected photo was common among all groups. That was the photo of lighthouse on cape surrounded by ocean (NJG36.0%, JPG40.5%, NZG16.7%). As Second top photo, NJG chose the lake on volcano with volcanic steam (24.0%). JPG selected the solid magma in volcanic crater (23.8%) and the lake (23.8%). These two photos might be chosen as the characteristic landscape image of NZ because those are unfamiliar sceneries in Japan. In NZG, it was hard to find out the characteristic scenery because the groups of selected photos were decentral.

For keywords about the landscape image (KLI), noun showing plants and landscape, noun showing animals, noun showing color, adjective indicating impression, and proper noun were answered. As KLI of NZ, FOREST, MOUNTAIN or HILL was answered 29.6% as total. And GREEN, DYNAMIC or BROAD was answered 22.2 % for each in NJG. People would have the image of landscape that broad and dynamic mountain and hill are spread in NZ. On the other hand, JPG answered BROAD(35.0%), MEADOW and GRASSLAND(27.5%), SKY(25.0%), WILD(25.0%) as KLI. Though it also shows broad image, JPG would have the image of broad glass land instead of mountain or hill.

It revealed the difference of landscape cognition between NJG and JPG. There was not obvious difference on the photo selecting exercise. However, JPG recognized the photo taken at NZ as Japanese landscape photo. For KLI, JPG indicated broad glass land, and NJG shown the landscape consisted of broad forest and mountain.

Keywords: Japan, New Zealand, Landscape Cognition, Landscape

HGG01-P03

Room:Poster

Time:April 29 18:15-19:30



## Analysis of Scenery Transition and Residents' Opinion in Dalai Lake Nature Reserve

HAN, Guorong<sup>1\*</sup> ; FURUYA, Katsunori<sup>1</sup>

<sup>1</sup>Graduate School of Horticulture, Chiba University

### Introduction

Grassland scenery has been diminishing in Inner Mongolia in People's Republic of China. It is said that increase in farmland and desertification of grasslands are the cause of diminishing grasslands. This is a serious issue for the Mongolians who make a living from pasturing. In this research, Dalai Lake Nature Reserve, which is located in the Hulunbuir Grasslands has been selected as a study subject. The objective is to clarify the transition of the scenery in the nature reserve by extracting scenery factors in relation to usual lives of the residents in the area.

### Study Methods

An opinion research was conducted between the end of December, 2013 and the middle of January, 2014. The survey subjects were the residents who are nomadic in the grasslands of Dalai Lake Nature Reserve. Interviews were conducted and 409 responses were obtained. In this research, demographics of the respondents and the composition factors of grassland scenery in Dalai Lake Nature Reserve were confirmed. The composition factors of grassland scenery were studied in three different time frames: 10 years ago, present, and future vision (for example, 10 years later). For this research of scenery composition factors, 25 factors had been obtained from the initial literature research, and typical factors had been pre-selected among those for multiple choice questions. Multiple answers were accepted for this question, and an open answer section was also provided. Responses to the grasslands management which local residents would expect were also obtained. A chi-square test was applied to statistical analysis.

### Results

Scenery factors of Dalai Lake Nature Reserve obtained from literature research included; 1) natural scenery such as lake, river, swamp, wild animals, and wild vegetation, 2) cultural landscape like Mongolian gels, and 3) factors which developed along with economic development, including electricity, mining and building.

The demographics of respondents showed that residents within the nature reserve counted 236; therefore, the number of the effective responses has been determined as 236. The average age of the respondents was 41.1 years old. These respondents include 170 Mongolians (72%), the Hans (23%), and the Evenk (5%). The following factors are the ones that all effective respondents selected as typical scenery composition factors of 10 years ago: wild animals, wild vegetation, grasslands, and river, whereas 99% selected lake, sandy soil, and livestock. Only 1% selected railroad, ger camp, signboard, tourism facilities, and camping car. Next, the following factors are the ones that all effective respondents selected as current factors: village, railroad, sandy soil, and livestock, while 232(98%) selected roads and electric lines. Following these, 229(97%) selected mining field. The factor mentioned by the least respondents was wild animal with 54 respondents (23%). Lastly, in the question of future scenery composition factors, the following ones are those that all respondents selected: wild vegetation, grasslands, livestock, and river. Road was selected by 233 respondents (98%), and lake by 227 (96%). A small number of respondents selected mining field (41 respondents, 17%) and electric wire (50 respondents, 21%). Comparing the scenery composition factors of 10 years ago and those of current, natural scenery factors decreased from 93% to 60%. On the other hand, future natural scenery factors counted 87%.

In terms of grasslands management which residents would expect, major responses were as following: 1) maintain status-quo (103 respondents, 44%), unplanned succession (79 respondents, 34%), and reinforce management (51 respondents, 22%).

### Conclusion

This study clarified the scenery which residents in the nature reserve area have in mind and specified it in three different time frames: 10 years ago, present, and future vision (approximately 10 years later). Grasslands management which residents would expect has been also captured.

Keywords: Dalai Lake Nature Reserve, Scenery Transition, Resident, Scenery factors, Opinion, Grasslands

HGG01-P04

Room:Poster

Time:April 29 18:15-19:30



Dalai Lake Reserve

## Research on Comparison of Races in Terms of Evaluation of Natural Landscapes in the Republic of Fiji

KOSUGE, Takashi<sup>1\*</sup> ; FURUYA, Katsunori<sup>1</sup> ; VERMA, Mukesh<sup>2</sup>

<sup>1</sup>Graduate School of Horticulture, Chiba University, <sup>2</sup>Hard, Social Sciences, Fiji National

### Methods

1) after collecting Natural landscape photos of Japan and Fiji national countries, Fiji 33 photos and Japan 39 photos of WATERFALL, FOREST, SEASHORE, RIVER, FARMLAND, SWAMP, MOUNTAIN, and LAKE were selected from each country, which sum up to a total of 72 photos, 2) these photos were categorized in groups by 141 citizens and each group was labeled with a name, 3) the same students evaluated these photos according to preference (5-scale) and exoticism (3-scale), and 4) they were asked to select three photos which they believe to represent the unique characteristics of the Fiji, so that landscape that exhibit the unique characteristics of each ethnic can be extracted. I stayed in Fiji August-December 2013. And A research was run among the Fiji residents during stay. I used a investigation by interview. Then answers were collected from 141 respondents. Cluster analysis (Ward's method, squared Euclidean distance, 3) was applied for the analysis of photo categories, and Mann-Whitney U Test was applied for the analysis between ethnic groups.

### Considerations and Research results

Firstly, the difference in classification of the pictures of SWANP was observed between the two races. Fijians classified SWANP and FOREST into different groups, and they included SWANP in the category of RIVER. On the other hand, some Indians included SWANP in the category of FOREST and some included SWANP in the group of RIVER.

Secondly, regarding classification of LAKE, both Fijians and Indians classified LAKE into the same group as SEASHORE. In Fiji, where the percentage of water area in the land is extremely low, there is a possibility that LAKE are not recognized as such. Regarding classification of SEASHORE, both races divide BEACHE into two broad categories: landscapes of sandy BEACHE where there are only a few rocks and trees, and rocky BEACHE where rocks and reefs are common.

In the analysis of preference, significant differences were detected with the six pictures. Five of the six pictures were landscapes of Fiji, and one of them was a landscape of Japan. Furthermore, in the analysis of exoticism, significant differences were seen with the four pictures. Three of the four pictures were landscapes of Fiji, and one of them was a landscape of Japan. Concerning preference of the pictures of the landscapes of Fiji, the value of Fijians is 4.06 higher than that of Indians. Regarding selection of the pictures typical of Fiji, there was a variance between Fijian and Indian residents. Fijians selected the pictures of FARMLAND (21 %), MOUNTAIN (17 %) and SEASHORE (17 %), while on the other hand Indians chose the pictures of SEASHORE (44 %), RIVER (14 %) and SWANP (12 %). The reason for Fijians' choice may be that they think fields of taro, which is the staple food in Fiji, and mountains extending into villages as traditional landscapes of Fiji. On the other hand, the reason for Indians' selection may be that they associate landscapes of BEACHE with a scattering of resort spots in Fiji.

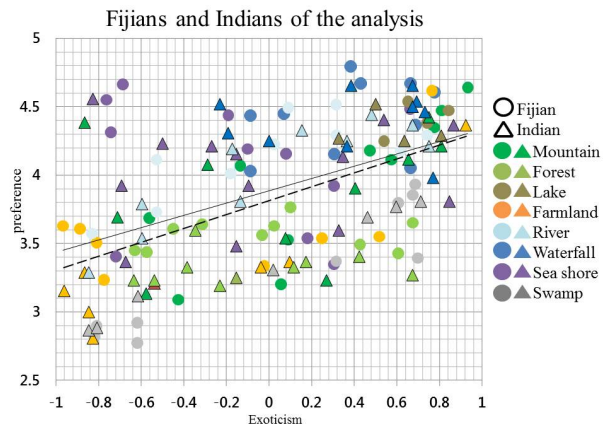
Fijians' preference was in the order of WATERFALL (4.43), LAKE (4.41), RIVER (4.14) and SEASHORE (4.09), and Indians' preference was in the order of WATERFALL (4.41), LAKE (4.33), SEASHORE (4.08) and RIVER (4.02). That is to say, both races preferred the pictures of waterfront landscapes. Particularly, the pictures of SEASHORE may be considered as familiar landscapes of Fiji. Most of the pictures of WATERFALL and LAKE were from Japan, and they are unfamiliar sights in Fiji and considered as exotic landscapes (the pictures of Japanese landscapes). However, the pictures of SWANP were not very much preferred compared to other pictures of waterfronts. There was not much big difference in preference between Fijians and Indians excluding the six pictures with which significant differences were detected. However, there was a difference in that Fijians preferred traditional landscapes whereas Indians preferred landscapes of seashores.

Keywords: Landscape evaluation, Republic of Fiji, Fijians, Indians, Comparison

HGG01-P05

Room:Poster

Time:April 29 18:15-19:30



## Study on natural amenities in off-limits area: imagination of virtual activities received from landscape

MIZUKAMI, Shogo<sup>1\*</sup>

<sup>1</sup>Department of Public Policy, School of Sociology, Bukkyo University

### Introduction

In urban areas, there is little space that has been kept natural although it is now recognized that natural elements such as green space, water features or wildlife habitat, etc. increase the value of an environment. However, human influences on natural habitats interfere with restoring natural spaces to their original condition.

It is difficult to maintain such green space and limit its availability to people. In fact, it is often the case that areas with a high level of undisturbed natural habitats are off-limits areas.

For example, storm-water reservoirs for flood control in urban areas are off-limits, concrete-covered, fenced-in spaces. However, a variety of wild fauna and flora manage to make their habitats in some reservoirs. In other words, reservoirs are an example of artificial yet informal urban green spaces, where spontaneous wild vegetation grows. However, clearly reservoirs were not planned as natural spaces.

Although these spaces are off limits, people can enjoy a view of natural growth from the wall of the reservoirs. On the other hand, due to the physical boundary, people cannot get in touch with natural elements due to perceptual constraints.

Viewing such restricted areas has a beneficial effect as a solution for symbiosis with nature because human development and natural preservation are opposed to each other.

This study clarifies people's impressions of the spontaneous and wild vegetation in reservoirs. Moreover, this study considers the affordance research for environment afford provision of behavior to perceiver as seen in the case of flying stone. Flying stone is a concrete block put into a river bed. This paper presents a new way for people to virtually take part in nature-friendly activities. This study explains how imaginary contact with nature by viewing spontaneous vegetation in off-limits, informal urban green space creates satisfaction.

### Methods

#### Research Questionnaire 1

In a Tokyo suburb, 108 reservoirs were selected for this study. We surveyed shapes, size, location, and surrounding environment and explored possibilities of whether the space was a beautiful landscape and from what perspective.

We conducted an awareness survey regarding environment and landscape with 88 residents living around three reservoirs. Correlative relationship was applied to analyze the relationship between question items.

#### Research Questionnaire 2

Another study was conducted in Kyoto with 175 university students who responded to questions about the image of flying stones on the Kamogawa River. Responses were given as free descriptions. A text mining approach was applied to analyze symbolic representations for water-friendly activities.

### Results and Considerations

The results show that most of the reservoirs were concaved and had good views of open space. Therefore, reservoirs have a high potentiality to be urban green space, where people can view spontaneous natural habitats. Reservoirs are artificially made. The results also showed vegetation succession has possibilities for creating transient esthetic appraisal. However, questionnaire results showed that residents who lived around reservoirs feel that the naturally occurring vegetation is not beautiful.

The results of affordance research were as follows. Flying stones provide an image of physical behavior. for getting across a river or playing in the water. The image is a trigger for the imagination of virtual water-friendly activities. Symbolic representation of environmental signatures is a device that affords imaginary familiarity with environmental elements.

Keeping a view of nature in off-limit green spaces leads to an imaginary sense of familiarity with nature.

Symbiosis with nature increases the value of an environment in urban. Image of nature-friendly activities have a commonality of body. Therefore, symbolic representations for nature-friendly activities have a functional role as a landscape appraisal standard.

Keywords: off-limits area, amenity of nature, symbol of water-familiar, affordance

The questionnaire was consisted with two main part, survey about figure of the coastal mindscape and individual backgrou

MATSUSHIMA, Hajime<sup>1\*</sup>

<sup>1</sup>Research Faculty of Agriculture, Hokkaido University

In this study, the image of coastal landscape as the mindscape were compared between Japanese university students and Russian university students by the questionnaire survey.

The questionnaire survey were conducted to 24 university students of Irkutsk city as Russian university students and 73 university students in Sapporo city as Japanese university students.

Furthermore, 12 Russian students who studied in the university in Sapporo city were added as Russian students in Japan.

The questionnaire was consisted with two main part, survey about figure of the coastal mindscape and individual background of respondents. As a result, the sandy beach and sea were the major component of mindscape. Because most respondents enjoyed sea bathing as recreational use, it was guessed that the viewpoint from the beach were dominated and inland area, like coastal dune, was not described.

On the other hand, Russian university students described more emotional words as beautiful, calm, bright, etc. in addition to major components.

There was no difference in a drawn composition type, but Russian university students described more natural components, mainly coastal plants, than Japanese. About the shore protection, the Russian student did not image in particular it at all.

Keywords: mindsape, coastal landscape, figure, drawing method, Japan, Russia

## Landscape Appreciation on Green Passages with Waterway in Edogawa Ward, Tokyo

SADO, Susumu<sup>1\*</sup> ; FURUYA, Katsunori<sup>1</sup>

<sup>1</sup>Graduate School of Horticulture, Chiba University

### Introduction

Edogawa Ward equipped itself with the first water nature park in Japan in 1974, and sterilized purified water has been utilized in this park. By 1996, water nature parks with natural water had been also established with considerations for ecosystem. The focus of this study is inhabitation of living creatures and human usage in relation to differences between purified water and natural water. The objective of this study was determined to clarify the following three points at two green passages in Edogawa Ward: 1) impressions among the users, 2) behavior of users, and 3) inhabitation of living creatures. Comparing the aquatic life, more variety of living creatures was identified in natural water, and fewer in purified water.

### Study Methods

First, an opinion survey about impressions of green passages was conducted among the green passage users. A survey questionnaire was directly handed out to 288 users on the 24th and the 28th of July and the 4th of August, 2013. The following four items were tested in this study: 1) if they like it, 2) if they feel good, 3) if the water is clean, and 4) if there are many living creatures. Following this questionnaire, a behavioral study was executed in order to compare the results of the opinion survey and the actual usage of green passages. This behavioral study was administered between 10:00 and 14:00 on the 25th and the 31st of July, 2013. The subjects of this research were fish, crustacean, reptiles (turtles), and amphibians (frogs). This research was conducted between 9:00 and 17:00 on the 17th, the 18th, and the 31st of July, 2013. The research area of the green passage was segmented into 27 sections.

### Results

The impression survey concluded that over 98% of the users had favorable impressions of both green passages from the results of two questions: *if they like it* and *if they feel good*. As for the question *if there are many living creatures*, 74.5% responded *very many* or *many* in the green passage with many natural water streams. Although the difference is small, relatively smaller figure of 65.6% responded *very many* or *many* in the one with purified water streams.

The behavioral study result showed that the most popular usage among the eight categories was *playing with water* with over 25% of usage. The result was same with both green passages. Similar tendencies were detected with both passages with other activities which followed the most popular *playing with water*: *resting*, *walking*, and *exercising*, in order of popularity.

The inhabitation research confirmed 14 kinds of aquatic habitat on the green passage with natural water, and nine kinds on the one with purified water. Among the confirmed aquatic habitat, reptiles and amphibians such as the Chinese three-keeled pond turtles, Mississippi common sliders, and Japanese toads were observed on the green passage with natural water; however, they were not found on the green passage with purified water. In addition, the average number of creatures per 100 meters counted 14.7 on the green passage with natural water, but the figure on the green passage with purified water counted only 7.0. More than double the difference was detected between the two.

### Considerations

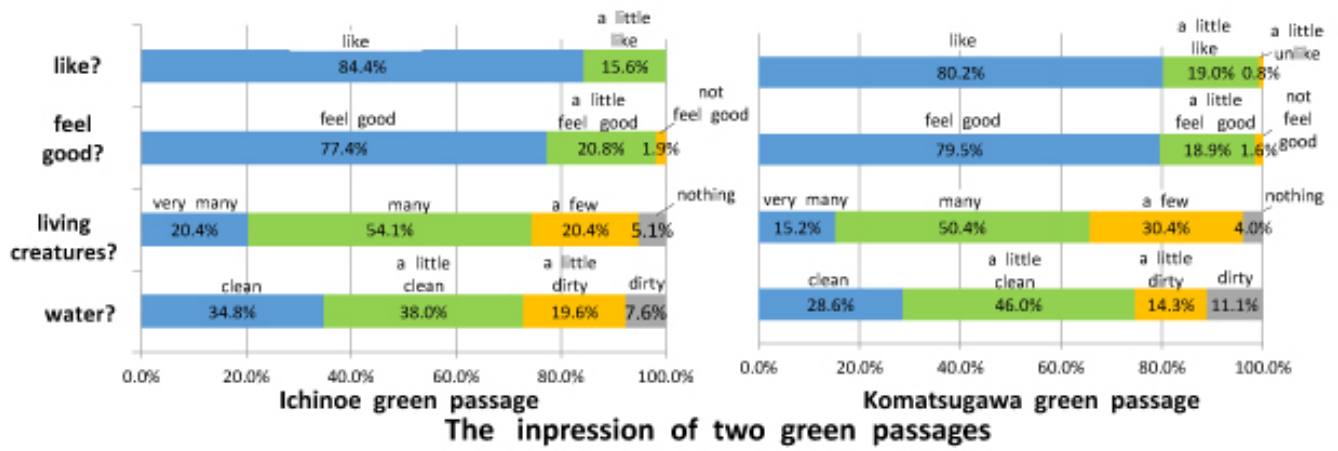
Based on the research results of the two green passages, the difference in the inhabitation situation has been clarified. However, there were no significant differences detected in users impressions of the scenery and in their behavior. From these results, it can be inferred that the differences in aquatic habitat on the green passage does not have a significant influence on users impressions with the scenery or on their behavior. Futures researches on other factors such as vegetation and surrounding environment of a green passage, including grass and woods, shall further clarify favorability of sceneries and user behaviors.

Keywords: Edogawa ward, green passage, appreciation, impression, usage, creature

HGG01-P08

Room:Poster

Time:April 29 18:15-19:30



## The Development of Large-scale Upland Farming and Farmland Use in Hokkaido : A Case Study of Otofuke Town

SASAKI, Toru<sup>1\*</sup>

<sup>1</sup>Sapporo Gakuin University

Japanese agriculture falls into a decline. Especially, farmland resources very important as a factor of production are decreasing. From 1961 to 2010, farmlands decreased by 25% in Japan. On the other hand, in Hokkaido, farmland is not decreasing so much.

This presentation tries to explain the characteristics of large-scale upland farming and condition of farmland use in Otofuke town.

Keywords: Farmland use, Upland crops, Wheat, Large-scale Farming, Otofuke Town

## Change of forest use and current state of coppice forest in Nenoshiroishi near Sendai

MATSUBAYASHI, Takeshi<sup>1\*</sup> ; KANO, Arika<sup>2</sup> ; UCHIGASAKI, Aya<sup>3</sup>

<sup>1</sup>Tohoku Fukushi University, <sup>2</sup>Research Student, Miyagi University of Education, <sup>3</sup>East Japan Railway Company

Coppice forest had been repeatedly felled in an interval of about 15 to 30 years in order to produce and provide fuel wood and charcoal. A charcoal production worker produced 1,500kg of the charcoal in the winter of 2009-2010 in Nenoshiroishi near Sendai. The felled area is approximately 800 square meters. The amount of production of charcoal was approximately 3,000,000kg per year in Nenoshiroishi in the 1930s, therefore the felled area is calculated approximately 1.6 square kilometers per year at that time. After the fuel revolution in the late 1950s and the early 1960s, felled area rapidly decreases, and trees have grown to large sized. In recent years, mass mortality of oak trees has been expanding rapidly in Nenoshiroishi. Growth of the tree is considered to one of the causes of mass mortality of oak trees.

Keywords: coppice forest, forest use, mass mortality of oak trees, Sendai

## Utilization of local resources in agricultural cooperatives in Inner Mongolia,China

SEKINE, Ryohei<sup>1\*</sup> ; SASAKI, Toru<sup>2</sup> ; SUDE, Siqin<sup>3</sup>

<sup>1</sup>Tohoku University, <sup>2</sup>Sapporo Gakuin University, <sup>3</sup>Inner Mongolia University

This study considers about the regional action mainly on the sales of dried beef established with agricultural cooperative modality in Xilingol League, Inner Mongolia Autonomous Region, China that it lived by mainly in live stock farming before 1990s. Agricultural cooperative in China is a new co-operative association institutionalized from 2007 as a position improving local economy. Dried beef is winter excellent products in this area. The agricultural cooperative targeted in this study produces dried beef by oneself, and sells it by oneself at the store established in Xilinhot City that is local metropolis of Xilingol League. It is administered by 25 households live in Bulgan County. They got an adjunct to 300,000 yuan from the government in 2009 to establish this cooperative. This study discusse about the business processes after the establishment of this cooperative and the relations with local resources.

## Placing sediment budgets in the socio-economic context for management of sedimentation in Lake Inle, Myanmar

FURUICHI, Takahisa<sup>1\*</sup> ; WASSON, Robert<sup>2</sup>

<sup>1</sup>Department of Science, IT, Innovation and Arts, Queensland Government, Australia, <sup>2</sup>National University of Singapore, Singapore

In soil erosion and sedimentation research in developing countries, scientists are expected to be better involved in quantifying mechanisms and rates of sediment movement and objectively demonstrating their impacts. Soil erosion and sedimentation in the ca. 3,800km<sup>2</sup> Lake Inle catchment, Myanmar have been of both local and national concern given the significance of the lake to the economy, environment, and culture. Sediment budgets that include a focus on different sedimentation rates in various sink environments around and in the lake were constructed for this lake catchment. The sediment budgets showed that deltas stored more than half of the sediment transported to the lake area, and that, despite the relatively smaller storage mass, the highest specific storage was found at river mouths. Socio-economic assessment identified diverse perspectives on impacts of sedimentation. Of those perspectives, increasing difficulty in water transportation was recognized as a common, significant problem among stakeholders. Proposals for management of sedimentation therefore emphasize that a priority should be given to controlling sedimentation at river mouths.

### <Reference>

Furuichi,T., Wasson, R.J., 2011. Placing sediment budgets in the socio-economic context for management of sedimentation in Lake Inle, Myanmar (Burma). In: *Sediment Problems and Sediment Management in Asian River Basins* (ed. Walling, D.E.), IAHS Red Book 349, 103-113.

Keywords: sedimentation, sediment budget, socio-economic assessment, Lake Inle, Myanmar

## Regional Governance of Forest and its Fringe - case of South India -

KIMOTO, Koichi<sup>1\*</sup> ; S., Arun das<sup>2</sup>

<sup>1</sup>Hiroshima Jogakuin University, <sup>2</sup>University of Mysore

In recent years, on a global scale, forest issues are being "organized". The "facts" of a serious deforestation and "needs" of appropriate protection, as the international public opinion, becomes the general framework of forest policy in each country and region, and under the framework various policies have been implemented. In the late of the 1980s, it may be said that the short turn from the timber-oriented forest government to the community based forest management and governance is a beginning of such a trend. Since the 1990s, many of research such as various case studies of the present situation of forest, a critique of forest policies and foreign aids, and theoretical studies including the commons theory, have been accumulated.

In India, Joint Forest Management (JFM) which was launched at the beginning of 1990s has been showing a certain "recovery" in the forest rate. However, since the late 1990s, various problems such as land acquisition and competition and the human ? wildlife conflict spout out. Indeed, under the JFM program, we might be able to recognize the results of certain "improvement" in both the macro level of forest rate recovery and micro level of participatory activities in village. On the other hand, it has been overlooked the issues related with the forest "region" including the forest and its fringe areas. The success of forest policy, so to speak, has dug out the forest "region" issues.

Even if the community based forest management will be developed continuously, the problem of the forest "region" must be considered with a peculiar frame of its own. As the forest "purification" by the setting of "National Park" and an enclosing of legal and/or physical, the doughnut-shaped chaotic area around the forest appears like sprawling phenomenon in the sub-urban area.

In this study, we are trying to overview of the problems in the forest "region" based on our field survey in Karnataka, India.

Keywords: Protected Areas (PAs), National Park, Region, Governance, India

## Hydrologic Environment in Rangwa Caldera on Lake Victoria, West Kenya

OTSUKI, Yoshinori<sup>1\*</sup> ; UEDA, Gen<sup>2</sup>

<sup>1</sup>Graduate School of Science, Tohoku Univ., <sup>2</sup>Graduate School of Environmental Studies, Tohoku Univ.

In this presentation, we discuss on the hydrologic and physical geographic environment of sustainable settlements in the Rangwa Caldera, situated on the coast of the Lake Victoria, west Kenya.

## Borehole use and management in agro-silvo-fishery settlements around Lake Victoria, Kenya: water use rules

UEDA, Gen<sup>1\*</sup> ; OTSUKI, Yoshinori<sup>2</sup>

<sup>1</sup>Graduate School of Environmental Studies, Tohoku University, <sup>2</sup>Graduate School of Science, Tohoku University

This study is an interim report on the use and management of boreholes, whose importance as a domestic water source becomes greater as one goes far from Lake Victoria, in the sub-area (former Suba District) of Homa Bay County, Nyanza Province, Kenya. As for one of the boreholes outlined in 2013, the water level rose during the rainy season, the daily change in the water level corresponded to control by the water users' association, and not all member households could fetch water within the daily stipulated time table. Water use of this particular borehole was on the "first come, first served" basis, and it alternated between one queue for those who transported water with a donkey and the other queue for those carrying by human power. Individual boreholes scattered in the research area had a variety of "queueing system" rules reflecting different geographical and other conditions. The water use rule of each borehole can be seen as a historical product of people's attempt to level off inequality in water use in each settlement. It is indispensable for a better understanding of sustainable water use and livelihood security to investigate such rules.

Keywords: water resources, rule, Kenya, Tropical Africa

## Pig raising frontiers in Tropical Africa: Changing small and medium sized piggeries and their regional system in Kenya

UEDA, Gen<sup>1\*</sup>

<sup>1</sup>Graduate School of Environmental Studies, Tohoku University

Although Eastern and Southern African regions have experienced dramatic growth in the pig raising industry since the early 1990s, its enterprise reality has not yet been well researched. This study takes Nyeri County, Central Province and Homa Bay County, Nyanza Province, both in Kenya, as examples of "pig raising frontiers" in Tropical Africa where pigs are introduced as new livestock. It examines changing entrepreneurial activities that small- and medium-sized pig raisers have performed since their beginning, particularly between 2009 and 2012. Zero-grazing is affected by increasing feed prices, and free ranging/scavenging in urban and peri-urban areas causes crop damages and hygienic problems. These are pointed out as the main reasons which stimulate shift among breeding, fattening and integrated production in an enterprise, and which even trigger withdrawal from pig husbandry. The study also illuminates locational conditions and the regional system of rural and urban pig raising, all of which influence the change in the economic sector. Since the frontier experiences constitute a variety of trial and error, and changes, in achieving a success, their cases suggest potential factors that may promote distribution and sustainability of pig husbandry in Tropical Africa as a quick means to supply food and alleviate poverty.

Keywords: pig husbandry, small and medium sized producers, Kenya, Tropical Africa

## The value of coral and its change in Kushimoto, southern Kii Peninsula

SAKITA, Seishiro<sup>1\*</sup>

<sup>1</sup>Graduate School of Environmental Studies, Nagoya University

In the tropical and subtropical regions, coral is given the status important as one of the symbolic living things of the marine environment. Especially, in the consideration of resource use, coral is generally treated as a physiographic factor which provides a coral reef ecosystem and is often related to local fishing. Meanwhile, the use of coral itself has been seldom brought up for discussion.

Kushimoto is one of the regions in Wakayama Prefecture, and is located in the southernmost end in Kii Peninsula. Owing to the influence of the Kuroshio Current, the subtropical marine biota, typified by coral assemblages, has been produced in the western coastal waters of Kushimoto, and some local residents who lived in the area have collected and used coral as resources. In Kushimoto, coral was usually collected by gathering the casted corpses on the littoral zone, and sometimes by skin diving. Mainly, people has used coral as a material of slaked lime to make mortar, or for processing as a souvenir thing. The scale of these productions was not much extensive, but the use of coral in Kushimoto has been practiced and continued in relation to other local resource uses. For instance, to make mortar, other materials which were collected or produced in the region, such as seaweed and whale oil, were also used with slaked lime made from coral. And when making slaked lime, old timber and thinnings were used as fuel at the sequence of calcination.

Such collection and use of coral in Kushimoto were at least continued until 1970s, and then, these activities have been completely abandoned now. Instead, since the designation of some parts of the coastal area in Kushimoto as a national park in 1970, the coral and coastal environments have become an object of conservation. Therefore, a collection and use of the coral which inhabits the coastal waters of Kushimoto have been forbidden. And also, following such a increasing of the evaluation to the coral as an important factor of the marine environment, it brings an expectation of the value of coral as tourist attractions.

Besides, in recent years, the temperature of the nearshore waters in Kushimoto tends to rise notably, and it brings about the increase of a number of species and cover degree of coral which inhabits the coastal waters of Kushimoto. Given this situation, the increase in coral has a negative effect on regional fishery. On the other hand, large amounts of corallivorous organisms such as *Acanthaster planci* and *Drupella* spp. have been caused a problem for the conservation of coral since 2000s. Thus, the conditions of natural and social environments which surround the coral inhabits the coastal waters of Kushimoto have been constantly changing.

In this presentation, I would like to show the structure of resource use focusing on coral once formed in Kushimoto, and examine how the value of coral has been changed up to the present to consider the relationship between coral and people.

Keywords: coral, natural resource use, marine environmental conservation, Kushimoto

## PALEO-ENVIRONMENTAL HISTORY AND KOSA (DUST AND SAND STORM) FLUCTUATION AT ARID - SEMI-ARID REGIONS IN EAST ASIA

KASHIMA, Kaoru<sup>1\*</sup>

<sup>1</sup>Department of Earth and Planetary Sciences, Faculty of Sciences, Kyushu University

There are two methods to monitor environmental changes and desertification at arid and semiarid regions. The first one is the short-term monitoring, and examined the changes during several years or decades by meteorological, hydrological, geophysical and geochemical observations. The second one is the long-term monitoring, and presumed changes of environment during hundreds or thousands years using geologic and geographical methods. Although a lot of expeditions have reported short-term changes, the reports for long-term environmental changes have been limited because it takes a lot of efforts to take efficient samples to presume in detail environmental histories.

Department of Earth and Planetary Sciences, Kyushu University has started international research project to make long-term monitoring of desertification in East Asia to correspond with the East Asian Environmental Problems Project of Kyushu University. In cooperation with Mongolian Academy of Sciences, National University of Mongolia, Xinjiang University in China, the filed surveys have been done to obtain samples for long-term monitoring at lakes, ponds and marshes in Mongolia and north western China using geological and geographical methods. Our researches presumed long-range (about hundreds or thousands years) changes of the lowering of lake levels and under ground water levels, the reducing of forest areas and the expanding of deserts in those regions. The desertification has been accelerated in these two hundred years in both regions.

Keywords: Xinjiang Uyghur, Climatic changes, Desertification, Mongolia, The Global Warming, KOSA (Dust and Sand Storm)

## Visualization of liquefied layers using GPR in Watarase flood plain, central Kanto

SETO, Masayuki<sup>1\*</sup> ; ICHIKAWA, Minami<sup>2</sup> ; KITAZAWA, Toshiyuki<sup>2</sup> ; NAKAMURA, Yosuke<sup>1</sup> ; TAMURA, Toshikazu<sup>2</sup>

<sup>1</sup>Fukushima University, <sup>2</sup>Rissho University

At the Watarase flood plain, central Kanto, there were many cracks and sand mounds caused by liquefaction in 11, Mar 2011. Various liquefaction models have been proposed based on a profile observation of the old liquefaction and experiment. This study tried visualization of liquefied underground layers. We carried out boring investigations and GPR explorations in Watarase flood plain. Core samples show typical lower river deposits. There was loosely-deposited sandy layer near the groundwater level which was 2m deep. We traced liquefied layers using GPR (Ground Penetrating Rader) which can display the reflection profile about 5m deep with frequency of 250 MHz. By the comparison of core records with GPR images, we confirmed that GPR image is applicable to the distinction of sand, sandy clay and clay layers. Moreover, we found sharply shaped reflection patterns in sandy layers near 200cm deep. Width and height of the pattern is 0.5-2.5m and 0.2-0.95m respectively. Interval of sharp-shaped reflection patterns are 1-20m. The interval is related between the GPR survey line and the location of deformed layer. We considered that these sharp shaped reflection patterns were shown liquefied sandy layers. GPR is thus available for the visualization of the invisible liquefied layers.

Keywords: GPR, Liquifaction, 3.11 Mega quake

## Coastal geomorphology as a proxy of large paleothrust earthquakes along the Andaman Trench

ANDRADE, Vanessa<sup>1\*</sup> ; RAJENDRAN, Kusala<sup>1</sup> ; RAJENDRAN, C. P.<sup>2</sup>

<sup>1</sup>Indian Institute of Science, Bangalore., <sup>2</sup>JNCASR, Bangalore.

Estimating hazards from earthquakes and tsunamis along subduction zones is of significance to coastal communities. Here, we discuss the coastal geomorphology of selected sites in the Andaman Islands, which lie within the rupture zone of the 2004 Sumatra-Andaman earthquake. As part of the near-source region, these islands witnessed considerable geomorphic changes, both before and after the 2004 earthquake, which may be related to the maturity of a megathrust subduction zone earthquake cycle. Assuming that these geomorphic landforms are properly preserved and attributed to the right sources, it is possible to build the history of large paleothrust earthquakes for the Andaman Islands. Given that these landforms are a result of similar processes through time, our sites are broadly divided as regions that subsided or were uplifted in 2004.

At Hut Bay and Interview Island, uplifted coralline terraces were mapped, as were stream inlets that cut through the newly-formed as well as older terraces. Samples collected from these locations include wood pieces from trees embedded in the stream bank, shells from pebble-rich layers along the exposed bank as well as coral fragments from the terraces themselves. At Port Blair, large stretches of land subsided in 2004. While several farmlands remain inundated beneath the present-day tidal-line, several mangroves trees died in situ, their roots being preserved in the shallow subsurface. Along a stream bank, a similar root horizon was identified 1m below the present day surface which was sampled at multiple locations. Additionally, a shell sample was collected from within the paleo root-zone.

The ages of these samples were estimated using AMS radiocarbon dating, and they cluster at AD 1100, AD 1500, and AD 1900. Though these geomorphic landforms may be the result of other coastal processes, either regional or global, we believe that these ages, with corroborating evidence from several studies in the Andaman Islands and from coastlines in Sri Lanka, mainland India, Sumatra, and Thailand are representative of large earthquakes in recent history, some of may have been tsunamigenic.

Keywords: 2004 Sumatra-Andaman earthquake, Coastal geomorphology, Andaman Islands, Uplifted terraces, Subsided lowlands, Paleothrust earthquakes

## Volumetric changes of various rocks during weathering and their geologic significance

CHIGIRA, Masahiro<sup>1\*</sup> ; NAKATA, Eiji<sup>2</sup> ; OYAMA, Takahiro<sup>2</sup>

<sup>1</sup>Disaster Prevention Research Institute, Kyoto University, <sup>2</sup>Central Research Institute of Electric Power Industry

A rock volume may change during weathering, which would have various importance in earth surface processes. However, little is known on the volumetric change. We summarize our research results of various rock types and refer to its geomorphological importance. Basic idea is so-called isocon concept, which assumes immobile chemical elements during weathering and calculate a volume change from density and chemistry of rock before and after weathering (Grant, 1986). We assume TiO<sub>2</sub> is the immobile element.

### Granitic rocks:

Volumetric change may be different between granite and granodiorite/quartz diorite. White et al. (2002) reported that granodiorite and quartz diorite are isovolumetric during weathering. Chigira (2002) reported that granite expands 50% during weathering, which is consistent with Folk and Patton (1982) who estimated the volume change from the inflection of a pegmatite vein in a weathering zone. These expansions lead to spheroidal weathering or micro-sheeting.

### Sandstone:

Matsuzawa (2008) studied the weathering of sandstone of the Cretaceous Izumi Formation in Ehime and estimated 20-30% expansion during weathering, which closed joint openings.

### Mudstone:

Calculation from the data of Chigira (1988) for the Quaternary Haizume Formation in Niigata suggested that mudstone expanded 10-30% during weathering in the upper part of the dissolved zone. Such expansion may facilitate downslope soil creep.

### Vapor-phase crystallized tuff:

Calculation from the data of Chigira et al. (2002) for vapor-phase crystallized tuff of the Shirakawa ignimbrite in Fukushima suggested its weathering was isovolumetric except for the topmost part, in which fabric collapsed and the rock shrank.

### Tuff breccia:

We studied the weathering of tuff breccia of the Miocene Tomari Formation in Aomori, which suggested that it occurred with 20-50% expansion. So-called active faults in the Higashidori nuclear power plant site are apparent active faults made by rock expansion during weathering.

Chigira, M. 1988. *J. Japan Geol. Soc.* 94, 419-431. Chigira, M., Nakamoto, M., and Nakata, E., 2002. *Engineering Geology* 66, 111-125. Folk, R.L., and Patton, E.B., 1982. *Zeitschrift fur Geomorphologie N. F.* Bd 26, 17-32. Matsuzawa, M. 2008, Master thesis of Kyoto University. Grant, J.A., 1986. *Economic Geology*, 81, 1976-1982. White, A.F., 2002. *Chemical Geology* 190, 69-89.

Keywords: weathering, volumetric change, active fault

## Use of rock properties in classification of weathering grades: A Sri Lankan case study

UDAGEDARA, Dashan T.<sup>1\*</sup> ; OGUCHI, Chiaki T.<sup>2</sup>

<sup>1</sup>Graduate School of Science and Engineering, Saitama University, <sup>2</sup>GRIS, Saitama University

Rocks utilised for the Samanalawewa project, have undergone severe weathering after they were excavated late 90's. The rate of weathering is incomparably high with respect to the normal soil formation processes. Different weathering grades of rocks that were used as construction materials, foundation materials and road aggregates are found in the project area. Consequently, they have been threatening to the sustainability of the project. The access adit and rip-rap zone of the dam are vulnerable to damage owing to the rapid weathering. Even though charnockite, marble, biotite and garnet granulitic gneisses were utilized for the project, only pyrite-sillimanite-garnet gneiss has shown extensive weathering. The rapid weathering of this rock is being observed since the commissioning of the project. Rocks were subjected to a petrographic study under the optical microscope. Point load strength, slake durability, loss on ignition and water content tests were employed to distinguish weathering grades. Water-rock interaction was experimented to study the pyrite oxidation. Comparatively to charnockite and marble, pyrite-sillimanite-garnet gneiss is weaker according to point load strength and slake durability indices. Rock strength and chemical properties illustrates that the weathering process takes place at a rapid and a normal stages. It is mainly observed on set of weathering. Corroded grains boundaries and decayed minerals in the rock are consequences of weathering induced by the acidic water generated by pyrite oxidation. The abundance of pyrite in pyrite-sillimanite-garnet gneiss is uneven. Thus, different weathering grades of the rock can be seen over the study area. Extensive fractures, which might be generated during tectonic activities or during excavations, facilitate better interaction with the atmosphere. It also effectively reduces the strength of the rock. It is another reason for differential weathering.

**Keywords:** Point load strength index, Rapid rock weathering, Loss on ignition, Samanalawewa project, Pyrite oxidation, Pyrite-sillimanite-garnet gneiss

## Experimental Study on Deterioration and Durability of Bricks due to Salts

NGUYEN, Thi hai duong<sup>1</sup> ; OGUCHI, Chiaki T.<sup>2\*</sup>

<sup>1</sup>Graduate School of Science and Engineering, <sup>2</sup>GRIS. Saitama University

In Vietnam, heavy construction materials such as bricks are often used because there are many floods. However, the deterioration due to weathering has been found at general houses and historic brick buildings. To investigate deterioration of bricks used in these buildings, the present study performed salt weathering experiments using 6 bricks produced in Vietnam, Japan and China; red brick (RD), beige brick (BG), Vietnam brick (VN), amber brick (AB), brown brick (BR) and refractory brick (RF). These bricks were cut into cylindrical with a size of 3.5 cm in diameter and 7.0 cm in height. After examined rock properties such as physical, mechanical chemical and mineralogical characteristics, two types of salt weathering experiments were performed under 15-35 °C and 20 °C atmosphere. The saline solutions used in this study are 4%-Na<sub>2</sub>SO<sub>4</sub>, 8%-Na<sub>2</sub>SO<sub>4</sub>, 10% Na<sub>2</sub>CO<sub>3</sub>. Results of the experiments show that the deterioration mechanism of bricks is explained that 1) when the salt is absorbed and crystallizes inside brick, micropores of brick are extended by crystal expansion pressure and make cracks, 2) strength of the brick increases slightly by salt crystallization, but decreases gradually by salt deliquescence, and 3) with repeating of 1) and 2), bricks will be damaged. Even chemical and the mineralogical characteristics are almost equal except for BG, physical and mechanical characteristics are different, which controls durabilities of these bricks.

Keywords: salt weathering, brick, Vietnam, experiment, durability factor, salt susceptibility index

## Channel migration processes observed in 2013 in the upper reaches of the Azusa River, central Japan

SHIMAZU, Hiroshi<sup>1\*</sup>

<sup>1</sup>Rissho University

The upper reaches of the River Azusa in central Japan is a braided gravel-bed river running down Japan Alps. They are characterized by frequent landform changes occurring in the riverbed. This area is located in the high conservation area in the Chubu-Sangaku national park and thus physical processes of river are preserved. This study is the first step to clarify the fluvial processes of a braided gravel-bed river during a flood event.

The geomorphological maps of the observation site were made by the Research Group for Natural History in Kamikochi in every summer from 1994. These maps recorded annual landform changes of the riverbed. Sediment transport and/or major landform changes, such as channel migration, occurred once or twice in several years in severe heavy rain events more than 120 millimeters per day during the snowmelt flooding season in late May and/or the rainy season in June and July.

Interval shooting cameras were set up in 2011. These have taken the images of the riverbed and recorded the condition in every 15 or 20 minutes since 3 July 2011, only in the daylight and twilight. Channel migration in the observation area during the flood event was recorded on 19 June 2013, 166 millimeters of daily rainfall. The rain event began at night of 18 June. Water level began to rise early in the morning of 19 June. The heavy rainfall more than 13 millimeters per hour was recorded from 3 a.m. to 5 a.m. and from 7 a.m. to 9 a.m. The river was above bank-full stage at 12:00 a.m. and this condition continued until night. Highest water level was recorded at 16:15. Although water overflowed on gravel bars and shallow branching channels were formed before the bank-full stage, the landform of the main channel was still in the same condition. Changes of patterns of the water surface and movement of woody debris flowing downstream show that during the bank-full stage the channel landform changed and the main channel was migrated. The channel migration was not caused by lateral shifting with lateral erosion. Channels were buried and new channels were excavated tracing the shallow branching channels.

Keywords: channel migration, geomorphic process, braided river, flood, interval shooting camera, Azusa River

## Risk evaluation of steep slope failure using a slope angle and mean curvature

NISHI, Hayata<sup>1</sup> ; OGUCHI, Chiaki T.<sup>2\*</sup>

<sup>1</sup>Civil and Engineering Department, <sup>2</sup>GRIS. Saitama University

According to the previous techniques for the evaluation of slope failures, only steep slopes are taken into account. However, the influence of earthquakes on slope failures has not been considered on the hazard map delivered by local government. After the Great East Japan Earthquake occurred in 2011, Necessity for considering earthquakes on to slope failure evaluation is increasing. Therefore, the present study focused on risk evaluation of steep slope failures caused by earthquakes. Within various techniques, a technique proposed by National Institute for Land and Infrastructure Management, was adopted in this study. With comparing manual and GIS calculations to obtain the parameters of slope angle and mean curvature, the degree of the risk was evaluated. The target slope is Mt. Shinobu, in Fukushima Prefecture. After examination , it is resulted in that the evaluation using GIS is useful as well.

Keywords: Slope failure, Risk evaluation

## Limit of mountain growth in the development of experimental landforms

OUCHI, Shunji<sup>1\*</sup>

<sup>1</sup>Faculty of Science and Engineering, Chuo University

A series of experiments with rainfall-erosion and uplift of various rates, in which a square (60×60 cm) mound of a mixture of fine sand and kaolinite is uplifted at a constant rate under the artificial mist-type rainfall, suggests the existence of threshold uplift rates. In the run with the uplift rate below the lower threshold, drainage networks develop as the surface is slowly uplifted. The erosion is exclusively fluvial and no high slope develops. When the uplift rate becomes higher than this lower threshold, uplift exceeds erosion on the divides of drainage basins, which developed with fluvial erosion, and hills grow and slope processes start working. The divides grow into low mountain ridges with the uplift and slope failures become dominant. When the relief grows high enough, large landslides occur concentratedly. The average height and relief lower with the landslides, but the ridges soon grow again with the uplift till the next concentration of large landslides, and this process proceeds repeatedly. Uplift and erosion seems to become balanced to keep average height and relief roughly constant and landscapes similar. Assuming the existence of the critical slope controlled by the strength of mound-forming material and the rainfall intensity, the experimental landform is considered to reach a dynamic equilibrium condition at a certain relief regardless of the uplift rate. However, when the uplift rate is in the range between the lower and the upper thresholds, both relief and average height become higher with the uplift at higher rate. A simple equilibrium or steady state seems difficult to be expected with the critical slope. Although the maximum slope in a 1 cm grid becomes higher than 80 degree in all runs, considering that the angle of repose of dried mound-forming material is about 34 degree, it is rather difficult to take this maximum slope as the critical slope. The observation of the experiment suggests that large landslides require triggering events to occur, and without triggering events slopes can grow higher. Large landslides often occur when the rainfall is resumed after halting the rainfall for the measurement. This resumption of rainfall can be the major triggering event in the experiment. The interval of measurement is not exactly constant but does not vary so much among runs. As far as the resumption of rainfall after the measurement is the major triggering event, hills can grow higher with the uplift at higher rate. Moreover, fluvial processes can work more with the uplift at lower rate to widen valleys and therefore increase the area of lower slope. Average slope, relief, maximum height, and average height all become lower. In this way experimental landforms can have average height and relief corresponding to the uplift rate. This condition may be called quasi steady state. When the uplift rate is higher than the upper threshold, on the other hand, relief grows to the limit determined by the width of deposition area. In this case further increase in uplift rate cannot increase the height or relief any more, and this condition apparently does not agree with the condition of equilibrium.

Erosion rate is considered to increase with average slope, and some people pointed out that the relation is nonlinear. In the experiments the average value of the highest slope in a 1 cm grid shows similar linear increase with relief regardless of the uplift rate, but they become to show no clear relationship after relief reaches about 60 mm when landslides become dominated in the landform change process. Erosion rate also increase linearly with average slope first, but it becomes almost constant after the dominance of large landslides in the process of landform development. The relation between erosion rate and average slope seems necessary to be reconsidered with taking uplift rate into account.

Keywords: rainfall-erosion experiment, limit of mountain growth, threshold uplift rate, critical slope, landslides

## Evolution of river profile of experimental mountain building

OGAMI, Takashi<sup>1\*</sup> ; OUCHI, Shunji<sup>1</sup>

<sup>1</sup>College of Science and Engineering, Chuo University

River profiles and their evolution during mountain building are investigated and the characteristics of river profile under mountain steady-states are examined by rainfall-erosion experiments under various uplift rate. Miniature landforms are developed with constant uplifting of sand-block (mixture of fine sand and kaolinite) and artificial rainfall. Four experiments are operated under the uplift rate of 0.2 mm/h, 0.5mm/h, 1.2 mm/h and 5.0 mm/h. Based on landform measurement, 1 cm grid elevation models are constructed. Streams are generated by basin analysis with the elevation models.

Relationship between the slope of channel ( $S$ ) and the catchment area ( $A$ ) are examined. Plots of  $\log S$  and  $\log A$  ( $S$ - $A$  plots) show convex, linear and slightly concave forms as mountain building progress. In the mountain steady-states, the  $S$ - $A$  plots show slightly concave forms, and the forms are stable until end of uplifting. It is deduced that  $S$ - $A$  plots become linear forms if they are at steady-state by stream-power incision model. But our result shows that  $S$ - $A$  plots under steady-state shows slightly concave forms, expressing that channel slopes at downstream becomes relatively steep than those deduced by the model. This situation should be result of downstream increasing sediment flux, which is important factor of graded river but neglected by the traditional stream-power incision models.

Keywords: rainfall-erosion experiment, uplift, river profile, equilibrium, sediment flux

## Experimental study of the effect of partial uplift on river channels

NAKAUCHI, Takuya<sup>1</sup> ; ENDO, Noritaka<sup>1\*</sup>

<sup>1</sup>Kanazawa Univ.

Flume experiments were conducted to examine the effects of uplift on river channels in which the uplift area was restricted to the middle reaches. Experimental landform was evolved by exerting fine water mist on the slope consisting of a mixture of fine sand and clay, and the uplift was realized by jacking up the partial area of the flume bottom. The conventional idea that the occurrence of water gaps was determined by the balance between rates of uplift and downward erosion is true locally. The rate of down erosion is, however, variable due to the change of channel paths in the meso-scale. The avoidance of flowing in the uplift area tends to cause a new confluence and higher stream power producing larger erosion rate. A confluence makes the possibility of forming water gap high. The avoidance of the uplift area, however, does not always induce a confluence, in which the water gap is not generated.

Keywords: river channel, uplift, laboratory experiments

## Current status and issues of grain-size analysis using a digital image method and a laser diffraction method for sedimen

NANAYAMA, Futoshi<sup>1\*</sup> ; FURUKAWA, Ryuta<sup>1</sup>

<sup>1</sup>Geological Survey of Japan, AIST

Grain size measurement is the most fundamental physical information in evaluating the characteristics of various materials, the analytical technology. These are JIS standardized clearly by the association of powder process industry and engineering, Japan. In geomorphological field, we are carried out the grain size analysis of volcanic ash, mud, sand, and gravel using in combination of settling tube method, laser diffraction scattering method (LD), sieve classification method and the precipitation method in generally. According to currently technology, it is possible that the LD of each company to measure the particles of a wide range of 10nm to 3mm in a short period. However, we believe that a technical problem for analyzing nature sediments still now because these are not a powder of industrial products with same physical properties.

For example, we know a large scattered light intensity can be achieved in the shorter wavelength of the incident light because it is confirmed by measurement of the fine particles of submicron order, strength is not enough laser light. Moreover backscatter increases depending on the shape of non-spherical particles, tend to shift the fine particle side is confirmed grain size. Further, when using an algorithm for determining the particle size by inverse calculation using the Mie theory, it is necessary to set the user side of the value of the absorption coefficient and the particle refractive index.

This assumption is a very annoying problem for the user.

Recently, the particle size measurement in the field of powder technology, the development of new analytical instruments using digital image analysis method has been increasing. In this method, it is acquired the two-dimensional image of the particle is first digitally imaged by pixel division using the CCD camera and divided into two sub-methods, static (JIS Z 8827-1:2008; ISO 13322-1) and dynamic (JIS Z 8827-2:2010; ISO 13322-2). The methods may be used either, a process that takes as a digital image the particles, the statistical processing on a personal computer is the same.

Analysis method using a digital image of a single particle is clear, it is easy to be trusted from the user side. In addition, the use of the digital image, various particle shape parameter as well as information about the particle size distribution and the particle size of each definition different, for example, can be analyzed at the same time the value aspect ratio, elongation, circularity, HS circularity, convexity, solidity, etc.. Further, it is possible to obtain also the physical properties such as transmittance and intensity. We believe that it is analyzed in conjunction with the particle size measurement result data on physical properties and particle shape these, and becoming a new standard for particle size analysis in the future.

The present study includes the result of "Research and Development of Margin Assessment Methodology of Decay Heat Removal Function against External Hazards" entrusted to Japan Atomic Energy Agency by the Ministry of Education, Culture, Sports, Science and Technology of Japan (MEXT).

Keywords: laser diffraction method, digital image method, sediment, grain-size analysis, current status, issues

## Causes of gravel-sand distribution in upstream part of the river revealed from changes in lithology and form of detritus

UTSUGAWA, Takako<sup>1\*</sup> ; SHIRAI, Masaaki<sup>1</sup>

<sup>1</sup>Department of Geography, Tokyo Metropolitan University

Downstream fining of fluvial clastic sediments has been generally attributed to two processes, "hydraulic sorting" and "sand grains production", the former is that finer grains are transported farther than coarser grains, while the latter implies crushing and abrasion of gravels. In this study, we investigated that how the two processes operate on this tendency along the tributary of Watarase River, the major branch of the Tone River on the basis of field survey and measurement of finer grains (4 to 0.5 mm in diameter). Lithological composition of each grain size fraction from cobble to coarse-grained sand (128-0.5 mm in diameter) with 1  $\phi$  (phi scale) intervals and roundness were obtained with digital microscope.

Changes in lithological composition of cobble – pebble, granule and very coarse sand fractions are not explained only with "hydraulic sorting" of clastic grains. It implies that crushing and abrasion of gravel – very coarse sand fractions and consequent "sand grains production" occur at the studied area.

Whereas, coarse sand fraction (1-0.5 mm) shows remarkable features that (i) change in lithological composition along the tributary was not recognized and (ii) grains become rounded in downstream direction. These facts suggest that abrasion of the grains occur dominantly than crushing in coarse sand fraction and "sand grain production" may not be efficient to grains smaller than coarse sand. Therefore, it will be important to research the distribution of coarse sand and finer grains in bed material along the river in order to reveal the transition from "producing process" to "sorting process", erosion – transport processes of clastic sediments and a development of sedimentological geomorphology along the river.

### References

- Frings, R. 2011. *Journal of Sedimentary Research* 81 : 52-63.  
Kodama, Y. 1994. *Journal of Sedimentary Research* A64(1) : 68-75.

Keywords: gravel, sand, crush-abrasion, lithological component, roundness, tributary of Watarase River

## Earth-surface processes on the basis of instrumental observations in Takidani-ike lake-catchment system, central Japan

ITONO, Taeko<sup>1\*</sup> ; KASHIWAYA, Kenji<sup>1</sup> ; OCHIAI, Shinya<sup>1</sup>

<sup>1</sup>Kanazawa University

Lacustrine sediments contain both high-resolution regional environmental records and global information in lake-catchment systems. They are also of great use for reconstructing short-term environmental changes (precipitation, water discharge, etc.) and understanding earth-surface processes (erosion, transportation, sedimentation) in the lake-catchment system.

Process understanding is essential for clarifying causal relations in earth surface phenomena and proper interpretation of sediment information. Instrumental observation (monitoring) is of great use for the process understanding. This study deals with the instrumental observation for a small pond-catchment system (Takidani-ike) near Kanazawa University. The pond is storage reservoir. It is used for agricultural irrigation in summer. Therefore the water level shows highly fluctuation. Our observation consists of sediment sampling with trap, water level measurement, temperature measurement, and precipitation measurement. Observation in Takidani-ike using sediment trap has continued since June 2000.

Observational and analytical results for Takidani-ike show that; the sedimentation rate (both monthly and seasonal sedimentation) is expressed as a function of two factors; precipitation intensity (external factor) and water level change (system factor, closely related to size of erodible area). The correlation for the seasonal relationship is better than one for the monthly relationship, suggesting that reservoir effect in the catchment should be considered. The results also show that mineral grain size may be used as proxies for sedimentation rate.

Keywords: lake-catchment system, earth-surface process, pond sediment, sedimentation rate

## Characteristics and production processes of coastal huge blocks in the Miyako Island

SHIMAZU, Hiroshi<sup>1\*</sup> ; SETO, Masayuki<sup>2</sup>

<sup>1</sup>Rissho University, <sup>2</sup>Fukushima University

There are many coastal huge blocks in the Miyako Island. Some were brought from the sea bottom by tsunamis. Most of others were made by landslides of the coastal cliffs. Previous studies showed the dynamics of the production of such huge blocks from the coastal cliffs of Ryukyu limestone. Development of notches formed near the sea level and vertical cracks on the surface of the marine terraces near the cliffs caused the instability of the rock mass and finally it were torn into coastal huge blocks. This process indicates that the height of the cliff relates the block form and size. However there are large variety of form and size of coastal blocks in Miyako Island. Although smaller blocks are distributed in front of the higher cliff in the Boraga beach, huge blocks with vegetated top are distributed in front of the 20 meters high cliff in Higashi-hennazaki. This Study aims to describe the characteristics and distribution of coastal blocs and discuss production processes of the blocks.

In the Miyako Island the Ryukyu limestone covers the semi-consolidated sandstone or mudstone called the Shimajiri formations. These are unconformable. The Ryukyu limestone is hard and permeable rock and the Shimajiri formations are soft and impermeable rocks. These two layers outcrop on the cliffs and their boundary usually occurs high above the sea level. Groundwater springs or seeps from the boundary on the cliff. The water erodes the Shimajiri formations along the boundary. This process causes the notch-like form at the boundary. At the Braga beach the height of the cliff is more than 40 meters and the boundary of the layers, where groundwater springs, locates 14-20 meters high above the sea level. Development of the notch-like form caused instability of the limestone layer. And then the layer collapsed and produced limestone blocks. They rolled down to the beach breaking into smaller blocks. At the Aragusuku and Urasoko fishing port coasts the blocks were produced by same process. At the Higashi-hennazaki the boundary locates several meters above the sea level. Groundwater sapping forms notch-like form at the boundary. At the Shimajiri coast the Ryukyu limestone appears on all the cliff. A notch was formed at the sea level by the wave process. On these type of coasts the limestone cliffs were torn into huge blocks. The blocks with vegetation on the top of them were deposited along the coast.

Keywords: huge block, geomorphic process, coastal cliff, spring, Ryukyu limestone, Miyako Island

## Late Quarternary tectonic development at the northeastern margin of Tibet revealed by $^{10}\text{Be}$ and $^{26}\text{Al}$

SHIRAHAMA, Yoshiki<sup>1\*</sup> ; MIYAIRI, Yosuke<sup>2</sup> ; HE, Honglin<sup>3</sup> ; FU, Bihong<sup>4</sup> ; KANO, Ken-ichi<sup>5</sup> ; ECHIGO, Tomoo<sup>6</sup> ; YOKOYAMA, Yusuke<sup>2</sup> ; IKEDA, Yasutaka<sup>1</sup>

<sup>1</sup>Department of Earth and Planetary Science, Graduate School of Science, The University of Tokyo, <sup>2</sup>Atmosphere and Ocean Research Institute, The University of Tokyo, <sup>3</sup>Institute of Geology, China Earthquake Administration, <sup>4</sup>Institute of Geology and Geophysics, Chinese Academy of Sciences (IGGCAS), <sup>5</sup>Faculty of Science, Shizuoka University, <sup>6</sup>Geo-Research Institute

Tibetan Plateau has been growing up due to collision between the Indian and Eurasian plates and expanding its area laterally by invading marginal forelands and making them involved into deformation. The mechanism of expansion at the northeastern margin of the plateau is still a subject of much debate due to the scarcity of tectonic researches. In the Kumkol Basin at the northeastern margin of the plateau we made detailed geomorphological mapping using satellite images, and revealed that there is a huge anticlinorium that consists of many thrusts and folds covered with significantly deformed fluvial or fluvio-glacial fans or terraces along the Pitileke River. The development and deformation rate of the anticlinorium would give an important clue to understanding the growth mechanism of the plateau. In order to estimate the deformation rate, we dated depositional surfaces by surface exposure dating by using cosmogenic radionuclides (CRNs), such as  $^{10}\text{Be}$  or  $^{26}\text{Al}$ . Field investigations were conducted in 2011 and 2013, and mainly pebbles of vein quartz were collected at 22 points on the surface of fans and terraces. Depth-profile samples were collected also from 3-m deep sections at two points; each depth profile of  $^{10}\text{Be}$  and  $^{26}\text{Al}$  concentrations were analyzed for the exposure age, erosion rate, and inheritance by the Monte Carlo simulation. In addition, grain-by-grain CRN concentrations were measured for surface samples from two points to estimate the origin of sediments. Following three inferences were obtained: (1) the sediments of the lower part of terraces and the present river contain reworked sediments; (2) depositional processes and erosion processes are strengthened in the glacial and interglacial period, respectively; (3) the uppermost two steps of terraces were formed before the MIS6 and in the transition period from MIS6 to MIS5, respectively.

Keywords: Tibetan Plateau, Qaidam Basin, tectonic landform, surface exposure dating

## Longitudinal distribution of incision rates in the Oshika Gorge, Tottori prefecture using terrestrial cosmogenic $^{10}\text{Be}$ :

WATAKABE, Takuma<sup>1\*</sup> ; KODAMA, Yoshinori<sup>2</sup> ; MATSUSHI, Yuki<sup>3</sup> ; MATSUZAKI, Hiroyuki<sup>4</sup>

<sup>1</sup>Graduate School of Regional Sciences, Tottori University, <sup>2</sup>Faculty of Regional Sciences, Tottori University, <sup>3</sup>Disaster Prevention Research Institute, Kyoto University, <sup>4</sup>School of Engineering The University of Tokyo

We determined longitudinal changes of incision rates in the 3 km long Oshika Gorge, Tottori prefecture, Western Japan, by exposure dating of a series of granitic strath terraces using terrestrial cosmogenic  $^{10}\text{Be}$ . Thereby we discuss development of a waterfall sequence zone and an incised meander zone. The bedrock of the gorge consists of granite. We collected 24 granite samples from surface of erosional terraces. The oldest exposure age of a strath terrace was 50.2 kyr (relative height from river-bed is 11.0 m) and the youngest exposure age was 1.2 kyr (relative height is 1.2 m). Incision rates in the Oshika Gorge varied from 0.24 mm/yr to 1.40 mm/yr. Those of step-pool sequence zones and large boulder scatter zones were about 0.64~1.40 mm/yr, which showed increasing tendency toward downstream. Those of the waterfall-pool sequence zone were 0.24~0.57 mm/yr, which showed rapid increase toward downstream. This means that gradient of the waterfall-pool sequence zone has been under increasing conditions in these c.a.50 kyr, resulting from river-bed roughness increase according to waterfall-pool growth. The incised meander zone is located just upstream adjacent to the waterfall-pool sequence zone. Incision rate of the incised meander zone was 0.36 mm/yr, which was slower than that of step-pool sequence zones and faster than that of the waterfall-pool sequence zone. In this reach, alternate gravel bars were developed because of lower gradient and as a result, lateral migration of the river occurred and the incised meander zone was developed.

Keywords: bedrock river, incision rate, cosmogenic nuclide  $^{10}\text{Be}$ , waterfall-pool sequence, incised meander zone

## Basin-averaged erosion rates of Yakushima using cosmogenic $^{10}\text{Be}$ in river sediments

SHIROYA, Kazuyo<sup>1\*</sup> ; MATSUSHI, Yuki<sup>2</sup> ; MATSUZAKI, Hiroyuki<sup>3</sup>

<sup>1</sup>Geological Survey of Japan, AIST, <sup>2</sup>Disaster Prevention Research Institute, Kyoto University, <sup>3</sup>Department of Nuclear Engineering and Management, School of Engineering, The University of Tokyo

Quantitative understanding of erosion rates under several geomorphic and geological settings is important to discuss the process of erosion. We investigated basin-averaged erosion rates from cosmogenic  $^{10}\text{Be}$  in quartz grains from river sediments in Yakushima. Erosion rates in Yakushima are relatively low within a similar range to those in regions of several times lower rainfall than Yakushima. This finding suggests that rainfall is not necessarily a causal factor of landform evolution. In this presentation, we focus on a pattern of hillslope erosion and a process of landform evolution in Yakushima.

This research project has been conducted as the regulatory supporting research funded by the Secretariat of Nuclear Regulation Authority (Secretariat of NRA), Japan.

Keywords: Yakushima, Basin-averaged erosion rate, precipitation, cosmogenic Be-10

## Temporal variation of Kurobe River Sediments revealed by TL and ESR signals in quartz

YOSHIDA, Msanori<sup>1\*</sup> ; TOYODA, Shin<sup>1</sup> ; NINAGAWA, Kiyotaka<sup>1</sup> ; TAKADA, Masashi<sup>2</sup> ; SHIMADA, Aiko<sup>3</sup>

<sup>1</sup>Department of Applied Physics, Faculty of Science, Okayama University of Science, <sup>2</sup>Department of Geography, Nara Women's University, <sup>3</sup>Application Support Team, JEOL RESONANCE Inc

While the ESR signals of the E1' center in quartz was used to investigate the origin of the loess in MIS 1 and 2 (Toyoda and Naruse, 2002) and of the sediments in the Sea of Japan (Nagashima et al., 2007). Shimada (2008) showed that TLCI (thermoluminescence color image) may be useful for similar qualitative study on river sediments. In the present study, the wavelength-temperature two dimensional thermoluminescence measurement was employed, together with the ESR measurements, to investigate the temporal change of these characteristics observed in fluvial sediments of the Kurobe river.

Eight sediment samples were collected from the present river bed along the Kurobe River in 2012 and 14 samples in 2013. They were sieved into two grain size fractions of 500-250 $\mu$ m, 250-75 $\mu$ m. Quartz grains were extracted using chemicals, heavy liquid, and an isodynamic magnetic separator. The obtained quartz grains were heated at 300 degree Celsius for 1 hour to erase the inherited signals. Each sample was then separated into 9 subsample aliquots for gamma ray irradiation up to 2640 Gy, which are for ESR measurements. Other aliquots for TL measurement were given a dose of 809 or 857 Gy with wrapping the tubes with Al foil in order to keep the samples in the dark.

TL measurements were performed by using the two dimensional TL apparatus. We measure the TL emission spectra during heating up to 450 degree Celsius. Red emission (538 to 658 nm) was observed between 140 and 250 degree Celsius (Low Red) and 290 and 370 degree Celsius (High Red) and Blue emission (379 to 538 nm) was between 103 and 211 degree Celsius (Blue). The integrated counts were taken as the intensities of the red and blue emissions. The results of ESR measurements will be given in the presentation together with the TL results.

Keywords: ESR, TL(thermiluminescence)

## Distribution pattern and formation processes of potholes in Oshika, Tottori: role of pothole on river incision processes

KODAMA, Yoshinori<sup>1\*</sup> ; INOUE, Yuuki<sup>2</sup>

<sup>1</sup>Fac.of Regional Sciences, Tottori-Univ., <sup>2</sup>Under Graduate, Fac.of Regional Sciences, Tottori-Univ.

Potholes on the Oshika River bed near Takaganma, Misasa-Town, Tottori, Western Japan were surveyed. Surrounding terrace development revealed that there potholes were formed within 3,600 years. Plan view survey illustrated a line distribution pattern of potholes, resulting from longitudinal vortices generated in flood flows. Longitudinal profiles (Fig.) showed that bottom levels of potholes were close to or towards to those of the present river bed. In general, potholes have a role of effective drilling erosion on a hard bedrock elimination with few sediment loads in the river incision processes.

Keywords: potholes, pothole developing processes, line distribution, river incision processes, balloon photos, The Oshika River, Tottori, Japan

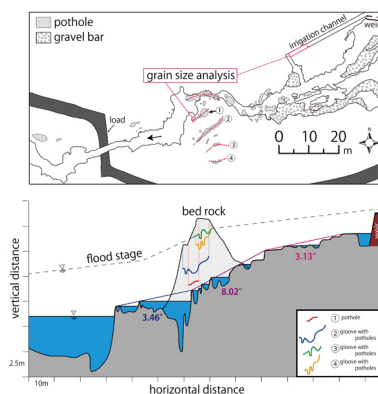


Fig. Plan view and long profiles of Takaganma-Potholes, Misasa Town, Tottori Pref., Japan

## Accumulation patterns of in-channel modern deposits in the lower Stung Sen River

NAGUMO, Naoko<sup>1\*</sup> ; SUGAI, Toshihiko<sup>2</sup> ; KUBO, Sumiko<sup>3</sup> ; OKAZUMI, Toshio<sup>1</sup>

<sup>1</sup>ICHARM, PWRI, <sup>2</sup>Graduate School of Frontier Sciences, University of Tokyo, <sup>3</sup>School of Education, Waseda University

The Stung Sen River flows down the central region of Cambodia, is the main tributary in the Tonle Sap drainage basin. It develops fluvial lowland in its downstream and the longitudinal profile is very flat, with the slope of less than 0.1 ‰. Monsoonal precipitation provides seasonal flood every year in the fluvial lowland and cyclic water level changes of the Tonle Sap Lake about 8 m in the river mouth, therefore the river seems to change sediment transportation processes in each season. While meander scrolls formed by channel migration and back marsh are found in the floodplain throughout the year (Nagumo et al., 2013), four types of channel bars are recognized within the river channel about 10 m lower than back marsh during dry season. Outcrop observations at concave type channel bars revealed the alternate layers of reverse-graded sand and mud layers, and inserted plastic pieces with date stamps indicated that the deposits are quite new and have been partly replaced to reflect flow regime changes of the river. Such sedimentary structures suggest that minute fluctuations of water level and discharge control bar construction, and would be important source to understand recent flood history and patterns.

Keywords: fluvial lowland, meander, monsoon, water level fluctuation, Lake Tonle Sap, Cambodia

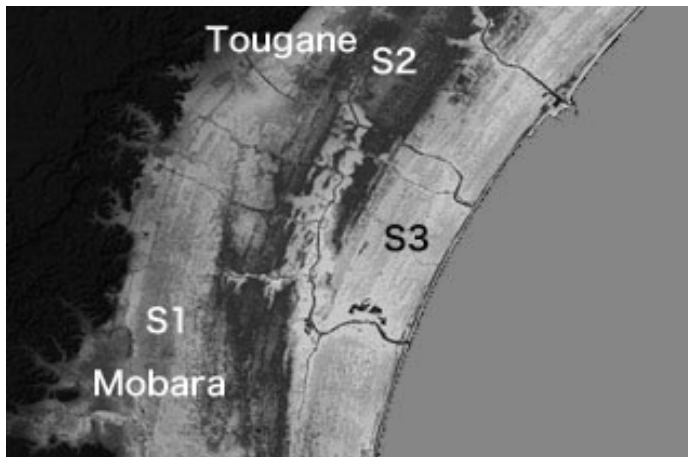
## Development of Strandplain Ridges Group in the Kujukuri Coastal Plain by LiDAR DEMs

OOI, Shinzou<sup>1\*</sup> ; NANAYAMA, Futoshi<sup>2</sup> ; NAKASHIMA, Rei<sup>2</sup>

<sup>1</sup>GSI/AIST, <sup>2</sup>AIST

The DEM data based on an Airborne laser survey was fixed recently, and it became possible also in the Kujukuri Coastal plain to use this DEM data. Then, this DEM data analyzed the microtopography of the plain. And the development of the Kujukuri Coastal plain, especially the north-south difference were considered.

Keywords: Kujukuri Coastal Plain, Strandplain ridge, LiDAR DEMs



## Controlling factor on evolution of late Pleistocene to Holocene sequences in Nara Basin

HORI, Kazuaki<sup>1\*</sup> ; ITO, Nobuaki<sup>1</sup> ; TAKADA, Masashi<sup>2</sup>

<sup>1</sup>Department of Geography, Graduate School of Environmental Studies, Nagoya University, <sup>2</sup>Department of History, Sociology and Geography, Faculty of Letters, Nara Women's University

Many researches on late Pleistocene to Holocene sequences (Chuseki-so) have been carried out in coastal lowlands. In contrast, stratigraphy and evolution of alluvial plain located above the coastal lowlands is less well known. We focus on Nara Basin to clarify stratigraphy and evolution of alluvial plain.

Two borehole cores (MK1, MK2) were taken at Matsukasa, Yamatokoriyama city located in the middle part of the basin. Sedimentary facies analysis and AMS radiocarbon dating were performed. Stratigraphy of late Pleistocene and Holocene deposits was built by analyzing existing borehole columns and radiocarbon ages. Additionally, an incised valley formed beneath the Kawachi Plain located near the Old Yamato river mouth during the sea-level lowstand was reconstructed by analyzing existing borehole logs. Sediment accumulation rate of the basin mainly during the last two millennia was estimated from depth of remains shown in archaeological reports published by Archaeological Institute of Kashihara, Nara prefecture.

Radiocarbon ages obtained from the cores suggest that thickness of Holocene deposits is less than approximately 3 m and they have mainly accumulated after 2,000 cal BP. The timing is not related to sea-level change of Osaka Bay. Sea-level change would affect change of river-bed gradient at Kawachi Plain near the river mouth. However, Kamenose narrow segment in Ikoma Mountain is located between Kawachi Plain and Nara Basin and is composed of Cretaceous and Neogene igneous rock. Rock hardness may have resulted in small incision rate of the river bed at the segment, and influence of the sea-level change above the segment was little.

Geological section of Nara Basin shows thickness of Holocene deposits on south area is larger than that of north area. Discharge and drainage area of south district are ca. 2.3 times larger than those of north district. This may be related to the difference in thickness of Holocene deposits.

Depth of remains during the era of Yayoi to Kamakura suggests that increase in sedimentation rate occurred after Asuka era. Existing pollen analysis results indicate that second growth forest probably influenced by human activity had already occurred in and around the basin at Kofun era. Therefore, it is possible that artificial effects in the basin caused increase in sediment production and influenced formation of late Pleistocene to Holocene sequences in Nara Basin.

Keywords: Late Pleistocene to Holocene sequences, inland basin, borehole log, Nara Basin

## Quantitative Evaluation of Microtopography in the Riverside Land of the Mizunashigawa River, Japan

OGURA, Takuro<sup>1\*</sup> ; AOKI, Tatsuto<sup>2</sup>

<sup>1</sup>School of Humanities, Kanazawa University., <sup>2</sup>School of Regional Development Studies, Kanazawa University.

This research did the quantitative assessment of how the amount of encroachment changed and microtopography change in the outside area of the new dike, which modify the land, of Mizunashi River. The origin of this river is the mount Unzen which is well known of its eruption in 1990. This area is unique because of the artificial preparation of the soil; its base-level of erosion was reset. Thus, this area cannot be discussed by the usual landform evolution, but quantitative assessment.

The result of the research showed that the effect of the change can be divided into 4 periods. There was no large-scale debris flows and erosion of the lateral had progressed with the formation of the micro watercourse network in the 7 years since the 1998. debris flows in the riverside land stabilized as the result of the terrain became stable in 2005.

There were debris flows that occurred intensively in a short period while 2005 to 2008. They were large enough to cause the outflow of the vegetation of the surface layer. As a result of these debris flows, the lateral erosion changed to the downward erosion. After those debris flows, the passage was fixed.

There was a rapid recover of the flora in 2011. This increased the stability of the outside area of the bank.

### Overview of the area

It has been more than 20 years since the Heisei eruption; however, a light rain amount of about 20 ~30mm rainfall time can cause debris flows in the Mizunashi River. To minimize the damage of the volcanic disaster, constructions for the erosion control are still continuing.

### Results and the research method

#### Calculation of bare land ratio by GIS

Putting the base-level of the erosion to the 1998, as the time lapses the ratio of the bare land decrease. For instance the bare land area was 91.62[%] in 2003, but in 2005 it became 50.32[%]. However, the ratio of the 2008 was 58.66[%] and after 2008 the ratio is repeating a micro increase and decrease.

#### Calculation of the flow path extending ratio

The calculation is about the the ratio of the flow path extending of the same waterway since 2008. The result of the calculation shows the quantitative assessment of the immobilization of the channel. This is shown by the result of the 2008, 2011 and 2013, in these three years the ratios are 1.11 and 1.10.

#### Measure of the erosional cross section and local observation

The survey date show the width of gully is 8.27[m]. This is approximately equal to the size of the width and gully erosion in the upper reaches. This date can be seen in the report of 2011 by the Unzen reconstruction office. Calculating the average erosion speed ( $v$ ) from the base level of erosion and the maximum deepening speed ( $Mv$ ) from the maximum depth of erosion, the results are  $v=4.66$ [cm/year] and  $Mv=20.6$ [cm/year]. These results show two things. First, the lateral erosion has the bigger scale than that of lower erosion. Second, the direction of the erosion changed recently from horizontal to down.

Keywords: geomorphological process, gully erosion, debris flow, GIS, Unzen Volcano

## Timing of sediment discharge events on a welded tuff slope in Chugoku Mountains, Japan

WAKATSUKI, Tsuyoshi<sup>1\*</sup> ; YAMADA, Ryuji<sup>1</sup>

<sup>1</sup>National Research Institute for Earth Science and Disaster Prevention

Many slope disasters were occurred by a heavy rain on July 28, 2013 in Yamaguchi and Shimane Prefectures. In particular, a number of shallow slope failures and debris flows occurred on mountain slopes underlain by rhyolite-dacite welded tuff in the Tsuwano Town, Shimane Prefecture and the adjacent Ato District, Yamaguchi City. The debris flows eroded the sidewalls and the riverbed of the flow channel, and outcrops of deposits accumulated by sediment discharge events older than 2013 appeared intermittently. From five outcrops along two channels, we collected 11 chip samples of the woods that may have buried and died at the time of the sedimentation. We performed <sup>14</sup>C dating of them, and the calendar-calibrated radiocarbon ages showed a 0.6 - 52 Ka BP. Sedimentary structures suggest that these ages correspond to the occurrence time of debris flows and slope failures in the past.

Keywords: <sup>14</sup>C dating, debris flow, slope failure, soil slip

## The characteristic of roots distribution on the slopes in Izu-Oshima where landslides were occurred by Typhoon No.26

MURAKAMI, Wataru<sup>1\*</sup> ; OGAWA, Akiho<sup>1</sup> ; OGAWA, Yasuhiro<sup>1</sup> ; DAIMRU, Hiromu<sup>1</sup>

<sup>1</sup>FFPRI

Large-scale landslides were occurred in Izu-Oshima by Typhoon No.26 on October 16, 2013. By the urgent investigation after the disaster, it is reported that the landslides were occurred in the part within about 1m from the slope surface and the few rhizomes were on the slip surface. We surveyed the distribution of the fallen trees (species, height, the root depth, and the extensions (widths) of the roots) on the slope near the landslide. The surveyed fallen trees were a lot of *Eurya japonica*, and were the order of *Ilex crenata var.hachijoensis*, *Prunus lannesiana var. speciosa*, and *Camellia japonica*. Most of the surveyed fallen trees were about 5-7m in height, and the high one was 10m or less. The root depth of most fallen trees was 60-80cm; however, the root depth had the difference by the tree species. The *Camellia japonica* and the *Prunus lannesiana var. speciosa* had comparatively deep roots. On the other hand, the *Eurya japonica* and the *Ilex crenata var.hachijoensis* tended to be distributed shallowly the root systems. As a factor to which the root systems are not deeply distributed, a peculiar properties of soil situation of the volcano is pointed out. In this survey, the difference of characteristics of the tree species on the surveyed slopes was guessed as a cause, too.

Keywords: Izu-Oshima, Typhoon No.26, landslide, roots distribution

## Verification of incision rate estimation based on the geomorphological history of river terraces in Kaligandaki, Nepal

YOSHIDA, Takahiro<sup>1\*</sup> ; SUGANUMA, Yusuke<sup>2</sup> ; MAEMOKU, Hideaki<sup>3</sup>

<sup>1</sup>The Graduate University for Advanced Studies, <sup>2</sup>National Institute of polar research, <sup>3</sup>Housei university

The Himalaya is the highest mountains of the world. To estimate long-term (1 ~100 kyers) uplift history of the Himalaya, erosion rates of the incised river have been used with presuppose of dynamic equilibrium between tectonics and aggradations. This estimation is based on the correlations of the river terraces, however, depositional processes of the terraces usually have not been described in detail.

The Kaligandaki is the one of the longest river across the Nepal Himalaya. The long-term uplift history of the Himaraya has been estimated from the distribution of Holocene and Pleistocene terraces along the Kaligandaki river. In this study, we carried out the detailed geomorphological and sedimentological survey at the upper and middle part of the Kaligandaki River to verify the correlations of the river terraces. The fluvial terraces at the upper part of the Kaligandaki river is thought to be originated to the local sediment supply from three phases of the glacial events, although the middle part of the terraces are fluvial sediment. This indicates that correlations of the river terraces along the Kaligandaki river is not suitable for the estimations of incision rate and uplift history of the Himalaya.

Keywords: Himaraya, Geomorphology, Kaligandaki, Fuluvial terrace

## Field measurements on the reduction of wave height on a fringing reef: A study from the Miibaru coast, Okinawa Island

TAKEISHI, Yu<sup>1\*</sup> ; AOKI, Hisashi<sup>2</sup> ; MAEKADO, Akira<sup>3</sup> ; HIROSE, Takashi<sup>3</sup>

<sup>1</sup>Graduate School of Humanities and Social Sciences, University of the Ryukyus, <sup>2</sup>Faculty of Business Administration, Daito Bunka University, <sup>3</sup>Faculty of Law and Letters, University of the Ryukyus

To investigate the relationship between reduction of wave height on a fringing reef and the water depth at the reef edge, field measurements were carried out on Miibaru coast with a fringing reef in Okinawa Island, Japan. The ratio of the shore break height (the height of final breaking waves near the shoreline) to the wave height at the reef edge,  $H_b/H'$ , which denotes the degree of the reduction of wave height on a reef, was found to decrease with decreasing water depth at the reef edge. This result indicates that the reduction of wave height on a reef is greatly controlled by water depth on a fringing reef.

Keywords: Reduction of wave height, Coral reef, Fringing reef, Water depth, Okinawa Island

## Experiments on Salt Weathering in Cold Environments : Effects of Dissolved Salts on Frost Shattering

SATO, Masato<sup>1\*</sup> ; HATTANJI, Tsuyoshi<sup>2</sup>

<sup>1</sup>Graduate School of Life and Environmental Sciences, University of Tsukuba, <sup>2</sup>Faculty of Life and Environmental Sciences, University of Tsukuba

Weathering experiment was carried out to investigate the effects of dissolved salts on frost shattering using four types of rocks (two tuffs, one sandstone and one andesite) and three types of salt solutions (sodium chloride, sodium sulphate and magnesium sulphate). Cubic specimens with a side of 5 cm in length were immersed in saturated salt solution of NaCl, Na<sub>2</sub>SO<sub>4</sub>, MgSO<sub>4</sub> or distilled water for 72h. After immersion, the specimens were covered with foil and subjected to up to 80 freeze-thaw cycles in a cold chamber where the temperature ranges from -30 °C to 10 °C within twenty four hours.

Freezing points of salt solutions were decreased by dissolved salts. In particular, the saturated solution of NaCl did not freeze under -25 °C. The linear strain on the surface of specimens was measured with strain gauge during freeze-thaw cycle. The specimens immersed in salt solutions showed greater freezing strain than those immersed in distilled water. Specimens with MgSO<sub>4</sub> solution produced the large strain. In most cases, the strain strongly correlated with Weathering Susceptibility Index (WSI). The decreasing rates of the longitudinal wave velocity and the Equotip hardness value during freeze-thaw cycles also correlated with WSI.

Keywords: salt weathering, frost shattering, cold environments, freezing strain, laboratory experiment

## The volume expansion of pyroclastic rocks by the crystal growth of Halloysite at the Higashidoori

NAKATA, Eiji<sup>1\*</sup> ; OUYAMA, Takahiro<sup>1</sup> ; TORIGOE, Yuji<sup>2</sup> ; MIWA, Tadashi<sup>2</sup> ; CHIGIRA, Masahiro<sup>3</sup>

<sup>1</sup>Central Research Institute of Electric Power Industry, <sup>2</sup>Tohoku Electric Power Co., Inc., <sup>3</sup>Disaster Prevention Research Institute Kyoto University

We find the ground deformation by volume expansion of pyroclastic rocks at the Higashidoori Nuclear power station site. The Tomari formation is strongly altered by light brown colored weathering with halloysite crystallization. The Tomari formation mainly consists of lapilli tuff including andesitic lava. The Gamanosawa formation is laid on the Tomari formation consists of alternated sandstone, mudstone, conglomerate and tuff layers. These stratum are covered by the middle terraces deposit including the Toya tephra: 110 ka and Towada red tephra: 80 ka. Towada red tephra in the middle terrace deposit is not deformed on this site.

The convex deformation is formed absorbing the water of montmollironite in fault zone (clay rich zone). Strongly weathered surface rocks of the Tomari and Gamanosawa formation are also deformed toward upper parts around fault zone. This deformation is also formed regardless of fault zone.

Montmollironite distributes at the deeper area (the Tomari formation) which consists of weakly weathered rocks. Halloysite crystallized from montmollironite at shallow area. Plagioclase disappears with the crystallization of halloysite by XRD results. Halloysite which formed tube shapes covered the all over the materials are changed the shape to aggregation of fan shapes by SEM observation. Halloysite crystals increases a distance of the space between minerals under the micro scopic observation.

To assume that Ti is immobile elements with weathering in the rock, the volume of weathered rocks (lapilli tuff: the Tomari formation) increases in 1.3 to 1.5 times to compare with fresh rocks.

Montmollironite crystallizes the surface of minerals at first. After crystallization of montmollironite, halloysite crystallizes on the montmollironite to be affected by weathering at shallow depth.

Crystal growth of halloysite causes the volume expansion of rock and the deformation of ground surface. The old faults plane and joints slip as the appearance reverse faults by crystal growth at this site.

Keywords: Halloysite, Volume expansion, Higashidoori

## Characteristics and Development Processes of Wetlands on Landslide Masses in Hachimantai Volcanic Group, NE Japan

SASAKI, Natsuki<sup>1\*</sup> ; SUGAI, Toshihiko<sup>1</sup>

<sup>1</sup>the University of Tokyo

Wetlands are widely distributed in the mountainous regions in Japan, and are subject to protection and conservation because of their beautiful landscapes and their peculiar biota. Considering not only their climate and hydrological conditions but also their geomorphological conditions is necessary to characterize development processes and environmental responses of wetlands. In tectonically active and warm humid regions like Japan, landslides are one of the most important factors for mountain development. Recently the role of landslides creating biodiversity and landscape diversity has been much attracted attention in the field of ecology and geomorphology (Geertsema *et al.*, 2007). This study focuses on wetlands as one of the representative landform units composing landslides and presents their characteristics and development processes in Hachimantai volcanic groups which have been deformed by many landslides. 'Wetlands' generally includes various types of water-rich conditions. In this study, as their primary components we focus on 'bogs' and 'ponds', and define 'bogs' as grasslands in moisture conditions.

Hachimantai volcanic group stands in Ohu backbone range and is composed of some Quaternary complex basaltic or andesitic stratovolcanoes. Their bodies are being collapsed by landslides characterized by a variety of body size and structures: some have deformed into several numbers of sliding blocks. Wetlands occur in almost all large scale landslide bodies. Its climate is categorized in Japan Sea side climate pattern as heavy-snow.

We investigated the characteristics of wetlands using remote sensing images and digital elevation models and analyzed the relationship with landforms by GIS. Then we reconstructed the development process of typical wetlands located both in and out of the landslide masses by the analyses of the sediment including <sup>14</sup>C dating, tephra identification, carbon content measuring and grain size analysis.

On landslide masses 33.2 % (185 of the 599 in total) wetlands stood and area rate was 63.7 %. Most wetlands out of landslides stood on the volcanic original surface along the ridge line of Ohu mountain range or some were in the craters of Hachimantai volcano. The formers are the small bogs formed by meteoric-water (snow) cultivation in the nivation hollows. On the other hand, those on the landslide masses scattered widely. Large landslide masses frequently had ponds cultivated by ground water in the large and deep depressions along the scarps and in the small ones among pressure ridges.

In Oyachi, a wetland in a landslide, black mud and organic sand and silt (representing for bog and forest), sand and gravel (disturbance), clay and silt (pond) and peat (bog) deposited from their bottoms. Wetlands typically develop under the stable circumstance from ponds to bogs, and finally to forests. In the case of Oyachi, at BC 4000-3500 the bog changed to the pond, the former developmental stage, probably because the landslide activity formed the dam, and then it developed to the bog with stabilization of the slopes and the water discharge. On the other hand, the development process of Okuno-maki, a wetland out of landslides, were probably directly affected by climate changes. Diminishing erosion along with decreasing snow accumulation in the nivation hollow and warming of melt season climate toward the Medieval Warm Period enabled to be the bog. In contrast, landslide activities and denudation of landslide masses control the developmental stages of wetlands. Consequently, various ages and types of wetlands are presumed to coexist in humid mountains with large landslide masses.

### Reference

Geertsema *et al.* (2007): Influence of landslides on biophysical diversity -A perspective from British Columbia. *Geomorphology* 89, 55-69.

Keywords: wetland, landslide, development process, Hachimantai

## Comparison between two chronological methods - in situ TCN and WRT applied to periglacial landforms in Kiso Mountains

ENDO, Ryo<sup>1\*</sup> ; SUGAI, Toshihiko<sup>1</sup> ; EZURE, Yasuhide<sup>1</sup> ; MATSUZAKI, Hiroyuki<sup>1</sup> ; MATSUSHI, Yuki<sup>2</sup>

<sup>1</sup>The University of Tokyo, <sup>2</sup>Kyoto University

A lot of types of chronological methods have been suggested in the field of earth science. Chronological methods are classified into absolute dating methods and relative dating methods. Absolute dating methods contain isotopic age or tree-ring chronology for example, and they provide the age as numerical values. Otherwise, relative dating methods are the methods which detect the time series of the formation of geomorphology or deposition. However, they cannot fix the age without the absolute age data (Watanabe, 1990).

Two chronological methods - in situ Terrestrial Cosmogenic Nuclides (TCN) and weathering-rind thickness (WRT) -are subjected. These two methods are especially effective in high mountain areas as it is difficult to find radiocarbon samples or key tephra layers (Aoki, 1994). These two methods were compared using terminal moraines in the cirques (Aoki, 2000). However, this comparison is not made in other mountainous terrains, and it is made in Kiso Mountain Range in this study.

In order to compare these two methods, samples were taken from multiple ridges in the eastern part of Mt Kisokomagatake, and Shirabidaira. Six samples were taken from 3 ridges and 2 depressions of triple ridges, and one sample from Shirabidaira. In order to obtain the exact formation age, we selected the bedrock or the oldest boulder filling the depression and collected their surface layer of 4 cm or less in thickness

Each sample is divided in two, one for TCN and the other for WRT.

<sup>10</sup>Be exposure dating method is subjected as TCN. The samples are chemically preprocessed and at MALT (Micro Analysis Laboratory, Tandem Accelerator), University of Tokyo. The exposure age is calculated by means of the formula as follows(\*)

$$T = -1/\lambda \ln\{(1 - \lambda N/P)\} \quad (*)$$

T: Exposure Age [yr] λ:Decay constant [1/yr] N: Number of isotopes [atoms/g] P: Production rate of isotopes [atoms/(g • yr)]

Weathering-rind is a discolored part of rocks. It is formed due to oxidation or hydration. Though the age is nearly in portion to WRT, its correlation depends on the rock type, sampling point and so on. In this study, samples were cut so that the weathering-rind can be observed as clearly as possible.

In 7 samples, radioactive ages are in either late Pleistocene or Holocene. Weathering-rind was observed and detected for 5 samples. There is a positive correlation between WRT and the exposure age. The primary regression equation is as follows : WRT [mm] = 0.367 × (Exposure age [kyr] ) + 1.16. The correlation coefficient is about 0.85. This suggests that in order to get the exposure age of multiple ridges, WRT is also an effective method to a certain extent. Therefore, mean weathering rate ( = 0.367 mm/kyr) can be gained by calculating a primary regression line that shows the relationship of the WRT and the exposure age. This weathering rate is the same in the order of magnitude as that ( = 0.283 mm/kyr) estimated from Seki and Koizumi (1992).

Keywords: In-situ Terrestrial Cosmic Nuclides, Weathering-rind Thickness, Periglacial landforms, Kiso Mountain Range

## Tree-line change since the Last Glacial from the pollen profile at the Hiroppara peat bog, central Japan

YOSHIDA, Akihiro<sup>1\*</sup>

<sup>1</sup>Center for Obsidian and Lithic Studies, Meiji University

To better understand the interaction between the human and environment in past period, this study reconstructed vegetation history and climate change since the late Pleistocene at the Hiroppara peat bog (1,400m a.s.l.), central Japan, from the pollen and micro-charcoal profiles at HB-1A cores. Arboreal pollen assemblages and influx of the cores indicated the vegetation history and climate change since the Last Glacial Maximum as follows; 1) ca. 30,000~19,000 cal BP, grassland and wasteland distributed due to decreasing the tree-line; 2) ca. 19,000 cal BP, around the site was covered with a mixed forest of boreal conifers and cool-temperate deciduous, because the tree-line passed the altitude of site; 3) ca. 16,000 cal BP, *Betula* forest expanded; 4) ca. 12,000 cal BP, a cool temperate deciduous broad-leaved forest consisting of *Quercus* subgen. *Lepidobalanus* and *Carpinus* was distributed; 5) ca. 4,000 cal BP, temperate conifer such as *Taxaceae-Cupressaceae*, *Tsuga*, and *Abies* increased; 6) secondary forest of *Pinus densiflora* and *Larix kaempferi* plantation increased in ca. 500 and 100 cal BP, respectively. It is highly possible that the tree-line change impacted strongly the human activities since the Last Glacial Maximum.

Keywords: pollen analysis, vegetation history, tree-line, obsidian, prehistoric age, central Japan

## Vertical crustal movements along the Japanese coastlines inferred from the Quaternary and recent sea-level changes

OKUNO, Jun'ichi<sup>1\*</sup> ; NAKADA, Masao<sup>2</sup> ; ISHII, Masayoshi<sup>3</sup> ; MIURA, Hideki<sup>1</sup>

<sup>1</sup>NIPR, <sup>2</sup>Faculty of Sciences, Kyushu University, <sup>3</sup>MRI

Observed relative sea-level (RSL) changes during the past 130 kyr are mainly caused by change of ocean volume, tectonic crustal movement and glacio-hydro isostatic adjustment (GIA) of the Earth in response to the redistribution of ice and water loads. Here we examine the tectonic crustal movements along the Japanese coastlines on three typical timescales (50 yr, 6 kyr and 125 kyr) based on several sea-level observations and their predictions due to GIA process and recent melting of mountain glaciers and both polar ice sheets. We use the observations of RSL based on tide gauge and Holocene RSL observations and the altitudes of marine terraces formed at the last interglacial (LIG) phase at about 125 kyr. The rates on a timescale of 50 yr are derived from tide gauge data, thermosteric sea-level changes due to thermal expansion of the oceans and predictions due to the GIA for the last deglaciation and also recent melting of the mountain glaciers and both polar ice sheets. Those for 6 kyr and 125 kyr are based on the RSL observations and the predictions by GIA modeling, considering uncertainties for temporal changes in eustatic sea-level for the mid- to late-Holocene and LIG phase. The inferred rates for 50 yr are significantly different from those for 125 kyr in most sites, particularly for sites along the coastline from eastern Hokkaido to northeastern Japan, Shikoku and south Kyushu facing the Pacific Ocean. In these regions, the rates for 125 kyr and 50 yr are positive (uplift) and negative (subsidence), respectively. Also, the observed RSL changes at 6 kyr BP are consistent with the inferred RSL changes using the rates for 125 kyr and GIA-predictions in many sites, but inconsistent with those for 50 yr in most sites except for a few sites. These results suggest that the rates on a timescale of 50 yr are not representative of the tectonic crustal movements for timescales longer than 6 kyr in most sites along the Japanese coastlines. The inferred rates on these timescales may be useful in discussing the recurrence of megathrust earthquake with its interval of about 1 kyr like the 2011 off the Pacific coast of Tohoku Earthquake.

Keywords: crustal deformation, sea-level change, Quaternary, tide gauge, thermometric sea-level

## Prehistoric human activity around the Hiroppara wetland, central Japan: a case study in and around the obsidian sources

HASHIZUME, Jun<sup>1\*</sup> ; SHIMADA, Kazutaka<sup>2</sup> ; SUDA, Yoshimitsu<sup>1</sup> ; ONO, Akira<sup>1</sup>

<sup>1</sup>Center for Obsidian and Lithic Studies, Meiji University, <sup>2</sup>Meiji University Museum

The Hiroppara wetland is located about 1.5 km to the north of Wada-toge, a well known obsidian source 1,400 m above sea level. Many prehistoric sites and geological obsidian sources are scattered around this area.

Through general surveys and small-scale excavations conducted by the former Wada Board of Education between 1989 and 1991, several prehistoric sites were identified around the wetland. In 2011, the Center for Obsidian and Lithic Studies (COLS), Meiji University began a new research project on this wetland and the prehistoric sites around it. Our research goal is to reveal the relationship between human activities in and around the obsidian sources and paleoenvironmental changes during the late Late Pleistocene (Upper Palaeolithic) to the Early Holocene (Incipient to Early Jomon period). This presentation is a preliminary report of our research, with a particular focus on the results of our archaeological excavations.

On the basis of results of previous surveys and our observations of the topographical features around the wetland, we distinguished the archaeological landscape around the wetland into seven sites, which we numbered from I to VII. The COLS has set up an excavation area 1 (EA-1) at site I and excavation area 2 (EA-2) at site II.

Excavations at EA-1, the Hiroppara I site, and EA-2, the Hiroppara II site, have revealed the following:

### 1. EA-1

- 1) This site yields evidence of an Early Upper Palaeolithic lithic industry from layer 6 (under the Aira-Tn tephra).
- 2) The latter part of the Late Upper Palaeolithic industry, represented in layers 2b and 3, primarily features bifacial points with a blade core.
- 3) Incipient to Early Jomon period assemblages are found in layers 2a and 2b.

### 2. EA-2

- 1) The early part of the Early Upper Palaeolithic industry, from layers 4a and 4b, yields an "obsidian concentration" characterized by a dense lithic concentration in a small area mainly composed of large lithics. Layers 4a and 4b contain the Aira-Tn tephra and a ground-edge stone ax made from tremolite rock.
- 2) The latter part of the Late Upper Palaeolithic industry, from layer 3, appears to be a knife-shaped tool industry using a developed blade technique.
- 3) Jomon pottery of the early part of the Initial Jomon with pebble concentrations and a pit, arrowheads, and cobble tools.

These new findings expand the scope of information about multilayered prehistoric occupations at the Hiroppara I and II sites. In addition, it has allowed us to extract a significant amount of information on prehistoric human behavior with specific regard to exploitation, transportation and consumption of obsidian during the late Late Pleistocene to the Early Holocene. However, these issues require further study.

Keywords: Obsidian sources, Central Japan, Hiroppara wetland, Hiroppara site group, Jomon period, Upper Palaeolithic

## Prehistoric obsidian exploitation in the Central Highlands obsidian sources and excavations of the Hiroppara site group

SHIMADA, Kazutaka<sup>1\*</sup>

<sup>1</sup>Meiji University Museum

The Center for Obsidian and Lithic Studies, Meiji University (COLS) has conducted archaeological and palaeoenvironmental excavations at the Hiroppara wetland and prehistoric site group (sites I and II) located 1,400m of the Kirigamine mountains in Nagawa Town, Nagano Prefecture, Japan. This paper presents a review of the Central Highlands obsidian source area where Hiroppara is located and its circumstances of prehistory, and preliminary results of Hiroppara excavations. Many sites assigned to the Upper Palaeolithic and the Jomon periods have been discovered in and around the Central Highlands. The site distribution of both periods shows distinctive patterns. The Upper Palaeolithic sites concentrate in relatively high-altitudinal zone over 1,000m close to the obsidian sources, while the Jomon sites shows dense-distribution on the hill slopes in low-altitudinal zone below 1,000m. This ebb and flow pattern reflects historical changes between the Upper Palaeolithic and the Jomon periods in the technology of obsidian acquisition, the way of land-use in the source area, the group organization, and the obsidian circulation system. The emergence of an obsidian mining site in the initial Jomon is one of representatives of those changes in the relationship between humans and obsidian. Data for archaeological chronology and changes in palaeoenvironment in the Central Highlands, however, are less accumulated than other areas, resulting in insufficient explanation for changes in human activities in and around obsidian sources. Multidisciplinary research on the Hiroppara wetland and site group provide us with a useful set of data concerning archaeological and palaeoenvironmental changes that represents a limited narrow area. The excavations of Hiroppara by COLS have been conducted three times in 2011, 2012, and 2013. The excavations at sites I and II have unearthed several cultural layers ranging from the Early and Late Upper Palaeolithic to the earliest Jomon. Palaeoenvironmental data during the late MIS 3 and the early Holocene have been obtained from microfossil analyses on the peat cores from the Hiroppara wetland. Though further analyses and integration on obtained data are still required, the Hiroppara wetland and site group will allow us to make an explanatory model for relationships between prehistoric humans and palaeoenvironment in and around obsidian sources of the Central Highlands.

Keywords: the Upper Palaeolithic, the Jomon, the Central Highlands, obsidian sources, the Hiroppara wetland, microfossil analysis

## Discovery of fresh water diatom from aeolian sediments in the conical pit structure in the Arsanjan area, south Iran

HISADA, Ken-ichiro<sup>1\*</sup> ; TSUNEKI, Akira<sup>2</sup> ; CHIBA, Takashi<sup>1</sup>

<sup>1</sup>Graduate School of Life and Environmental Sciences, University of Tsukuba, <sup>2</sup>Graduate School of Humanities and Social Sciences, University of Tsukuba

It is well known that the life of ancient people was greatly influenced by various natural conditions, such as climate, topography, and geology. In particular, geology is not only important as a source of raw material for stone tools and residence construction material, but also as a provider of groundwater and mineral resources. Furthermore, soil is generated from weathered bedrocks, and soil is a key influence on vegetation. Thus, when ancient people considered the natural conditions for first settlement locations, geology would have been a crucial factor in these conditions. The present paper offers a preliminary examination of interaction of the humankind - Iranian Zagros Mountains.

One of the most important discoveries among the humankind studies was the existence of many Middle Paleolithic and Epi-Paleolithic cave sites in the Arsanjan area, south Iran. One of the caves, named A5-3 (Qar-e Tang Sikan), produced a large amount of Middle to Epi-Paleolithic stone implements. Thus the Arsanjan area is one of the most suitable areas for the study of human evolution and cultural transition from the Middle/Late Paleolithic to the Epi-Paleolithic/Neolithic periods. This means that the investigation of this area can possibly provide opportunity for the better understanding of the evolution of modern *Homo sapiens* and of the interface of geology-archaeology.

We accomplished the trench survey recently. The results of B3 trench survey (4 X 4 m square) at A5-3 (Qar-e Tang Sikan) are as follows (Hisada and Tsuneki, 2013). The culture layers are divided into ten layers. Layers 1 to 3 correspond with Late Paleolithic to Proto Neolithic. Six samples from layers 2 and 3 indicate approximate 36,000 BP. Layers 4 to 10 are included into Middle Paleolithic culture layers. It is noteworthy that structure 3 was discovered from layer 7. Structure 3 presents a circular form on plan, 1 m in long axis and 0.7 m in short axis. In profile, it is conical and depth is about 50 m. Cave limestone bedrock is used as a bottom wall of the conical shape, and concrete-like harden wall with pebbles and clays is used as the other one. The concrete-like wall might be built after cutting soil surface. The filling of the conical shape structure is light orange color clay, 50 cm in thickness. This clay presents a bimodal pattern, 5 phi and 11 phi in grain size analysis, and consists of quartz, muscovite and hydroxylapatite. The color of the clay is characteristics (10YR7/6, 6/6 etc) and conspicuous from other soil. Based on the color and clay-seized sediments, it can be concluded that they are aeolian sediments. This conical structure may be intended to be a water-reserved place keeping water oozed from the limestone wall (Hisada and Tsuneki, 2013). Thus, the clay might be deposited in this conical pit, 50 cm deep. This laying down at the pit seems to be prevented from erosion and transportation because the pit was full of water. Very recently, it is clarified that clay bed yields diatom, *Pinnularia* spp.. This genus indicates a living in fresh water (Watanabe et al., 2005). The ages for layer 7 are inferred before 51,000 BP, because layer 5 is dated as 50±2Ka and the ages for the boundary between layers 6 and 7 are 51±2Ka based on the photoluminescence measurement (Ito, in pers. comm.).

Keywords: West Asia, Paleolithic ages, Iran, water-reserved place

## Quantitative detection of event deposits in the piston core of Beppu Bay, central Kyushu, Japan

YAMADA, Keitaro<sup>1\*</sup> ; TAKEMURA, Keiji<sup>2</sup> ; KUWAE, Michinobu<sup>3</sup> ; IKEHARA, Ken<sup>4</sup> ; YAMAMOTO, Masanobu<sup>5</sup>

<sup>1</sup>Division of Earth and Planetary Sciences, Graduate School of Science, Kyoto University, <sup>2</sup>Beppu Geothermal Research laboratory Institute for Geothermal Science, Kyoto University, <sup>3</sup>Center for Marine Environmental Studies, Ehime University, <sup>4</sup>Institute of Geology and Geoinformation, AIST, <sup>5</sup>Faculty of Environmental Earth Science, Hokkaido University

Particle transportation and deposition is repeated by various phenomena to be caused by constant cycle of water and atmosphere (non-event) and sudden phenomenon (event) such as earthquake, volcanic eruption, flood, and a stratum is formed. Therefore we can know paleo-disaster or climate change from the stratum. In addition, because the deposit caused by event (event deposits; Shiki, 1998) supplied a lot at a time, it is very important for solving formation process of the stratum. In recent years, due to analysis technique development high resolution/precision study in sedimentology is increasing (Katsuta *et al.*, 2007). For this reason, details of the sedimentation mechanism and the environmental change are more clearly, but on the other hand influence of development on age models and various analyses is actualized. Therefore clear distinction of event and non-event is one of the important problems.

In Beppu Bay, the detailed age model to omit major events was constructed by Kuwae *et al.*(2012). Event deposits were identified by sighting based on facies, CT images, magnetic susceptibility and wet bulk density. This method can identify event deposits seamlessly, but it is a problem to depend on the personal experience and to have difficult to quantitative detection. Therefore we tried quantitative detection of event deposits by the statistical method and compared the detection result and the sighting result in Kuwae *et al.*(2012). The BP09-3 core (about 9.3 m long) using this study which was used in Kuwae *et al.*(2012) was obtained at the deepest place in the head of Beppu Bay.

Generally, because the source and sedimentation process of event deposits are greatly different from non-event deposits, chemical composition, particle composition or other profiles have difference. Therefore, in this study, we defined event deposits as “ the sediment which has significantly different composition or physical properties ” , we tied the quantitative detection of the event sediment using test for outliers. Analysis data are particle composition of very fine sand which sampled every 2 cm from the core, and we used MSD method (Wada, 2010) which is the robust and multivariate method for test. As a result, 47 events were detected. The detected event in this study and the sighting event in Kuwae *et al.*(2012) are relatively congruent, so it is thought that detective method using this study is useful for quantitative detection of event deposits. However, there are problems that 1) one is not to be able to detect minute event sediments enough and 2) the other is difficult to recognize the border of event deposit and non-event deposit. Because the event layer which was not able to detect is thin relative to sampling interval, it is thought that event layer was diluted by non-event deposits. Because there is no a meaningful difference in composition of the neighborhood of border, clear border detection using only test for outliers is difficult. It is necessary to evaluate and reflect event attenuation (vertical change) and preservation potential to solve these problems.

Keywords: Beppu Bay, Event deposits, Quantitative detection, Particle composition

## Paleolithic human activity and summer temperature recorded in oxygen isotope of *Semisulcospira* from Sakitari-do archeolo

FUJITA, Hikaru<sup>1</sup> ; SONE, Tomomi<sup>1</sup> ; KANO, Akihiro<sup>1\*</sup> ; OKUMURA, Tomoyo<sup>2</sup> ; FUJITA, Masaki<sup>3</sup> ; YAMASAKI, Shinji<sup>3</sup> ; KATAGIRI, Chiaki<sup>3</sup>

<sup>1</sup>SCS Kyushu University, <sup>2</sup>JAMSTEC, <sup>3</sup>Okinawa Pref. Mus. & Art Mus.

Sakitari-do archeological site is located in Gyokusen-do cave system in Nanjo City, Okinawa Prefecture. Since 2009, this site has yielded important remains including a 12.4-ka-old human canine (Yamasaki et al., 2012). One of the noticeable animal remains is *Eriocheir* crub. Large and uniform size of the forceps indicates individuals of autumn season when this crub grows into an adult. Paleolithic people may have stayed in this cave during autumn and eaten *Eriocheir* crub.

In order to examine this hypothesis, this study focuses on *Semisulcospira* shell that was excavated together with *Eriocheir*. *Semisulcospira* is a freshwater gastropod that grows spiral shell. It is known that change in the water temperature was recorded in oxygen isotope of a series of samples collected along the spiral growth axis (Kano et al., 2008). If the Paleolithic people ate the gastropod, the oxygen isotopic value of the outermost sample indicates when it was taken. We analyzed the gastropod shell from two Paleolithic layers (19 ka and 12.4 ka) of the Sakitari-do site, as well as modern *Semisulcospira* collected a stream 5 km east from the site in late November 2013.

Paleolithic specimens from the Sakitari-do often exhibit a sign-shaped oxygen isotopic curve. Amplitude of the change is ~2 permil that corresponds to ~8 degree temperature change under stable water isotopic composition. More importantly, the outermost value locates on an autumn position in many specimens, which support the hypothesis based on *Eriocheir* remains. In contrast, the modern *Semisulcospira* specimens that lack the sign-shaped pattern were young individuals that born in early summer. They recorded temperature change from summer to November. Comparing the summer oxygen values, the modern specimens are 1-1.5 permil lower than the Paleolithic specimens. If the oxygen isotopic value has been constant, it can be evaluated that the Paleolithic summer water was 4-6 degree cooler than the modern summer water.

Kano, A., Suzuki, S., Hori, M. (2008) Information recorded in oxygen isotopic profiles of freshwater gastropod *Semisulcospira livertina*. *Ann. Bull Hiroshima Univ. Taishaku-do site Research Center.* 22, 47-61.

Yamasaki, S., Fujita, M., Katagiri, C., Kunikida, D., Matsuura, S., Suwa, G., Oshiro, I. (2012) Excavations (2009?2011) at Sakitari-do cave site, Nanjo city, Okinawa prefecture ?a new Late Pleistocene paleoanthropological site- *Anthropological Science (Japanese Series)*, 120, 121-134.

Keywords: Paleolithic age, oxygen isotope, Okinawa

## Environmental changes of prehistoric culture of the Ryukyu, reconstructed by sedimentological studies of Haneji-naikai.

GOTANDA, Katsuya<sup>1\*</sup>; YAMADA, Kazuyoshi<sup>2</sup>; HARAGUCHI, Tsuyoshi<sup>3</sup>; SETO, Koji<sup>4</sup>; HAYASHIDA, Akira<sup>5</sup>; YONENOBU, Hitoshi<sup>6</sup>

<sup>1</sup>Faculty of Policy Informatics, Chiba University of Commerce, <sup>2</sup>School of Human Sciences, Waseda University, <sup>3</sup>Department of Geosciences, Graduate School of Science, Osaka City University, <sup>4</sup>Research Center for Coastal Lagoon Environments, Shimanu University, <sup>5</sup>Department of Environmental Systems Science, Doshisha University, <sup>6</sup>Graduate School of Education, Naruto University of Education

The beginning of agriculture in Ryukyu Islands goes back to the 10th-12th century (Takamiya and Itoh, 2011). Land clearing for farm lands accelerated soil discharge into water systems in Ryukyu Islands due to heavy rain in summer. In a closed bay, finer-grained clastics can remain sub-merged for long periods, causing adverse effects in fishery.

In this study we will report on the analytical results for sediment cores recovered from Haneji-naikai. Haneji-naikai is a bay closed by the Yagachi and Okubu Islands. Its maximum water depth is 10 m with the area is 10km<sup>2</sup>. The Nasata river flows into the Haneji-naikai. In 2010 and 2012, 3-m and 24-m long sediment cores were recovered from the center of the bay. These were used to reconstruct the past environmental changes and human activities. The latter longer cores consisted of clay and silt with shell fragments from the surface up to the 16-m depth, while the lower part was composed of gravels. The radiocarbon dates of terrestrial plant fragments were 2880±40, 4210±30, 6150±40 and 31680±220 at the depths of 7.42 m, 10.78 m, 14.84 m and 23.90 m, respectively. The cores were subsampled at an interval of 2.3 cm to analyze carbon, nitrogen and sulfur (CNS) contents, magnetic susceptibility and visible color reflectance. It is considered that the Haneji-naikai was dried up around 30000 yr BP probably due to marine regression. The changes in TOC, TN and TS were recognized from 4m in depth, showing drastic decrease from 4m in depth. This suggests that the deforestation induced by agricultural activities have begun since 1000 yr BP in this region.

Keywords: Haneji-naikai, CNS analysis, Magnetic Susceptibility, Human activity, Ryukyu Islands

## Paleoenvironments analysis for the past 50 ka based on TOC and TN of the sediment cores INW2012-1 and -2, Lake Inawashiro

WATANABE, Kei<sup>1\*</sup> ; NAGAHASHI, Yoshitaka<sup>2</sup> ; HIROSE, Kotaro<sup>3</sup> ; KUMON, Fujio<sup>4</sup>

<sup>1</sup>Graduate School of Science, Shinshu University, <sup>2</sup>Faculty of Symbiotic Systems Science, Fukushima University, <sup>3</sup>Graduate School of Systems and Technology, Fukushima University, <sup>4</sup>Department of Environmental Sciences, Faculty of Science, Shinshu University

The total organic carbon (TOC) and total nitrogen (TN) were measured at 2 cm interval for the long sediment cores (INW2012-1, INW2012-2) taken from a central site of 90 m depth in Lake Inawashiro in Fukushima Prefecture. Depth-age relationship has been established based on six <sup>14</sup>C data, and the bottom of the drilled core, about 28 m, is estimated as old as 48 ka. Sample interval is 50 to 100 years.

The compilation of information on lithology, TOC and TN concentrations, C/N ratio and water contents of INW2012-1 and -2 enable us to reveal the paleoenvironments of Lake Inawashiro from the early stage to the present with high temporal resolution. Deep condition of Lake Inawashiro started 42,000 years ago and then the lake has been constantly deep until now. Temporal change of TOC concentration of Lake Inawashiro shows the quasi-periodical fluctuation similar to the marine isotope curve known as LR04, and corresponds well to that of TOC concentration of Lake Nojiri in Nagano Prefecture. Vegetation change revealed at the Yanohara, moor in Fukushima Prefecture corresponds with the TOC fluctuation of TOC in the lake. Therefore, Temporal change of the TOC concentration in Lake Inawashiro seems to be controlled mainly by climate, probably temperature, and can be one of the useful paleoclimate records in the Tohoku region, Japan.

Keywords: Lake Inawashiro, TOC, TN, C/N, paleoenvironments, paleoclimate

## Environmental Changes based on the variations of the grain size distributions of MD179 cores, off Joetsu, Sea of Japan

TAKIZAWA, Michiru<sup>1\*</sup> ; SUGAI, Toshihiko<sup>2</sup> ; MATSUMOTO, Ryo<sup>3</sup>

<sup>1</sup>Graduate School of Frontier Sciences, University of Tokyo (current PASCO Corporation ), <sup>2</sup>Graduate School of Frontier Sciences, University of Tokyo, <sup>3</sup>Gas Hydrate Research Laboratory, Organization for the strategic Coordination ,Meiji University

### 1.Introduction

Climate change during the Quaternary period experienced a 10,000year<sup>2</sup>glacial<sup>1</sup>interglacial cycle. This cycle has an influence on land formation. In Japan, the sea level changes, in coastal areas, and the variations of precipitations, at up stream and middle stream areas, change the riverbeds. Thus the marks from climate changes are expected to be archived around the rivers. However, the long term and continuous records hardly remain on the land, due to weathering and erosion. On the other hand, owing to the more stable environment, the continuous records are expected to remain on the seafloor(Tada et al., 1999). In this study, to reconstruct the correlation between the land formations and climate changes, the variations of the grain size distributions during past 130 ka on the East marginal area of Sea of Japan was revealed.

### 2.Study Area and Methods

There are a lot of Paleoenvironmental records concerning the Sea of Japan. In this study, 3 cores, which were sampled during the MD179 cruise in the Umitaka Spur and the Unnamed ridge off Joetsu, are used and the variations of grain size distributions of these cores were revealed. The Umitaka Spur is located in the continental slope. Moreover the sedimentation rate off Joetsu is very rapid (Nakamura et al., 2013; Ishihama, et al., in press) and the supply from the island arc is active (Freire et al., 2009). The supply from the Tateyama Mountains has the highest amount in Japan. So the of these supply are speculated to contribute to the sediment off Joetsu.

In this study the age models of these cores are constructed by using tephrochronology, radiocarbon dating, oxygen isotope ratio of foraminifer (Ishihama et al., in press) and additional data from tephra and radiocarbon dating. The organic matters in 485 samples from the 3 cores were removed by 10%H<sub>2</sub>O<sub>2</sub>. Then the grain size distributions of these are analyzed by using SALD3000S (Laser diffraction particle size analyzer).

### 3.Result

The sediments off Joetsu are composed mainly of suspended load. The coarser sediments that contain little fine sand existed during the interglacial age. The variations of the median grain sizes off Joetsu have a similar pattern to the glacial cycles.

In general, it is assumed that the grain sizes of seafloor sediments become smaller as it gets farther from the land. Nevertheless, in this area, the variations in the size of the sediment supplied from land driven by the glacial cycles, have a large influence on the grain sizes of sediments in the study area, because of (1) the active supply from the rivers and (2) the narrow continental shelf.

However, in the case of the rapid rise in sea level, for example after LGM, the formation of alluviums in coastal zone is speculated to have an influence on the size of the sediment in study area.

### References

- Freire, A. F. M. et al. (2009) *Journal of the Sedimentological Society of Japan*, 68:117-128.
- Ishihama, et al. (in press) *Journal of Asian Earth Sciences*.
- Kashiwaya (1989) *Journal of Geography*, 98:725-730.
- Nakamura, Y. et al. (2013) *Journal of the Japanese Association for Petroleum Technology*, 78:79-91.
- Tada, R. et al. (1999) *Paleoceanography*, 14:236-247.

Keywords: Seafloor cores on MD179, Umitaka Spur, grain size analysis, Last Interglacial Age

## Developing process of the erosional landform and the developmental mechanism of slope failure in Shirasu area

IGARASHI, Ryusuke<sup>1\*</sup> ; SUGAI, Toshihiko<sup>1</sup> ; IMURA, Ryusuke<sup>2</sup>

<sup>1</sup>Graduate School of Frontier Sciences, The University of Tokyo, <sup>2</sup>Graduate School of Science and Engineering, Kagoshima University

Pyroclastic flow deposits are distributed throughout Japan, dotting the country's landscape. In Kagoshima Prefecture, in particular, the cliff overlain by " Shirasu " deposits has undergone repeated slope failures during a period of several decades, which is an extremely short timeframe for such activity (Tsukamoto, 1993). Ito pyroclastic flow deposits are part of a huge pyroclastic flow that occurred approximately 29,000 years ago (Machida and Arai, 2003); these deposits span an area of approximately 90 km from Aira Caldera, which was the source of Shirasu deposits (Yokoyama, 2000). Although the stratigraphic relationship between the erosional landform and the Shirasu deposits of volcanic ash and gravel layers is important, little research has been conducted on this topic. Among the current and the former incised valleys engraving Shirasu plateau, an ancient fossil valley has been identified; however, the factors contributing to the ceasing of its growth remain unknown (Yokoyama, 2000). This study examined the relationship between the developmental mechanism of slope failure and the long-term development process of the erosional landform in the Shirasu distribution area to clarify the region's geomorphological evolution. In this presentation, we focus on the Satsuma Peninsula, which includes a part of the Shirasu plateau in northern area. In the peninsula, ancient shallowly incised valleys remain on the plateau, while the current deeply incised valleys have been dissecting the plateau. A landform classification map was made by interpretation of color aerial photograph in 1975 and by analysis of samples obtained from the plateau cliff that developed through erosion-denudation processes such as slope failure and erosion of Shirasu by running water; strength measurements were performed with a Schmidt hammer.

The valley width decreases rapidly from the main stream valley to the tributary valley and in the current incised valley, from downstream to upstream corresponding to the high-density distribution of failures in this site. The failure substance can be easily transported downstream because the " Shirasu " rapidly changes fine sand and silt after the failure. The failure at the valley wall slope has likely been continued by the valley width expansion of the current incised valley. Incision can be estimated from the beginning edge of the downstream side of the original Shirasu located in the place that is near to the East China Sea of the Satsuma Peninsula west, and has progressed in the upstream side gradually. This is probably because that the attitude of the Shirasu deposition surface is low, and the incised valley bottom is close to the base level of erosion, which has been almost stable during the last 7ka.

It is considered that lateral erosion of current incised valleys has continued during the time whereby failure has occurred in the vicinity of the lower end of the incised valley wall. From a long-term perspective, it can be said that the failure potential is high for current incised valleys dominated by width enlargement processes.

Keywords: Shirasu, Slope Failure, Records, Geomorphological Development, Southern Kyushu

## Total organic carbon fluctuation from the lake sediments in central Japan during the past 200 ka

KIGOSHI, Tomohiko<sup>1\*</sup> ; KUMON, Fujio<sup>2</sup> ; TAWARA, Takaharu<sup>3</sup>

<sup>1</sup>Interdisciplinary Graduate School of Science and Technology, Shinshu University, <sup>2</sup>Faculty of Science, Shinshu University, <sup>3</sup>Wakayama Prefectural Government

Lake sediment is a useful recorder of paleoclimate in the mid-latitude regions. However, the life span of a lake is shorter than that of the marine sediments or polar ice sheets in the most cases. Furthermore, a general condition of a lake may be disturbed by an accidental event. Then, we try to combine a climate proxy of total organic carbon (TOC) records from several lake sediments central Japan, and have compiled an average TOC in the past 200 ka which may correspond to the regional climate change.

Used data include Lake Biwa (BIW07-5, 6 core: 0-50 ka, BIW08-B core: 0-200 ka), Lake Nojiri (NJ88+NJ95 core: 0-72 ka), Takano Formation (TKN-2004: 38-160 ka). The time resolutions in those data are between 20-100 years. TOC data of the six sediment cores were normalized as dividing a data by standard deviation. Their fluctuation curves of the normalized TOC were matched by the method of Lisiecki and Lisiecki (2002). Then the matched normalized data were interpolated at 100-year interval by polynomial interpolation method.

The compiled TOC fluctuation in central Japan is well correspond to the D18O curves of the marine sediments (LR04) and the Greenland ice core (NGRIP) respectively both in the orbital and millennial time scales. In late MIS (marine isotope stage) 7 and MIS 1, the compiled TOC values are generally high. In MIS 6, 4 and 2, the TOC values are generally low, and their temporal fluctuation is not so large. The compiled TOC in MIS 5 is characterized by large fluctuation in orbital scale. In contrast, the compiled TOC in MIS 3 shows many peaks which correspond with the repetition of cold stadials and warm interstadials, known as D-O cycle.

This result suggests that the normalized TOC may be a useful proxy of paleoclimate for the past 200 ka, which can be correlated with other sediments or climate records by the many marker tephra beds in central Japan.

Keywords: Total organic carbon, past 200 ka, central Japan

## Morphosis of the Oyster shell bed and Diatom assemblage in Tokyo bay

NOGUCHI, Marie<sup>1\*</sup> ; ENDO, Kunihiko<sup>2</sup> ; KASHIMA, Kaoru<sup>1</sup>

<sup>1</sup>Kyushu University, <sup>2</sup>Nihon University

Recently, oyster shell beds and reefs have been found in various places in Tokyo bay. Six shell bed types can be recognized on the basis of their lithology (YOKOYAMA et.al., 2004). Topographic and paleogeographic changes closely related to the Holocene Jomon Transgression, have been investigated by reconstructing the migration of oyster shell beds, which are good markers of paleoshorelines, throughout the wide inner bay during the rising stage of sea-level. However, ecology of benthos and diatom assemblages is not clear about oyster shell bed types(Endo et.al.,2013 ). This study describes taphonomic processes of the oyster reefs well exposed in Tokyo bay, Sanbanze. The oyster reefs of Sanbanze have grown up during about 5 years. The growth of oyster reefs was rapid but nowadays it is reduced due to change of oyster environment as consequences of Torrential rain and Typhoon. We started to do research 5 years ago in Sanbanze. We are making a report on oyster shell bed types and ecology of diatom assemblage in this area.

Keywords: Tokyo bay, oyster shell bed, diatom

## A possibility of influence of deposition in dam-lake to deep marine environments around the Japanese Islands

SHIRAI, Masaaki<sup>1\*</sup> ; OMURA, Akiko<sup>2</sup> ; HAYASHIZAKI, Ryo<sup>1</sup> ; UTSUGAWA, Takako<sup>1</sup>

<sup>1</sup>Tokyo Metropolitan University, <sup>2</sup>University of Tokyo

It is well known that dams construction on river caused decrease in sediment supply and serious coastal erosion. While, taking into account similarity of grain size, deposition in dam-lake may also cause decrease in deep marine hemi-pelagic depositional rate. Mass accumulation rate (MAR) during ca. 100 years around the Japanese Islands were estimated with Pb-210 radioactivity concentration.

Core samples were obtained with multiple corer (core length <60 cm) on the R/V Tansei-maru from off the Enshu, Kumano and Niigata regions in the central Japan. Subsamples sliced with 1 or 2 cm thick were dried, crushed and measured by an ORTEC High Purity Ge gamma spectrometer housed in the Department of Geography, Tokyo Metropolitan University with a 48 hour counting. MAR was estimated from Pb-210 radioactivity concentration and dry bulk density of other subsamples measured with the Shimadzu Accupyc 130 gas pycnometer housed in Atmosphere and Ocean Research Institute, the University of Tokyo.

In the off Enshu area, MAR of two core samples obtained from small basin on the outer ridge-Nankai Trough slope (ca. 2500 m water depth) were estimated for this study. Although one core did not show change in MAR, the other core showed decrease in MAR around 1930-1940. In the off Kumano area, MAR of two core samples obtained from bottom of the Kumano Trough (ca. 2100 m water depth) were estimated. Both core showed decrease in MAR around 1940-1960. In the off Niigata area, MAR of a core sample obtained from bottom of submarine canyon on the SE slope to the Mogami Trough (ca. 400 m water depth) was estimated. The core showed decrease in MAR around 1960-1970.

Although estimated ages of decrease in MAR have considerable error, it is remarkable that decrease in MAR was estimated from all the studied areas. Contemporaneity of decrease in MAR and dams construction and similarity of the grain size between hemipelagic sediment and dam sediment suggest that deposition in dam-lake may influence sediment supply to deep marine hemipelagic environment.

Keywords: dam, hemipelagi deposits, mass accumulation rate

## Seismic history of the last 5500 years reconstructed from the topographic development of the Furen-ko barrier system

NANAYAMA, Futoshi<sup>1\*</sup> ; SHIGENO, Kiyoyuki<sup>2</sup> ; HASEGAWA, Takeshi<sup>3</sup> ; WATANABE, Kazuaki<sup>1</sup> ; ISHIWATA, Kazuto<sup>5</sup> ; IKEDA, Yasuo<sup>4</sup> ; UCHIDA, Yasuhito<sup>6</sup>

<sup>1</sup>Geological Survey of Japan, AIST, <sup>2</sup>Meiji Consultants Ltd., <sup>3</sup>Ibaraki University, <sup>4</sup>Kushiro Branch, Hokkaido University of Education, <sup>5</sup>Betsukai Museum, <sup>6</sup>Geological Survey of Hokkaido, HRO

There are some active barrier (island) systems in eastern Hokkaido. Since 2011, we have been investigating the Hashirikotan barrier spits in the northern part of Furenko barrier system facing the Sea of Okhotsk/ Nemuro Strait because five branches of spits (BR1-BR5) are clearly observed. According to GPS topographic survey, GPR exploration, hand drilling survey, grain size analysis, AMS 14C dating and tephra chronology, we already got some important geomorphological results as follows.

As a first point, the Furenko barrier system has been established since 5.5 ka, and there were two lagoon-expanding stages at 5.2 and 4.0 ka estimated by volcanic ashes, Ma-e and Ma-d from Mashu volcano. As a second point, the youngest BR5 has occurred after the 17th century and BR4 caused by the last seismic up rifting in the 17th century because it was covered with two historical volcanic ash layers, Ta-a and Ko-c2 from Tarumai and Komagatake volcanoes. BR2 caused by the seismic up rifting in the 9th century because it was covered with B-Tm from Baitoushan volcano in AD 929. BR3 and BR1 were undated clearly, but we are able to assume that BR3 rifted in the 12-13th century and BR2 rifted at 4.0 ka. These two BRs were covered with large eolian dune layers just after emerging each BR.

Since 2003, it was clearly that the great earthquakes (Mw8.5~) have been occurred at an interval of 500 years along the southern Kuril subduction zone. Especially coastal area raised almost 1 or 2m just after the great earthquakes due to the post-seismic displacements. But conversely land subsidence has been continuing at a rate 8.5mm/year since the 17th century until now. We express that geomorphological evolution of the Furenko barrier system has been controlled by the seismotectonics along the southern Kuril subduction zone.

This work was supported by JSPS KAKENHI Grant Number 23540539.

Keywords: Lake Furen-ko, barrier spit, topographic development, Nemuro Strait, sea-level change, seismic history

## Late Quaternary tephtras and basin fill sediments under Ukinuman, Murayama city in the north part of Yamagata basin, Nort

SUZUKI, Takehiko<sup>1\*</sup> ; KASAHARA, Amao<sup>1</sup> ; YAGI, Hiroshi<sup>2</sup> ; IMAIZUMI, Toshifumi<sup>3</sup> ; YOSHIDA, Akihiro<sup>4</sup>

<sup>1</sup>Tokyo Metropolitan University, <sup>2</sup>Yamagata University, <sup>3</sup>Tohoku University, <sup>4</sup>Meiji University

Yamagata basin, one of the tectonic basins aligning along the west part of Ou Backbone Range, Northeast Japan Arc, exists between hills and mountains. Active faults concentrate along the west margin of the Yamagata basin. In the north part of the basin where more active faults were recognized than the south part of the basin, not only marginal faults bordering hills and mountains but also isolated faults in central part of the basin were recognized by Yagi et al. (2001). In order to establish the history of fault activity and landform development in the basin, chronological and sedimentological studies on the basin fill sediments beneath the ground surface is necessary. In this study, an all-core boring (MR-13-1) with a depth of 101.00 m was carried out at Ukinuma (81.40 m a.s.l.), Murayama City, Yamagata Prefecture in October to November, 2013. Preliminary results are as follows.

### Stratigraphy

Fine sediments dominate less than 64.60 m in depth, composing of silt to organic silt except three sand and gravel layers with thickness of <1.65 m. Sediments between 64.60 and 101.00 m in depth consist of an alternation of silt, sands, and gravels. Depths of tephtras already identified are 3.34-3.47 m, 35.34 m, and 75.86-76.24 m.

### Tephra

A gray to white ash-fall deposit with a depth of 3.34-3.47 m contains hornblende ( $n_2=1.670-1.673$ ) and orthopyroxene ( $\gamma=1.709-1.714$ ). Refractive indices of glass shards is  $n=1.499-1.500$ . These characteristic properties show that this ash is correlative to Hijiori-Obanazawa Tephra (Hj-O, 11-12 ka; Machida & Arai 2003).

A thin white vitric tephra (4 mm in thickness) at 35.34 m in depth characterized by bubble-wall to stripe types of glass shards ( $n=1.496-1.500$ ; SiO<sub>2</sub>: 78.44 wt.%, Al<sub>2</sub>O<sub>3</sub>: 12.05 wt.%, CaO: 1.08 wt.%, FeO: 1.12 wt.%, K<sub>2</sub>O: 3.21 wt.%, Na<sub>2</sub>O: 3.40 wt.%) (containing a small amount of quartz) is correlated to Kikai-Tozurahara Tephra (K-Tz, 95 ka; Machida & Arai 2003).

An ash-fall deposit with a depth of 74.86-75.17 m was detected. This tephra contains orthopyroxene ( $\gamma=1.724-1.730$ ), quartz, and sponge to fiber types of glass shards ( $n=1.498-1.502$ ), and is possibly originated from volcano in the vicinity.

In presentation, chemical compositions of glass shards in tephtras mentioned above and ages by carbon 14 dating will be reported.

Keywords: Yamagata basin, Underground geology, Tephra, Late Quaternary, Boring core

## Late Quaternary tephra and basin fill sediments under northeast part of Yonezawa basin, Northeast Japan

KASAHARA, Amao<sup>1\*</sup> ; SUZUKI, Takehiko<sup>2</sup> ; KITAMURA, Akihisa<sup>2</sup> ; KATO, Shinji<sup>4</sup>

<sup>1</sup>Graduate student, Tokyo Metropolitan University, <sup>2</sup>Tokyo Metropolitan University, <sup>3</sup>Shizuoka University, <sup>4</sup>NEXCO East

We report tephra distributed under the northeastern part of the Yonezawa Basin, in the southern part of the Northeast Japan Arc. The Yonezawa Basin is the one of the inland tectonic basins along the backarc side of the Ou Backbone Mountains. There is a wetland which delimited by the small fans in the southern and western margins and by the mountains in the northern and eastern margins around the Lake Hakuryu in the northeastern part of the Yonezawa Basin, which called Oyachi (Yoshida, 1955). We observed two cores, B7-1-2 and B7-1-14, both drilled at Fukanuma, Takahata Town at the southern margin of the wetland. Both core obtained at distance of about 200 m, and about 90 m long.

Both B7-1-2 and B7-1-14 cores have well developed peat deposit. Silt and peat deposit contains about 1-20 cm thick thin sand layers repeatedly. Well sorted granule thin layers and pebble thin layers which contains max 4 cm in diameter are observed at the middle and lower part of the sediments, but poorly lateral continuities. In addition, both cores are not drilled through the Quaternary deposit under the Yonezawa Basin.

In the B7-1-2 core, Numazawa-Kanayama tephra (Nm-KN; 62-65 ka: Suzuki and Soda, 1994) is in 31.59-31.655 m depth, Aso-4 tephra (Aso-4; ca. 87 ka: Aoki et al. 2008) is in 44.16-44.23 m depth as a blocky form, and two-pyroxene crystalline ash (B7-1-2L) is in 79.14-79.16 m depth, are observed.

In the B7-1-14 core, Nm-KN is in 27.33-27.34 m depth, two-pyroxene crystalline ash (B7-1-14E) is in 75.47-75.485 m depth, and glassy ash contains babble-wall type of glass shards (B7-1-14G) is in 83.97-84.07 m depth, are observed. Furthermore, a beige ash patch observed in 39.385-39.39 m depth would correlate to Ontake-Nagawa tephra (On-NG; 85.1 ka: Nagahashi et al., 2007).

We could not observed a AT bed in the both cores, however, we detected babble-wall type of glass shards from correlate to AT in the gray silt bed in 21.62-21.63 m depth between a peaty silt bed in the B7-1-2B core (not sequential sampled). In addition, B7-1-2L and B7-1-14E are correlate to each other because of its height above sea level and petrographic features.

It is concluded that height above sea level of Nm-KN and B7-1-2L/B7-1-14E indicate sediments in the both cores deposited almost horizontal form. Deposition rate simply calculated and estimated from age and depth of Aso-4 in the B7-1-2 core is about 0.5 m/kyr, which shows slightly larger value than 0.22-0.35 m/kyr (Suzuki et al., 2013) based on tephrochronology obtained in the Aizu Basin to the south of the Yonezawa Basin recently. This deposition rate is generally reconciling rate if it is assumed that deposition rate of the Yonezawa Basin floor depends on the activity of the Yonezawa Basin Western Margin Fault which slip rate is 0.4-0.5 m/kyr.

Keywords: Yonezawa basin, Underground geology, tephra, Late Quaternary, Boring core

## The age of the Inubou Group in the Choshi district, Chiba Prefecture, Japan, based on tephra correlation

TAMURA, Itoko<sup>1\*</sup> ; YAMAZAKI, Haruo<sup>1</sup> ; MIZUNO, Kiyohide<sup>2</sup>

<sup>1</sup>Dep. Geography, Tokyo Metropolitan Univ., <sup>2</sup>AIST, GSJ

Numerous widespread tephra layers of late Pleistocene and Holocene age have been known since the early 1970s and greatly contribute to paleoenvironmental reconstruction in the Japan islands and adjacent seas. This study has identified a new widespread tephra using the trace element composition of volcanic glass determined by ICP-AES analysis and the stratigraphy.

In1 tephra is found at lowest part of the Naarai Formation in the Inubou Group, Choshi district, Chiba Prefecture, accumulated during Pliocene to Early Pleistocene. Ikg1 tephra is found in upper Ikego Formation in the Miura Group, Kanagawa Prefecture, accumulated during Pliocene. B25 tephra is found at Horinouchi Formation in the Kakegawa Group, Shizuoka Prefecture, accumulated during Pliocene to Early Pleistocene.

In1, Ikg1 and B25 tephtras are white and fine grain. The thickness of these deposits range from cm(Ikg1) to 22cm(B25). These tephtras mainly consist of glass shards of bubble-wall type. The glass shards of these are poor in K<sub>2</sub>O (<2 %) and La (<15 ppm) and rich in Y(>40 ppm), which give low La/Y (about 0.3) and high Ba/La (about 30). These characteristic chemical compositions of glass in tephtras erupted from the Tohoku area (Mizuno, 2001).

The age of In1 tephra is estimated at about older than 3 Ma based tephrochronology in Choshi area (Tamura et al.,2007). The age of Ikg1 is estimated at about older 3.1Ma based biostratigraphy and magnetostratigraphy (Utsunomiya et al, 2012 and Utsunomiya, 2013). The B25 tephra is estimated at about older 2.9Ma based on tephrochronology (Tomita and Kurokawa, 1999 and Kurokawa and Tomita, 2000).

This tephra correlation indicates that the age at lowest part of the Inubou Group is estimated older than 3.1 Ma.

Keywords: Plio-Pleistocene, Tephra correlation, Inubou Group, Depositional age, Marker Tephra

## Underground electrical resistivity and soil water content on the surface around former river channel of Tone River

NAKANO, Takayuki<sup>1\*</sup> ; KOARAI, Mamoru<sup>1</sup>

<sup>1</sup>GSI of Japan

Land liquefaction occurred in a land reclaimed water area such as former river channel induced by the 2011 off the Pacific coast of Tohoku Earthquake. The land liquefaction was a biased distribution even in former river channel. We assumed that groundwater level and/or shape of former river bed (depth of former river) have a significant influence though the factor of this phenomenon is various. Therefore, we conducted electrical prospecting (2-D electrical resistivity prospecting) on former river channel of Tone River around Kozaki Town, Chiba Prefecture, to estimate a distribution of groundwater level and/or shape of former river bed from underground distribution of electrical resistivity. In addition, we considered a relationship between underground distribution of electrical resistivity and soil water content on the surface by measuring soil water content on the surface along the electrical prospecting line. In this survey area, there are data of layer profiles (trench survey profiles) and boring core stratigraphes by the National Institute of Advanced Industrial Science and Technology (AIST) and the Chiba Prefectural Environmental Research Center (CERC) (Mizuno et al., 2013; Miyaji et al., 2013).

Electrical prospecting was performed by the pole-pole array in 280m length, electrode intervals of 1m and until 15m deep. Measurement of soil water content was performed by volumetric soil water content sensor (by the method of responding to changes in the apparent dielectric constant) and weight water content sensor (by alternating current two electrode method). These measurements of soil water content were performed intervals of 10m on the electrical prospecting line, and three times in each measurement points and each sensors. We used these average values.

Electrical resistivity profile indicated clearly difference between reclaimed soil in the former river channel with relative high electrical resistivity (more than 20-30 ohm-m) zone and a ground out of former river channel with relative low electrical resistivity (less than 20-30 ohm-m) zone. The position where the boundary of these zones reaches near the surface was correspondent with a boundary of land liquefaction (sand volcano) area by the 2011 off the Pacific coast of Tohoku Earthquake. It is possible that the underground distribution of electrical resistivity is affected by a soil property more than soil water content. Distribution of groundwater level was unclear though it was estimated to be 1.5m in depth from that usual electrical resistivity of saturated sand is 80-100 ohm-m (The Japanese Geotechnical Society, 2003). As a groundwater level near this survey area by the boring survey (Mizuno et al., 2013) was 0.7m in depth, it is possible that electrical resistivity near the groundwater level is higher than 80-100 ohm-m.

As a result of compared the soil water content on the surface with the electrical resistivity beneath the surface, there was a correlation that weight water content is low in a high electrical resistivity. However, there was not a correlation between volumetric soil water content and electrical resistivity. Also, it was not able to confirm the relationship between soil water content and groundwater level because of the groundwater level was not able to estimate from the distribution of electrical resistivity.

This result indicated a detection of the shape of former river bed and a correlation between the soil water content on the surface and the electrical resistivity beneath the surface. We would like to find out an index with land liquefaction in former river channel due to perform a ground penetrating radar survey in the same field.

Keywords: former river channel of Tone River, Kozaki Town, electrical prospecting, distribution of electrical resistivity, soil water content

## Geological survey for liquefaction-fluidization phenomena: damage and survey by PD-CPT

KAMEYAMA, Shun<sup>1\*</sup>; KAZAOKA, Osamu<sup>1</sup>; SHIGENO, Kiyoyuki<sup>2</sup>; SUZUKI, Yoshiyuki<sup>2</sup>; FUKUMA, Tetsu<sup>3</sup>; MORISAKI, Masaaki<sup>1</sup>; YOSHIDA, Takeshi<sup>1</sup>; KAGAWA, Atsushi<sup>1</sup>; SAKAI, Yutaka<sup>1</sup>; KIMURA, Michio<sup>1</sup>; OGURA, Takayuki<sup>1</sup>

<sup>1</sup>Research Institute of Environmental Geology, Chiba, <sup>2</sup>Meiji Consultant Co., Ltd, <sup>3</sup>ACE Sisui Kogyo Co.,Ltd

2011 off the Pacific coast of Tohoku Earthquake and the aftershock brought heavy damage in the various places in East Japan. At a public high school in Mihama ward, Chiba city, remarkable liquefaction - fluidization phenomena occurred in a part of the bicycle place. Sand spouted out the surface of the ground and the ground level sank partially 30 - 40cm height.

In the part that the level of the ground surface changed, we investigated portable dynamic cone penetration test every 1.5 - 2m densely horizontally.

As a result of investigation by portable dynamic cone penetration test, the situation of the subsidence of the ground surface and relations with geological structure became clear.

We can grasp the hardness of the layer in exact depth by portable dynamic cone penetration test, but it is only hardness. We cannot confirm a particle size and the sedimentation structure of the stratum by portable dynamic cone penetration test.

It becomes the high investigation into precision more by comparing geological survey with portable dynamic cone penetration test. Because stratum sample may expand and contract when we pull up stratum in geological survey, this is because it can correct depth by comparing it with the result of portable dynamic cone penetration test.

Keywords: Liquefaction-Fluidization, The 2011 off the Pacific coast of Tohoku Earthquake, Chiba city, Man-made Strata, Geological survey, Portable Dynamic Cone Penetration Test

## Geological survey for liquefaction-fluidization phenomena: New method of geological survey by new ACE liner

SHIGENO, Kiyoyuki<sup>1\*</sup>; SUZUKI, Yoshiyuki<sup>1</sup>; FUKUMA, Tetsu<sup>2</sup>; KAZAOKA, Osamu<sup>3</sup>; KAMEYAMA, Shun<sup>3</sup>; MORISAKI, Masaaki<sup>3</sup>; YOSHIDA, Takeshi<sup>3</sup>; KAGAWA, Atsushi<sup>3</sup>; SAKAI, Yutaka<sup>3</sup>; KIMURA, Michio<sup>3</sup>; OGURA, Takayuki<sup>3</sup>

<sup>1</sup>Meiji Consultant Co., Ltd, <sup>2</sup>ACE Sisui Kogyo Co.,Ltd, <sup>3</sup>Research Institute of Environmental Geology, Chiba

Thinking about origin by collecting the stratum in the alluvial lowland that is the main living surface of us is very important. Liquidizing-fluidizing phenomenon occurs mainly in man-made strata distribution area in Chiba Prefecture, surface subsidence local area of more than 50cm occurs in the Tohoku-Pacific Ocean Earthquake in 2011. As one of the causes liquidizing-fluidizing, greater potential impact of geological structure of the deep alluvium and man-made strata of shallow has become high (Kazaoka et al., 2012). This improved ACE liner ((Japanese patent application No.3669495) in order to clarify the mechanism and certification of liquidizing-fluidizing point in the layer, and man-made strata deeper and man-made strata that has been soil filled with the dredged sand in shallow underground in this study because it was able to taken the state of the oriented and non-disturbing, observe various structures of the layer, and reports a research method.

Survey results, as well Geoslicer (Nakata et al., 1997) and, without having to be re-liquefaction during drilling the sand hard cohesive soil soft to subsurface 8m, new ACE liner became recoverable in undisturbed sample. Survey results, as well Geoslicer (Nakata et al., 1997) and, without having to be re-liquefaction during drilling the sand hard cohesive soil soft to subsurface 8m, new ACE liner became recoverable in undisturbed sample. On the other hand, there is the core shrinks during drilling and fall of the sand layer at the bottom device to prevent falling of the sample does not operate, loose sand layer is dehydrated deformation during press-fitting part. I believe you require improved by updating technology and experience accumulated in the future.

Keywords: Liquefaction-Fluidization, The 2011 off the Pacific coast of Tohoku, Chiba city, Man-made Strata, Geological survey, ACE liner

## Geological survey for liquefaction-fluidization phenomena: Geological cross section of man-made strata and mechanism

KAZAOKA, Osamu<sup>1\*</sup> ; KAMEYAMA, Shun<sup>1</sup> ; MORISAKI, Masaaki<sup>1</sup> ; SHIGENO, Kiyoyuki<sup>2</sup> ; SUZUKI, Yoshiyuki<sup>2</sup> ; KAGAWA, Atsushi<sup>1</sup> ; YOSHIDA, Takeshi<sup>1</sup> ; KIMURA, Mitsuo<sup>1</sup> ; SAKAI, Yutaka<sup>1</sup> ; OGURA, Takayuki<sup>1</sup>

<sup>1</sup>Research Institute of Environmental Geology, Chiba, <sup>2</sup>Meiji Consultante Co., Ltd

Terrible liquefaction-fluidization phenomena happened partially with subsidence, 10-50 m width and 20-100 m length, less than 1m height in northern Tokyo bay reclaimed land on the 3011 off the Pacific coast of Tohoku Earthquake. Large amount of sand and groundwater spouted out in the terrible subsided parts. But there are little subsidence and jetted sand outside of the terrible subsided part (RIEGC, 2011).

Continuous box core samples from surface to 5-7 m depth could be taken at the each 3-5 m length from little subsided part to terrible subsided part in Chiba city. Detailed litho-stratigraphy and liquefaction-fluidization parts were studied on the continuous box core samples and large relief peel on the core samples. These data indicate as follows.

1. The thickness of man-made strata is 5-7 m. The thickness increases to subsided part.

2. Man-made strata is composed of Dumped Association, Upper Filling Association and Lower Filling Association. Two Filling Associations were made by sand pump method from bottom sediments in the Tokyo bay. Upper Filling Association consists of lowermost, lower, upper and uppermost bandle.

3. Litho-facies of each man-made strata is as follows.

Dumped Association: This association is composed of 1.5-2.2 m thick sandy silt to silty fine sand layers with siltstone brocks and rock gravels. Sand dike with yellowish brown sand and gray sand distribute rarely

Uppermost Bandle of Upper Filling Association: this bandle is composed of 0.2-0.8 m thick yellowish brown laminated fine-medium sand layers. Upper part of this bandle lost primary sedimentary structures and loose. The base of this bandle consists of laminated coarse-very coarse sandy shell fragment layers.

Upper Bandle of Upper Filling Association: This bandle is composed of 0.4-1.8 m thick gray medium sand layers. Shell fragment layers often interbedded in this sand layers. The sand layers lost primary sedimentary structures and very loose.

Lower Bandle of Upper Filling Association: This bandle is composed of 0-1.8 m thick gray silt layers. Lower part of the silt layer sometimes show slump structures.

Lowermost Bandle of Upper Filling Association: This bandle is composed of 0.7-1.8 m thick gray shelly medium sand layers. Shell fragment layers often interbedded in the shelly sand later. Top of this bandle consists of loose medium sand without primary sedimentary structures. The medium sand injected in the upper silt layers.

Lower Filling Association: This association is composed of 0.5-3.5 m thick yellowish gray laminated relatively dence matrix free good sorted fine-medium sand layers. This association may deposited removed filling sand by wave action on shoreface.

4. Liquefaction-fluidization parts are in man-made strata, top of the lowermost bandle, upper bandle and uppermost bandle of the Upper Filling Association.

5. Subsidence part distribute in thin part of lower bandle and thick part of upper bandle of the Upper Filling Association. The aboves show that subsidence concern with the liquefaction-fluidization part of the upper bandle of Upper Filling Association.

Keywords: Liquefaction-Fluidization, The 2011 off the Pacific coast of Tohoku Earthquake, Tokyo bay reclaimed land, Man-made Strata, Geological survey by continuous box core, Mechanism

## Revised stratigraphy of the upper Quaternary in Yufutsu Plain and Shikotsu Pyroclastic flow upland, central Hokkaido

KOMATSUBARA, Junko<sup>1\*</sup>; KOMATSUBARA, Taku<sup>1</sup>; TANABE, Susumu<sup>1</sup>; HONGO, Misao<sup>2</sup>; UEKI, Takeyuki<sup>3</sup>; NAKASHIMA, Rei<sup>1</sup>; ISHIHARA, Takeshi<sup>1</sup>

<sup>1</sup>AIST, <sup>2</sup>Alps Technical Research laboratory Co. Ltd., <sup>3</sup>Chiba Institute of Science

Upper Quaternary stratigraphy in Yufutsu Plain and Shikotsu Pyroclastic Flow Upland, southern Hokkaido is revised based on review of previous studies and three boring core analysis, which includes sedimentary facies, pollen, diatom, shell assemblages and paleomagnetic analysis.

Active folds have been assumed beneath Yufutsu Plain and Shikotsu Pyroclastic Flow Upland because they are located southwest of the active faults along the eastern margin of the Ishikari Lowland, but neither displacement nor continuity of the folds has been specified. The detailed stratigraphy of the Shikotsu Pyroclastic Flow Upland is unknown due to lack of boring surveys for stratigraphic research. To establish subsurface stratigraphy in Yufutsu Plain and Shikotsu Pyroclastic Flow Upland to specify the fold activity, we take three boring cores (BT1, YF1 and CT1). BT1 and YF1 are 4.25 km apart along the coastline, the former is on the Yufutsu anticline axis and the latter is on the west side of the axis. CT1 is in the center of the upland.

In BT1 core we found two characteristic units: First unit is estimated as MIS11 for its abundant *Fagus* pollen, and second unit is estimated as MIS7 for its marine strata which yields cool temperature pollen assemblages. CT1 core is composed MIS7 marine deposits, MIS6 conglomerate, and MIS5 marine deposits. Two unidentified tephra layers found in MIS7 marine deposits in CT1 core may be traceable up to the north of the Shikotsu Pyroclastic Flow Upland.

Keywords: Ishikari lowland, Yufutsu plain, boring survey, Quaternary stratigraphy, Pleistocene

## Geological overview of the Mobara District: Quadrangle Series, 1:50000, GSJ/AIST

NANAYAMA, Futoshi<sup>1\*</sup>; NAKAZATO, Hiroomi<sup>2</sup>; OOI, Shinzou<sup>3</sup>; NAKASHIMA, Rei<sup>1</sup>

<sup>1</sup>Geological Survey of Japan, AIST, <sup>2</sup>NARO, <sup>3</sup>GSI

Between 2010 and 2014, geological and geomorphological research for the Quadrangle Series, 1:50000 of the Mobara district was performed by Geological Survey of Japan, AIST. In this poster presentation, we presents the proto version of geological map due to have opinions from everyone.

The Mobara district is located in the northeastern part of Boso Peninsula of the Kanto region. The district partly includes the Pacific Ocean in the eastern district. The land area is geomorphological divided into hills, diluvia uplands, river terraces, alluvial lowlands and Kujyukuri strand plane. The hills and uplands occupy the southwestern to western and northwestern part of the district, respectively. The hills constitute parts of the Kazusa Hills and the uplands are parts of the Shimosa Uplands. River terraces and alluvial lowlands are distributed along Ichinomiya River, Isumi River and Murata River. The Murata River runs through the northwestern district flows into the Tokyo Bay. On the other hand, the Ichinomiya River runs through the central district eastward into the Pacific Ocean. Also the Isumi River runs through the southern district eastward into the Pacific Ocean.

In the Mobara district, there are mainly two stratigraphic units, the lower to middle Pleistocene Kazusa Group and the middle to upper Pleistocene Shimosa Group, trending northeast to southwest and gently dipping northwest. Furthermore Upper Pleistocene terrace deposits with Kanto Loam, Holocene terrace deposits and alluvial deposits arc mostly distributed along the Ichinomi, Isumi and Murata Rivers.

The Kazusa Group is divided into seven formations, Otadai, Umegase, Kokumoto, Kakinokidai, Chonan, Kasamori and Kongochi Formations. These were conformably deposited upward the continuous change of the sedimentary environments from the lower bathyal through upper bathyal to inner shelf.

Keywords: Chiba Prefecture, Mobara District, Quadrangle Series, 1:50000, GSJ/AIST, Geology, Geomorphology, overview

## Subsurface geology of the Shimizu Lowland and the Miho Peninsula along the northern Suruga Bay, central Japan

ISHIHARA, Takeshi<sup>1\*</sup> ; MIZUNO, Kiyohide<sup>1</sup>

<sup>1</sup>Geological Survey of Japan, AIST

We conducted the drilling survey, core analysis, and boring data analysis to clarify the subsurface geologic structure of the Shimizu Lowland and the Miho Peninsula, the Shizuoka Prefecture, central Japan. GS-MMB-1 was drilled in the northern Miho Peninsula. GS-MMB-1 is composed of the gravelly layer, sandy and muddy layer with burrows and shell fragments, and gravelly layer in ascending order.

In the Shimizu Lowland, a buried incised valley is along the right bank of the Tomoe River. The basal altitude of the incised valley appears to be decrease upstream, suggesting that coastal area of the Shimizu Lowland has been relatively uplifting.

Keywords: Shimizu Lowland, Miho Peninsula, Subsurface geology, Boring survey

## Reconstruction of tectonic movements using ravinement surfaces: A case study for the subsurface geology of the Osaka

SAKURAI, Minao<sup>1\*</sup> ; MASUDA, Fujio<sup>2</sup>

<sup>1</sup>Graduate School of Science and Engineering, Doshisha University, <sup>2</sup>Faculty of the Science and Engineering, Doshisha University

Ravinement surfaces are produced when the sea floor is eroded into a flat surface by the action of waves or tides during a marine transgression. They are preserved in the transgressive deposits as a sharp erosion surface. In a geological cross section across the ancient shoreline, primary ravinement surfaces appear as a subhorizontal line slightly dipping toward the sea. In a cross section, comparing successive ravinement surfaces deformed by tectonic movement allows for the reconstruction of relative tectonic movement. For example, when successive ravinement surfaces are parallel, the entire region has subsided or uplifted uniformly. However, when the lower ravinement surface dips more steeply than the upper ravinement surface, this indicates differential subsidence. With sufficient data, ravinement surfaces can be used to reconstruct the deformation history of an area in three dimensions. Furthermore, because many ravinement surfaces in Quaternary sediments are associated with transgressions related to glacio-eustatic sea level changes, the age of the surfaces can be determined and used to estimate the rate of tectonism. We used the reconstruction of tectonic movement derived from ravinement surfaces to reconstruct the shallow subsurface geologic structures of the Osaka Plain, an intra-arc basin in the Japan island arc. For this study, we constructed cross sections from drill hole data extracted from a civil engineering drilling database. Our study revealed that, in different areas of the Osaka Plain, the land had been uplifted and differentially subsided toward the sea; a relatively large uplift occurred near a flexure zone, and the rate of the tilting of an anticline was constant.

Keywords: ravinement surface, tectonic movement, intra-arc basin, Quaternary, drilling database

## Effects of the offshore barrier against the 2011 Tohoku Earthquake Tsunami and related Recovery Process

MORI, Nobuhito<sup>1\*</sup> ; WILLIAM, Pringle<sup>1</sup> ; YONEYAMA, Nozomu<sup>1</sup>

<sup>1</sup>Disaster Prevention Research Institute, Kyoto University

In this study, the effectiveness of an offshore breakwater for the 2011 off the Pacific Coast of Tohoku Earthquake Tsunami was examined by two-dimensional (2D), quasi three-dimensional (quasi-3D) and three-dimensional (3D) numerical models. First, both 3D numerical models were applied to the behavior of tsunami inundation for Kamaishi Bay in Iwate Prefecture where an offshore deep-water breakwater was installed against an assumed tsunami before 2011. The numerical results indicate 20% error of maximum inundation height compared with the post-event tsunami survey on the land. It is found that the offshore breakwater significantly reduced the tsunami height on the land. The reduction of tsunami height on the land gave about 30% tax revenue in comparison with similar locations with or without breakwater. Based on the results the construction and or rebuilding of damaged offshore breakwaters can be considered as a viable option against tsunami particularly in vulnerable areas

Keywords: tsunami, offshore barrier, disaster reduction, recovery

## The Agri-Reconstruction Project and Rapeseed Project for Restoring Tsunami-Salt-Damaged Farmland after the GEJE

NAKAI, Yutaka<sup>1\*</sup> ; NISHIO, Takeshi<sup>1</sup> ; KITASHIBA, Hiroyasu<sup>1</sup> ; NANJO, Masami<sup>1</sup> ; SAITO, Masanori<sup>1</sup> ; ITO, Toyoaki<sup>1</sup> ; OMURA, Michiaki<sup>1</sup> ; ABE, Miyuki<sup>1</sup> ; OGUSHI, Yukie<sup>1</sup>

<sup>1</sup>Tohoku Univ, Grad School Agricultural Sci.

The Graduate School of Agricultural Science, Tohoku University, launched an Agri-Reconstruction Project in 2011 immediately after the March 11 Great East Japan Earthquake disaster, and this continues to date. The project's objective is to support the agricultural, forestry and fisheries reconstruction process in the tsunami disaster area. The activities have been implemented through more than 40 research projects along the Tohoku region including the Rapeseed Project for Restoring Tsunami-Salt-Damaged Farmland.

Immediately after the disaster, damaged farmlands were surveyed and salt-tolerant rapeseed varieties from Brassicaceae and related species were used to restore the soil. The plants came from the gene bank developed at the Graduate School of Agricultural Science, and were planted on damaged farmland in Sendai, Iwanuma and Higashi Matsushima cities. The varieties used to restore the soil depended on the specific damage.

As part of the project, the production and sale of edible as well as fuel oil obtained from rapeseed plants was organized in coordination with the Miyagi Prefecture Sendai City government, a number of private companies and other partners. This enterprise continues to date.

Besides using the salt-tolerant varieties of Brassicaceae plants in tsunami-damaged fields they are also used overseas in the rehabilitation of salt-damaged farmlands.

Keywords: earthquake, tsunami, reconstruction, rapeseed, salt damage

## Evacuation response of fishermen during the 2011 Great East Japan Tsunami and present recovery status

SUPPASRI, Anawat<sup>1\*</sup> ; YASUDA, Mari<sup>1</sup> ; ABE, Yoshi<sup>1</sup> ; FUKUTANI, Yo<sup>1</sup> ; IMAMURA, Fumihiko<sup>1</sup>

<sup>1</sup>International Research Institute of Disaster Science (IRIDeS), Tohoku University

The 2011 Great East Japan tsunami severely damaged or destroyed most of the fishing ports and facilities along the Sanriku coast. Fishing boats can be considered as the most important thing for fishermen as their activities are mostly depending on their boats. By getting out offshore to protect their boats from tsunamis is a custom in Japan but this is considered as a risky action. Interviews with fishermen were conducted to investigate their evacuation response, experience and opinion of the recovery status after the 2011 tsunami. We found that most of fishermen who did not decide to get out offshore but evacuated to high ground was although felt deploring in losing their boats but in all cases, they believed that their own lives are the most important. Knowing about tsunami characteristic of fishing port is also important. Tsunami generally arrives the Sanriku areas as fast as 30 min because of the deep sea and short distance from the earthquake epicenter. By this reason, boats can reach to the safety zone of 50 m sea depth very soon as well. However, boats in Sendai Plain will need about one hour to the deep sea. For the recovery, all of the villages are still facing problems resulting from land subsidence when the ports are partly submerged during high tide. In addition, land ownership is another issue that delays any recovery process as local governments need their permissions before doing any kind of construction. Although there are some small differences in detail, they have decided to move the entire community to high ground. Local residents feel that constructing high seawalls are unnecessary because there will be no more houses on the low part of the land and the local governments are trying to solve these problems neutrally.

Keywords: 2011 Great East Japan tsunami, Tsunami evacuation, Fishing port

## A method to determine the area of tsunami inundation level 1 and level 2 for pre- and post-disaster situation

MUHARI, Abdul<sup>1\*</sup> ; IMAI, Kentaro<sup>1</sup> ; SUGAWARA, Daisuke<sup>1</sup> ; IMAMURA, Fumihiko<sup>1</sup>

<sup>1</sup>IRIDeS, Tohoku University

After the 2011 tsunami, a new approach in the land use planning is introduced and starting to be applied in some areas in Japan. An area that is likely to be affected by the high frequency, but low impact tsunamis -calling as Level 1. It will be used in a separated function in an area that is likely to be affected by low frequency but high impact tsunamis -calling as Level 2. The countermeasures adopted in both areas are different as well. The physical structures will be improved to minimize the effects of the medium-to-low tsunamis to human as well as prosperies in the area of tsunami Level 1. In the area of tsunami Level 2, the coverage of flooded area is much wider. Thus, evacuation facilities and education are the major efforts to save lives. This study aims to address the process on how we can distinguish the boundary between area Level 1 and Level 2. We firstly exercise the use of numerical simulations to establish the framework in assigning area Level 1 and Level 2 at a post-disaster area. Next, we examine the possibility to apply similar techniques in a pre-disaster area. We demonstrate that distinguishing areas of tsunami inundation Level 1 and Level 2 is not only important for the reconstruction in the post-disaster areas, but also necessary to mitigate the future tsunamis in pre-disaster areas.

Keywords: Tsunami inundation area Level1, Tsunami inundation area Level2, numerical simulation, GIS modeling

## Advanced researches of Earthquakes and Tsunamis -Towards disaster mitigation on Earthquakes and Tsunamis-

KANEDA, Yoshiyuki<sup>1\*</sup> ; KAWAGUCHI, Katsuyoshi<sup>1</sup> ; ARAKI, Eiichiro<sup>1</sup> ; MATSUMOTO, Hiroyuki<sup>1</sup> ; NAKAMURA, Takeshi<sup>1</sup> ; KAMIYA, Shinichiro<sup>1</sup> ; ARIYOSHI, Keisuke<sup>1</sup> ; HORI, Takane<sup>1</sup> ; HYODO, Mamoru<sup>1</sup> ; TAKAHASHI, Narumi<sup>1</sup> ; BABA, Toshitaka<sup>1</sup> ; NAKANO, Masaru<sup>1</sup> ; CHOI, Jin-kyu<sup>1</sup> ; NISHIDA, Shuhei<sup>1</sup>

<sup>1</sup>Japan Agency for Marine-Earth Science and Technology

Based on lessons learned from the 2011 East Japan Earthquake/Tsunami, we recognized the importance of real time monitoring of these natural hazards. As a real time monitoring system, DONET1 was already deployed and DONET2 is being developed constructing the dense ocean floor networks around the Nankai trough Southwestern Japan. DONET observatories detected offshore tsunamis 15 minutes earlier than onshore stations at the 2011 East Japan Earthquake, and provided the significant information of the tsunami amplification process between off shore and on shore. Using these systems, we can detect not only early earthquakes and tsunamis but also low frequency tremors, slow earthquakes and micro earthquakes in the inter-seismic or pre-seismic stage, which provide useful information for the estimation of seismic stage. As the conclusion, the integration of the real time monitoring data and advanced simulations such as the recurrence cycle of mega thrust earthquakes, tsunami inundation, seismic response on buildings/cities and evacuation, is the very important methodology towards future disaster mitigation programs and related measures. We will explain disaster mitigation researches on earthquakes and tsunamis around the Nankai trough.

## Sociocultural and Economic Aspects in Restoration after Tsunami Hit: Minamisanriku, Miyagi, Japan

KIMURA, Naoko<sup>1\*</sup>

<sup>1</sup>GSGES, Kyoto University

This research discusses sociocultural and economic aspects through description of initiatives taken by local people and organizations in Utatsu area, Minamisanriku, Miyagi Prefecture, for reconstruction after the Great East Japan Earthquake and huge tsunami hit in March 2011. Utatsu is located on the coast of Isatomae-Bay, the Pacific Ocean. The key industry of town is fishery, however, the number of people involved in fishery has decreased since 1990, and the town also has issue related to aging of population year by year. Like any afflicted people by huge tsunami induced by the earthquake, Utatsu residents had to move to another area located higher hillside and start to rebuild their life. This research focuses on two initiatives: a painting-art project and *miso* factory (*miso* is fermented soybean paste, a traditional preservative food in Japan) managed by local housewives. Interviews were conducted to some key stakeholders of those initiatives, and its results were qualitatively analyzed. The interview revealed some positive changes in mind among participants, especially young generation, as well as problems and obstacles long-deep rooted in the local socio-economic structure of the area, for example, mental conflicts between communities, concerns to influence of radionuclides from Nuclear Power Plant accident in Fukushima. The research concludes with a view regarding a possible way forward to their sound rebuilding and reconstruction.

Keywords: tsunami, reconstruction, community, sociocultural and economic aspects, Minamisanriku

## Living with Natural Hazards; Tsunami

SANTIAGO-FANDINO, Vicente<sup>1\*</sup>

<sup>1</sup>Independent Environmental Advisor

Tsunamis are a common natural hazard originated by earthquakes, landslides, volcanic eruptions and even meteorological conditions. These events have hit coastal areas particularly along the Pacific Ocean (Rim of Fire), Eastern Mediterranean Sea and the northern part of the Indian Ocean resulting in large impacts to the environment and coastal settlements.

Adaptation by organisms and ecosystems after being hit by tsunamis follow nature's processes for adaptation to the new realities, which also applies in the case of mankind but in this case intelligence, reasoning and complex social structures makes the process more complex reflecting in turn in how the restoration and reconstruction process may develop and its success.

Efforts made to reconstruct and restore impacted areas have proven to be very complicated and controversial oftentimes, this mainly due to differences of opinion on the approaches to be taken and decision-making processes added to the societal aspects. Moreover, lack of direct and effective participation of impacted communities, sectorial and top down decision-making further exacerbates the debate resulting in reducing trust by the locals, diminished resilience and increases emigration amongst other aspects.

Tsunamis are complex natural events requiring the integration of sound research and knowledge, the same is required to understand local communities where traditions, customs and societal components are crucial before decision making. Living in Tsunami exposed areas call for building trust with authorities as well as developing early warning and disaster prevention policies, appropriate defence systems and mechanisms, provision of education and awareness raising as well as the understanding of the affected communities needs, capabilities as well as their customs and traditions together with their living environment. Proactive and integrative policies rather than sectorial and reactive top down ones bring all these elements together whereby strengthening local communities, increasing resilience and allowing the reconstruction and restoration process to be effective and successful.

## Local community and Tsunami-lesson from 2011 eastern Japan mega earthquake

HARUYAMA, Shigeko<sup>1\*</sup>

<sup>1</sup>Mie University

The coastal plain facing Pacific Ocean in north-eastern Japan was suffered by Tsunami and mega-earthquake at 2011 Easter Japan Mega-Earthquake. Still now, the regional planners are preparing for appropriate resuscitation or reconstruction for mitigation in the disaster-stricken areas. In this study, the authors tried to clarify local community activity for disaster prevention at the moment of Mega-earthquake occurrence and Tsunami intrusion. The lower Abukuma river basin and coastal and fluvial landforms comparing with former Tsunami intrusion referred to historical records on this site and local communities based on different landform units of the lower Abukuma river basin were selected for analysis to avoid disaster risk level using questionnaire survey. The local community activities were designed by strong leadership of community, former experience of disaster, preparedness of evacuation drill, work sheering experience of community building up social capital in each region. The land use pattern and recent land use change processes in this study area are analyzed and the rapid land use change dealing with urbanization is another trigger of disaster risk level enlargement under the disaster. The future disaster prevention work and disaster mitigation planning should be argued with local community social capital.

Keywords: Tsunami, Local community, landform

## Fluvial Environmental Changes of the Ayeyarwady Delta: Case Study for Nyaungdon Borecore Area

KAY THWE, Hlaing<sup>1\*</sup> ; SHIGEKO, Haruyama<sup>2</sup> ; AYE, Maung maung<sup>3</sup>

<sup>1</sup>Researcher, Graduate School of Bioresources, Mie University, <sup>2</sup>Professor, Graduate School of Bioresources, Mie University, <sup>3</sup>Professor, Department of Geography, University of Yangon

The Ayeyarwady River is one of the largest rivers in Myanmar and drains an area of 85,534 km<sup>2</sup>. The study area is mainly located in the central part of deltaic of the Ayeyarwady River belonging to Nyaungdon Township, Ayeyarwady Region. The main purpose of this study is to clarify geomorphologic land classification mapping and fluvial features of the Ayeyarwady River Delta derived from aerial photos, Landsat +ETM7 Global Digital Elevation Model Version 2 with GIS and RS linkage and to check long term natural environmental restoration of the lower Ayeyarwady River at Nyaungdon drilling point in Ayeyarwady Region. The volume of sediment deposited rate and discharge rate should be accumulated rapidly before Holocene period because we could clarify with the results of <sup>14</sup>C dating of the organic materials including each layer and all core drilling samples, concept of paleo-geography and geomorphologic evolution, landform development of the study area.

Keywords: Ayeyarwady River Delta, Geomorphologic land classification map, sedimentary facies, drilling bore core, discharge, radiocarbon age

## The Impact of Joint Forest Management on Household Income and Forest Condition: The Case of Madhya Pradesh, India

SAKURAI, Takeshi<sup>1\*</sup> ; ISAKA, Masashi<sup>2</sup>

<sup>1</sup>Institute of Economic Research, Hitotsubashi University, <sup>2</sup>Graduate School of Economics, Hitotsubashi University

Joint Forest Management (JFM) is a benefit-sharing scheme between rural households and the state government. Rural households are the user of forest resources for their livelihood, such as grazing, fuel woods, wild foods, etc., while the state government is the owner of the forest land and trees in the forest and makes revenue from the sales of forest resource such as timber, medicinal plants, etc. In the past, the state government used to protect the state forest from rural households, but the protection had been becoming more costly due to the increasing population and as a result forest resources had been depleted. JFM scheme was formally introduced by the central government in 1988 to provide rural households with incentive for forest management by benefit sharing, and each state government adopted JFM since then. Under JFM scheme, rural households have to regulate their use of forest resources for their livelihood and they are promised to will a significant share (e.g. 50%) of timber sales revenue.

Although JFM has been implemented for almost 20 years in most states in India, its impact on the welfare of rural households and forest condition has rarely investigated quantitatively. Thus, the objective of this paper is to tackle this remaining question. This paper utilizes a two-year panel data of 360 households and the satellite images of forest around their residential places. The panel data were collected in 1998 and 2008 in 60 villages spread over 6 districts in Madhya Pradesh.

Our analyses show that JFM neither increased nor decreased household income per capita although household income per capita increased significantly during the 10 year period investigated. It implies that the restriction of forest use did not have any negative effect on the welfare of rural households, but that the benefit sharing was not realized or did not increase household income. The latter is consistent with the fact that most timber trees are still immature to harvest. On the other hand, forest condition was improved during the 10 year period in villages where JFM was implemented. The improvement of forest resources is considered to be caused by forest protection from grazing and tree plantation as part of JFM activities. In conclusion, the state government has benefited from JFM, while rural households have not benefited from JFM although they have not decreased their welfare at least in the short-run.

Keywords: joint forest management, impact assessment, panel data, household income, forest condition, India

## Forming the Inter-mediate Region between Urban and Rural in India - a case of Mysore city, Karnataka -

SUNDERRAJ, Arun das<sup>1</sup> ; KIMOTO, Koichi<sup>2</sup> ; R., Umakanth<sup>1</sup> ; HR, Vishwanatha<sup>1\*</sup>

<sup>1</sup>University of Mysore, <sup>2</sup>Hiroshima Jogakuin University

The fragmentation of agricultural land due to inheritance and partial selling has put the farming community into marginal farmers. A marginal farmer owning less than one acre of land, losses complete livelihood from his land. He becomes a partial non agriculture worker along with his farming occupation. Ultimately, leading to permanent change in occupation. In the later period he disowns the farming activity and migrates to the fringe of the nearby city. The CBD pressure on fringe begins as ripples from the city towards fringe. Consequence of this the fringe pressure ripples towards the farming and forest land. This has vice versa effect from Rural to Urban Fringe. The rural pressure which emanates from outer country land towards city mounts up its pressure on Fringe.

This paper discusses about the process of expanding cities, its pressure on fringe, the rural farming land, shifting occupation and bouncing effect towards city. A fast growing city like Mysore city bounded by farming land of Mysore and Chamaraja districts is a good example to explain the situation of many cities of India which are experiencing similar process and bouncing effect.

Keywords: Inter-mediate Region, Land Use and Cover Changes, Population Pressure, Urban - Rural, India

## Time-serial trend of built-up area of China - A preliminary consideration of statistical data

DOI, Haruhiro<sup>1\*</sup>

<sup>1</sup>Faculty of Education and Welfare Sciences, Oita University

The research group of SLUAS (Research project of "Towards Sustainable Land Use in Asia" Grant-in-Aid for Scientific Research(S) 2009-2013, Yukio Himiyama) has executed several research field trips in various regions of China. The author fortunately has chance to join the field trips and to observe several land-use conditions and land-use changes on the way. As a result of those research field trips, the author confirmed that the built-up area remarkably expanded by fast growing economy of big cities in the coastal area such as Beijing and in those cities not only the industrial development but also the housing development and shopping malls are developed actively in the suburban area. On the other hand, the author also felt that the cities in the inland area, however, it is late comparatively its economic growth from the coastal region, a built-up area growth is generated recently by the industrial and housing developments in the high rise apartment building etc. The present study intends to confirm such a personal impression about recent built-up area growth of China by using statistical material.

The objectives of the research are as follows. First object is to confirm time serial feature of the built-up area expansion. Second is to analyse the relation between the built-up area expansion and population scale. Third is to confirm regional difference of built-up area expansion by using regional division in China. And forth is to consider factors or the background of the built-up area expansion. So the author analyses the relations among built-up area expansion, a population increase, and GDP indexes. Findings concerning obtaining by these objectives are beneficial to estimate how a spatial expansion of the China city will become in the future.

The author set up hypothesis obtaining by the research are as follows. One is that built-up area expands according to a population increase and economic growth of a city. Second is that structural change of an economic condition of a city such as secondary industry and tertiary industry is reflecting its expansion of built-up area of a city. Third is that the growth wave of a city spreads from the coastal region to the inland area.

Keywords: built-up area, population, regional division, economic structure

## Study on the relationship between human activities. natural environment of food production in Xinjiang

XIAOKAITI, Aji<sup>1\*</sup> ; KONDOH, Akihiko<sup>2</sup>

<sup>1</sup>Graduate School of Sciences, Chiba University, <sup>2</sup>CEReS, Chiba University

Maintaining the food production force is a basic condition for ensuring the food security in Xinjiang Uygur Autonomous Region. In this study, We have carried out the factors analysis from both sides of the natural and social factors on food production in Xinjiang, using the unit area production volume as the main indicator of food production. In order to understand the temporal change of the unit area production volume in Xinjiang at first, We extracted the unit area production volume data from the Statistical yearbook in Xinjiang, and analyzed the secular change of food production in Xinjiang. The result shows that the unit area production volume had been growing steadily over the 1990-2003, but shows an unstable state since 2004, and has been reduced in 2008; In order to understand the spatial variation of the unit area production volume, We have created a difference image using GIS technique, between 2008 when the unit area production volume reduced, and 2003 when the unit area production volume had been continued growth to analysis the regional changes of food production. It shows that the regions which the unit area production volume decreased are distributed more in the area of the north and east of Xinjiang in 2008 comparison to 2003.

In order to understand the change factor of food production, the analysis has been done on the causes of changes in food production in Xinjiang, by extracting the data of the chemical fertilizer that was used for the food production, irrigation area, agricultural machinery and the rural electricity from the statistical yearbook, The result shows that the effective irrigation rate in Xinjiang after 2005 was reduced by the loss of irrigation facilities and equipments, and it is confirmed that these area are substantially matches to the region in which the unit area production volume decreasing. The data of the agricultural production material price, commodity retail price, agricultural products purchase price are also used for the same analysis, It was estimated that the rise of agricultural production material prices, has become a factor in reduction of food production indirectly through reduced production cost in 2008 that unit area production volume was reduced.

On its outer, using the TRMMB343 precipitation data and CRU TS3.21 temperature data, analyzed the natural factors of food production change. It shows that the trend of precipitation in decline, and the reduction position matches well with the area of unit area production volume are decreased. However, it is suspected that both of human activities and natural factors have been the impact jointly to the changes in food production in Xinjiang.

Keywords: Xinjiang Uygur Autonomous Region, Food production, Human activities, Natural environmen, GIS

## Framing Land Use Sustainability Research in Future Earth Context

HIMIYAMA, Yukio<sup>1\*</sup>

<sup>1</sup>Hokkaido University of Education

The Future Earth Initial Design issued late in 2013 emphasizes the importance of land use research related with sustainability. What are written about land use are not particularly new to land-use specialists, but what is significant is that land use is considered as a priority concern of Future Earth. The paper discusses how to frame land use sustainability research in Future Earth Context based on the achievements and experiences of IGU-LUCC (International Geographical Union Commission on Land Use/Cover Change), GLP (Global Land Project), SLUAS (Towards Sustainable Land Use in Asia Project) and others.

Keywords: Future Earth, land use, GLP, IHDP, IGU-LUCC

## RIHN Archives - for transdisciplinary research on global environmental studies

YASUTOMI, Natsuko<sup>1\*</sup> ; SEKINO, Tatsuki<sup>1</sup>

<sup>1</sup>Research Institute for Humanity and Nature

Research Institute for Humanity and Nature (RIHN) solicits, develops, hosts, and funds fixed-term research projects on pressing areas of interaction between humanity and nature. RIHN promotes coordinated, problem-centered, context-specific, and multi-dimensional science. RIHN projects can last from three to five years; they are always multidisciplinary and employ multiple methodologies, and they are supposed to offer solutions to the problems under study.

RIHN undertake an important task to accumulate their research products on transdisciplinary global environmental studies and resources for successors since almost all researchers leave RIHN after the end of their project.

"RIHN Archives" was developed in 2008 in order to accumulate and charge research products of RIHN research projects. It contains metadata of publications, reports, posters, handsouts and movies of seminars, evaluations, obtained data, maps, and so on. RIHN Archives database is open to public.

"RIHN Archives" itself is the record of transdisciplinary studies held in RIHN. Moreover, RIHN research projects have been conducted on objectives which should contribute to Future Earth. RIHN Archives must play an important role on planning new feasible studies to design futable earth.

Keywords: global environmental studies, interdisciplinary research, outreach

HSC25-01

Room:421

Time:April 30 09:00-09:15

## The reconstruction 2014 present circumstances after The 2011 TOHOKU Great Earthquake disaster

NISHIZAWA, Masaru<sup>1\*</sup>

<sup>1</sup>none

1. Suggest the collective bargaining with the authorities concerned with the important matter.
2. I am hoping the youth for a marked conception to our country.
3. Suggest the building serves both as a residence and a place of refuge.

Keywords: The 2011 TOHOKU Great Earthquake Disaster, The building serves both as a residence and refuge, youth, Reconstruction

## Application of Information on Seasonal Landscapes for Landcover Classification by Satellite Data

KUROKI, Takahito<sup>1\*</sup>

<sup>1</sup>Fukuoka Univ. of Edu.

We cannot ignore the influence of seasonal landscapes in landcover classification by Satellite data. Therefore in the analysis, we always have to select the data acquired in the best season for available landcover classification. The seasonal landscape change is also caused by human activities as well as natural conditions. The higher the resolution of the data used for classification, the influence on the landscape by human activity increases in the results. Considering human activity on the classification, it seems that we cannot obtain the realistic image for natural conditions. We do not have much interest in the influence of classification of natural conditions induced by landcover classification based on human activity and the countermeasure. In this study, seasonal landcover classifications based on human activity are analyzed in Aso volcano with remarkable seasonal change of landscape every year. Then, the accuracy is confirmed by such as sign of human activity that can be identified in the classified images. Finally, I discuss on the influence of the classification to that of natural conditions in the volcano and show a countermeasure for the problem in the classification. We used four ALOS data acquired in spring 2010, summer 2006, autumn 2007 and winter 2007 for the classification. The study area was classified into 6 items such as green grass, withered grass, forest, arable land, urban area, open burning area by the supervised maximum likelihood classification.

On the landcover classified maps of all seasons, similar distribution patterns were observed on forest of caldera wall and piedmont of central cone, and on arable land and urban area of caldera floor. On the other hand, distribution of different items was shown in crater rim and mountainside of central cone every season. They are green grass in September, green grass, arable land and withered grass in November, withered grass in February, green grass, withered grass and open burning area in April. On the classified maps, the large seasonal landscape changes at the grassland in crater rim and mountainside of central cone can be understood. From the interpretation of these changes, signs of human activity of boundary of management association for grassland, such as firebreak of open burning were identified clearly. However, this classification work could not induce appropriate classified images that represent the natural conditions in the volcano at the summit area and crater lake area of central cone, dissected valley of lava dome and past slope failure area in caldera wall. At the summit area of central cone, I selected the seasonal image that is easy to represent the distribution for each class of natural conditions. The items in the image were reclassified into the classes of natural conditions and the values of the power of 10 were given to them. Finally, I obtained the realistic landcover classification image at the volcanic area from the overlay analysis by using the reclassified images. Consequently, I clarified in this study that landcover classification representing the characteristics of natural conditions can be performed with high accuracy by using the information of seasonal landscapes based on human activities.

Keywords: Aso volcano, landcover classification, ALOS, seasonal change, natural condition

## Disaster information gathering depend on the geographic characteristics zone using geospatial information

KOARAI, Mamoru<sup>1\*</sup>

<sup>1</sup>GSI of Japan

In order to build a national land equipped with resilience, it is important to advance environmental preservation, land conservation and development which performed geographic division summarized the area where the geographic characteristics is similar. The author tried to classify into the about one hundred geographic characteristics zones of Central Japan for disaster prevention.

Geographic characteristics classification from the viewpoint of the disaster prevention was carried out by the following method. First, it classified into mountain, hill, volcano, plateau and lowland by landform classification. Next, about mountain, hill and volcano, it subdivided according to geology. About plain, it subdivided according to the ratio of plateau and lowland. High-risk areas, such as slope collapse, landslide, liquefaction and collapse of volcanic bodies, were extracted from the analysis of geospatial information, including DEMs, geological maps, landslide distribution maps, landform classification maps, etc.

In this presentation, the author will discuss how to use the geographic characteristics zone for emergency assistance at early stage. It is necessary to consider the disaster information gathering according to the difference of disaster characteristics on each geographic characteristics zone. The most important issue in mountain area is grasping of an isolated colony, and detection of an isolated colony is possible by overlay of slope collapse expected area and road network information. In the viewpoint of a catastrophic secondary disaster, extraction of the flooding area by a landslide dam is very important. Satellite SAR and airborne SAR were effective method in the case of deep collapses by the typhoon heavy rain of Kii Peninsula in 2011. In the disaster information gathering in early stages of a plain area, tsunami damage is very important. Satellite SAR was effective method for the detection and monitoring of the tsunami flooding area in the case of the Great East Japan Earthquake. From the viewpoint which carries out emergency assistance at early stage, the extraction of the heavy damaged area is required. The development of automatic classification technology about spill zone, failure zone and flood zone using polarization SAR is required.

Keywords: geographic characteristics zone, geospatial information, disaster information gathering, emergency assistance at early stage, synthetic aperture radar

## Towards detailed tsunami hazard assessment for specific regions

HIRATA, Kenji<sup>1\*</sup>; FUJIWARA, Hiroyuki<sup>1</sup>; NAKAMURA, Hiromitsu<sup>1</sup>; OSADA, Masaki<sup>1</sup>; OHSUMI, Tsuneo<sup>1</sup>; MORIKAWA, Nobuyuki<sup>1</sup>; KAWAI, Shin'ichi<sup>1</sup>; AOI, Shin<sup>1</sup>; YAMAMOTO, Naotaka<sup>1</sup>; MURASHIMA, Yoichi<sup>2</sup>; MURATA, Yasuhiro<sup>2</sup>; IN-OUE, Takuya<sup>2</sup>; SAITO, Ryu<sup>2</sup>; MATSUYAMA, Hisanori<sup>3</sup>; TOYAMA, Nobuhiko<sup>3</sup>; KITOH, Tadashi<sup>3</sup>; AKIYAMA, Shi'ichi<sup>4</sup>; KORENAGA, Mariko<sup>4</sup>; ABE, Yuta<sup>4</sup>; HASHIMOTO, Norihiko<sup>4</sup>

<sup>1</sup>NIED, <sup>2</sup>KKC, <sup>3</sup>OYO, <sup>4</sup>CTC

NIED began research projects regarding tsunami hazard assessment (THA) in Japan to support various kind of measures against possible tsunami attacks in future by sectors such as local governments, life-line companies, etc after the national tragedy caused by the 11st March 2011 Tohoku earthquake (Mw9.0) (Fujiwara et al., 2013, JpGU). One of the research projects is a research of probabilistic tsunami hazard assessments (PTHA) in which we consider all of possible tsunamis that may affect coastal regions in future. The research of PTHA consists of two subjects; (1) nation-wide probabilistic tsunami hazard assessment (NWPHTA) (Hirata et al., 2014, JpGU) and (2) detailed probabilistic tsunami hazard assessment for specific regions (DPTHASR). We briefly show outlines of (2) here.

The objective of DPTHASR is to bridge the gap between probabilistic tsunami hazard assessment and local measures for disaster prevention in city-scale. In the research and development process of DPTHASR, we are planning to conduct several kinds of tsunami inundation assessment for specific regions by using tsunami propagation and inundation simulations based on a non-linear long wave equation with staggered leap-frog, finite difference method (FDM) over a nesting grid system with the minimum grid size of 10 meters. As for presentation tools of DPTHASR, we are planning to present (a) inundation flow depth hazard curve (excess probability) at specified point and (b) probabilistic spatial distribution of inundation flow depth as well as we are also planning to investigate development of (c) probabilistic inundation flow velocity assessment that is closely related to tsunami destructive force against buildings, etc. and that can be directly applied to risk assessments. As the first attempt in researches regarding DPTHASR, we are investigating a probabilistic method of depth flow assessment in which both of probabilistic assessment for inundation flow depth distribution and inundation flow hazard curves (excess probability) are presented (Saito et al. 2014, JpGU).

For a high-precision forecast of inundation phenomena based on tsunami run-up calculation in DPTHASR, it is the most important to use fine and precise topographic data with detailed information on breakwaters and seawalls in coastal region and riversides. We make effort to collect these information and will have to investigate relationship between inundation flow assessment and destruction conditions of coastal infrastructures in near future. The Ministry of Land, Infrastructure, Transport and Tourism (MLIT) of Japanese Government recommends users for tsunami runup calculation to basically use high-precision topographic data acquired with airborne laser scanning (MLIT, 2012, Guideline for tsunami inundation forecasting). The Geospatial Information Authority of Japan (GSI) is progressively releasing the precise coastal topographic data acquired with airborne laser scanning. DPTHASR will be advanced using processed data, converted for tsunami simulation, created from high-precision topographic data acquired with airborne laser scanning by GSI.

Keywords: tsunami, hazard assessment, runup, probability, local tsunami forecast, utilization

## Evacuation passage from Tunami-map exercise with inhabitants

FURUTA, Noboru<sup>1\*</sup> ; CHUJYO, Yoshiteru<sup>1</sup> ; KOBAYASHI, Ikunori<sup>1</sup> ; KAWASE, Kumiko<sup>2</sup>

<sup>1</sup>Tokushima Bunri Univ., <sup>2</sup>Ehime Univ.

At the time of the south seas earthquake occurrence, the security of the refuge course is necessary. The investigation area is Shiwagi, Minami-cho, Tokushima. We identified the evacuation route as local inhabitants in students. We had you tell local people a number and the location of the person requiring nursing care. A person requiring nursing care is an elderly person, an infant, a person with a physical disability.

Keywords: Evacuation, tunami, DIG, ?obstruction, GIS

## The Significance of Partnership and Participatory Sharing of Geospatial Information through crisis mapping in Izu-Oshima

SETO, Toshikazu<sup>1\*</sup>

<sup>1</sup>Center for Spatial Information Science, the University of Tokyo

### 1. Introduction

Various platforms enable online-based plotting of disaster information map using reviews and other social networking services (SNS). Examples Ushahidi has been noted since the Great East Japan Earthquake for its usefulness in promoting rapid situational awareness in disaster areas. This platform also is used OpenStreetMap (OSM), a free mapping project used to generate background maps. Indeed, as regards natural disasters that occurred in Japan after year of the Great East Japan Earthquake, simplified versions of information sharing sites have been established by volunteers, such as Crowdfunder. Meanwhile, during the onslaught of Typhoon Wipha last October 2013, information sharing by volunteers progressed smoothly using the rapid launch of Crowdfunder.

However, the method of geospatial information gathering in the event of a crisis as a means of quickly relaying information in and out of disaster areas, as typified by crisis mapping using Ushahidi, is not fully and properly utilized in Japan. This study examines the role of information sharing and the development of geospatial information on the Web related to disaster response.

### 2. Sharing of geospatial information by participatory mapping in Izu-Oshima

To promote Izu-Oshima tourism around the Geopark with the aid of information technology, Izu-Oshima Tourist Association and other groups held the Hackathon and Mapping Party in January 2013. In this event, a detailed map created or developed smartphone applications for leisure by about 30 cooperating participants composed of OSM developers and mappers, as well as local residents involved in geopark's tour guide.

### 3. Cooperation with other organizations and launch of crisis mapping during the occurrence of Typhoon Wipha

After the event in January 2013, participants continue to engage in exchanges through a Facebook group, including participants of the island nature tour guide. For instance, users in Tokyo, who tuned in to the news regarding the occurrence of heavy rain and landslides brought by typhoon Wipha last October 16, intensified their information collection and uploaded data on the Web site very quickly. Twitter accounts with high reliability, such as that of "Izu-Oshima's disaster prevention", published information picked up by disaster prevention radio stations.

In another case, the Red Relief Image Map made by Asia Air Survey and slant ortho-photo data gathered by emergency shooting by some survey companies provided as a possible WMS layer through "e-com map" of the Research Institute for Earth Science and Disaster Prevention and Geoserver of the Code for Japan community. Such geospatial information can serve as the basic data for the estimation of location information, in which Crowdfunder helps screen information via SNS features. As such, the number of page views of Crowdfunder reached 12,000, and 248 reports are posted on Crowdfunder in about a month after the disaster. In addition, as information transfer throughout and mapping of the disaster area had become a major issue, it was reported in local as well as analog information of paper maps, such as the large-format guide to the Great East Japan Earthquake by the Nature and Tourism Association staff.

### 4. Conclusions

In Japan, crisis mapping that fully utilizes the Web, such as online maps, has come to be carried out quickly and serve as a source of understanding and cooperation between volunteers and various organizations. In this context, the need for information gathering and sharing at a high public degree in the initial disaster stage is recognized, triggered by the events of the Great East Japan Earthquake. In addition, even in areas where information technology and geospatial information have not been as highly developed compared with Izu-Oshima, the cases covered in this study revealed that stakeholders could work together through workshops to build a relationship aimed at advancing information sharing development.

Keywords: crisis mapping, crowdsourcing, Ushahidi, volunteered geographic information, Izu-Oshima island

## Study of natural disasters and terrain of Izu Oshima with Red Relief Image Map

CHIBA, Tatsuro<sup>1\*</sup>

<sup>1</sup>Asia Air Survey Co., Ltd.

### **Introduction**

In recent years, advances in LiDAR technology, detailed topographic data with high accuracy by eliminating the influence of the tree is now obtained. The contour by aerial photogrammetry so far, terrain under the trees is due to the estimation of operator that assumes the tree height, the difference of the laser measurement was evident. However, it is to express in scale in which it is easy to utilization of the whole picture microtopography measurement such results is difficult. Also shaded contour plot also altitude tints Figures it was not appropriate. I invented red relief image map method at the time of terrain reconnaissance of Aokigahara-Jukai of Mount Fuji in 2002. After that I've been used to field survey and interpretation of volcanic terrain around the country.

### **red relief image map**

The more red than at steep slope, as bright as ridge, expressed the darker the valley, red relief image map is a some false color image of certain ortho. Since the state overlapping the topographic map, without the use of specialized equipment, it is possible to obtain a natural three-dimensional feeling in one piece, a combination of a red relief image map and LiDAR DEM and revolutionized the field survey.

### **terrain of Izu-Oshima**

Also in Izu-Oshima, LiDAR DEM were detected, H24 by Tokyo, H25 by Tokyo, H18 by GSI has been carried out. In addition, as the foundation map information 5mDEM, measurement results of H24 have been published from the GSI.

This section shows a red relief image map of Izu-Oshima, we describe the features of the volcanic terrain that can be read from there.

Izu-Oshima, there is a caldera in the center, Mt central cone is located in the center. Mt shows the terrain of tuff cone crater is large in proportion to size, but I'm repeating the activity in which the bottom of the crater of the central vertical hole moves up and down, to overflow the lava. The eruption occurred at 1950-51 and 1986 in recent years. In addition, in the Izu-Oshima, fissure eruption many distribution on the outside of the caldera, C fissure eruption in 1986. It has been estimated that there is a fissure of Y5 drained the lava flow the steep slopes on the east side of Motomachi, but the exact location has not been clearly covered in trees. The red relief image map by the laser measurement of H18, Y5 fissure is visible clear, although confirmation has been difficult by many trees. After that, the field survey of the collapse can be accomplished by the typhoon disaster of October 2013, it was confirmed to be Y5 fissure.

### **Features of the terrain of the surface slope collapse**

The typhoon of October 16, 2013, a large debris flow disaster occurs at the Motomachi Kandachi area of Izu-Oshima. Wake of this disaster was the collapse of the surface layer of volcanic ash on the slopes, and this slope are crossed by Y5 fissure, debris flow was flowing down over the Motomachi lava flowed from there. For the valley of this lava flow is very shallow, became the disaster spill debris flow can not swallow. In addition, I describe the characteristics of the micro-topography in the poster.

Keywords: izu-ooshima, DEM, red relief image map, lava flow, LiDAR, surface failure

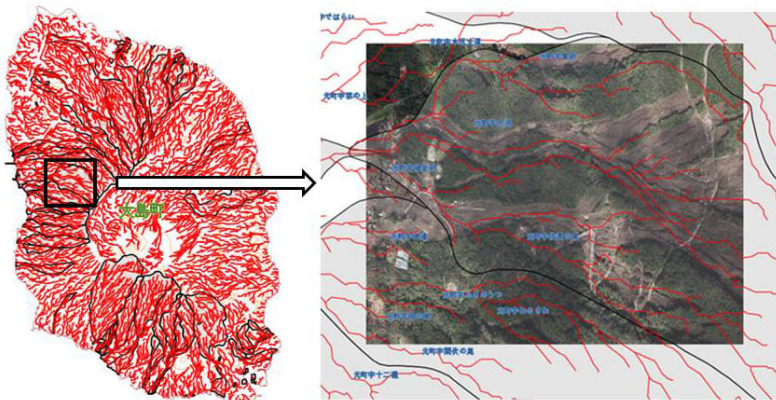
## Debris flow by Typhoon Wipha and creating maps with flow accumulation

SAWANO, Nobuhiro<sup>1\*</sup>

<sup>1</sup>Kanazawa Seiryō University

- 1. Typhoon Wipha**
- 2. Flow accumulation**
- 3. A case of Izu Oshima**
- 4. Web Publication**
- 5. Summary**

Keywords: Typhoon Wipha, Debris flow, Flow accumulation, Web publishing, Geoserver



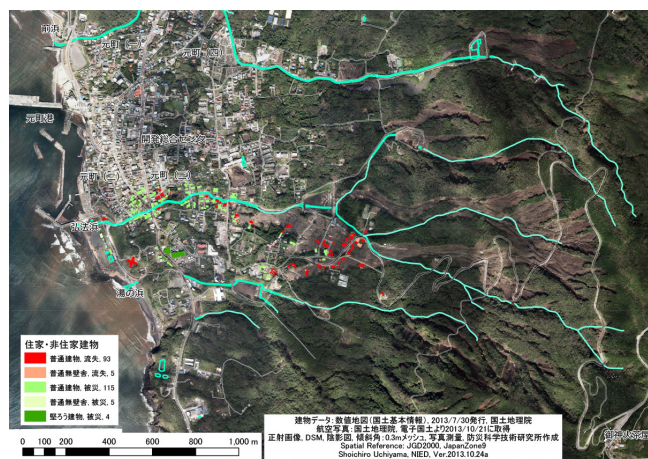
## The effort of prompt information-gathering - crisis response to damages by Typhoon Wipha (2013) on Izu Oshima island

UCHIYAMA, Shoichiro<sup>1\*</sup> ; SUZUKI, Hinako<sup>1</sup> ; USUDA, Yuichiro<sup>1</sup>

<sup>1</sup>National Research Institute for Earth Science and Disaster Prevention (NIED)

Disaster Information Laboratory (DIL) at National Research Institute for Earth Science and Disaster Prevention (NIED) integrates information provided related organizations and release to public in case of hazard strikes. This paper shows the effort of prompt information-gathering as crisis response by NIED at Izu-Oshima devastated by the typhoon Wipha in 2013.

Keywords: crisis response, information-gathering, structure from motion (SfM), typhoon Wipha in 2013, Izu-oshima



## Role of the cloud based GIS for disaster management system at Emergency Operation Center

GOTO, Shintaro<sup>1\*</sup> ; SAWANO, Nobuhiro<sup>2</sup> ; SAKAI, Toshikazu<sup>1</sup>

<sup>1</sup>Department of Environmental Systems Faculty of GEO-Environmental Science Rissho University, <sup>2</sup>Kanazawa Seiryō University

The cloud-based GIS center with the assumption that on the basis of the lessons learned in disaster information logistic support of the Great East Japan Earthquake 2011, ICS is introduced at the provincial level, to function under ICS concepts in the field Saitama Prefecture. The object of the invention is to organize the features and to operate by implementing it.

For this purpose, the contents of this study are as follows;

1. Study of cloud-based GIS data management perspective for the basic system
2. Application to the COP(Common Operational Picture) and the study of the utilization by the cloud of electronic results
3. Demonstration and calibration in collaborative disaster drill applying the ICS

Keywords: GIS, Incident Command System, Common Operational Picture, Information Management Process, Emergency Management Center

## Micro - Landform Mapping and Applications in Hilly Area Using LIDAR Data

BORJIGIN, Habura<sup>1\*</sup> ; GOTO, Shintaro<sup>2</sup>

<sup>1</sup>National Institute for Environmental Studies Center for Regional Environmental Research, <sup>2</sup>Rissho University Department of Environmental Systems Faculty of GEO-Environmental Science

The objective of this study is to develop the information to be provided for natural regeneration by investigating the relationship between Micro-Landform and vegetation in hilly area of Higashi-matsuyama City in Saitama Pref. The Micro-Landform was classified based on the conversion line of the slope angle derived from DEM (digital elevation model) generated from LIDAR (Laser Imaging Detection And Ranging). Furthermore, we summarized the classification situation of each Micro-Landform by every tree measurement. Finally, the relationship between vegetation and Micro-Landform in the study area was detected by analyzing the relationship between the summarized situation of Micro-Landform and the woody life type corresponding to the Micro-Landform classification using TWINSpan.

Keywords: LIDAR data, Micro-Landform, Vegetation, TWINSpan

## An influence of roadway on occurrence of slope failure and debris flow of the Izu-Oshima Typhoon Wipha (1326) disaster

SHIRAI, Masaaki<sup>1\*</sup> ; WATANABE, Makiko<sup>1</sup>

<sup>1</sup>Tokyo Metropolitan University

Vast slope collapse took place and debris flows struck the Motomachi-town foot of western slope of the Izu-Oshima Island on early morning 16, Oct. 2013. Field survey on the collapsed slope by *TMU Group for Izu-Oshima Typhoon Wipha (1326) Disaster Survey* was carried out 4 to 6, Dec. 2013.

One of the major concerns of the authors was an influence of roadway built after 1986 eruption on occurrence of 2013 slope collapse. Results of the survey are summarized as follows, (a) Collapse points originated from downslope side of the roadway (type-A collapse) were located on ridges and adjacent to collapse points originated from upslope side of the roadway (type-B collapse). (b) A large amount of debris of fallen tree which would have been transported by mud flow on the road was observed around the type-A collapse points. (c) A 1-0.5 m thick surface soil mass with tree and its dense roots was peeled from base of the retaining wall at the other small collapse. An appearance of the base of the retaining wall at the small collapse is similar with base of the retaining wall at type-A collapse.

Taking account into these results (a) to (c), it is inferred that type-A collapse would have occurred according to the following scenario, (1) rainwater and mud flow from type-B collapse flowed on the roadway, (2) around the curve on the ridge, rainwater/muddy water fell down from road surface to retaining wall and (3) surface soil mass (1-0.5 m thick) with dense tree roots and trunks was saturated by water and peeled from base of the retaining wall. Consequently, we conclude that the roadway was not a primary factor but secondary factor of the slope collapse, which expanded collapse area in this case.

Keywords: slope failure, Izu-Oshima, Typhoon Wipha (1326), roadway

## Reexamination of the 1960 Chilean tsunami disasters at the northern part of Amami Oshima island, Kagoshima Prefecture

IMURA, Ryusuke<sup>1\*</sup> ; ZAIZEN, Yui<sup>2</sup> ; KUSAHARA, Hitomi<sup>2</sup> ; TOMIYASU, Kosuke<sup>2</sup>

<sup>1</sup>Graduate School of Science and Engineering, Kagoshima University, <sup>2</sup>Faculty of Science, Kagoshima University

We've interviewed about the Chilean tsunami disasters of 1960 at the northern part of Amami Oshima island. Results of our investigation suggest that the 1960 Chilean tsunami heights exceeding 3-4 m were observed in the almost coastlines of the northern part of Amami Oshima island.

Keywords: Amami Oshima, 1960 Chilean tsunami, tsunami disasters

## Utilization of the natural hazard database by NIED - a case of utilization at Typhoon Wipha (2013) on Izu Oshima island

SUZUKI, Hinako<sup>1\*</sup> ; UCHIYAMA, Shoichiro<sup>1</sup> ; USUDA, Yuichiro<sup>1</sup>

<sup>1</sup>National Research Institute for Earth Science and Disaster Prevention (NIED)

This study introduces a case study on utilization of natural hazard database by NIED for extracting historical hazard events on Izu Oshima island suffering Typhoon Wipha in 2013. This powerful typhoon attacked on Motomachi area, and caused large-scale landslides. We searched the historical hazard events in this place from the natural hazard database to investigate relation between hazard this time and old events. Keywords for searching the database were "typhoon", "heavy rain" and "landslide". As a result, seven events were found between 1925 and present, and typhoon Ida in 1958 was a particularly massive scale. The typhoon Ida that caused large landslide in Motomachi area, which was devastated again by Typhoon Wipha, was named "Kanogawa typhoon" in Japan. Through these unification processes, we found two problems in our database:

- 1) No records about typhoon, heavy rain, and landslide before 1925 in this area
- 2) Little information about the date and time of occurrence and the extent

We will enrich these event records and information.

Keywords: natural hazard database, utilization, typhoon Wipha in 2013, Izu-oshima

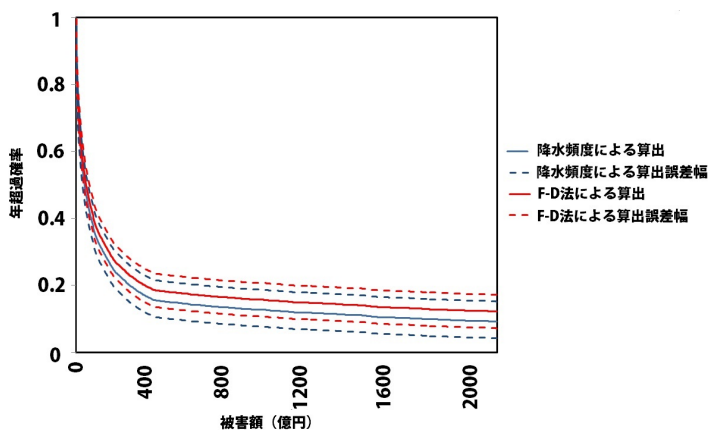
## A new methodology to assess the impacts of precipitation change on flood risk in Tokyo 23 ward Area

HIRANO, Junpei<sup>1\*</sup> ; DAIRAKU, Koji<sup>1</sup>

<sup>1</sup>National Research Institute for Earth Science and Disaster Prevention

In this study, we attempted to develop a new methodology for flood risk assessment in the Tokyo metropolitan area by considering the effect of precipitation change. By comparing the statistical distribution of the daily precipitation frequency for the whole study period, and those for flood occurrence days, we found that the distributions of the precipitation frequency for the flood occurrence days are corresponding to those for the whole study period. These results indicate that we can estimate flood damage based on frequency of daily precipitation. Based on these results, we estimated the flood damage for Tokyo based on distribution of daily precipitation frequency. We then created a flood-risk curve that represents the relationship between damage and exceeding probability of a flood. By comparing the newly developed flood-risk curve, based on the precipitation frequency, with those in the previous studies, we indicated that a newly developed flood-risk curve could evaluate the potential flood risk in Tokyo with high accuracy.

Keywords: Flood risk, Precipitation change, Risk curve, Tokyo metropolitan area



## Map Drilling of Disaster Prevention by Voluntary Group - An Example at Nasu Volcanic Area

FUKUSHIMA, Tamio<sup>1</sup> ; TAKAMORI, Shouji<sup>3</sup> ; INABA, Shigeru<sup>4</sup> ; NAKAMURA, Yoichi<sup>2\*</sup> ; NASU, Local governmnet<sup>5</sup>

<sup>1</sup>National Association For Diaster Prevention, <sup>2</sup>Utusunomiya University, <sup>3</sup>Promotion Council of Distric Continuity Management, <sup>4</sup>Disaster Prevention Qualiged Counselor in Tochigi, <sup>5</sup>Manucipal Governmnet of Nasu Town

A map drilling of volcanic disaster prevention by voluntary groups: An Example at Nasu volcanic area was hold in the area of Nasu active volcano. This evacuation drilling at Nasu municipal government for voluntary groups of town people was supported by National Association for Disaster Prevention, Promotion Council of District Continuity Management, and Disaster Prevention Quailed Counselor in Tochigi. This project was managed financially to perform for last two fiscal years between 2012 and 2013. As a result, present drilling was very effective, especially for community people living near active Nasu volcano, in order to learn evacuation managements at the future volcanic emergency.

Keywords: Disaster Prevention, Map Drilling, Volcanic Diaster, Active Volcano, Eruption, Voluntary Group

## Disaster risk reduction workshop utilizing GIS and Saba-meshi: A practice of the Department of Geography, Oita Univ.

KOYAMA, Takushi<sup>1\*</sup> ; DOI, Haruhiro<sup>1</sup> ; MORIMATSU, Maya<sup>2</sup> ; UCHIYAMA, Shoichiro<sup>3</sup>

<sup>1</sup>Department of Geography, Oita University, <sup>2</sup>Nihon Suido Consultants Co. Ltd., <sup>3</sup>NIED

The Department of Geography at Oita University held a disaster risk reduction workshop on November 3, 2013, for schoolchildren and their parents (A total number of participant was fifty one). The purpose of the event was to motivate the schoolchildren and their parents to aware of a disaster prevention and reduction in their daily life. The event consisted of the following two experiences: drawing a map using a geographic information system (GIS), and cooking rice using two 350ml aluminum cans and three 1L milk cartons (Survival *Meshitaki*). Survival *Meshitaki* is called *Saba-meshi* for short, and it is material for teaching about disaster prevention through practical experience.

After the event, the participants were requested to respond the questionnaires in order to evaluate the event. The results of the questionnaire showed that we received high evaluations from many participants on the experiences offered at the event. Therefore, we were able to raise the participants' awareness of disaster prevention and disaster reduction.

Furthermore, thirteen university students, who intend to become schoolteachers, participated the event as assistant staffs. They acquired in advance the fundamental skills of GIS and *Saba-meshi* by a preliminary training workshop. These are useful skills in the field of school education. The event, in conclusion, has given the participants and the students intending to be schoolteachers very effective experiences and practical knowledge respectively and the experience-based event such as this workshop is worth to be held repeatedly.

Keywords: Geographic Information System, Saba-meshi, Disaster risk reduction workshop, The 2011 off the Pacific coast of Tohoku Earthquake, Students intending school teachers, Oita Prefecture

## Liquefaction occurrence ratio and geomorphic conditions in the inland area caused by the Great East Japan Earthquake

AOYAMA, Masafumi<sup>1\*</sup>

<sup>1</sup>Japan Map Center

The area ratio of liquefied sites in the inland area caused by the 2011 off the Pacific coast of Tohoku Earthquake was estimated from the field survey and Google Earth images interpretation. In the Tone River lowland, the occurrence of liquefaction concentrated in the former river channel and pond, and the area ratio of liquefied sites is about 23%. The ground consisting of younger landfill age is more susceptible to liquefaction than that created by the older ones. Area ratio of Liquefied sites in the Tone River lowland is larger than the Osaki plain, Miyagi Prefecture. In the Osaki plain, the area of former river channels and ponds buried by loose sandy soils is less than the Tone River lowland.

Keywords: liquefaction, geomorphic classification, former river channel and pond, landfill age, 2011 off the Pacific coast of Tohoku Earthquake

HSC25-P07

Room:Poster

Time:April 30 18:15-19:30

## Problems on the disaster mitigation plan of the elementally and junior high school - a case study of Ishikawa Prefecture

AOKI, Tatsuto<sup>1\*</sup> ; HAYASHI, Kiyomi<sup>1</sup>

<sup>1</sup>School of Regional Development Studies, Kanazawa University

Keywords: Elementally and junior high school, Manual for disaster mitigation, Hazard Map, Evacuation

## Tsunami hazard inventory survey of utilize for municipalities

OHSUMI, Tsuneo<sup>1\*</sup> ; NAKAMURA, Hiromitsu<sup>1</sup> ; HIRATA, Kenji<sup>1</sup> ; OSADA, Masaki<sup>1</sup> ; FUJIWARA, Hiroyuki<sup>1</sup>

<sup>1</sup>National Research Institute for Earth Science and Disaster Prevention

A tsunami hazard inventory is important for tsunami disaster mitigation due to earthquakes, and also for a Tsunami hazard assessments. The tsunami hazard assessments project for Japan was started since 2012 by NIED (Fujiwara, *et al.*, 2013, Hirata, *et al.*, 2014). We performed inventory survey on utilization of the tsunami hazard assessments to Ibaraki and Chiba prefectures, which damaged municipalities of the tsunami during the 2011 off the Pacific Coast of Tohoku Earthquake. First stage, we surveyed the crisis management departments of the Ibaraki and Chiba Prefectures. Second stage, we surveyed 10 municipalities of Ibaraki prefecture and 18 municipalities of Chiba prefecture. Tsunami hazard inventory was carried out with a description of the Tsunami hazard assessments as the introduction. To discuss the possibility of the use of the municipality of tsunami hazard assessments current status and Issues of tsunami measures, organize the opinion and negative opinion aggressive to report the problem extraction.

Keywords: tsunami, hazard, public disclosure, disaster mitigation, probabilistic

## Reconstruction of paleo earthquake intensity

INOUCHI, Yoshio<sup>1\*</sup> ; OKUMURA, Yuka<sup>2</sup> ; NAMEKI, Katsuhiko<sup>3</sup>

<sup>1</sup>Faculty of Human Sciences, Waseda University, <sup>2</sup>School of Human Sciences, Waseda university, <sup>3</sup>Graduate School of Human Sciences, Waseda University

Many drastic earthquakes have been occurred historically in Japan. In order to reduce damages caused by those earthquakes, data concerning frequency, magnitude and influenced areas of each earthquake are inevitable. Here, we report measuring method of paleo intensity of historic earthquakes at arbitrary selected stations based on empirical formulas. Based on data regarding position of epicenter and magnitude of each paleo earthquake, intensity of paleo earthquake at arbitrary site is estimated. At the beginning, these data were used to recognize earthquake triggered turbidites at several lakes. The results show that lower threshold of triggering turbidites are 45gal in Lake Biwa and 79gal in Lake Inawashiro, respectively. Usage of this kind of method will enable us to reconstruct paleo earthquake data which have no written record.

Keywords: paleo earthquake, intensity of quake, sediment

## An overview on current status of public disclosure for tsunami hazard information in and around Japan

OSADA, Masaki<sup>1\*</sup> ; NAKAMURA, Hiromitsu<sup>1</sup> ; HIRATA, Kenji<sup>1</sup> ; OHSUMI, Tsuneo<sup>1</sup> ; FUJIWARA, Hiroyuki<sup>1</sup>

<sup>1</sup>National Research Institute for Earth Science and Disaster Prevention

A probabilistic tsunami hazard assessment research work is currently conducting by the National Research Institute for Earth Science and Disaster Prevention (NIED) (Fujiwara et al, 2013, Hirata et al., 2014). It is well recognized that output from such assessment should be transferred to the public as understandable and utilizable informations in various stages on hazard prevention works. From this point of view, as part of this project, we make a brief survey on how and what sort of hazard informations local residents are receiving from administrative authorities or agencies in and around Japan. Survey is focused on hazard map which is reachable through internet. In this paper, results are summarized in two categories, 1) type of maps and 2) distribution methods. Category 1 is able to divide into four subgroup; 1a is due to tsunami height map at shore (ex. Australia), 1b is tsunami inundation depth map which are based on the simulations on worst, most probable case, or probabilistic case (ex. most of Japanese prefectures, Indonesia, Oregon and Washington, USA), 1c is tsunami evacuation map in which zones to be quit are shown according to the warning level (Wellington, NZ, Oregon and Hawaii, USA), and 1d tsunami regulation map which prohibits (Oregon, USA). These maps are based on probabilistic or deterministic assessment outputs. Tsunami hazard informations are available mainly in style of the poster (downloadable in PDF format) although Web mapping (ex. Hawaii, USA) or GIS format (ex. Australia) can be found. Later seem to urge a user to secondary or further utilization. This survey suggests that it should be to provide tsunami hazard assessment results in various ways of presentations which meet user's purposes.

Keywords: tsunami, hazard information, disclosure, hazard map, utilization

## Pore water pressure in slopes composed of multi-layer geological structure

IMAIZUMI, Fumitoshi<sup>1\*</sup> ; MIYAMOTO, Kuniaki<sup>2</sup>

<sup>1</sup>Graduate School of Agriculture, Shizuoka University, <sup>2</sup>Faculty of Life and Environmental Sciences, University of Tsukuba

Increasing in pore water pressure in the slopes during heavy rainfall events is considered as an important factor inducing landslides. Sliding surface of many of these landslides locates on the boundary between different rock/soil strata. We need to know spatial distribution of the pore water pressure in slopes composed of multi-layer geological structure in order to explain occurrence mechanism of these landslides. Many of prior studies generally analyzed slope stability under condition that the pore water pressure is same as the hydrostatic pressure. These studies ignored influence of depth profile of hydraulic parameters on magnitude of the pore water pressure. We, therefore, tried to understand spatial distribution of the pore water pressure on the basis of the continuity equation and equation of motion for seepage flow in two-dimensional slopes with multi-layer soil structure. Our study clarified that the water velocity as well as the depth profile of the pore water pressure are affected by depth profile of the hydraulic conductivity in the saturated zone. Pore water pressure agrees with hydrostatic pressure in case that the saturated zone develops on the impermeable soil layer. Meanwhile, pore water pressure is smaller than hydrostatic pressure in case that bottom of the saturated zone contacts with unsaturated zone. In this case, magnitude of the pore water pressure depends on the difference in the hydraulic conductivity between upper and lower layers. In addition, pore water pressure is highest at a layer boundary. Our analysis results agree with the general landslide characteristic that the sliding surface locates on a layer boundary.

Keywords: landslide, pore water pressure, multi-layer soil structure, seepage flow

## Landsliding phenomenon under abnormal weather conditions: a case study

WANG, Gonghui<sup>1\*</sup> ; SUEMINE, Akira<sup>1</sup> ; MATSUURA, Sumio<sup>1</sup> ; ARAIBA, Kiminori<sup>2</sup>

<sup>1</sup>Disaster Prevention Research Institute, Kyoto University, <sup>2</sup>National Research Institute of Fire and Disaster

To examine the initiation and movement mechanisms of landslides occurring during abnormal weather conditions, we have been monitoring a landslide on Nisenotani area in Miyazaki Prefecture, Japan. The monitoring items include the weather conditions (rainfall and air pressure), moisture content of surficial soil layers, groundwater table, and displacements (by means of borehole wire extensometer, surficial extensometer, and total station). Cracks appeared on the slope after a heavy rainfall and borehole investigation revealed that this landslide is a large compound one, consisted of several sub-blocks. Our dense monitoring is performed on a small block of the toe part, and our results showed that: (1) landsliding was initiated by a heavy rainfall, but was not less affected by small rainfall; (2) landsliding varies with air-tide; (3) lower part of the sliding sub-block had been continuously compressed; (4) the sliding surface and the compressed soil layer had been effectively identified by means of a surface-wave technique.

Keywords: Abnormal weather, air pressure, Rainfall, landsliding, groundwater table

## Extreme Rainfall Effect on Slope Hazards along Mountain Roadway

WANG, Chao-wen<sup>1\*</sup> ; YOSHIMI, Kazuhiro<sup>1</sup> ; YAMADA, Tadashi<sup>1</sup>

<sup>1</sup>Graduated School of Science and Engineering, Chuo University

Due to the global climate changes, the scale and frequency of natural disasters are more difficult to predict and measure. Extreme rainfall often brings astonishing amount of water and causes very serious damage in the mountain areas. And for different environment conditions, the slope hazards induced by rainfall would be different like geology, topography or location. Therefore in this research, the authors considered the elevations, slope aspect, slope gradient and geology to compare and analysis the rainfall effect on slope hazards by using the historic landslides records. And the major method of rainfall analysis is the snake line model that is using dual-indexes of rainfall- short term rainfall intensities and accumulated rainfall data. Short term rainfall intensities mean hourly rainfall, 3 hourly rolling rainfall, 6 hourly rainfall and so on. The most important of these rainfall analyses are trying to find some regulars in occurrence of slope hazards. Furthermore, the authors also collected different hazard types in order to try to get the rainfall characteristics of different disasters. In this research, the authors used the Da-Jia River upstream region (Taiwan) as the case study. In this region, over than half area the slope gradient is larger than 55%. Through the results of the analyses, the authors get some important conclusions. Firstly, in the environment conditions, the effects of slope gradient, elevation, and geology are obvious. Secondly, the effect of slope aspect is according to the rainfall events. Finally, in extreme rainfall events, the trend of occurrence time in different hazards can be observed. According to the above conclusions, it can be effective to make decisions to prevent disasters and reduce lost.

Keywords: Landslides, Rainfall

## Shallow Landslide Susceptibility Mapping for Selected Areas in the Philippines Severely Affected by Super Typhoon Haiyan

RABONZA, Maricar<sup>2\*</sup> ; FELIX, Raquel<sup>1</sup> ; ORTIZ, Iris jill<sup>1</sup> ; ALEJANDRINO, Ian kaye<sup>2</sup> ; AQUINO, Dakila<sup>2</sup> ; ECO, Rodrigo narod<sup>1</sup> ; LAGMAY, Alfredo mahar francisco<sup>2</sup>

<sup>1</sup>University of the Philippines Diliman, <sup>2</sup>Nationwide Operational Assessment of Hazards, Department of Science and Technology

Super Typhoon Haiyan, considered as one of the most powerful storms recorded in 2013, devastated the central Philippines region on 8 November 2013. In its wake, Haiyan left 6,190 fatalities, 28,626 injured and 1,785 missing, as well as damage amounting to more than USD 823 million. To mitigate damage from similar events in the future, it is imperative to characterize hazards associated with tropical cyclones such as those brought by Haiyan, with detailed studies of storm surges, landslides and floods. Although strong winds and powerful storm surges up 15-17 feet were the primary causes of damage, landslides studies are also vital in the rehabilitation of typhoon damaged areas. Cities and municipalities of Leyte (7,246.7 sq. km) and Samar (13,121 sq. km) provinces, the heaviest cities area during the onslaught of Haiyan, require detailed and up-to-date hazard maps for their rebuilding and disaster mitigation programs. In order to delineate areas susceptible to rainfall-induced shallow landslides and generate a worst-case scenario hazard map of the two provinces, Stability INDEX MAPPING (SINMAP) software was used over a 5-meter-resolution Interferometric Synthetic Aperture Radar (IFSAR)-derived digital elevation model (DEM) grid. SINMAP has as its theoretical basis in the infinite plane slope stability model. Topographic, soil-strength and hydrologic parameters (cohesion, angle of friction, bulk density and hydraulic conductivity) were used for each pixel of a given DEM grid to compute for the corresponding factor of safety. The landslide maps generated using SINMAP are found to be highly consistent with the landslide inventory derived from high-resolution satellite imagery dated 2003 to 2013. The landslide susceptibility classification found in the landslide hazard maps are useful to identify no-build, areas that can be built upon but with slope intervention and monitoring as well as places that are safe from shallow landslides. These maps complement the debris flow and structurally-controlled landslide hazard maps that are also being prepared for rebuilding Haiyan's devastated areas.

Keywords: Natural Hazards, Landslide, Hazard Mapping

## Calculation of Shallow-Landslide Rainfall Threshold for Libon, Albay, Philippines Using TRIGRS

ALEJANDRINO, Ian kaye<sup>1\*</sup> ; ALEMANIA, Maneka kristia<sup>1</sup> ; AQUINO, Dakila<sup>1</sup> ; ECO, Rodrigo narod<sup>1</sup>

<sup>1</sup>DOST Project NOAH

In a rainfall event caused by a cold front and a low pressure area during the 14th until the 21st of February 2008, the Albay province experienced several landslides with \$4.6 million in damages to infrastructure alone. Aside from delineating areas that are highly susceptible to landslide, it is important to determine shallow-rainfall threshold aid in the development of an early warning system. The study area was carried out on an area in Libon town in Albay with approximately 1000 residents living near the high hazard area. Using TRIGRS software (Transient Rainfall Infiltration and Grid-based Regional Slope-stability analysis), 6 different sustained rainfall intensities with the duration of 24 hours were simulated to a 5-meter resolution IFSAR (Interferometric Synthetic Aperture Radar)-derived DEM (Digital Elevation Model). Topographic, soil strength, and hydrologic parameters were assigned to each pixel of the given DEM grid to compute for the factor of safety using the theory on Infinite Plane Slope Stability to produce a shallow-landslide susceptibility map. The values of the different rainfall intensities were selected to represent different rainfall events equal (1.26mm/hr), less than (.5 and 1mm/hr) and greater than (1.5, 2.73, 7.5 mm/hr) the infiltration rate of the soil. After comparison, there were no observed differences in the hourly variation of the Factor of Safety Maps for 1.26 mm/hr and greater intensities. The rainfall threshold determined to be 4.5 to 5mm of effective accumulated rainfall on which the pixels that failed ( $FS < 1$ ) matched the landslide inventory from 2003-2014 and the shallow-landslide hazard map. This study shows that in determining rainfall thresholds for shallow landslides the effective infiltration rate and hydraulic diffusivity of the soil serves as factors on how fast the slope reaches instability during a rainfall event. The results of this study may be treated as the worst case possible due to the sustained intensities and may be further improved through simulations using data of actual rainfall events, considering varying rainfall intensities and durations.

Keywords: Landslide, Shallow, Rainfall, GIS, Albay, Philippines

## Sensitivity of the initiation of debris flow to initial soil moisture

HU, Wei<sup>1\*</sup> ; XU, Qiang<sup>1</sup> ; WANG, Gonghui<sup>2</sup> ; VAN ASCH, T.w.j.<sup>3</sup> ; HICHER, Pierre-yves<sup>4</sup>

<sup>1</sup>State Key Laboratory of Geo-Hazard Prevention and Geo-Environment Protection, Chengdu University of, <sup>2</sup>Disaster Prevention Research Institute, Kyoto University, Japan, <sup>3</sup>Faculty of Geosciences, Utrecht University, Heidelberglaan 2, 3584 CS, The Netherlands, <sup>4</sup>LUNAM University, Ecole Centrale de Nantes, CNRS UMR 6183, France

The initiation of debris flows is commonly attributed either to fluidization as a result of rainfall induced landslides or to gully erosion induced by concentrated run-offs. A series of flume tests have been performed to show how the initial soil moisture influences the initiation of debris flows. At the start of each experiment, surface run-off was generated over loose granular deposits, triggering debris flows. These experimental debris flows enacted different scenarios according to the small variations among the initial soil moistures. In the loose granular deposits with initial soil moistures ranging from 1% to 5%, most run off water could infiltrate and trigger a landslide, which accelerated within one second to speed over 1 ms<sup>-1</sup> and then transformed into a debris flow. In the same soil deposits with initial moistures >5% or <1%, the debris flow was initiated by slow gully erosion with episodic events of damming and breaching due to small-scale landslides occurring on the side-slopes of the erosion valley. The slope failures were not triggered by positive pore pressure but by a decrease in suction due to the wetting of the soil. This suction decrease in initially unsaturated slopes explains why the transformation of these slope failures into debris flows are due not only to an increase of pore pressure leading to soil liquefaction, which is one of the expected triggering mechanisms, but also to a loss of the cohesive strength of the soil.

Keywords: debris flow, soil moisture, initiation

## Gully development on flows and deep-seated slides in the Mangaoporo catchment, North Island, New Zealand

PARKNER, Thomas<sup>1\*</sup>

<sup>1</sup>College of Geoscience, University of Tsukuba

Mass movements and gully erosion are widespread phenomena in many steep, erosion prone catchments. Understanding gully erosion on unstable slopes is important for the management of slopes as well as for management of river systems, as large quantities of sediment are supplied by gully erosion directly into river systems causing off-site damage.

The development of gullies on unstable slopes is not well understood. In this study gully development on slopes affected by mass movements was analysed in 14 headwater catchments of the Mangaoporo catchment, North Island, New Zealand. Bedrock consists of Cretaceous-aged, highly crushed and sheared mudstones and sandstones. Deforestation by European settlers at the beginning of the 20th century for pastoral farming was followed by reforestation for wood production from the 1980s. Sequential aerial photographs from 1939 to 2005 were interpreted to map mass movements and the development of gullies. Digital elevation models were extracted from aerial photography using ERDAS to assess the applicability of the commonly applied topographic threshold approach for gully incision.

Flows of varying depth occurred in all catchments underlain by mudstone, while the catchment consisting of alternations of mudstone and sandstone were affected by deep seated sliding and secondary shallow sliding. Deep (few meters to 15m) gullies were located at the toe of mass movement bodies. Such gullies developed oversteepened sidewalls, which in turn initiate extensive mass movements at the gully walls. Shallow (about 1 -2m deep), hundreds meter long gully arms extended upslope. Topographical changes by active flows and slides caused stream capture or gully destruction. Cracks and scraps functioned as incision pathways.

The topographic threshold approach is not appropriate for unstable slopes, as the mass movement topography exhibits irregular drainage pattern and gully incision depends on the morphology of mass movements. New approaches need to be developed for gully incision on unstable slopes to understand the spatial and temporal variability of incision dynamics on unstable slopes.

Keywords: gully erosion, flow, slide, New Zealand

## Quantifying the seismic response of slopes: observed and modelled amplification from the Port Hills of Christchurch

MASSEY, Chris<sup>1\*</sup> ; KAISER, Anna<sup>1</sup> ; HOLDEN, Caroline<sup>1</sup>

<sup>1</sup>GNS Science

**ABSTRACT:** Before the Christchurch 2010/11 earthquake sequence the influence of site effects on landslide triggering during earthquakes was reported in many studies, but evaluating these effects has been difficult through lack of high-resolution data, especially the lack of local ground motion instrumental observations. As a result of the Christchurch 2010/11 earthquake sequence we now have high temporal and spatial resolution data, including subsurface geotechnical and geophysical information that allows quantification of the amplification relationships between the near surface geology, topography and seismic inputs.

This paper presents preliminary results on site effects in the Port Hills of Christchurch caused by near surface material impedance contrasts and slope morphology. Results from small scale temporary arrays installed on several of the large rock slopes that failed repeatedly during the earthquakes suggest amplification factors of up to 300% of peak ground acceleration when compared to free field rock outcrop peak ground accelerations. These are corroborated not only by two dimensional seismic site response analyses using synthetic earthquake motions as inputs to the models but also by comparing recorded ground motions from borehole and surface seismometers.

Based on these findings it is apparent that particular slope shapes and material contrasts can significantly amplify peak ground accelerations during earthquakes. At present in New Zealand such amplification effects are not routinely taken into account when designing earthworks or structures on slopes or in landslide risk assessments.

Keywords: Earthquake induced landslides, topographic amplification, earthquake hazards

## Distribution loess landslides triggered by the 1920 Haiyuan earthquake and their formation mechanisms

HUANG, Runqiu<sup>1\*</sup> ; PEI, Xiangjun<sup>1</sup> ; HAN, Xiangsen<sup>1</sup> ; ZHANG, Xiaochao<sup>1</sup>

<sup>1</sup>Chengdu University of Technology

The 1920 Haiyuan Earthquake ( $M=8.5$ ) is one of the strongest earthquakes in Chinese modern history, and directly resulted in more than 200,000 people dead. The Earthquake induced a large number of landslides. Among them, we investigated 544 landslides in the meizoseismal area, and found that the distributions of the landslides are mainly concentrated in the southeastern part of the seismogenic fault, but the relationship with the NW-trending seismogenic fault is not noticeable. Further investigation indicated that such distribution is mainly controlled by two types of factors. One is the nearly SN-trending secondary faults concealed under the loess cover. The other one is the thickness of the loess. The landslide is more intensive in those areas with thicker loess and the density of the landslides decreases with the decreasing in the loess thickness, while landslides occurring in the bedrocks are very rare.

Investigation shows that the sliding surface of a large number of loess landslides is extremely gentle with the apparent friction angle ranging between 8 -11 degrees. Liquefaction phenomenon was found on a large number of areas in loess tableland along both sides of the river in the meizoseismal area. This is likely one main reason for the occurrence of landslides with very gentle sliding surface angle. Laboratory testing of undisturbed loess of these regions indicated that the sand content ranges from 3% to 15%, silt content is about 65% - 85%, clay content between 10% - 20%, and thus this kind of soil belongs to silt. But the sand content showed uneven distribution and high sand content occurred in local area. Dynamic triaxial tests showed the saturated loess could suffer from liquefaction failure.

However, there existed a large number of low angle slip surface, large runout and high mobility loess landslides in the slope zone with low underground water level. Loess is characterized by large pores with high compressibility and low strength. Scanning electron microscopy revealed that cement of loess particles were dispersed particulate, distributed discontinuously attached to the particle surface or accumulated at the point of the contact in the skeleton, the adhesive strength is very low. The earthquake occurred in December of that year's winter. Due to very low water content of loess, relatively dry shallow loess easily shattered and collapsed under strong shaking of extreme earthquake. Therefore this caused occurrence of the high-speed and long runout landslide.

Finally, we conclude that because of the special geological characteristics of loess, there are more than two types of landslide mechanism: one is the liquefaction occurring on the loess layer affected by the groundwater level; the other one is the collapse of loess structure under strong earthquake.

## Geomorphological and Geological Features of The Collapsing Landslides Induced by The 2009 Padang Earthquake.

NAKANO, Maho<sup>1\*</sup> ; CHIGIRA, Masahiro<sup>2</sup>

<sup>1</sup>CTI Engineering Co., Ltd., <sup>2</sup>Disaster Prevention Research Institute, Kyoto University

The Mw7.6 Padang earthquake in 2009 attacked the northwest of Sumatra, Indonesia, and triggered many landslides, which killed at least 130 people at one village. We made satellite image interpretations, field investigations, and laboratory tests to identify the geomorphological and geological features of these landslides. As a result, we found that the number of landslides was 159, materials that slid were pumice fall deposits, and their sliding surface was made within the base of the pumice layer where pumice grains were mixed with underlying lahar and heavily weathered. These landslides had the following characteristics: 1) they occurred in the areas with pumice beds with >3 m thickness, which was controlled by the distance from their source; 2) the pumice fall deposits had a slope-parallel layering, which had been cut at the foots of slopes; and 3) the mixed layer at the base of the pumice beds was heavily weathered to be clayey materials with abundant halloysite.

We made an isopach map of the pumice fall deposits, which is so-called Qhpt and believed to be from Maninjau Caldera. The isopach contours, however, showed that Qhpt is from Tandikat Volcano, and that landslides occurred in clusters in the areas with pumice beds thicker than 3.5 m.

Qhpt beds had slope-parallel bedding, but they were undercut by subsequent river incision. Interpretations of stereoscopic satellite images and field surveys showed that there are four terraces along the Magung River, and Qhpt covers widely distributed higher terraces (Lh) of lahar younger than 80 ka and middle terraces (Lm) but are cut by lower terraces (Ll1 and Ll2) as well as small nearby tributary gullies. This undercutting likely reduced the support of Qhpt beds from downslope.

The mixed layers, in which sliding surfaces were formed, were heavily weathered and very weak; weaker than the main Qhpt above and the lahar below. XRD analyses showed that pumice grains of the main part of Qhpt scarcely had halloysite but pumice grains and weathered lahar in the mixed layers were rich in halloysite. The formation of halloysite could be attributed to the interaction between the materials of the mixed layers and the water coming through Qhpt beds; water, which gets Si and other chemical components from the volcanic glass of pumice, may become stagnant in the mixed layers because they are much less permeable than the Qhpt beds above. This would be a preferable condition of halloysite formation.

Infinite slope stability analysis using geotechnical parameters, pumice bed thickness, and slope angles, which we obtained, suggested that landslides with sliding surfaces within the mixed layers could be triggered by the shaking of the 2009 Padang earthquake. The natural water contents of the materials of the mixed layers exceeded their liquid limits, which suggests that they would behave like a liquid after remodeling.

The geological history, which is volcanic eruption, weathering, and undercutting by river incision as stated above, is typical in tropical volcanic areas. That means we can make a hazard map of such a catastrophic landslide induced by earthquakes on the basis of geological development.

Keywords: 2009 Padang earthquake, Halloysite, Collapsing landslide, pumice fall deposits, weathering

## The seismic signals from the model slope failure and erosion tests

FENG, Zheng-yi<sup>1\*</sup> ; YU, Chia-cheng<sup>1</sup>

<sup>1</sup>National Chung Hsing University, Taiwan, ROC

High intensity rainfalls in mountainous areas often induce floods. The floods could erode riverbank slopes and cause them to landslide. This study selected Landao Creek of Huisun Experimental Forest (Nantou, Taiwan) as the in-situ test site for the model slope failure and erosion tests. We built a large size model soil slope and an artificial landslide dam in Landao Creek for the tests. The Nengau agricultural channel at the upstream of Landao Creek was setup to control the inflow to Landao Creek. Therefore, the artificial landslide dam were overtopped when the retention space were full by the inflow water. Consequently, the dam breached and caused the model soil slope to be eroded by the flooding water. The model soil slope failed partially due to the erosion and generated seismic signals during the slope materials sliding down. We installed of several accelerometers sensor on the model soil slope to collect seismic signals generated. We present two test results in this study. The seismic signals were analyzed using the Hilbert-Huang Transform for time-frequency spectrograms. We explored the characteristics of seismic signals due to the model soil slope sliding and the flooding. In addition, we can use the time-frequency spectrograms to identify the timings when the model slope slid repeatedly.

Keywords: Landslide, slope, erosion, seismic signal, flood, dam

## Characteristics of the slope failures in Izu-Oshima Island on Oct. 16, 2013, inferred from seismic waveform records

DOI, Issei<sup>1\*</sup> ; KAMAI, Toshitaka<sup>1</sup> ; WANG, Gonghui<sup>1</sup> ; MORITA, Yuichi<sup>2</sup>

<sup>1</sup>DPRI, Kyoto Univ., <sup>2</sup>ERI, Univ. of Tokyo

On Oct. 16, 2013, large-scale slope failure took place due to extreme rainfall in Izu-Oshima Island in Japan. The precipitation reached over 90 mm per hour from 1:00 to 5:00 before and during the period when the failures took place. Through geological surveys by us and Natural Disaster Research Council, piping holes were observed on the collapsed slopes, which suggested that the ground water spouted due to high water pressure. It is important to grasp the detailed behaviors of water and sediment movement in order to reduce the slope disaster in the volcanic regions.

Signals of failures and their related sediment movements were recorded many times by several seismometers installed around by Oshima Volcano Observatory of ERI, Univ. of Tokyo. The seismic signals were observed almost at the same time at several stations. Four major signals were detected from 2:00-3:00, while at least a few tens were observed from 3:00-5:00. These signals had unclear initial phases and long (several minutes) durations. The amplitudes increased almost at the same time at the beginning among the stations, while the times when they attained the maximum values were earlier at the stations located in the upper side of the slope. These facts indicate that the vibrations were firstly generated in the upper side of the slope, then moving toward the downside.

Acknowledgments: We used meteorological data recorded by JMA.

Keywords: slope failure, seismic waveform, sediment movement

## Friction law of gouges from monotonic and cyclic shear tests - implications for rockslide triggered by earthquakes

DONG, Jia-jyun<sup>1\*</sup> ; TETSUHIRO, Togo<sup>2</sup> ; LAI, Jun-rong<sup>1</sup> ; YANG, Che-ming<sup>1</sup> ; LEE, Chyi-tyi<sup>1</sup> ; SHIMAMOTO, Toshihiko<sup>2</sup>

<sup>1</sup>Graduate Institute of Applied Geology, National Central University, Taiwan, <sup>2</sup>State Key Laboratory of Earthquake Dynamics, Institute of geology, China Earthquake Administration

The differences of soil strength under static and dynamic loading have been well recognized. This study utilized rotary shear apparatus to elucidate the friction coefficient of gouge materials under monotonic and cyclic shearing conditions. A rigid block model incorporating the velocity/displacement dependent friction law from monotonic tests was adopted to simulate the dynamic shearing behavior. Basically, the friction coefficient under maximum shearing velocity was well depicted. However, the friction coefficient under zero velocity for dynamic shearing tests was overestimated. A frequency factor, which taking the healing effect into account, was successfully incorporated into the friction law to simulate the variation of the friction coefficient under dynamic loading condition. The modify friction law with consideration of the cyclic shearing frequency was used to evaluate the triggering of a dip slope rockslide during earthquake. It is illustrated that the cyclic shear induced from the earthquake is critical for the initiation of large scale rockslide. The influence of seismic loading on earthquake-triggered rockslide can thus be evaluated quantitatively.

Keywords: monotonic and cyclic shear, velocity and displacement dependent, friction coefficient, rotary shear test, gouge, earthquake triggered rockslide

## Fast Shear Behaviour of Granular Material and Rapid Landsliding Phenomena

JIANG, Yao<sup>1\*</sup> ; WANG, Gonghui<sup>2</sup> ; KAMAI, Toshitaka<sup>2</sup>

<sup>1</sup>Graduate School of Science, Kyoto University, <sup>2</sup>Disaster Prevention Research Institute, Kyoto University

Many rapid landsliding events are normally catastrophic in which granular masses flow with extremely low friction. In order to prevent and mitigate the disaster, it is essential to better understand their mechanisms of initiation, motion and deposition. Although a great deal of research and attention has been focused on the unusual physical features for rapid landsliding events, the dependence of frictional properties on particle characteristics and test conditions has not yet been clearly understood. In the present research, we performed a set of experimental studies to examine the grain-scale frictional properties. We used two kinds of glass beads to examine how particle size affected the strength and stability of granular materials by employing a large ring-shear, and sheared the samples by changing the shear rate from 0.1 to 100 mm/s under different normal stresses (50, 100, 200, 400 kPa). It was found that the influence of shear rate on the residual shear strength for glass beads was negligible, while the stress fluctuation was observed for different particle sizes. Three distinct spectral peaks were identified in the frequency spectra for the two glass beads by utilizing Discrete Fourier Transform (DFT) method. According to the frequency spectra, we found that the stress fluctuation of glass beads was closely related to the particle size. Then we analyzed the role of particle size in the fast shear behaviour of granular materials and their relationship to the rapid landsliding behavior of rock avalanche.

Keywords: fast shear behavior, rapid landsliding, glass beads, particle size, shear rate, stress fluctuation

## Changes in particle size distribution of clayey material at a catastrophic landslide base

TSOU, Ching-ying<sup>1\*</sup>; CHIGIRA, Masahiro<sup>1</sup>; FENG, Zhengyi<sup>2</sup>; HIGUCHI, Kohei<sup>3</sup>

<sup>1</sup>Disaster Prevention Research Institute, Kyoto University, Uji, Japan, <sup>2</sup>Department of Soil and Water Conservation, National Chung Hsing University, <sup>3</sup>Department of Civil Engineering, National Cheng Kung University

In August 2009, a catastrophic rockslide avalanche was initiated by a cumulative rainfall of 1676.5 mm by Typhoon Morakot in the southern mountainous region of Taiwan. The landslide occurred on slopes extending from head scarp to the opposite riverside with a fall height of 830 m and generated the runout distance of 3.2 km long. The mobility of the landslide was high, indicating by its low apparent friction angle of 14 degrees and velocity of 70 to 120 km hr<sup>-1</sup> in 95 s. The landslide claimed more than 400 people dead and missing when the village of Shiaolin was destroyed directly in the path of the landslide. We found clayey material in many locations at the base of the landslide deposits. Two samples S1 and S2 and one sample D1 of clayey material were respectively collected from the base of the remaining debris in the lower part of source area and the base of the deposits in the depositional area. Their mineralogy and particle size distribution were analyzed using an X-ray diffractometer (Rigaku Gaigerflex RAD IIB) and a laser diffraction particle size analyzer (Shimadzu, SALD-3100), respectively. The X-ray analysis indicates that the samples are the same material, in terms of texture and mineralogy, consisting of illite, chlorite, quartz, feldspar, and calcite. Besides, particle size analysis shows that samples S1 and S2 of the source area had two particle size modes at 15 μm and 50 – 100 μm, and sample D1 of the depositional area had one mode at 15 μm. This difference between the samples may reflect pulverization during movement of the material from the source area to the depositional area. The overall particle size distribution is narrower in sample D1, and the mean grain size (D<sub>50</sub>) decreased from 11.03 μm in sample S2 to around 8.96 μm in sample D1. Sample S1 has larger amounts of finer fractions than do samples S2 and D1, and its distribution curve has a flattened top in comparison with the other two samples, which could be attributed to intense shearing between bedrock and debris. The results suggest that the clayey material at the landslide base and the increasing fine-grained content of the clayey material during shearing are assumed to have a significant impact on its long, rapid movement.

Keywords: rockslide avalanche, high mobility, clayey material, particle size distribution

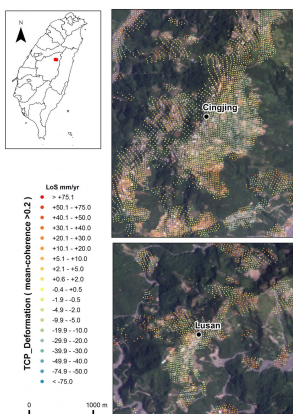
## Application of TCP-InSAR technique for the Deep-Seated landslides detection and monitoring at Cingjing village, Taiwan

LIU, Shouheng<sup>1</sup> ; LIN, Chingwei<sup>1</sup> ; CHEN, Roufei<sup>2\*</sup> ; ZHANG, Lei<sup>3</sup>

<sup>1</sup>Department of Earth Sciences, National Cheng Kung University, Taiwan, <sup>2</sup>Department of Geology, Chinese Culture University, Taiwan, <sup>3</sup>Department of Land surveying and Geo-informatics, Hong-Kong polytechnic university, Hong-Kong

Taiwan located at an active mountain belt and subtropical climate environment, severe gigantic landslide that have caused considerable damages commonly occurred in mountainous areas. After the 2009 Hsiaolin landslide that caused 450 casualties, how to identify potential sites of Deep-Seated landslides, evaluate their activity and susceptibility become an important issue. In the past few years, our research team has processed many slope failures that have caused considerable damages by using airborne LiDAR Digital Elevation Model (DEM), and implemented related analyses for the goal of deep-seated landslide. Cingjing village located at Centre Taiwan is well known as one of the three high altitude agriculture area in mountainous regions. In this study, we using TCP-InSAR interferometry from ALOS/PALSAR images to detect and monitoring the landslide activity and its susceptibility of deep-seated deformation over a large area. The method obtains more ground deformation information than other InSAR approaches, providing more comprehensive analytical results for the slope related hazard studies. Our TCP-InSAR result shows a significant subsidence pattern around the Cingjing area. Comparing the surface deformation data and the field investigation records, several imperceptible deep-seated landslide locations are found and the boundaries can be identified as well as the spatial distribution of instability to them. The deposition pattern also implies different landslide development types on the slopes. This case study shows the great potential of TCP-InSAR evaluating the slope activities and deformation in the vegetated mountain area. Combined with topography signatures from high resolution digital elevation model data, it will be an effective way to determine the stability of slopes and potential hazard locations over a large area.

Keywords: Deep-Seated landslides, TCP-InSAR technique, Airborne LiDAR, Cingjing village



## Preceding topographic features of catastrophic landslides in an accretion complex in the Kii Mountains

CHIGIRA, Masahiro<sup>1\*</sup> ; MATSUSHI, Yuki<sup>1</sup> ; TSOU, Ching-ying<sup>1</sup> ; HIRAISHI, Narumi<sup>2</sup>

<sup>1</sup>Disaster Prevention Research Institute, Kyoto University, <sup>2</sup>previously Fukada Geological Institute

Slope movements is one of the major processes of denudation as well as erosion and transportation by rivers or glaciers, and many slope movements themselves are induced by river or glacier erosion. We investigated the linkage of river erosion, deep-seated gravitational slope deformation, and catastrophic landslides in the Kii Mountains Japan, where occurred tens of catastrophic large landslides during 1889 Totsukawa typhoon and 2011 typhoon Talas. The consequent fatalities were 168 and 56, respectively. The Kii Mountains is underlain by the Cretaceous to Neogene Shimanto accretional complex in large areas and has paleosurface remnants in higher elevations. The paleosurfaces have been newly incised by rivers, of which the Kumano River catchment occupies the central part of the Kii Mountains. The new incision of the Kumano River proceeded with the upstream propagation of knickpoints, which developed well-defined convex slope breaks on interfluvial slopes. High-resolution DEMs clearly delineated deep-seated gravitational slope deformations, which are characterized by scarps, linear depressions, and bulges, aligned along the convex slope breaks, suggesting that they were induced by gravitational instability induced by the erosion undercutting. The catastrophic landslides during the 1889 Totsukawa typhoon and 2011 typhoon Talas occurred had been preceded by deep-seated gravitational slope deformation on newly incised inner valley slopes. Most of the landslides had sliding surfaces along undulating minor faults, probably thrusts, which might have made rock bridges when shearing along preferably oriented parts of the faults occurred. Catastrophic slope failure may occur when those rock bridges are finally fractured.

Keywords: gravitational slope deformation, landslide, accretion complex

## Recognition of large scaled deep-seated landslides using high resolution topography and case studies in Taiwan

HO, Dia jie<sup>1\*</sup> ; LIN, Ching-wei<sup>2</sup>

<sup>1</sup>(1)Disaster Prevention Research Center National Cheng Kung University, <sup>2</sup>(2)Department of Earth Sciences National Cheng Kung University Tainan Taiwan

High resolution topography and topographic characteristics of large scale deep-seated landslides (landslide area >10 ha) are used to interpret large scale deep-seated landslides in an area of 4980.8 km<sup>2</sup> and a total number of 1607 potential large scale deep-seated landslides are recognized. The results show that main distribution of potential large scale deep-seated landslides in Kao-Ping River watershed is near structural lineaments and both sides of the river.

Two cases discussed in the study are on the right bank of Baolai River in Baolai, Kaohsiung City and on the left bank of Luliao River in Yanping Township, Taitung County. Typhoon Trami (08/20~08/22), Typhoon Kong-Rey (08/27~08/29) and Typhoon Usagi (09/19~09/22) are main typhoon events of 2013.

Potential landslide area, average slope angle and main lithology of case I is 96.6 ha, 31.1° and argillite. GPS data show a maximum horizontal displacement of 27.6 cm to southwest and a maximum subsidence of 20.5 cm after Typhoon Trami and Typhoon Kong-Rey. Surface extensometer data show the extension amount of 8 cm and 5 cm after three typhoon events. Potential landslide area, average slope angle and main lithology of case II is 6.4 ha, 32.5° and slate. A landslide with an area of 2 ha happened in the range of case II after Typhoon Usagi. These two cases indicate that rainfall and riverbank erosion are important factors on triggering large scale landslides.

Keywords: deep-seated landslides, GPS

## The Assessment of Landslide Displacements Using Digital Photogrammetry and Numerical Analysis

CHANG, Kuang-tsung<sup>1</sup> ; LIN, Chun-te<sup>1\*</sup> ; SU, Miao-bin<sup>2</sup> ; CHENG, Min-chieh<sup>1</sup>

<sup>1</sup>Department of Soil and Water Conservation, National Chung Hsing University, Taichung 402, Taiwan., <sup>2</sup>Department of Civil Engineering , National Chung Hsing University, Taichung 402, Taiwan

Instead of comparing remote sensing images between before and after a landslide event, this study compares aerial photographs over the years with the velocities of surface movements of landslide to evaluate the feasibility of aerial photographs as a monitoring tool. Before the total collapse of the slope of Freeway No.3, there were signs showing sliding of the slope, but no equipment was set up for monitoring. We use GIS to discriminate aerial photographs of different years to evaluate the displacements of specific objects or marks. From 2002 to 2004, the average displacement was 49.5cm, and the average displacement rate was 23.7cm/yr; from 2004 to 2007, the average displacement was 22.5cm, and the average displacement rate was 7.3cm/yr.

According to time-dependent creep behavior, the primary creep might have occurred from the beginning of the excavation in 1998 to 2004. And the secondary creep was from 2004 to 2007, so the velocity was comparatively lower than the previous stage. As for the tertiary creep, the displacement rate might rise since 2007 till the total collapse in 2010. The software Plaxis 2D based on the finite element method will be used to analyze the displacement process of the slope. The numerical model is set up according to the digital terrain model (DTM) of the slope. The numerical results will be calibrated with the results of the digital photogrammetry. We expect to obtain the creep behavior of the slope such as the slope strength reduction with time and the changes of surface displacement rate with time.

Keywords: digital photogrammetry, Freeway No.3 landslide, displacement rate, creep

## Deformation Analysis of the Pliocene-Pleistocene Sedimentary Rocks Mountain using Lidar Data

ASAHINA, Toshihiro<sup>1\*</sup>

<sup>1</sup>PASCO CORPORATION

### 1.Introduction

Be a topic for the deformation of the Shimanto Supergroup in the Oigawa River basin and in the Kii Peninsula in many cases. How deformation of sedimentary rocks of the Pliocene to Pleistocene age strata earlier age and lower strength than the Shimanto Supergroup is in progress, I report on the basis of the analysis result of airborne Lidar data. The study area is the mountain in Tsunan of Niigata Prefecture around located on the border between Nagano and Niigata Prefecture. Geologically, the study area is located in the south side of the Matsunoyama dome and the Uonuma formation of Pliocene to Pleistocene age is widely distributed.

### 2.Mountain block geology and geomorphology

The northwestern part of Tsunan is a steep mountain of 1100m altitude from 200m, where the Uonuma formation, being of sand, silt, alternating beds of silt and sand, massive silt and volcanic rocks, is distributed. The investigation mountain has a monoclinic structure facing the Shinanogawa River on geological structure, which the Uonuma formation dips 40 degrees from 15 degrees SE generally and shows a monotonic spread to the whole.

In this area, a number of landslides have occurred, but at the time of the earthquake in northern Nagano Prefecture (March 12 2011, M6.7, depth: 8km, epicenter: Sakae village in Nagano Prefecture), the large plane slip presumed to be caused by this earthquake has occurred.

### 3.Lidar data

An airborne Lidar survey was conducted on May 14, 2013 for the morphological analysis of the northwest mountain of Tunan. Lidar measurement was carried out in the range of about 30km<sup>2</sup> by ALS60 system. The Lidar point data were interpolated using a natural neighbor method on a grid with 1.0m spacing.

In order to understand the characteristics of the mountain deformation, I analyzed the mountain terrain in the following procedure.

#### 1)Analysis 1

a.Classification of slope gradient (a grid with 5.0m spacing),b.Extraction of the cells of 40 degrees from 15 degrees slope gradient,c.Analysis of surface structure,d.Extraction of bedding surface slopes that is likely to cause a slip

#### 2)Analysis 2

a.Image analysis,b.Extraction of linear deformation terrain , such as a lineation or an edge,c.Extraction of deformation terrain surface, such as a depression zone,d.Integrated analysis of analysis 1 and 2

#### 4.Discussion

The GIS analysis of the cells obtained by the process of Lidar data and GIS processing has revealed that the slopes which are considered to bedding plane are found very widely in the mountain. Furthermore, based on the morphological features obtained, the two mountain blocks with a trace of a slip plane as the bedding planes were extracted. These mountain slopes have a characteristic of both showing a bedding plane sliding surface morphology on the terrain surface and the irregular linear trough. The largest linear trough is running diagonally across the hillside slope, and its extension reaches 600m from 550m. The thickness of the terrain block forming a linear trough is about 10m from 6m maximum. These morphological features suggest that the bedding surface played a major role in events that may have caused the extensive deformation and collapse of the edifice. The above is a morphological characteristic that is not found in such the Shimanto Supergroup.

These are important key points in extracting mountain deformation due to the bedding slip.

#### 5.Conclusions

By the analysis of Lidar data, it has been confirmed the distribution of distinctive slopes to suggest that the edifice extensive deformation has occurred in the past in this area.

#### 6.References

Takeuchi, K., et al. (2000) Geology of the Matsunoyama Onsen District. With Geological Sheet Map at 1:50,000, Geol. Surv. Japan, 76p. (in Japanese with English abstract 5p.).

Yanagisawa, Y. et al. (2001) Geology of the Iiyama district. With Geological Sheet Map at 1:50,000, Geol. Surv. Japan, 144p. (in Japanese with English abstract 6p.).

Keywords: Lidar, surface morphology, bedding plane slip, line trough, edifice deformation

## Interaction between river bed condition and debris flow in Ichino-sawa subwatershed of Ohya-kuzure landslide, Japan

TSUNETAKA, Haruka<sup>1\*</sup> ; HOTTA, Norifumi<sup>1</sup> ; IMAIZUMI, Fumitoshi<sup>2</sup> ; HAYAKAWA, Yuichi S.<sup>3</sup>

<sup>1</sup>Life and Environmental Sciences, University of Tsukuba, <sup>2</sup>Graduate School of Agriculture, Shizuoka University, <sup>3</sup>Center for Spatial Information Science, The University of Tokyo

In recent years, there has been significant concern about large-scale sediment movements, such as deep-seated landslides, that are expected to occur more intensively due to changes in rainfall patterns. These landslides not only induce immediate sediment disasters downstream but also produce a large amount of unstable sediment that is transported gradually following the landslide. Most of the unstable sediment residing in a deep-seated landslide area is first discharged as debris-flow forms. Thus, after the occurrence of landslides, debris flows have a long-term affect on the watershed regime through their impact power, riverbed aggradation, and the production of turbid water, among other effects.

To facilitate better prediction of debris flows from landslide areas, this study investigated the interactions among topographic conditions, bed-material conditions, and debris flow events in a headwater catchment where a deep-seated landslide had occurred.

The study site was the Ichino-sawa subwatershed in the Ohya-kuzure basin, Shizuoka Prefecture, Japan. The basin experienced a deep-seated landslide about 300 years ago and is currently actively yielding sediment with a clear annual cycle. During the winter season, sediment moves from the hillslope to the channel bed because of freeze-thaw activity and weathering. In the summer season, the deposited sediment is discharged incrementally by debris flows related to storm events.

Topographical surveying and grain-size analysis were carried out several times between November 2011 and November 2013. Point cloud data were acquired during the topographical surveying, using a ground-based laser scanner, and used to create a high-resolution digital elevation model. Grain-size analysis was conducted in the upper, middle, and lower parts of the study site. A line-grid method was employed for the in situ analysis, and the fine particle fraction was determined by sieving the sampled materials. Debris flow occurrences were also being monitored in the same period by a sensor-triggered video camera. Rainfall was observed during the summer season for comparison with debris flow occurrence and magnitude.

Several debris flows with different magnitudes were observed during the study period. Although rainfall events in the early spring season altered bed inclination, the thickness of deposited sediment, and the grain-size distribution of the bed material, more significant changes were detected after the debris flows. While the initial grain-size distribution in early spring was roughly identical over the study site, the subsequent grain-size distribution changed differently, according to location. The source, transport, and deposition areas of the debris flows were different among different rainfall events, resulting in different transitions in geomorphic conditions at different locations. The lower part of the study site changed from a source area to a deposition area through the summer season.

A comparison of the topographic conditions, bed-material conditions, and debris flow events indicated that, in addition to the conditions of the triggering rainfall, topographic and bed-material conditions affected debris flow occurrence and magnitude. These interactions could be observed in the deep-seated landslide area, where a substantial and continuous supply of sediment prevents stabilization of the channel bed through exposure of bedrock or by armoring of bed materials.

Thus, to predict the long-term impact of large landslides, it is necessary to assess the subsequent debris-flow discharge considering the sediment dynamics and changes in topographic and bed-material conditions in the landslide area.

Keywords: debris flow, deep-seated landslide, topographic condition, grain size distribution

## Deep seated landslides along the geological structure in Chishan River Watershed, southern Taiwan

LIAO, Chi-yueh<sup>1\*</sup> ; LIN, Ching-weei<sup>2</sup>

<sup>1</sup>) Disaster Prevention Research Center National Cheng Kung University, <sup>2</sup>Department of Earth Sciences National Cheng Kung University Tainan Taiwan

Landslide is the common nature hazard in Taiwan. The Typhoon Morakot in 2009 brought huge precipitation and induced severe hazards in south-central and eastern Taiwan. Except the landslides, debris flow and flooding hazards induced by Typhoon Morakot, the large scaled deep seated landslides deserve more attention because they may cause the destructive disaster.

The Chishan River watershed which covered 750 km<sup>2</sup> is selected as study area. The study area is mainly compose of metamorphic and sedimentary rocks. Within the study area, 313 sites greater than 10 ha with sliding topographic features of deep seated landslide such as crown main escarpment, down slope scarp ,and lateral cracks are recognized from LiDAR derived 1 m resolution DEM, and we noticed the distribution of these sites is close to the structure in our study area. In order to know the influence of structure in the development of deep seated landslides, landslide density are calculated. The landslide density decreases with increasing distance and there are 79% of. deep seated landslides developed along the structure with a 1km buffer zone. The Result indicates that deformation zone associated structure is crucial in the development of deep seated landslides in the study area.

Keywords: Chishan River watershed, deep seated landslides, geological structure

## Natural-technological disasters of recent years in Japan and Russia: social and economic consequences

PETROVA, Elena<sup>1\*</sup>

<sup>1</sup>Lomonosov Moscow State University

During the last decade, natural hazards impacts on people, the environment, urban and industrial areas, infrastructure and other technological systems were increasing, causing large social, environmental and economic damages in many countries. The number and severity of natural-technological accidents and disasters were also increasing all over the world, because of these impacts. The term "natural-technological" applies to an accident (disaster) in the technosphere (including industrial plants, power stations, transport, infrastructure facilities, communication lines, etc.) triggered by any natural process or phenomenon. Their growth is accounted for: 1) by observed increasing in frequency and intensity of various natural hazardous events; 2) by much more complicated structure and complexity of modern technological systems and facilities exposed to natural hazards, and 3) by increasing advancement of economic activities and population into the regions at natural risk. The most severe consequences for people and the environment have the so-called Natech-accidents, which are accompanying by release of dangerous substances (like chemicals or oil), and accidents at nuclear power stations.

One of the most large-scaled natural-technological disasters having enormous social, environmental and economic consequences occurred on March 11, 2011 in Japan due to a massive 9.0-magnitude earthquake off the northeast coast of Honshu Island, which triggered a more than 30-meter tsunami. The disaster not only caused a large direct and indirect damage to the people (about 20 thousand fatalities) and economy of the country (more than \$500 billion), but also influenced on regional, national and international development reaching a truly global scale. It clearly demonstrated high vulnerability of a human society and modern technosphere to natural disasters; even in a country like Japan that is highly developed and well-prepared to natural risks. A distinctive feature of events, such as of the 2011 Tohoku earthquake, is their multihazard and synergistic nature, as a disaster spawns a secondary disaster that increases the impact on people and technosphere, resulting in simultaneous occurrences of numerous technospherical accidents. The secondary effects of natural-technological accidents can be even much more serious, such as at "Fukushima-1" nuclear power plant. These impacts are the more severe the higher are the population density and concentration of industrial facilities and infrastructure (especially hazardous and vulnerable objects) in disaster-affected areas. In addition, all rapid reaction forces and resources tend to be primarily fighting natural disaster; it limits the capability to eliminate secondary technological impacts, especially in those situations when transport facilities and required infrastructure are destroyed, and economic communications are broken.

The lessons of the Tohoku disaster should be taken into consideration while placing, constructing and operating nuclear power plants and other high-risk facilities. It is necessary to consider carefully possible intensity and frequency of all potential impacts, including natural hazards.

In Russia, natural-technological disasters with catastrophic consequences occur not so often. However, their possibility should be taken into account, especially in the economic development of areas at high natural risk, which is, for example, the Far Eastern region exposed to earthquakes, tsunamis, volcanic eruptions, floods, strong winds, storms, heavy rain- and snowfalls and other natural hazards. The most severe damages caused the Sakhalin earthquake in 1995, which was the most destructive in the Russian history. Severe social and economic consequences cause floods, for example, the flood in the autumn 2013. Natural-technological risk to the regions of Russia was evaluated using a database that was created by the author.

Keywords: natural hazards impacts, social and economic consequences, natural-technological risk, natural-technological disaster

## The Egyptian Tempest Stele: an Example of Ancient Natural Disaster

PETROVA, Anastasia<sup>1\*</sup>

<sup>1</sup>Institute of Oriental Studies, Russian Academy of Sciences

Some Ancient Egyptian texts tell us about violent storms and rains. One of the most impressive ancient accounts of natural disasters is the so-called Tempest stele (1550 BC), which describes a very destructive storm happened under Ahmose I, the king of Egypt's 18 dynasty. The upper portion of the stele describes the catastrophe. Many essential details are given, such as the specific noise, overall darkness etc. Numerous houses were washed into the river; temples, tombs and pyramids were badly damaged. The main features of the storm can be highlighted: torrential rain; darkness; and loud noise, probably caused by a thunder or a wind, or both. It evidently occasioned large-scale flooding, property damage, and loss of life. After describing the events, the stele gives account of the restoration works made by the king to repair the damages made by this great disaster. There are Egyptologists who believe the stele to be propaganda put out by the pharaoh, the "tempest" being the depredations of officials of the embattled seventeenth dynasty of Egypt drawing upon the financial resources of the temples during the escalating conflict with the Hyksos. To my opinion, we don't have sufficient grounds to deny that the storm took place in reality. Nevertheless, the Tempest Stele actually is a political propaganda, because the main purpose of the erection of the stele was to draw attention to the role of the king in coping with the disaster. Traditionally, the king was responsible for maintaining maat (a cosmic order as opposed to chaos), and this responsibility included protection from natural disasters. The main point of the specific political context of the Ahmose I's times was the struggle of what would become the 18th Dynasty to establish its rule in opposition to the Hyksos. This effort required success on two levels: the human and the divine, which meant what would be classified as the natural world today. To simply liberate the land from Hyksos rule was a necessary but not sufficient step to legitimate one's rule. The king also needed to demonstrate divine blessing meaning that the cosmic order of the natural world had been restored as well as the political world had been. The storm commemorated by the Tempest stele is not the only example of heavy storms in Egypt. It seems that hazards of that kind were more common than we now believe. What makes the Ahmose stele unique is the description of the details of such a severe catastrophe, which go beyond what is usually experienced by a regular storm and therefore might be the oldest description of a natural hazard. The catastrophe described in the Ahmose I's Tempest Stele can be considered one of the most ancient examples of natural disasters, which caused a huge impact on the society. This is also a significant example of a political propaganda, reflecting the situation when government uses a catastrophe and its consequences to its own benefit.

Keywords: natural disaster, social impact, history of disasters, ancient egypt

## Relationship between social and natural disasters

VIKULINA, Marina<sup>1\*</sup> ; VIKULIN, Alexander<sup>2</sup> ; SEMENETS, Nikolai<sup>3</sup>

<sup>1</sup>Research scientist, Faculty of Geography, Lomonosov Moscow State University, Russia, <sup>2</sup>Senior Research Fellow, Institute of Volcanology and Seismology, Russia, <sup>3</sup>Acting general director, Research and Production Company "EKOS", Moscow, Russia

The problem of reducing the damage caused by geodynamic and social disasters is a high priority and urgent task facing the humanity. The vivid examples of the earthquake in Japan in March 2011 that generated a new kind of threat ? the radiation pollution, and the events in the Arabic world that began in the same year, are dramatic evidences. By the middle of this century, the damage from such disastrous events is supposed to exceed the combined GDP of all countries of the world. The authors have developed the first database to include the largest geodynamic and social phenomena that occurred on Earth before 2005. We suggest the following phenomenological model based on the database (uniform with respect to the quantitative classification). All disasters are classified by size using a single logarithmic scale suggested by Rodkin and Shebalin in 1993. The base consists of 2000 disasters. The following phenomenological model is proposed: 1. The scale of disasters does not decrease with time. (Earthquakes in China in 1556 and 1976; the tsunami after the Sumatra earthquake in 2004, which can be compared in regards to the level of consequences only with the World Flood or a series of floods that occurred approximately 13000 years BP). 2. There were a minimal number of disasters in the 15th century; during which there were not a single disaster with  $J = I$  and  $II$ ; from that time the number of such disasters gradually increases; in the 20th century there were 20. 3. The number of disasters is characterized by cycles, which are a few thousand years long; the available longterm measurements confirm this (for example, the overflow of the Nile observed over more than 5000 years or deformations of the Earth surface in the last few thousand years based on the geodynamic, seismotectonic, and paleoseismic data). 4. Natural and social disasters together are distributed uniformly in time, while only natural and only social disasters are distributed nonuniformly, i.e. disasters group.

5. The proportion of the social disasters has a tendency to increase in time, which confirms the viewpoint of V.I. Vernadskii about the constantly increasing role of humans and society in the noosphere. It was shown that natural and social disasters are interrelated. The Earth from the point of view of the disaster theory evolves according to the definite laws of the unique bio-socio-geodynamics. The investigation and understanding of the nature of this mechanism that "mixes the disasters" will allow us in the future to formulate a scientific hypothesis and/or a law on the basis of the phenomenological model that we suggest in this work and use it in the system of expert global process management. In the aspects of modern methods of studying of the global disasters, the authors suggest an approach to understanding global disasters based on modern data. The global disaster is an event damage from which cannot be liquidated by the joint resource. Irreversible process of death of a modern civilization can become a consequence of a global disaster.

Keywords: geodynamics, society, magnitude of disaster, interaction of disasters, impact of society

## The numerical model of natural hazards development in the environment stressed by opposing forces

KUDIN, Valery<sup>1\*</sup>

<sup>1</sup>Lomonosov Moscow State University, Faculty of Geography

Natural hazards include earthquakes, tsunami, volcanic eruptions, floods, etc. The time of appearance of such significant events within hundreds of years can be considered as random. In most cases, the dangers' amplitudes are not amenable to prediction, i.e. their size is also random. From the mathematical point of view, the deposition of natural hazards is described by exponential dependence, which is connected with the involvement of the own "mass" of danger. In the presence of opposing forces in a first approximation, these processes are described by the Verhulst equation. It is a particular variant ( $Q < 0$ ,  $A = L$ ) of the total autonomous differential equations of the 2nd order for the function  $x(t)$  on time  $t$ , i.e.  $dx/dt = N + L \cdot x + Q \cdot x \cdot x$ , where  $N, L, Q$  are constants of equation with initial conditions  $t(n)$  and  $x(n)$ .

The complete solution of this equation with arbitrary initial conditions has bulky appearance, although the logistic curve reflects it qualitatively quite well. However, these solutions allow us to reveal a violation of the principle of stability of numerical solutions of the logistic equation  $x(n+1) = x(n) \cdot (1 + a \cdot (1 - x(n)))$ , where  $a = A \cdot (t(n+1) - t(n))$ , when the derivative  $dx/dt$  is replaced by the value for  $(x(n+1) - x(n)) / (t(n+1) - t(n))$ .

It is shown that the instability of the processes with the opposing factors invoked by jumps of initial conditions on consecutive segments. For certain values of the parameters of the differential equation associated with capacity of the stressed environment, both volatile and deterministic modes of development of the variable  $x(t)$ , normalized to unit, can be formed. An example of the Verhulst model with parameter  $A$  shows the dependence of the solutions  $x(t)$  at time intervals  $t(n+1) - t(n)$  and tabular values of  $x(n)$  and different a jumps of initial conditions. Negative inclinations of dependency associated with the tabular values  $x(n)$  are shown. Thus, there appears a situation, which leads to the release of the variable  $x$  from the corridor, normalized per unit, of sustainable values. For each  $a$ -case, the changes in the structure of  $x(t)$  in time look diverse and complex.

Therefore, the numerical logistic equation can be taken as a numerical model for the development of natural hazards in the geographical environment, characterized by capacity (option  $a$ ) of a tension of opposing factors.

Keywords: natural hazards, model, numeric equations, stability

## Studies on the understanding of haiku composed by earthquake disaster of East Japan on 11. 3. 2011

AOKI, Yoji<sup>1\*</sup>

<sup>1</sup>Student of Open University of Japan, <sup>2</sup>Member of Kuramae Hiku Club, <sup>3</sup>Translator of Haiku International Association, <sup>4</sup>Professor of Aomori University

Studies on the understanding of haiku composed by earthquake disaster of East Japan on 11. 3. 2011

Aoki, Yoji (student of Open University of Japan), Chida Sosuke (Kuramae Haiku Club), Jambor Kinuko (translator of Haiku International Association) and Hitoshi Fujita (Professor of Aomori University)

The damage of the Fukushima nuclear power plant and the East Japan big earthquake, the east part of Japan received big impact on the March 11, 2011. Many haiku poet composed haiku poems to the impact of the nuclear power plant accident and the earthquake disasters. Of these haiku what was published in the magazine, 234 haiku on the home page were to be used in the data. Copies of haiku were shown to 19 people of the general public and the poet, and we asked whether they can understand them, or they are impressed by them. 2354 haiku was chosen in total. 124 haiku was chosen average.

10.1 average people, understand of haiku and the distribution of the two-peaked mountain with 8 and 13 people was observed. Haiku understood by more than half of people were relatively large and 132 (56.4%), so it was found that haiku is yet the useful means of communication of mind for the Japanese today. As for the impressive haiku, it has the maximum value in 0 and at 1.4 person average, and decreases the distribution of people. 91 (38.8%) haiku were impressed by more than two people. To convey the emotion equally to many people, it showed difficulties. Taking the correlation of the number of people impressed with the number of people evaluated, it showed weak association of 0.515. The results suggested that haiku could be understood by a lot of people, but could give the impression variously.

According to the evaluation method in the Haiku Society, one point in haiku which was able to understand, to give two points to haiku that was impressed, we calculated the total score. Correlation of the number of people understood and the people impressed indicates 0.731, the stronger association was obtained. This is a result of the score added points. As it was not a very strong connection, so the individual differences affect the evaluation of haiku.

By the principal component analysis in the factors respondents, six-axis was obtained with eigen value greater than 1.0. This indicates that there are many different preferences in the evaluation by the respondents. The axis with maximum eigen value has the largest explanatory power, and showed the severity of the evaluation. We estimate 5-axis remaining as the evaluator's preferences for haiku.

The highest scored Haiku observed 2 haiku of 20 points.

(1) Mud certification of graduation, mud portrait digging under the debris by Tsunami (Sinogo SONE)

(2) Finding my mother in turning disaster's debris, light snow falling (Minu KASHIWABARA)

(3) Children crying bright hopes for their future a graduation ceremony (Nagahiko KAMIGORI)

(1) described the scenery that the photographs of deceased persons and the certification of diploma by deceased became muddy by the tsunami, people are digging them after the disaster in the damaged areas.

(2) described the scenery that light snow was falling, while people are removing the disaster debris of earthquake to find their mother of missing, at the neighborhood home.

(3) was praying for the pupil who were singing the graduation song with full of tears to be lighten

We thought that both of them were touched deeply by sadness.

Reference

Haiku: <http://blog.goo.ne.jp/humon007/e/fcc6b3e8f8dc3ca1cbc6a2177d6d0637>

Acknowledgments: Cooperation was obtained from Kuramae Haiku Club (Tokyo Institute of Technology) and Blue Ridge Haiku Association (Roanoke City, Virginia) for the investigation of haiku. The Haiku used in this study was introduced by the site.

Keywords: earthquake disaster of East Japan on 11. 3. 2011, haiku poet, understandings and deep impressions

## Hazard Mapping of Structurally Controlled Landslides in Leyte, Philippines Using High Resolution Digital Elevation Model

MONTALBO, Kristina rochelle<sup>1\*</sup> ; LUZON, Paul kenneth<sup>1</sup> ; LAGMAY, Alfredo mahar francisco<sup>1</sup>

<sup>1</sup>Nationwide Operational Assessment of Hazards, Department of Science and Technology, Philippines, <sup>2</sup>National Institute of Geological Sciences, University of the Philippines, Diliman, Quezon City, Ph

Structurally controlled landslides are one of the most destructive natural hazards that have occurred in the Philippines. The 2006 Guinsaugon Landslide, which was produced by the displacement of the Philippine fault, is a classic example of such hazard that took more than 1,000 lives and displaced more than 19,000 residents in the municipality of St. Bernard, Southern Leyte. Frequent monitoring and assessment should be done across the Philippine archipelago. The purpose of this study is to locate structurally controlled landslide prone areas with the aid of Coltop3D, Matterocking and Conefall using a high resolution digital elevation model (5 m resolution Interferometric Synthetic Aperture Radar images). The study area is set in the municipality of Ormoc, Leyte where the Philippine fault also cuts through and trending northwest. Discontinuity sets were identified using Coltop3D software that simulates a 3D model of the digital elevation model showing the dip and dip direction of different discontinuities. Lineation analysis and rose diagrams were made to verify the discontinuity sets in the area. Matterocking computes and estimates the locations where rock instabilities can occur according to the identified discontinuity sets that may allow sliding. Conefall was then used to compute and estimate the potential rockslide extent. Results show that the area has zones of potential rockslides with generated simulation of rockslide propagation extent. There is a high probability of landslides in Ormoc area where continuous monitoring of such danger zones should be done.

Keywords: structurally controlled landslides, geohazard, philippine fault, discontinuities, landslide mapping, structures

## Developing Automatic Delineation of Alluvial Fans for Rapid Hazard Assessment in Aurora Province, Philippines

ORTIZ, Iris jill<sup>1\*</sup> ; AQUINO, Dakila<sup>1</sup> ; NORINI, Gianluca<sup>3</sup> ; SALVOSA, Sheena<sup>1</sup> ; LLANES, Francesca<sup>1</sup> ; GALANG, Jan albert macario<sup>1</sup> ; ECO, Narod<sup>1</sup> ; VELEZ, Maria clara zuluaga<sup>4</sup> ; LAGMAY, Alfredo mahar<sup>1</sup>

<sup>1</sup>Nationwide Operational Assessment of Hazards, Department of Science and Technology, <sup>2</sup>National Institute of Geological Sciences, University of the Philippines, Diliman, Quezon City, Phi, <sup>3</sup>Istituto per la Dinamica dei Processi Ambientali, Consiglio Nazionale delle Ricerche, Italia, <sup>4</sup>Universita degli Studi di Napoli Federico II, Napoli, Italy

On Nov. 14, 2004, flashfloods from Subsob River struck Barangay(village) Paltic in Dingalan, Aurora Province around 4 a.m. when most residents were asleep - leaving hundreds homeless and 135 people dead. The series of floods caused by Violeta, Winnie, and Yoyong until December 2004 killed at least 300 people in Dingalan, Aurora alone. Mud buried 300 houses and residents were forced to stay on rooftops or seek higher ground. Because of these incidents, measures were devised to improve available geohazard maps to raise public awareness about landslides, debris flows and alluvial fans. This study developed a method to rapidly identify alluvial fans, thereby, hastening geohazard mapping in the region. Alluvial fans are fan shaped geologic formations deposited from tributaries from a mountainous terrain which flows out from the sudden break of a slope. Intense rainfall increases the discharge of sediments and water on these areas which could induce disastrous events such as flooding and debris flows. In this study, manual and automated methods in delineating fans in Aurora Province were compared. Manual delineation of alluvial fan boundaries were done through the contour lines generated from the 10-meter synthetic aperture radar (SAR)-derived digital elevation model (DEM). However, manual mapping of alluvial fan boundary which makes use of topographic interpretation of geomorphic features is subjective and time consuming. Biases were addressed by the second method by including factors such as 1) fan area of slope ranging from 1 to 8 degrees, 2) contributing stream networks from fan apex to fan toe , and 3) the fan potential lateral extent within the buffer zones based on the relief of the sediment source area in the GIS-based model. The outputs were compared with the manually delineated fans. Manual delineation identified 14 alluvial apex of 14 alluvial fans in 6 municipalities affecting 36 barangays . On the other hand, automated method identified 183 apex of 126 alluvial fans in 7 municipalities affecting 105 barangays. Although greater number of fans and wider fan area were identified using the automated method, manual delineation is still needed to check the results especially in volcanic regions. In addition, inactive alluvial fans are not accounted by the automated method.

Keywords: alluvial fan, natural hazard mapping, geohazard, GIS, Aurora, Philippines

## Strong Explosive Eruptions of Kamchatkan Volcanoes in 2013

GIRINA, Olga<sup>1\*</sup> ; MANEVICH, Alexander<sup>1</sup> ; MELNIKOV, Dmitry<sup>1</sup> ; NUZHDAEV, Anton<sup>1</sup> ; DEMYANCHUK, Yury<sup>1</sup> ; PETROVA, Elena<sup>2</sup>

<sup>1</sup>Institute of Volcanology and Seismology FEB RAS, KVERT, <sup>2</sup>Lomonosov Moscow State University, Geographical faculty

There are 30 active volcanoes in the Kamchatka, and three of them (Sheveluch, Klyuchevskoy, and Karymsky) continuously active. In 2013, two of the Kamchatkan volcanoes ? Sheveluch and Klyuchevskoy - had strong explosive eruptions.

Powerful explosive eruption of volcanoes is the most dangerous for aircraft because in a few hours or days in the atmosphere and the stratosphere can produce about several cubic kilometers of volcanic ash and aerosols. Ash plumes and the clouds, depending on the power of the eruption, the strength and wind speed, can travel thousands of kilometers from the volcano for several days, remaining hazardous to aircraft.

The eruptive activity of Sheveluch Volcano began since 1980 (growth of the lava dome) and is continuing at present. Strong explosive events of the volcano occurred in 2013: on June 26, on October 18, and on December 03: ash plumes rose up to 10 km a.s.l. and extended about 200-400 km, respectively, to the south-west, south-southeast, and north of the volcano. A form of pyroclastic flow deposits with run-out 12 km accompanied these explosive eruptions. Ashfalls occurred at Klyuchi Village (on June 26) and Ivashka Village (on December 03). Activity of the volcano was dangerous to international and local aviation.

Klyuchevskoy volcano had two eruptions in 2013: moderate Strombolian explosive eruption from October 14, 2012, till January 15, 2013; and strong Strombolian-Vulcanian explosive and effusive eruption from August 15, 2013, till December 20, 2013. There were four lava flows to effuse on the north-west, west and south-western volcanic flanks. Probably a flank eruption began at the pass between Klyuchevskoy volcano and Kamen volcano on October 06. Culmination of strong Vulcanian explosive activity of the volcano occurred on October 15-20: ash column rose up to 10-12 km a.s.l. and ash plumes extended to the different directions of the volcano according to cyclonic activity in the this area. Phreatic ash plumes on the fronts of lava flows rose up to 5 km a.s.l. Weak ash falls were noted at Klyuchi Village on October 09 and 13, and Mayskoe Village on October 16. Activity of the volcano was dangerous to international and local aviation.

Keywords: explosive eruption, volcano, Kamchatka, Sheveluch, Klyuchevskoy

## Magnitude of the Solomon Tsunami of February 6, 2013

HATORI, Tokutaro<sup>1\*</sup>

<sup>1</sup>nome

The great earthquake occurred on February 6, 2013 at the junction of Solomon and New Hebrides trenches (10.738S, 165.138E, 28.7km depth, M8.0, USGS). Moderate tsunami was widely observed in the Pacific zone (WC/ATWC, NOAA, JMA). The tsunami killed 10 persons and 590 houses destroyed at Nendo Is.(Santa Cruz Is.) located near the source region. The estimated source lies 250km length toward E-W direction. Judging from the attenuation of tsunami height with distance, tsunami magnitude is determined to be  $m=2$  that the grade is the mean value for earthquake magnitude. For tsunami magnitude, semi-amplitudes of the following regions are relatively large: 20cm at Crescent City, California, 18cm at Maui, Hawaii, 17-19cm in Galapagos and Coquimbo, South America and 40cm at Hachijo Is., 19cm at Chichijima ,Japan. The pattern of amplitude distribution is similar to other Solomon-Vanuatu tsunamis.

Keywords: Solomon Tsunami, Tsunami magnitude, February 6, 2013, Tsunami source, amplitude deviation

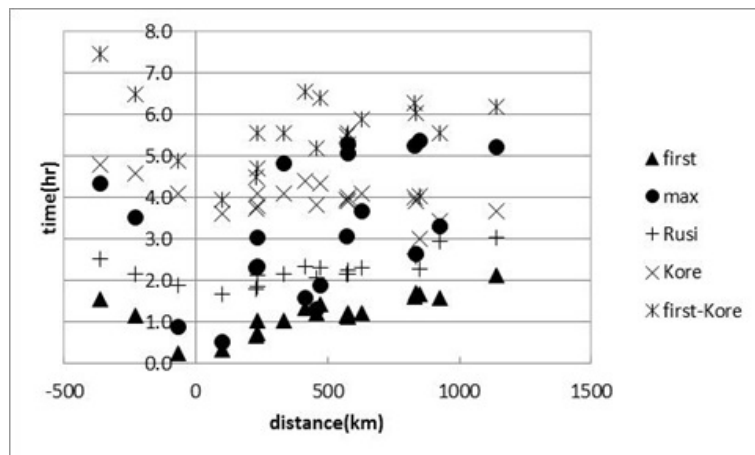
## Arrival times of reflected waves and the maximum phases of tsunami?the 1993 Hokkaido Nansei-oki Tsunami

ABE, Kuniaki<sup>1\*</sup> ; OKADA, Masami<sup>2</sup> ; HAYASHI, Yutaka<sup>3</sup>

<sup>1</sup>none, <sup>2</sup>MRI, <sup>3</sup>MRI

Tsunami maximum phases are frequently attained by reflected waves. Arrivals of reflected waves were studied in relation with arrivals of maximum phases. Arrival times of reflected waves are calculated from combination of refraction diagrams of direct wave and arbitral reflected wave. The arrivals are recognized in coincidence between the prediction and the observation. Under this circumstance travel times of first and maximum waves were obtained for the 1993 Hokkaido Nansei-oki Tsunami and predicted travel times of reflected wave from Russia, Korea and double reflected waves from Honshu and Korea are plotted in figure 1. As the result arrivals of maximum phases are classified into three groups. First one, the direct wave from the source, is earlier arrivals before the reflected wave from Russia. Second one is a group found between arrival times from Russia and Korea. This is recognized as reflected wave from arbitral coast of Eurasia continent. Third group is one found at arrival times shorter than those of the double reflection. This group is interpreted from double reflections from coast near the source and Korea.

Keywords: Tsunami, maximum phase, late arrival, reflected wave, 1993 Tsunami



## Quantitative comparison of the 2011 Tohoku earthquake and past tsunami heights

SATAKE, Kenji<sup>1\*</sup> ; TSUJI, Yoshinobu<sup>2</sup> ; HARADA, Tomoya<sup>3</sup> ; ISHIBE, Takeo<sup>1</sup> ; NISHIYAMA, Akihito<sup>1</sup> ; KUSUMOTO, Satoshi<sup>4</sup>

<sup>1</sup>Earthquake Research Institute, the University of Tokyo, <sup>2</sup>ERI, the University of Tokyo, Now at Fukada Geological Institute, <sup>3</sup>CIDIR/ERI, the University of Tokyo, <sup>4</sup>ERI, the University of Tokyo, Now at Dia Consultants

The tsunami heights from the 2011 Tohoku earthquake were on the average 1.5 times the 1896 Meiji Sanriku tsunami, 3 times the 1933 Showa Sanriku tsunami, 4 times the 1960 Chilean tsunami, and 14 times the 2010 Chilean tsunami along the Sanriku coast. The Sanriku coast is a typical ria coast, a sawtooth-shaped irregular coastal shape, and the local variation of tsunami heights is very significant. We carefully selected the sites where the past measurement points are known, and comparisons were made at the same villages or small-scaled bays (roughly a km scale).

Along the Sanriku coast, the median value of 1896/2011 tsunami height ratio at 83 measurement points is 0.69, and a correlation coefficient is 0.34. The median 1933/2011 ratio at 94 points is 0.33 with a correlation coefficient of 0.47. The 2011 tsunami was higher along the southern Sanriku coast (Miyagi prefecture). In the central Sanriku coast (Iwate prefecture), the 2011 tsunami was 1.2 times the 1896 tsunami and 2 times the 1933 tsunami. The comparison was made at 98 points for the 1960 tsunami with a median ratio of 0.25, and at 12 points for the 2010 tsunami with a median ratio of 0.07. The correlation coefficients are lower, 0.17 and 0.14 for the 1960 and 2010 Chilean tsunamis, than the past Sanriku tsunamis. All the Sanriku tsunamis (1896, 1933 and 2011) had different earthquake source area and types, but the tsunami height distributions were similar, indicating that the tsunami heights are more sensitive to the local topography for the near-field tsunamis. The lower correlation with the Chilean tsunami may be due to the fact the dominant period of incoming tsunami was more than twice longer for the trans-Pacific tsunamis.

Comparisons with the two Chilean tsunamis were also made on the Ibaraki and Chiba coasts. The tsunami heights were compared at 24 points for the 1960 tsunami and 14 points for the 2010 tsunami. The median 1960/2011 ratio is 0.62, while the median 2010/2011 ratio is 0.28. The correlation coefficients with the 2011 tsunami heights are higher, 0.63 and 0.41 for the 1960 and 2010 Chilean tsunamis. The high correlation may be due to general decrease of tsunami heights toward south, and the fact that the tsunamis were locally high near peninsula such as Asahi city in Chiba prefecture.

We used the 2011 tsunami heights at 120 points measured and reported by Tsuji et al. (2011 BERI); the 1896 tsunami heights reported by Yamana, Iki and Matsuo, the 1933 heights by Matsuo, Kunitomi and ERI, the 1960 heights by Comm. Field Investigation and Japan Meteorological Survey, and the 2010 heights by Tsuji et al. and Imai et al. The full data and reference are given in Tsuji et al. (Pageoph in press).

**Keywords:** The 2011 Tohoku earthquake, tsunami, 1896 Sanriku tsunami, 1933 Sanriku tsunami, 1960 Chile tsunami, 2010 Chile tsunami

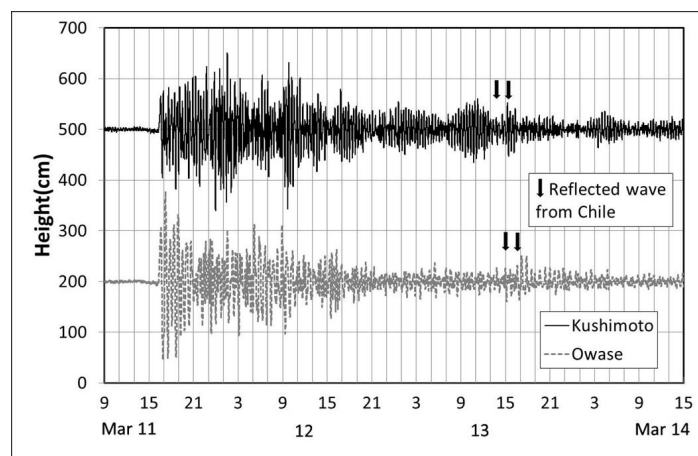
## Tsunami reflected from Chilean coast and observed in Japan - the 2011 off Tohoku Tsunami

OKADA, Masami<sup>1\*</sup> ; ABE, Kuniaki<sup>2</sup> ; HAYASHI, Yutaka<sup>1</sup>

<sup>1</sup>MRI, JMA, <sup>2</sup>None

We identified reflected waves from Chilean coast at Kushimoto and Owase tide stations in Japan on the 2011 off Tohoku Tsunami. It is based on amplitude increases at predicted travel times. The travel times were calculated by using the tide gage records of the 2011 tsunami at Talcuano in Chile and those of the 1960 Chilean Tsunami observed at Kushimoto and Owase. For the latter we noticed reflected waves from Chilean coast and obtained the travel times between Chile and Japan. Then, two phases of large amplitude of the 2011 tsunami observed at Talcuano were selected, and travel times of 46.7, 47.9 hrs for Kushimoto and of 48.1, 49.3 hrs for Owase were estimated. Amplitude increases at the predicted times were recognized in both tide stations. Waveforms and predicted travel times are shown in Fig.1. The identification is supported by amplitude increases at almost same travel times for two different tide stations.

Keywords: tsunami, Chile, Japan, reflected wave, 2011 tsunami



## Disaster Warning System in Thailand through Enterprise Engineering Perspective

LEELAWAT, Natt<sup>1\*</sup> ; SUPPASRI, Anawat<sup>2</sup> ; IMAMURA, Fumihiko<sup>2</sup>

<sup>1</sup>Tokyo Institute of Technology, <sup>2</sup>Tohoku University

### Introduction

*Identify, assess and monitor disaster risks and enhance early warning* has been set as one of the five priority areas of action in the Hyogo Framework for Action 2005-2015. This study is a part of our research project on disaster warning process management analysis as well as Leelawat et al. (2013).

### Enterprise Engineering & DEMO

Enterprise engineering is an interdisciplinary field focusing on investigating of each aspect of the enterprise, including a business process, information flow, and organizational structure (Dietz, 2006). While most of the current modeling tools (e.g., BPMN) cannot achieve the enterprise engineering principles, *Design and Engineering Methodology for Organizations (DEMO)* (Dietz, 2006; Perinforma, 2012), an enterprise engineering and business process modeling language, has capability to demonstrate the validity of some principles (Dietz & Hoogervorst, 2012). Thus, DEMO has been selected in this study.

### Data Collection

(Primary and Secondary) Data collection took place during Aug.-Dec. 2013. The face-to-face interviews with the acting Director of National Disaster Warning Center (NDWC) of Thailand and the Director of the Seismological Bureau, Thai Meteorological Department (TMD) were conducted in Sep. 2013 through the semi-structured style interviews, together with the observation.

### Findings and Discussion

There are 2 main actual players in the Thai warning system as mentioned. The case has been analyzed by DEMO. According to Perinforma (2012), the *Organization Construction Diagram (OCD)* and *Transaction Product Table (TPT)* have been created to show the compact form of the system. DEMO shows its capability to express the sketch of the organization, together with some interesting issues.

First, we can understand the authority and responsibility from OCD and TPT. It can be seen that announcement decision is authorized to only NDWC (i.e., one actual warning announcer). It is a good practice because it does not create the confusion that may occur from many announcing sources.

Second, through the TPT, we can see the chain of warning message announcement, from monitoring information to seismological information. It means that the duty of declaring seismological disaster and declaring warning is separated to different actor roles which in turn increase the performance because each executor can focus on their responsibility works and increase the accuracy since the seismological information has been confirmed by the initiator.

Third, by comparing with Japanese case, it can be seen that the warning system in Japan is mainly executed by one organization (i.e., JMA) while Thai case contains 2 main organizations plus other 4 monitoring organizations regarding to the aspect of information. One reason is probably from the different government hierarchical structures which separated the expertise into each departments (in different ministries) in Thai case.

### Acknowledgements

The study was supported by the ACEEES and the Risk Solutions 2013 project of Tokyo Tech. The authors would like to acknowledge Capt. Song Ekmahachai (acting Director of NDWC), Mr. Burin Wechbunthing (Director of Seismological Bureau), Prof. Junichi Iijima (Tokyo Tech), and Dr. Jing Tang for their advice and support.

### References

- Dietz, J. L. G. (2006). *Enterprise Ontology - Theory and Methodology*. Heidelberg: Springer-Verlag.
- Dietz, J. L. G., & Hoogervorst, J. A. P. (2012). The Principles of Enterprise Engineering. In *Advances in Enterprise Engineering VI* (pp. 15-30). Heidelberg: Springer Berlin Heidelberg.
- Leelawat, N., Suppasri, A., & Imamura, F. (2013). Analyzing the essence of the disaster warning system in Japan. In *Proceedings of the Second International Education Forum on Environment and Energy Science 2013*.

---

HDS27-05

Room:418

Time:May 1 10:00-10:15

Perinforma, A. P. C. (2012). *The Essence of Organisation Version 1.2*. South Holland: Sapio.

Keywords: Design and Engineering Methodology for Organizations, Disaster Management, Enterprise Engineering, Thailand, Tsunami, Warning System

## A methodology for near-field tsunami inundation forecasting and its application to the 2011 Tohoku tsunami

GUSMAN, Aditya<sup>1\*</sup> ; TANIOKA, Yuichiro<sup>1</sup>

<sup>1</sup>Institute of Seismology and Volcanology, Hokkaido University

We develop a new methodology for near-field tsunami inundation forecasting (NearTIF). This method required site-specific pre-computed tsunami inundation and pre-computed tsunami waveform database. Information about tsunami source of an event is required as an input for the method to work. By this method, we will not attempt to obtain a reliable earthquake source model for an event. Instead, any available information about tsunami source such as earthquake moment magnitude, earthquake fault model, or tsunami source model will be used. After information about the tsunami source is obtained, tsunami waveforms at near-shore points can be simulated in real-time during an event. Simulating tsunami waveforms by solving the linear shallow water equation on low-resolution bathymetric data does not take long time, therefore it is suitable to be used in real-time. By using root mean square analysis, a scenario that gives the most similar tsunami waveforms in the database is selected as the best-fit site-specific scenario. Then the corresponding pre-computed tsunami inundation of the best scenario is selected as the tsunami inundation forecast.

The pre-computed tsunami database is built from thrust earthquake scenarios of simple rectangular fault models with moment magnitude ranged from Mw 8.0 to 9.0. We arrange a total of 56 reference points along the subduction zone off the east coast of Honshu, Japan as the center top of the fault planes. The points are grouped into four depth categories of shallowest, upper intermediate, lower intermediate, and deepest plate interface. The earthquake scenarios for each depth category have moment magnitude range of Mw 8.0 to 9.0, Mw 8.0 to 8.9, Mw 8.0 to 8.8, and Mw 8.0 to 8.7, respectively, from the shallowest to the deepest plate interface, making a total of 532 scenarios.

Sites are chosen based on their coastal geomorphology (i.e. bay, lagoon, isthmus) or location of coastal community. Virtual observation points at which tsunami waveforms is computed are placed strategically near-shore, around a bay at depth of deeper than 30 or 50 m depending on the bathymetry.

We test the algorithm to hindcast tsunami inundation along the Sanriku coast that was generated by the 2011 Tohoku earthquake. To produce accurate tsunami inundation map, accurate information about tsunami source is required. We used source models for the 2011 Tohoku earthquake previously estimated from GPS, W phase, or offshore tsunami waveform data. These source models could be available before tsunami hits the shore. The forecasting algorithm is capable of providing a tsunami inundation map that is similar to that obtained by numerical forward modeling, but with remarkably faster speed. Using a regular laptop computer, the time required to forecast tsunami inundation in coastal sites from the Sendai Plain to Miyako City is approximately 3 min after information about the tsunami source is obtained. We found that the tsunami inundation forecasts from the GPS (5 min), W phase (5 min and 10 min) fault models, and tsunami source model (35 min) are reliable for tsunami early warning purposes and considerably similar to the observation. This method can be used to develop a future tsunami forecasting systems with a capability of providing tsunami inundation forecasts in the near field locations.

Keywords: near-field tsunami inundation forecast, pre-computed tsunami database, tsunami early warning

## An offshore type of GPS tsunami meter using QZSS and ETS-VIII satellites

TERADA, Yukihiro<sup>1\*</sup> ; HASHIMOTO, Gousei<sup>2</sup> ; MOTOHASHI, Osamu<sup>2</sup> ; YAMAMOTO, Shinichi<sup>3</sup> ; WADA, Akira<sup>4</sup> ; KATO, Teruyuki<sup>5</sup>

<sup>1</sup>Kochi National College of Technology, <sup>2</sup>Japan Aerospace Exploration Agency, <sup>3</sup>National Institute of Information and Communications Technology, <sup>4</sup>Hitachi Zosen Corporation, <sup>5</sup>The University of Tokyo

A new tsunami observation system has been developed, which employs the GPS technology to detect a tsunami before it reaches the coast. The GPS antenna attached on the top of a buoy floating at the sea surface is one of the important apparatus in this system. The estimated positions of the antenna includes not only tsunami but also all kinds of sea surface changes including wind waves, tides etc. The low pass and high pass filters are used for detection of tsunami. After a series of preliminary experimental studies, the operation-oriented experiments were conducted at two offshore sites. These results showed that a GPS buoy was useful to early detection of tsunami. And the Ministry of Land, Infrastructure, Transport and Tourism has established the GPS buoy system for monitoring sea waves with fifteen GPS buoys along the Pacific coast and Japan sea coast since the year of 2008. These system succeeded to detect the tsunami of the 2011 off the Pacific coast of Tohoku Earthquake.

Currently, the GPS buoy system uses RTK (Real Time Kinematic) method which requires land base for precise positioning of the buoy. This limits the distance of the buoy from the coast at most 20km. There are two problems to be conquered, one is the precise GPS positioning and the other is the data transmission methods. The algorithm of PVD (Point precise Variance Detection) method and PPP-AR (Precise Point Positioning method with Ambiguity Resolution) method are successfully under examination in the Muroto GPS buoy. Also, the satellite communication system using QZSS (Quasi-Zenith Satellite System) and ETS-VIII (Engineering Test Satellite VIII) were introduced for this GPS tsunami observation system experimentally.

Keywords: QZSS, ETS-VIII, GPS Tsunami Meter, PVD, PPP-AR

## Long-term deployment of Wave Glider for a real-time tsunami monitoring system using the Vector Tsunameter

HAMANO, Yozo<sup>1\*</sup> ; SUGIOKA, Hiroko<sup>1</sup> ; TOH, Hiroaki<sup>2</sup>

<sup>1</sup>JAMSTEC, <sup>2</sup>Kyoto University

We have been developing a real-time tsunami monitoring system by using the Vector Tsunameter(VTM), in which we use an unmanned surface vehicle called Wave Glider, manufactured by Liquid Robotics Inc. The WG, equipped with both an acoustic and a satellite communication modems, can be used to transmit data messages from the VTM to shore. In order to investigate the feasibility for this type of station-keeping operation, we made a long-term deployment of the WG at sea area. We deployed the WG on September 22, 2013 at 38 14.99N, 143 35.13E, water depth = 3420.1 m. We set 6 waypoints along a circle (200m in diameter) centered at the above position, so that the WG trace the watch circle. The experiment had been continued until the WG was caught by a drift net and delivered to the Kesenuma port on December 6,2013.

The 75-days deployment of WG gives valuable information on the performance of the WG. As for the feasibility of WG for the station-keeping operation, two problems become apparent. During the experiment, the WG sporadically escaped from the watch circle and drifted away following the ambient water current, and it returned to the circle after several days of trip. Four excursions occurred during the first 50 days, and the total of the excursion period is 20 days. For monitoring slow activities such as crustal deformation, this performance is acceptable. However, some improvements are required for monitoring the short period signals such as tsunami. The other problem is the reduction of speed over water occurred after about 2 months operation. In the middle of November, the speed abruptly decreased to less than 0.5 knots and remains low until the end of the experiment.

Based on the detailed analyses of the navigation data sets and inspection of the WG, we conclude that the twist of the umbilical cable, which connects the surface float to the sub-surface glider, triggered both the excursion and the speed reduction. The small size of the watch circle and the short distance between the waypoints (about 100 m) are main cause of the twist. The short distance causes large and frequent changes of glider heading. Since the float can not follow the abrupt changes of heading, differential rotation of the glider relative to the float arises and enhances the twist of the cable. This twist of the cable increases water drag to the WG, and the stress of the cable due to the twist inhibit the rotation of the WG. These effects reduce the movability of WG, and the speed reduction start the drift of WG following the ambient current motion. The twist of the cable mainly occurs while the WG follows the path along the watch circle. On the other hand, during the excursions, glider heading is fixed and rewinding of the cable was observed. This rewinding reduces the drag force to the WG and assist the WG in returning to its home circle.

Extreme reduction of the speed is observed after 2 months of deployments. Inspection of the WG right after the recovery indicates that the propulsion system of the sub-glider had been working well until the end of the experiment, whereas the float suffered by the biofouling of eboshi-gai (goose barnacle). The biofouling seems responsible for the speed reduction, but theoretical estimate suggests that the hydrodynamic drag due to the biofouling is not sufficient to explain the observed speed reduction. The twist of the cable and the biofouling both contribute to the speed reduction. These analyses suggest larger size of the watch circle may improve or solve the present two problems of the excursion and the speed reduction.

Keywords: tsunami, tsunameter, real-time observation, seafloor observatio

## Enhancement of GEONET Real-time Analysis System for Covering over Japan

YAHAGI, Toshihiro<sup>1\*</sup> ; MIYAGAWA, Kohei<sup>1</sup> ; KAWAMOTO, Satoshi<sup>1</sup> ; OSHIMA, Kennichi<sup>1</sup> ; YAMAGUCHI, Kazunori<sup>1</sup> ; MURAMATSU, Hiroki<sup>1</sup> ; OHTA, Yusaku<sup>2</sup> ; DEMACHI, Tomotsugu<sup>2</sup> ; MIURA, Satoshi<sup>2</sup> ; HINO, Ryota<sup>2</sup> ; SAIDA, Yuichi<sup>3</sup> ; DOUKE, Yuki<sup>3</sup>

<sup>1</sup>Geospatial Information Authority of Japan, <sup>2</sup>Graduate School of Science, Tohoku University, <sup>3</sup>Hitachi Zosen Corporation

Geospatial Information Authority of Japan (GSI) has been operating a continuous GNSS observation network system, known as GEONET (GNSS Earth Observation Network System), since 1994. Currently, GEONET consists of approximately 1,300 nationwide GNSS stations and its analysis center. Each station collects GNSS data with 1Hz sampling and those data are transmitted to the analysis center in real-time. GSI offers the observation data to the public in order to support various types of public surveys in Japan and precise positioning services using GNSS.

In the field of disaster prevention or mitigation, GEONET also plays very important roles by monitoring crustal deformation occurred by such as earthquakes or volcanic activities. In addition, after the 2011 off the Pacific coast of Tohoku Earthquake (Mw9.0), it is pointed out by a governmental committee that GEONET should be utilized for tsunami early warning by offering a first realistic estimation of moment magnitude (Mw) after large earthquakes. It is based on the fact that GNSS real-time positioning generally has big advantages in estimating moment magnitude (Mw) of the large earthquakes compared to short-period seismometers in terms of avoiding underestimation problem.

Since then GSI has been developing a new GEONET real-time analysis system, named REGARD (Real-time GEONET Analysis System for Rapid Deformation Monitoring), jointly with Tohoku University. It is designed for estimating permanent displacement field and Mw of giant earthquakes and notify the results in real-time. First, the GEONET data are processed by RTKLIB ver.2.4.1 (Takasu, 2011) for real-time GNSS positioning. We adopt both 'RAPiD' technique (Ohta et al., 2012) and the Early Earthquake Warning (EEW) information (Kamigaichi et al., 2009) for automated detection process of permanent displacements. Once the displacements are detected, corresponding fault source model is immediately estimated and the system sends the results to registered addresses by e-mail.

GSI launched its prototype system in April 2012 with 143 stations covering mainly Tohoku region and also has been evaluating its performances using archived data of some past earthquakes. We verified that the system successfully could estimate appropriate Mw values just after a couple of minutes in case of large events (e.g. Mw8.9 in the 2011 Tohoku earthquake), whereas it hardly detect proper values if the size of earthquake is less than Mw7.5. Based on the results and performances of the prototype system, we upgraded REGARD in 2013 for covering all over Japan by using most GEONET stations and enhancing its redundancy by carrying out two independent processing in parallel. This new system was launched in April 2014.

We present the evaluation results of the prototype system and introduce the upgraded REGARD including future plans focusing on exploiting to tsunami warning.

Keywords: GEONET, RTK-GPS, Real-time

## Tsunami inundation modeling of the 2011 Tohoku tsunami using the source estimated from the offshore tsunami records

BABA, Toshitaka<sup>1\*</sup> ; TAKAHASHI, Narumi<sup>1</sup> ; KANEDA, Yoshiyuki<sup>1</sup>

<sup>1</sup>JAMSTEC

As the number of offshore tsunami stations comes up, it is becoming possible to estimate tsunami source in real time by exclusively using offshore tsunami information. The issue we would like to discuss in this study is how accurate is it in terms of coastal tsunami prediction? In order to investigate this, we performed a tsunami inundation modelling of the 2011 Tohoku tsunami and compared with the tsunami field survey. We used the Saito et al. (2011) source model inverted from the offshore tsunami waveforms alone, although it was not a real-time solution, in the numerical simulation. The nonlinear Boussinesq equations were solved for the tsunami propagation because tsunami soliton fission was observed during the 2011 tsunami, which is split short-period waves around tsunami crest caused by combination of wave nonlinearity and dispersion. We also applied a variable nested algorithm which allows the spatial resolution of the study region to be easily increased. The finest grid spacing was set to be 2/9 arcsec (about 5m). The three dimensional shape of buildings and structures from lidar measurements were directly embedded on the digital elevation model to include the effect of them on tsunami inundation. Our dispersive tsunami code (JAGURS) was fully parallelized with MPI and OpenMP libraries so that the large scale dispersive modeling could be implemented within realistic computation time. According to Aida (1978), the geometric mean  $K$  and geometric standard deviation  $k$  was used to evaluate the reproducibility of the numerical simulation. For our numerical simulation results, the  $K$  and  $k$  were calculated to be 0.97 and 1.27, respectively. These values satisfy the adequacy criteria for tsunami numerical modeling established by the Japan Society of Civil Engineers (2002) ( $0.95 < K < 1.05$ ,  $k < 1.45$ ). Accordingly, the present study showed the reliability of the tsunami prediction procedure that uses tsunami sources obtained with the offshore tsunami records alone.

Keywords: 2011 Tohoku tsunami, Nonlinear dispersive theory, Simulation

## Real-time tsunami simulation and visualization system using rapid CMT solutions in Southeast Asia

INAZU, Daisuke<sup>1\*</sup> ; SAITO, Tatsuhiko<sup>1</sup> ; KUMAGAI, Hiroyuki<sup>2</sup> ; PULIDO, Nelson<sup>1</sup> ; FUKUYAMA, Eiichi<sup>1</sup>

<sup>1</sup>NIED, <sup>2</sup>Nagoya University

Southeast Asia, especially Indonesia and Philippines, is one of the most seismically active region in the world. NIED carries out real-time estimation of moment tensors of earthquakes and maintains a CMT catalogue in this region using the SWIFT system (Nakano et al. 2008), as well as waveform data from dense broadband regional seismic networks in Indonesia and Philippines, under a cooperative research with BMKG (Indonesia), PHIVOLCS (Philippines), and GFZ (Germany). Developing a rapid forecast/hindcast system of the tsunami is also necessary in particular for the tsunamigenic earthquakes.

We have been constructing an automated system for the tsunami simulation (Inazu et al. 2013 SSJ meeting). The current version of the system conducts simulations and visualizations of the followings procedures (1-4). The tsunami simulation is numerically carried out with a finite difference scheme from an initial condition given by a rectangular fault model.

- 1) Estimate a CMT solution by the SWIFT system.
- 2) Calculate the width, length, and slip amount of the rectangular fault model from  $M_w$  using an empirical scaling law. We here employ two scaling laws for the sake of evaluation of the uncertainties among the tsunami simulation results. Two parameters with small/large slip amount (or large/small rupture area) are then obtained for an estimated  $M_w$ .
- 3) Two fault mechanisms are obtained based on the double couple solutions, and then we expect four scenarios of the initial tsunami conditions. The seafloor deformation or initial tsunami condition are calculated by the Okada's (1985) theory for each scenario.
- 4) Carry out numerical simulations for the respective scenarios. We visualize the regional tsunami height distribution and the time series of the tsunami height at selected sites around the epicenter. The visualization is carried out in parallel to the simulation for an integral time interval. The maximum tsunami heights are displayed on a regional map and on coastal areas as well in parallel to the simulation.

We will present typical graphical outputs produced by the above procedures for several tsunami events.

Keywords: CMT, Tsunami, Rapid analysis

## Proper scoring systems with definite connections to information values of tsunami warnings

HAYASHI, Yutaka<sup>1\*</sup>

<sup>1</sup>Meteorological Research Institute

Necessary conditions which newly introduced method can improve forecast are, existing proper scoring system, and that the new method marks better score than the present method do. Up to now, these scoring system have never applied to tsunami warning system.

Some scoring rules being applied widely to binary forecasts in weather forecasting, such as having precipitation or not, have close connections to change of utility for users. These scores are based on assumption that all user know their cost to make counter measures (C) and loss in case of no counter measure (L). When the forecast says the event will occur, and all users are assumed to make counter measures. In addition, a simple probability density distribution of  $U(-C)/U(-L)$  is assumed for cost-loss model, where  $U$  is the utility function. In general, a score is calculated by using a targeted dataset, e.g., a fixed period of time, and frequencies: occurrence of targeted phenomena is forecasted and observed (hit:  $N_a$ ), forecasted but not occurred (false alarm  $N_b$ ), not forecasted but occurred (misdetection:  $N_c$ ), and not forecasted and not occurred (hit:  $N_d$ ). For example, equitable threat score ( $ETS \equiv (N_a - K)/(N_a + N_b + N_c - K)$ , where  $K \equiv (N_a + N_b)(N_a + N_c)/(N_a + N_b + N_c + N_d)$ ) is one of their scoring system.

In this paper, suitable scoring rules for tsunami warnings are derived by considering the characteristics of tsunami warnings and following assumptions.

(1) Scores can be defined without  $N_d$ , because counting  $N_d$  does not make sense for tsunami warning.

(2) In case of tsunami warning, users of forecasts can select actions to take a counter measure or not. In case of no warning, users do not take a counter measure. Change of utilities are  $U(-C)$  and  $U(-L)$  for taking a counter measure and for when a phenomenon happens without a counter measure, respectively.

(3) All users know the fault alarm ratio ( $FAR \equiv N_b/(N_a + N_b)$ ) of the warning, their utilities for each condition ( $U(-C)$ ,  $U(-L)$ ), and then their rational decision-making choose the option so that their expectation of utility ( $E_x(U)$ ) become maximum. Here, if  $U(-L)/U(-C) < FAR/(1-FAR)$  is satisfied, not taking a counter measure is the more reasonable decision. According to this assumption, larger the  $FAR$  is, larger the cost-loss ratio is, warning become easier to be ignored.

(4) Assuming three types of probability density functions on  $x=U(-C)/U(-L)$ . a) Uniform model:  $f(x)=1$ , b) Low-cost model:  $f(x)=2-2x$ , and (c) High-cost model:  $f(x)=2x$  for the range of  $0 \leq x \leq 1$ .

(5) The scores are set to be proportional to the information value of the warning. Here,  $\Delta U$  can be calculated as the integral corresponding to each distribution of (4) and utilities of selected actions at the  $N_a + N_b$  warnings based on the rational decision-making described in (3). Besides, if there were not for warning system, users should have lose utility as much as  $-U(-L)$  at every event. Then,  $V \equiv -\Delta U/((N_a + N_c)U(-L))$ .

Scores corresponding to models a)-c) in (4) are derived as follows.

a)  $V = N_a^2 / (2(N_a + N_b)(N_a + N_c))$ . For good warning which satisfies both  $N_a \gg N_b$  and  $N_a \gg N_c$ , the score can be approximated to  $V \doteq CSI/2$ , where  $CSI \equiv N_a/(N_a + N_b + N_c)$  is threat score or critical success index.

b)  $V = (2/3)(1-FAR)(1-M)(1+M/2)$ , where  $M \equiv N_c/(N_a + N_c)$  is missing ratio. For warnings with few misdetection which satisfies  $N_c \ll N_a$ , the score can be approximated to be  $V \doteq (2/3)(1-FAR)(1-M/2)$ .

(c)  $V = (1-FAR)^2(1-M)/3$ .

The proper score system thus changes according to the cost-loss ratio, which have close relation to preparedness. It is necessary to choose suitable forecast method using proper scoring system which is corresponding to a social structure. In the meeting, the author would like to discuss also on the problem for the practical application of the scoring systems.

Keywords: binary forecast, cost-loss model, expected-utility theory, rational decision-making, score

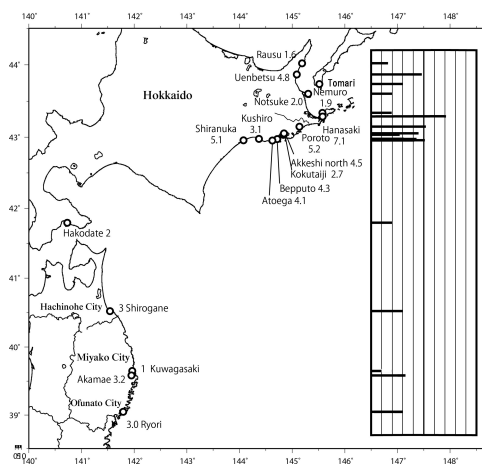
## Tsunami height distribution of the 1843 Tenpo Nemuro-oki earthquake

TSUJI, Yoshinobu<sup>1\*</sup>; HORIE, Takehito<sup>2</sup>; HASHIMOTO, Keisuke<sup>2</sup>; SASAKI, Takayuki<sup>2</sup>; MABUCHI, Yukio<sup>3</sup>; OKADA, Kiyohiro<sup>3</sup>; KUROYANAGI, Yousuke<sup>3</sup>; OOIE, Takayuki<sup>3</sup>; KURIMOTO, Masashi<sup>3</sup>; KINAMI, Takahiro<sup>4</sup>; IMAMURA, Fumihiko<sup>5</sup>

<sup>1</sup>Fukada Geolog. Inst., <sup>2</sup>Alpha Hydraulic Eng.Consultant, <sup>3</sup>Pacific Consultant, <sup>4</sup>Kubiki Techno., <sup>5</sup>IRIDeS, Tohoku Univ.

A large earthquake occurred in the sea area east offing Nenuro, Hokkaido at 6 AM, April 25, 1843 and is called Tenpo Nenuro-Oki earthquake whose magnitude is estimated at M7.5. A tsunami was accompanied with this earthquake, and hit the Pacific coast of Hokkaido and the east coast of Sanriku district, the north part of Honshu. Historical documents which record the tsunami were published by Musha (1941) and ERI, university of Tokyo(1984). It is recorded in the diary kept by a priest of Kokutaiji Temple at Akkeshi town, Kushiro district, Hokkaido that the Akkeshi branch office of the Tokugawa Government and huts of Ainu race were swept away in the residential area around the temple, and in Muko-Gishi area, north opposite coast of Akkeshi all houses were washed away and 34 Ainu people were killed. The official report written by an officer at Kushiro described that one hut and one barn were swept away at Betsufuto, about 36 kilometers east of Kushiro, and 2 houses were swept away at Atoega village. Documents written by the local meteorological observatory of Namuro described that 50 houses village were swept away at Hanasaki, about 8 kilometers south west of Nemuro Town, and survived people moved their residences to Honioi village about 6 kilometers north of Hanasaki. In this official report also it was recorded that a boy called Yamamoto Koshichi was lived on the coast of Notsuke peninsula. He experienced the tsunami there when he was 12 years old. He mentioned that the wave was divided into two waves in the offing of Notsuke coast, and the bigger wave hit the south coast of Shiretoko Peninsula. On the basis of those records, we conducted field survey for three times, and obtained the distribution of the tsunami height as the figure. The authors of the present study wish to express their thanks to JNES for its financial support in promoting our research.

Keywords: historical earthquake, historical tsunami, Hokkaido, Nemuro, Kushiro, Kuril trench



## A new calculation method for seabed displacement due to fault slip by boundary integration

AKIYAMA, Shinichi<sup>1\*</sup> ; FUJIWARA, Hiroyuki<sup>2</sup> ; HASHIMOTO, Norihiko<sup>1</sup>

<sup>1</sup>CTC, <sup>2</sup>NIED

In tsunami simulation, initial water level of tsunami is often considered to be equal to vertical displacement of seabed generated by a source fault slip. Exact solution for displacement due to rectangular fault slip in elastic half space (Okada, 1985) has been generally applied to calculate the seabed displacement.

In order to calculate the displacement due to the source fault which has irregular form using this solution, the source fault should be modeled by patching many rectangular small faults along the irregular surface. As a result, the source-fault model has portions in which the rectangular small faults are overlapped each other or not covered the fault surface. Then, calculated displacement from the fault model is overestimated near the overlapped area or underestimated near the uncovered area. This kind of displacement discontinuity is not negligible when the fault is located near the seabed, while it is negligible in the case that it is far from the seabed. Therefore, a new technique to take the irregular form into consideration accurately is required to solve the above problem.

Under such a background, we developed a new method to calculate displacement of seabed due to slip of the source fault using boundary integration. It is well known that deformation of the medium due to a fault slip is represented by the boundary integration for the medium surface and the fault surface by applying Green's theorem to the governing equation. Considering the seabed as an elastic half space, it can also be expressed only with the boundary integration for the fault surface. Calculating the boundary integration numerically, we introduce the linear element which is used by Boundary Element Method (BEM) into the proposed method to guarantee continuity of the displacement. However the numerical integration based on Gauss quadrature formulae at the point near the fault surface is broken down by the influence of singularity of Green's function. We apply the Projection and Angular & Radial Transformation (PART) method (Hayami and Brebbia, 1988) to the proposed method to evaluate the effect of the singularity accurately. We will present formulation, validation, verification and application of this method.

This research was carried out as part of Tsunami Hazard Assessment for Japan by National Research Institute for Earth Science and Disaster Prevention (NIED).

### Reference

Okada, Y. (1985) Surface deformation due to shear and tensile faults in a half-space, *Bull. Seism. Soc. Am.*, 75, 1435-1154.

Hayami, K. and Brebbia, C.A. (1988) Quadrature methods for singular and nearly singular integrals in 3-D boundary element method, (Invited paper), *Proc. 10th Int. Conf. on Boundary Elements*, Southampton, Computational Mechanics Publication with Springer-Verlag, Vol. 1, pp. 237-264.

Keywords: seabed displacement, fault slip, numerical calculation, boundary integration, singularity of Green's function, PART method

## Inundation hazard mapping toward probabilistic tsunami hazard assessment

SAITO, Ryu<sup>1\*</sup> ; FUJIWARA, Hiroyuki<sup>2</sup> ; HIRATA, Kenji<sup>2</sup> ; MURASHIMA, Youichi<sup>1</sup> ; MURATA, Yasuhiro<sup>1</sup> ; INOUE, Takuya<sup>1</sup> ; AKIYAMA, Shinichi<sup>3</sup> ; ABE, Yuta<sup>3</sup> ; MATSUYAMA, Hisanori<sup>4</sup> ; TOHYAMA, Nobuhiko<sup>4</sup>

<sup>1</sup>KOKUSAI KOGYO CO., LTD. (KKC), <sup>2</sup>National Research Institute for Earth Science and Disaster Prevention (NIED), <sup>3</sup>ITOCHU Techno-Solutions Corporation (CTC), <sup>4</sup>OYO Corporation

A method to obtain probabilistic hazard information on tsunami run-up and inundation area is described in this study, as part of the probabilistic tsunami hazard assessment research work [NIED]. A tsunami hazard assessment has been conducted to estimate frequency of exceedance wave height at several monitoring sites along coastal region, and to be useful for the study of coastal vulnerability, based on results from a tsunami simulation with an earthquake scenario and occurrence probability. Although the main target of a tsunami hazard assessment has contributed to quantify risk in critical infrastructure facilities, inundation hazard information for urban and river regions are also important. In a study of a probabilistic tsunami hazard assessment for Japan, tsunami exceedance wave height in coastal region is probabilistically derived from numerical modelling of tsunami sources available. However, horizontal resolutions in the model is only 50 m of minimum in a land region due to computational cost constrained by tsunami simulation for Japan, which is not enough resolution to assess inundation hazard mapping on a urban area. A detailed inundation hazard assessment is expected as a result of implementing smaller grid size than 50 m.

Here we provides a technical note for estimation of inundation hazard mapping resulted from a simulation run at horizontal resolution 10 m, and show their results at Rikuzentakata, one of example. A horizontal distribution of the probabilistic inundation is calculated from hazard curves on every grid cells in inundation area. Earthquake scenarios are set by many tsunami sources and occurrence frequencies around Japan trench. An annual exceedance probability of inundation when reaching threshold is calculated from tsunami sources and occurrence probability of the earthquake scenarios. This describes the benefit of tsunami inundation hazard mapping. We could successfully show this point clearly for the first time.

Keywords: Tsunami hazard, Tsunami inundation, Probability, Hazard curve

## Uncertainty for tsunami hazard caused by heterogeneous slip on the characterized source model

ABE, Yuta<sup>1\*</sup> ; HASHIMOTO, Norihiko<sup>1</sup> ; KORENAGA, Mariko<sup>1</sup> ; FUJIMOTO, Keisuke<sup>1</sup> ; AKIYAMA, Shinichi<sup>1</sup> ; FUJIWARA, Hiroyuki<sup>2</sup> ; HIRATA, Kenji<sup>2</sup>

<sup>1</sup>ITochu Techno-Solutions Corporation, <sup>2</sup>National Research Institute for Earth Science and Disaster Prevention

In preparation for probabilistic tsunami hazard assessment for the whole of Japan, we discuss uncertainty for tsunami heights due to a difference in slip distribution of source models.

In the process of probabilistic tsunami hazard assessment, tsunami heights at assessment points are estimated by numerical simulations. We calculate crustal deformations from source models, which are assumed as initial sea surface displacements, and then simulate tsunami propagations till tsunamis arrive in coastal sites. A simulation result changes depending on fault parameters of a source model such as magnitude, location, dip, strike, rake and slip distribution. Therefore, tsunami hazard includes uncertainties due to variability of fault parameters.

For the cases of subduction-zone earthquakes, focal mechanism is thought to be subject to a plate boundary in the characterized tsunami source model defined by probabilistic tsunami hazard assessment for the whole of Japan (Toyama et al., 2014, JpGU). On the other hand, magnitude, location and slip distribution are thought to have large varieties and their variabilities will create a large difference in tsunami height distributions. We therefore take account of the variabilities by calculating a number of source models with the different fault parameters. In this study, we give a qualitative verification for the variation in tsunami height due to slip distribution for the purpose of simplifying the hazard assessment process by using a probabilistic model for the uncertainty due to slip distribution. We examine a parameter study for several models with different slip distributions using two topography models, an uniform water depth model and a real ocean floor topography model. As the result, there is little to distinguish of geometric standard deviations between the two topography models, the values are 0.09 at a maximum.

This study was performed as a part of research for "Tsunami hazard assessment for the whole of Japan" in NIED.

Keywords: Tsunami, Probabilistic Hazard Assessment, Characterized tsunami source model, heterogeneous slip distribution

## Large slip area in characterized Tsunami source model toward Tsunami Hazard assessment

KORENAGA, Mariko<sup>1\*</sup> ; AKIYAMA, Shinichi<sup>1</sup> ; ABE, Yuta<sup>1</sup> ; HASHIMOTO, Norihiko<sup>1</sup> ; HIRATA, Kenji<sup>2</sup> ; FUJIWARA, Hiroyuki<sup>2</sup> ; MATSUYAMA, Hisanori<sup>3</sup> ; MURASHIMA, Yoichi<sup>4</sup>

<sup>1</sup>CTC, <sup>2</sup>NIED, <sup>3</sup>OYO, <sup>4</sup>KKC

In previously deterministic Tsunami hazard assessment, it had been ordinary method in setting tsunami source model that it is accountable for signature of historical tsunami events. Therefore it is difficult to evaluate of tsunami risk for future events unascertained focal area or magnitude and so on. On the other hand, in probabilistic tsunami hazard assessment, it's necessary to be designed for all potentially tsunamigenic earthquakes considering target region in principle, in planning phase of modeling of elastic fault parameter (Toyama et al., 2014, JPGU). For our purpose, on setting for characterized tsunami source model for probabilistic tsunami hazard, it is essential to characterize tsunami source model and include the statistical variability. We focused on the " heterogeneous slip distribution " of tsunami source, and studied on how to setting area ratio of large slip.

According to the distribution of the fault plane slip obtained from the wave source inversion studies of the 2011 off the Pacific coast of Tohoku Earthquake (2011 Tohoku tsunami), the ratio of large slip area is said to have contributed significantly to the tsunami wave height, the ratio of the area is much the same.

Therefore, in this study, we analyzed the ratio of seismic moment by unit area regardless of the assumed size of the fault element to all mean of seismic moment. As a result from inversion models of 2011 Tohoku tsunami source and other magnitude of 9 level source, three stage characterized modeling is required, it was found that the model which accounts for 30% of the total area of 2 times the average slip, and 10% of the total area of 4 times the average slip is appropriate. And two stage characterized model for magnitude 8 level sources, its large slip (twice the average) region accounts for 30%. Comparing the maximum coast wave heights simulated using characterized model above with a detailed inversion fault model, we verified that the former covering the latter.

This study was conducted by a part of research project in NIED for tsunami hazard assessment for the whole of Japan.

Keywords: tsunami, probabilistic hazard assessment, characterized fault model, heterogeneous slip distribution

## Large tsunami remote observations from high altitude using the induced magnetic field of tsunami.

TATEHATA, Hidee<sup>1\*</sup> ; HAMANO, Yozo<sup>2</sup>

<sup>1</sup>JMA, <sup>2</sup>JAMSTEC

On The 2011 off the Pacific coast of Tohoku Earthquake, massive tsunamis more than 10m attacked it in the wide range of Ibaraki from Aomori coast area. The tsunami warnings were not only sufficient but also no observation result of the tsunami, it was a big problem. The other side, at the Chichijima geomagnetic observation point had observed the tsunami induced magnetic field

As a result of example analysis for a past tsunami on Chichijima islands, the signal of the induced magnetic field was able to detect almost more than 1m tsunamis. The observation of the tsunami by the tsunami induced field has a weak point that sensitivity and a point of S/N ratio, but has a characteristic of the remote observation unlike the observation by tide gauges. If a geomagnetism sensor was installed in the hill of the Sanriku coast as a huge tsunami meter, they endured a massive tsunami and might continue observation without being destroyed.

We introduce the wave pattern of the prospective induced field of the tsunami and some character, if a sort of electromagnetic huge tsunami meter had been installed in the Sanriku coast.

Keywords: tsunami, Huge tsunami meter, induced magnetic effect

## Tsunami spectral analysis in and around Tokyo Bay

TAKIGAWA, Akira<sup>1\*</sup> ; MUROTANI, Satoko<sup>1</sup> ; HEIDARZADEH, Mohammad<sup>1</sup> ; WU, Yifei<sup>1</sup> ; SATAKE, Kenji<sup>1</sup>

<sup>1</sup>Earthquake Research Institute, University of Tokyo

Coastal areas in the Kanto region have been damaged by large tsunamis in the past. The reported tsunami heights from the 1923 M7.9 Kanto earthquake show a great difference between in and around Tokyo Bay. Attenuation of tsunami heights was observed at the mouth of the bay. For example, tsunami heights were less than 1.0 m inside the bay at Shinagawa, Funabashi, and Chiba, although they were 3.0-10.0 m outside the bay (Hatori et al., 1973, ERI special publication).

On the other hand, the tsunams from the 2011 Mw 9.0 Tohoku earthquake did not experience such attenuation. For example, tsunami heights were 1.46 and 2.84 m inside the bay at Tokyo and Funabashi respectively, although they were 1.45 and 1.60 m outside the bay at Tateyama and Kyonan (Sasaki et al., 2012, CEJ).

It is important to know why this difference occurs, when estimating tsunami damage to the metropolitan area for future earthquakes. Therefore we conducted spectral analysis of tsunami waveform obtained by numerical simulations, and found that the dominant wave period in the bay is different for each earthquake. It is around 100 min for the Kanto earthquake tsunami and around 70 min for the Tohoku one. We inferred that the 100 min period may result from the normal mode of Tokyo bay (Aida, 1996, Zisin) and the 70 min period from the normal mode of Sagami Bay (Imai et al., 2011, SSJ meeting). In future, we will examine the relation between these different periods and tsunami behaviors.

Keywords: Tsunami, Spectral analysis, Tokyo Bay, 1923 Kanto earthquake, 2011 Tohoku earthquake

## Wave period dependence of the tsunami energy decay based on observation: In the case of the 2011 Tohoku-oki Earthquake

TANOBE, Atsushi<sup>1\*</sup> ; IMAI, Kentaro<sup>2</sup> ; HAYASHI, Yutaka<sup>3</sup> ; IMAMURA, Fumihiko<sup>2</sup>

<sup>1</sup>Graduate School of Engineering, Tohoku University, <sup>2</sup>IRIDEs, Tohoku University, <sup>3</sup>Meteorological Research Institute

### 1. Introduction

2011 Tohoku-oki Earthquake caused serious damage. In the case of such a giant earthquake, transportation network suffer serious damage. Therefore ensuring sea route safety as the relief course is important for smooth relief and restoration activity. It is important that realize the decay process of tsunami to early ensure the security of the sea route. On the other hand, there is no clear and scientific standard to judge tsunami convergence (Hayashi et al., 2010).

In this study, we use the 2011 Tohoku-oki Earthquake tsunami wave form and show the characteristic of the tsunami decay process by the connection with time of the moving root mean square amplitude maximum onset and tsunami arrival time. And we paid attention to period, intended to clarify the characteristic of each decrement process.

### 2. Analysis

We targeted for analysis 20 points chose from observed tsunami wave form in the 2011 Tohoku-oki Earthquake that located in the Japanese Islands Pacific on shore and off shore station (observed by Japan Meteorological Agency, NOWPHAS, Geospatial Information Authority of Japan).

It is obvious that long sampling intervals can lead to a marked distortion of the wave properties (Rabinovich et al., 2011). We unified the sampling intervals for 30 sec and High-frequency filtering was used to remove sea level variations associated with synoptic atmospheric activity. We used the maximum of the moving root mean square amplitude to normalize the observed wave because of tsunami amplitude different from every observation point. After the Normalized process we analyzed that wave form.

Because the tsunami includes wave of various periods, and suggested decay process is different every period (Rabinovich et al., 2013). So we used band-pass 2-16 min, 16-32 min, 32-64 min, and 64-128 min filter to divide tsunami every periods. I calculated the moving root mean square amplitude and we analyzed it with a method of Hayashi et al. (2010) to define a decay coefficient.

In this study,  $t$  is the elapsed time from shock,  $M(t)$  is moving root mean square amplitude at  $t$ ,  $M_{max}$  is maximum of the  $M(t)$ ,  $T_m$  is time of onset  $M_{max}$ ,  $T_t$  is time of the first wave's maximum observed,  $TL$  is differences between  $T_m$  and  $T_t$ ,  $k$  is proportional constant every observation point,  $e$  is Napier's constant,  $\tau$  is decay time.  $\tau$  mean time required for the average amplitude being decay to  $1/e$ .

As a result of analyzed, the tsunami decrement process of each observation point is characterized by the longer period wave that attenuate later and shorter period wave that maximum wave late for arrival.

### 3. Conclusion

In this study, we used the tsunami wave pattern at the 2011 Tohoku-oki Earthquake and analyzed it. I discussion a factor to characterize a decay process of the tsunami energy, and get the following result.

- (1)Regardless of on shore or off shore, equilateral correlation has  $\tau$  and  $T_t$ , and on shore points tends to get longer than  $\tau$ .
- (2)For a wider tendency, tsunamis indicates that shorter period waves attenuate much faster than longer period waves in a short period.
- (3)Some observation point have a long  $TL$  about less than 32 min period.

### Acknowledgments

This work was partly supported by JSPS KAKENHI Grant No.24310132.

And I gratefully acknowledge the following organizations for providing with records for the 2011 tsunami: observed by Japan Meteorological Agency, NOWPHAS, Geospatial Information Authority of Japan

Keywords: tsunami, decay, decay time, period

## Oscillations starting immediately after the 2011 Tohoku earthquake in Japan Sea

MUROTANI, Satoko<sup>1\*</sup> ; IWAI, Maki<sup>2</sup> ; SATAKE, Kenji<sup>1</sup>

<sup>1</sup>ERI, the Univ. of Tokyo, <sup>2</sup>Yokohama City Univ.

The tsunamis from the March 11, 2011 Tohoku earthquake were recorded in the Japan Sea. At some tide gauge stations along the Japan Sea coast of Honshu and the Russian coast, sea surface disturbances were observed immediately after the earthquake, followed by tsunami propagated through the Tsugaru Strait between Honshu and Hokkaido. Using tsunami numerical computations from seafloor displacements including the effect of the horizontal displacement and seafloor slope, the oscillations starting immediately after the origin time were reproduced. We interpret that these tsunami forerunners were generated from horizontal motion of seafloor slopes in the Japan Sea.

The tsunami forerunners were particularly remarkable at Awashima (JCG), Sado, Noto Toyama and Fukaura (JMA) tide gauge stations along the Japan Sea coast of Honshu and at Rudnaya Pristan, Preobrazhenie, and Nakhodka stations along the Russian coast of Primorye (Shevchenko et al., 2013: Pageoph). The 2011 tsunami originated in the Pacific Ocean would pass the Tsugaru Strait 1.5 hours after the earthquake. It indicates that these forerunners were different from the tsunami originated in the Pacific Ocean.

We made the tsunami numerical computation to reproduce these forerunners from seafloor displacements in the Pacific Ocean and Japan Sea. We used the source model of Satake et al. (2013, BSSA). According to Tanioka and Satake (1996, GRL), if the ocean bottom contains steep slopes or steps, the effect of the horizontal displacement of ocean bottom cannot be neglected. Computation including this effect showed the oscillations starting immediately after the origin time. However, the short-period components about a few minutes are not well reproduced. Use of finer bathymetry grid than we used (30' and 5') may better reproduce the short-period components of the Japanese tide gauge stations. Seismograms at nearby stations suggest that some of the short-period components may be the seismic ground motion. When we applied low-pass filter to the observed waveforms, the agreement between the observed and synthetic waveforms on tide gauges became better.

Because the Russian stations are about 500 km away from the source area, we also computed the synthetic tsunami waveforms from seafloor displacements computed on the spherical Earth model (Sun et al., 2009: Geophys. J. Int.). However, the computed waveforms from the spherical models are not very different from those computed on Cartesian coordinate system. It is necessary to compute the tsunami waveforms using the finer grid including the shape of the bay.

Keywords: the 2011 Tohoku earthquake, the 2011 Tohoku tsunami, Japan Sea, seafloor displacement

## The 24 September 2013 tsunami in the Makran region, northwestern Indian Ocean

HEIDARZADEH, Mohammad<sup>1</sup> ; SATAKE, Kenji<sup>1\*</sup>

<sup>1</sup>Earthquake Research Institute (ERI), The University of Tokyo

Tsunami waves were observed in the northwestern Indian Ocean following the Mw 7.7 Pakistan inland earthquake on 24 September 2013. We analyze eleven tide gauge records as well as one DART record of this tsunami and perform numerical modeling of tsunami. The tsunami registered a maximum wave height of 109 cm in Qurayat tide gauge station (Oman). Spectral analysis showed that the most governing period of the tsunami waves was around 12 min though wavelet analysis showed that parts of the tsunami energy were partitioned into other period bands of 7 and 16 min. Distribution of aftershocks in the region showed that all of them were located inland indicating that the tsunami was generated by submarine geological phenomena triggered by the earthquake. Tsunami backward ray tracing showed that the tsunami source was possibly located at offshore Jiwani (Pakistan) and the tsunami was most likely generated immediately after the main shock. Tsunami modeling assuming a pile-up structure at the location of the new island was not successful in reproducing the observed sea level records. A landslide source with a length of about 15-20 km, a thickness of 100-150 m located at 61.72°E and 24.60°N seems capable of fairly reproducing the observed sea level records. This event was the second tsunami recorded in the Makran region since 1945, and may be evidence for hazards from landslide-generated waves following seismic activities.

Keywords: Northwestern Indian Ocean, Tsunami, Makran subduction zone, Landslide, Spectral analysis, Numerical modeling

## Pre-computed Tsunami Database with Additional Slip Near to the Trench for Tsunami Early Warning in Southern Java

SUNENDAR, Haris<sup>1\*</sup> ; TANIOKA, Yuichiro<sup>1</sup> ; GUSMAN, Aditya<sup>1</sup> ; LATIEF, Hamzah<sup>2</sup>

<sup>1</sup>Institute of Seismology and Volcanology, Hokkaido University, <sup>2</sup>Bandung Institute of Technology

We build tsunami database based on simple fault model scenarios for the Java trench subduction zone. We have 480 points along the subduction zone with distance between each other of 20 arc-min. This points are used as the center of simple fault model scenarios. Each point is the center of several fault models with different moment magnitudes. We used a magnitude to fault length and width scaling relationship for the fault model scenario. The moment magnitudes for the fault model scenarios are from Mw 6.3 to Mw 9.0 with interval of 0.3. The fault depth parameter is also a variable for the fault model scenario. We used depth between 10 km to 60 km with interval of 10 km.

From each fault model scenario we simulate tsunami propagation by solving the linear shallow water equations. We used bathymetry data based on Indonesian navy chart and GEBCO bathymetric dataset. The grid size for the tsunami simulation is 1 arc-min. The pre-computed maximum tsunami heights and tsunami arrival time at every point along the coast are stored in a database.

If a real earthquake occur at any location in the forecasting domain then the pre-computed tsunami heights from 16 scenarios are retrieved from the database. Theses 16 scenarios are those that are surrounding the actual hypocenter and each of the scenario has the closest higher or closest lower magnitude to the actual one. Then the tsunami heights from these scenarios are used in interpolation methods to get the tsunami height forecast. The tsunami heights from two scenarios with a same hypocenter and different moment magnitudes are interpolated by logarithmic interpolation. Then the tsunami heights with different depths and different epicenters are interpolated using linear interpolation and bilinear interpolation, respectively. The the interpolated tsunami heights is group into district administrative regions, then the maximum height for each administrative region is selected. The selected tsunami heights are categorized into three different warning levels. These levels are tsunami smaller than 0.5 m, between 0.5 m to 3 m, and larger than 3 m.

We apply this method to forecast the tsunami generated by the 1994 East Java earthquake. The 1994 earthquake is classify as a tsunami earthquake (Newman and Okal, 1998; Pollet and Kanamori, 2000). The earthquake moment magnitude was estimated to be Mw 7.6 (Abercrombie et al., 2001), Mw 7.8 (Bilek et al., 2006; USGS), Mw 7.9 (Pollet and Kanamori, 2000). Our result shows that the forecasted tsunami heights underestimate the actual tsunami heights. One of the main cause could be the fact that we used simple fault model scenarios which sizes were estimated from scaling relationship of magnitude to fault dimension of regular earthquake but not tsunami earthquake. Previous studies shows tsunami earthquake may generate large slip near the trench (Tanioka and Satake, 1996; Satake et al., 2013). Therefore to obtain a more accurate forecast, the fault model scenarios near the trench should represent fault model for tsunami earthquake event.

Keywords: pre-computed tsunami database, tsunami earthquake, tsunami early warning

## Simulation of tsunami inundation from future megathrust earthquake scenarios of Central Peru

MAS, Erick<sup>1\*</sup> ; ADRIANO, Bruno<sup>2</sup> ; PULIDO, Nelson<sup>3</sup> ; KOSHIMURA, Shunichi<sup>1</sup>

<sup>1</sup>International Research Institute of Disaster Science, IRIDeS, Tohoku University, <sup>2</sup>Graduate School of Engineering, Tohoku University, <sup>3</sup>National Research Institute for Earth Science and Disaster Prevention, NIED

Great tsunami events like the 2011 Great East Japan Earthquake and Tsunami might occur around the world in the future. In particular at areas of the Pacific Rim or the Andaman Sea as history has confirmed. In this study we will focus on the central coast of Peru on the western Pacific. The earthquake history of Peru accounts for many devastating tsunami disasters in the past (1555, 1586, 1609, 1630, 1655, 1678, 1687, 1746). The potential damage to national infrastructure exposed in Callao and Lima could yield to a heavy economical breakdown in Peru. It is of great importance to assess and estimate the future tsunami inundation scenarios in order to grasp the extent of possible damage and the severity of it. Consequently, this study evaluates the tsunami hazard and the related features of inundation at the central coast areas of Peru based on possible megathrust earthquakes.

The source model we used in this study (Mw = 8.90) was obtained from results of the interseismic coupling distribution in subduction areas using GPS monitoring data as well as historical earthquake recurrence information (Pulido et al., 2011). This slip model was used to generate twelve additional slip scenarios for strong ground motion simulation, by adding spatially correlated short-wavelength slip heterogeneities (Pulido et al., 2012).

Here, we used these thirteen scenarios to evaluate the tsunami hazard of Callao area in Peru. From results of strong ground motion simulations Pulido et al. (2012) reported that the slip scenario with the deepest along strike slip average (Mw = 8.86) was the worst case scenario for strong ground motion in Lima-Callao area. On the other hand, in this study the slip model with the largest peak slip (Mw = 8.87) yielded the highest tsunami inundation and maximum velocity near shore. Such differences on maximum scenarios for peak ground acceleration and tsunami height reveals the importance of a comprehensive assessment of earthquake and tsunami hazard in order to provide plausible worst case scenarios of strong ground motion and tsunami inundation.

### Acknowledgments

This study was carried out under the framework of the SATREPS project "Enhancement of Earthquake and Tsunami Disaster Mitigation Technology in Peru, project sponsored by the Japan International Cooperation Agency (JICA) and the Japan Science and Technology Agency (JST). Our appreciation goes to the Ministry of Education, Culture, Sports, Science and Technology (MEXT), National Research Institute for Earth Science and Disaster Prevention (NIED) and the International Research Institute of Disaster Science (IRIDeS), Tohoku University for their support.

### References

Pulido, N., Tavera, H., Aguilar, Z., Chlieh, M., Calderon, D., Sekiguchi, T., Nakai, S., and Yamazaki, F. (2012). Estimation of slip scenarios of mega-thrust earthquakes and strong motion simulations for Central Andes, Peru realizations (poster S33A-2505). In *American Geoscience Union Fall Meeting 2012*, number section III, pages 1?2, San Francisco, California, USA.

Pulido, N., Tavera, H., Perfettini, H., Chlieh, M., Aguilar, Z., Aoi, S., Nakai, S., and Yamazaki, F. (2011). Estimation of Slip Scenarios for Megathrust Earthquakes: A Case Study for Peru. In *4th IASPEI/IAEE International Symposium*, pages 1?6, Santa Barbara, CA, USA.

Keywords: megathrust earthquake, megatsunami, numerical simulation, tsunami Peru, scenarios

## Identification of submarine landslide tsunami sources: A probabilistic approach for the Gulf of Mexico

SHIGIHARA, Yoshinori<sup>1\*</sup> ; HORRILLO, Juan<sup>2</sup>

<sup>1</sup>National Defense Academy, <sup>2</sup>Texas A&M University at Galveston

The devastating consequences of recent tsunami events in Indonesia (2004), Japan (2011) have changed the perception about tsunami potential and have prompted a scientific response in assessing the tsunami hazard in regions even though an apparent low-risk or/and lack of complete historical tsunami record exists. Although a great uncertainty exists regarding the return period of large-scale tsunami events in the Gulf of Mexico (GOM), geological and historical evidences indicate that the most likely tsunami hazard could come from a submarine landslide triggered by a moderate earthquake. Under these circumstances, the assessment of the tsunami hazard in the region could be better accomplished by means of a probabilistic approach to include the uncertainty in the hazard analysis and thus to identify tsunami sources.

This study aims to customize for the GOM an existing probabilistic methodology to determine landslide-tsunami sources associated with return periods. The Monte Carlo Simulation (MCS) technique is employed to determine the uncertainty related to location/water-depth and landslide dimension based on normal/lognormal distributions obtained from observed data. Along fixed transects over the continental slope of the GOM, slide angle of failure, soil properties and seismic peak horizontal accelerations (PHA) are determined by publicly available data. These parameter values are used to perform slope stability analyses in randomly generated translational submarine mass failure (SMF) obtained from the MCS technique. Once the translational SMF is identified as tsunamigenic for a given recurrence rate, a preliminary tsunami amplitude can be estimated by using empirical formulations. Thus, the annual probability of a tsunamigenic SMF is determined by the joint probability with the annual PHA.

By using the probabilistic approach we identified tsunami sources associated with return periods from few thousands to 10,000 years for each fixed transects defined over the continental slope of the GOM.

Keywords: tsunami, submarine landslide, the Monte Carlo Simulation

## A stochastic analysis and an uncertainty assessment of tsunami wave height using a random source parameter model

FUKUTANI, Yo<sup>1\*</sup> ; SUPPASRI, Anawat<sup>1</sup> ; IMAMURA, Fumihiko<sup>1</sup>

<sup>1</sup>International Research Institute of Disaster Science, Tohoku University

In this paper, we conducted a stochastic tsunami hazard assessment including various uncertainties using a logic tree with targeting a region of the 3.11 Tohoku earthquake and investigated how heterogeneous slip faults generated by CRSP (Correlated Random Source Parameter) model influence the stochastic tsunami hazard assessment. In the assessment, observed tsunami wave height 6.7m in the 3.11 Tohoku Earthquake corresponded to 1112 year (0.50 fractile point), 1129 year (simple average) and 490 year (0.95 fractile point) for return period. Next, we investigated an influence that the number of slip patterns has on the results of the assessment. While the number of slip patterns had little impact on the results of the stochastic assessment in cases which a target wave height was comparatively low (2.0m), the return period at each fractile point was overestimated in case of 3 slip patterns and 5 patterns than 1 pattern when a target wave height was comparatively high (6.7m or 10.0m). We can conclude that the number of slip patterns had a great impact on the stochastic assessment depending on the target wave height. To clarify the uncertainties of tsunami wave height, we defined a 90 percent confidence interval and a coefficient of variation as indexes which can quantify the uncertainties of tsunami wave height. Basically, the 90 percent confidence interval had high value where the wave height at each fractile point was high. In addition, we confirmed that changing of maximum wave height due to changing of the asperity location in the assuming fault had a great impact on the coefficient of variations in the offshore point of the Ibaraki coast. The coefficient of variation in the offshore point of peninsula located in ria shoreline of the Iwate coast was comparatively higher than a result in closed-off section of bay located in ria coast. This result indicates an effect due to a characteristic topography in ria coast.

Keywords: probabilistic tsunami hazard assessment, uncertainty analysis, rogit tree, CRSP model

## Seismic and tsunami fragility of industries, revealed by the 2011 Tohoku-oki earthquake

KUWAHARA, Yasuto<sup>1\*</sup> ; HASEGAWA, Isao<sup>1</sup> ; YOSHIMI, Masayuki<sup>1</sup> ; NAMEGAYA, Yuichi<sup>1</sup> ; HORIKAWA, Haruo<sup>1</sup> ; NAKAI, Misato<sup>1</sup> ; MASUDA, Satoru<sup>2</sup>

<sup>1</sup>AIST, GSJ, <sup>2</sup>Graduate school of Economics and Management, Tohoku University.

We have developed seismic and tsunami fragility curves of industries by using damage data of industrial companies, estimated strong motions and estimated tsunami heights of the 2011 Tohoku-oki earthquake. The damage data were obtained from 7,019 industrial companies through inquiry surveys by the Regional Innovation Research Center of Tohoku University. As a damage level indicator for each company, we introduced a ratio of an economical damage of physical fixed assets excluding lands to previous balance of the physical fixed assets. The estimated strong motions of the 2011 Tohoku-oki earthquake at all the sites of the companies were from the database of the so-called QuiQuake system (Quick estimation system for shaking maps triggered by observation records) operated by the National Institute of Advanced Industrial Science and Technology (AIST). It is noted that the estimated data were obtained by taking account of seismic local site effects and the actually observed ones. The tsunami height data at each site of the company were obtained by interpolating the confirmed data compiled by the 2011 Tohoku Earthquake Tsunami Joint Survey Group (2013). It is found that a frequency-damage level distribution for each seismic intensity is well correlated with a binominal distribution where the only parameter characterizing the distribution is an average value of the damage levels in each seismic intensity. The tsunami fragilities are also obtained as a function of the tsunami height in the same way. These fragility curves can be useful not only to estimate economic damages for future huge earthquakes, but also to rapidly assess the damage just after earthquakes.

Keywords: Seismic, Tsunami, fragility curve, industry, the 2011 Tohoku-oki earthquake

## Compiling the source area data of large earthquakes occurred in Pacific Rim

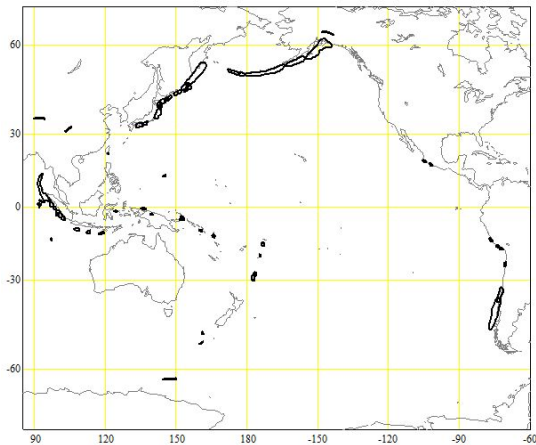
ISHIKAWA, Yuzo<sup>1\*</sup>

<sup>1</sup>Y. Ishikawa

The locations of hypocenters were usually plotted by some symbols. This way leads to misunderstand that the earthquake source is the point source. It was caused by the earthquake catalog of which location data were given as a point.

Now, the earthquake source are given by the area obtained by the one month aftershock distributions. Events of which magnitude are larger than 8.0 from 1970, using PDE earthquake catalog. Some large events were added in 20 century. The source areas of large earthquakes occurred in Pacific Rim were digitized.

Keywords: source area, large earthquake, Pacific Rim



## A set of characterized earthquake fault models for the probabilistic tsunami hazard assessment in Japan

TOYAMA, Nobuhiko<sup>1\*</sup>; HIRATA, Kenji<sup>1</sup>; FUJIWARA, Hiroyuki<sup>1</sup>; NAKAMURA, Hiromitsu<sup>1</sup>; MORIKAWA, Nobuyuki<sup>1</sup>; OSADA, Masaki<sup>1</sup>; MATSUYAMA, Hisanori<sup>2</sup>; KITO, Tadashi<sup>2</sup>

<sup>1</sup>NIED, <sup>2</sup>OYO CORPORATION

A set of characterized earthquake fault models are necessary for nation-wide probabilistic tsunami hazard assessment in Japan (Fujiwara et al., 2013; Hirata et al., 2014). It should include all possible earthquakes in future and should take into account various types of uncertainty.

In general, origins of tsunamis include a volcano, a landslide as well as an earthquake, but as the first step we focus on tsunamis that are caused by only earthquakes occurring near Japanese Islands. We introduce our strategy to construct a set of earthquake fault models for tsunami hazard assessment in Japan, showing examples of earthquake fault models along the Japan Trench.

The "Long-term Evaluation of earthquakes from Sanriku-oki to Boso-oki region (2nd edition)" (2011/11/25) by the Headquarters for Earthquake Research Promotion (HERP), Japanese government, defined 8 seismogenic segments along the Japan Trench. Based on these segmentations, we classify tsunamigenic earthquakes into 7 categories as follows; 1) "March 11, 2011 Tohoku earthquake-type" earthquakes, 2) maximum-sized class earthquakes, 3) other large-sized earthquakes, 4) earthquakes occurring in any single segment which HERP assessed its possible magnitude and/or location with recurrence interval, 5) tsunami earthquakes, 6) intra-plate earthquakes with normal faulting, and 7) moderated-sized earthquakes (HERP called this type "earthquakes which we cannot expect its magnitude and size"). HERP assessed earthquake potentials only in categories 1), 4), 5), and 6). To enhance the entirety of tsunami hazard assessment, we newly add the categories 2), 3) and 7), though no previous earthquakes in categories 2), 3), and 7) are known yet. We place earthquake fault on the upper boundary of the subducting Pacific Plate except earthquakes of the category 6).

Seismic moment,  $M_0$ , to a characterized earthquake fault model, is determined by an empirical scaling relation between  $M_0$  and fault area,  $S$ . To determine the empirical relation we first make a list of tsunamigenic earthquakes from the data base of "Size of tsunamis around Japan for 1498-2006" (<http://www.eri.u-tokyo.ac.jp/tsunamiMt.html>) by Abe. Next we assign  $M_0$  and  $S$  to listed tsunamigenic earthquakes, referring in previous studies (Sato et al., 1989) and then derive an empirical  $M_0$ - $S$  scaling relation for tsunamigenic earthquakes occurred in the area of the Pacific ocean side. There are some previous studies suggesting that rigidity is depth dependent, but we use a constant value of  $5 \times 10^{10} (\text{N/m}^2)$  as rigidity.

We introduce inhomogeneity in earthquake fault slip to define "large slip area (LSA)" and "extremely large slip area (ELSA)" by following a characterized ratio of high-slip area to entire fault area (Korenaga et al., 2014). For great earthquakes of  $M_w > 8.4$ , LSA is allowed to be located 3 patterns for along-trench direction and 3 patterns for trench-normal direction, thus total of 9 basic configurations, for each characterized earthquake fault model. ELSA can be allowed to be located along the upper edge in a LSA when the LSA is located adjoined the trench axis. For large earthquakes with the magnitudes less than  $\sim 8.3$ , that is the category 7), we consider only a LSA at the center of the entire fault area. In this case, variability of possible LSA location is taken into account by introducing an uncertainty value of possible LSA location in process of tsunami hazard curve calculation.

A set of characterized earthquake fault models that we place along the Japan Trench, spans from  $M_w$  7.0 to 9.4 at every 0.1 or 0.2 magnitude intervals. Total number of the models along the Japan Trench reaches more than 1800. It takes whole three months to complete non-linear tsunami simulations for all characterized earthquake fault models.

This study was done as a part of "Tsunami hazard assessment project for Japan" in NIED.

Keywords: tsunami hazard assessment, probability, characterized earthquake fault model

## Tsunami hazard assessment project in Japan

HIRATA, Kenji<sup>1\*</sup>; FUJIWARA, Hiroyuki<sup>1</sup>; NAKAMURA, Hiromitsu<sup>1</sup>; OSADA, Masaki<sup>1</sup>; OHSUMI, Tsuneo<sup>1</sup>; MORIKAWA, Nobuyuki<sup>1</sup>; KAWAI, Shin'ichi<sup>1</sup>; AOI, Shin<sup>1</sup>; YAMAMOTO, Naotaka<sup>1</sup>; MATSUYAMA, Hisanori<sup>2</sup>; TOYAMA, Nobuhiko<sup>2</sup>; KITOH, Tadashi<sup>2</sup>; MURASHIMA, Yoichi<sup>3</sup>; MURATA, Yasuhiro<sup>3</sup>; INOUE, Takuya<sup>3</sup>; SAITO, Ryu<sup>3</sup>; AKIYAMA, Shi'ichi<sup>4</sup>; KORENAGA, Mariko<sup>4</sup>; ABE, Yuta<sup>4</sup>; HASHIMOTO, Norihiko<sup>4</sup>

<sup>1</sup>NIED, <sup>2</sup>OYO, <sup>3</sup>KKC, <sup>4</sup>CTC

Tsunami hazard assessment (THA) is the most important information to take effective measures against possible tsunami attacks in future. After the national tragedy caused by the 11st March 2011 Tohoku earthquake (Mw9.0), NIED started a research project regarding TSA in Japan to support various kind of measures by sectors such as local governments, life-line companies, etc (Fujiwara et al., 2013, JpGU). Our research project consists of two components; (A) a research of probabilistic tsunami hazard assessments (PTHA) in which we consider all of possible tsunamis that may affect coastal regions in future and (B) a research to forecast coastal tsunami heights and inundation flow depths based on specified earthquake scenarios.

In the research (A) of PTHA, we began working on subjects of (1) nation-wide probabilistic tsunami hazard assessment (NW-PTHA) and (2) detailed probabilistic tsunami hazard assessment for a specific region (DPTHASR). Outlines of (1) NWPHTA are as follows; (i) we consider all of possible earthquakes in future including earthquakes that the Headquarters for Earthquake Research Promotion (HERP), Japanese Government, already assessed. (ii) We construct a set of simplified earthquake fault models, called "characterized earthquake fault models (CEFMs)", for all of the earthquakes mentioned above by following prescribed rules (Toyama et al., 2014, JpGU; Korenaga et al., 2014, JpGU). (iii) We solve a non-linear long wave equation, using staggered leap-frog, finite difference method (FDM), including inundation calculation as coastal boundary condition, over a nesting grid system with the minimum grid size of 50 meters, to calculate tsunamis for each of initial water surface distributions (under research for initial water surface calculation by Akiyama et al., 2014, JpGU) generated from a large number of the CEFMs. (iv) Finally we integrate information about coastal tsunami heights from the numerous CEFMs to get nation-wide tsunami hazard curves, defining excess probability, for coastal tsunami heights, incorporating uncertainties inherent in tsunami forward calculation and earthquake fault slip heterogeneity (Abe et al., 2014, JpGU). In the present step we are revising a prototype of NWPHTA in the case where possible tsunami sources are located along the Japan Trench as well as we are constructing a set of CEFMs in the case where possible tsunami sources are located along the Nankai Trough.

As for the research of (2) DPTHASR, we are going to develop new methods to assess inundation probability and inundation time, etc., through tsunami inundation simulations for a set of CEFMs using the same FDM over a nesting grid system with the minimum grid size of 10 meters including information of seawalls and breakwaters. Some of results from DPTHASR will be represented in a similar format of "Karte" (medical chart) to help understandings of tsunami hazard information by residents. In the present step, we are constructing a new method to assess probabilistic inundation depth distribution along with calculation of hazard curves for inundation depth at specified points on land (Saito et al., 2014, JpGU).

In the research (B), we are planning to construct a deterministic method to forecast coastal tsunami heights, inundation area and depth, etc. in specified sites in the scenarios that possible maximum-sized tsunamis strike there. These deterministic forecasts should be examined through comparisons with tsunami deposits distribution, historical materials, and instrument records.

Also, we are making a lot of effort to utilize probabilistic and deterministic tsunami hazard information by investigating actual usages of domestic/oversea tsunami hazard information (Osada et al., 2014, JpGU) and by investigating opinions and ideas from persons-in-charge of measures by local governments for tsunami disasters thorough questionnaire surveys with direct interviews (Ohsumi et al., 2014, JpGU).

This work partially functions to support activities of HERP.

Keywords: tsunami, hazard assessment, probability, scenario-type tsunami forecast, hazard map, utilization

## G-EVER Earthquake and Volcanic Eruption Risk Management Activities and Asia-Pacific Region Hazard Mapping Project

TAKARADA, Shinji<sup>1\*</sup> ; ISHIKAWA, Yuzo<sup>1</sup> ; BANDIBAS, Joel<sup>1</sup> ; G-EVER, Promotion team<sup>1</sup>

<sup>1</sup>Geological Survey of Japan, AIST

The Asia-Pacific Region Global Earthquake and Volcanic Eruption Risk Management (G-EVER) Consortium among the geo-hazard research institutes in the Asia-Pacific region was established in 2012. G-EVER aims to formulate strategies to reduce the risks caused by earthquakes, tsunamis and volcanic eruptions worldwide. The First Workshop on Asia-Pacific Region Global Earthquake and Volcanic Eruption Risk Management (G-EVER1) was held in Tsukuba, Japan from February 22 to 24, 2012. During the workshop, the G-EVER1 accord was approved by the participants. The Accord consists of 10 recommendations such as; enhancing collaboration, sharing of resources, and making information of the risks of earthquakes and volcanic eruptions freely available and understandable. The G-EVER Hub website was setup to promote the exchange of information and knowledge about volcanic and seismic hazards among Asia-Pacific countries. Establishing or endorsing standards on data sharing and analytical methods is important to promote data and analyses results sharing. The major activities of G-EVER include participation in global risk reduction efforts such as the Integrated Research on Disaster Risk (IRDR) Program, Global Earthquake Model (GEM) and Global Volcanic Model (GVM). The 2nd G-EVER International Symposium and the 1st IUGS&SCJ International Workshop on Natural Hazards was held in Sendai, Tohoku Japan on October 19-20, 2013. We endorsed Sendai Agreement during the symposium (<http://g-ever.org/en/sendai/>). Several G-EVER Working Groups and projects were proposed such as; (1) Risk mitigation of large-scale earthquakes WG, (2) Risk mitigation of large-scale volcanic eruptions WG, (3) Next-generation volcanic hazard assessment WG, and (4) Asia-Pacific region earthquake and volcanic hazard mapping project.

The Asia-Pacific region earthquake and volcanic hazard mapping project aims to make an advanced online information system that provides past and recent earthquake and volcanic eruption information (e.g. age, location, scale, affected areas and fatalities) and risk assessment tools for earthquake and volcanic eruption hazards. A printed map will also be published as the new version of the Eastern Asia Geological Hazard Map of the Commission for the Geological Map of the World (CGMW). The online hazard mapping system will provide useful information about earthquake and volcanic hazards in an interactive and user-friendly interface. Past and recent large-scale earthquakes and volcanic eruptions, tsunami inundation areas, and active faults distributions will be shown on the map. Links to major earthquakes and volcanic eruptions databases will be available in the system. The earthquake and volcanic eruption hazard mapping project will be implemented with the cooperation of major research institutes and organization in the Asia-Pacific region such as PHIVOLCS, CVGHM, GNS Science, EOS, USGS and CCOP.

Keywords: Earthquake, Volcano, Risk, Hazard, Hazard Map, Asia Pacific

## Observing Schumann Resonance by demodulating High Frequency Waves

CAO, Bingxia<sup>1\*</sup>; ZHOU, Hongjuan<sup>1</sup>

<sup>1</sup>Harbin Institute of Technology at Weihai

The limited dimensions of the Earth cause the waveguide between the surface of the Earth and the conductive ionosphere to act as a resonant cavity for electromagnetic waves in the ELF band so that Schumann Resonance (SR) occurs there. It has been suggested that SR may be used to monitor global temperature variations. SR has been used to study the lower ionosphere on Earth and suggested as one way to explore the lower ionosphere on celestial bodies. A new field of interest using SR is related to short-term earthquake prediction. The manmade noises in the ELF band was a problem for observing. A new way to observe SR based on cross-modulation in the low ionosphere is discussed.

The effect of cross-modulation was established by Yampolski et al. between SR and HF signals experimentally. The HF signals called Round-the-world signals (RWS) and large antenna arrays of the radio telescope UTR-2 were used. But the problem is whether the SR can be seen only with a simple antenna. If the answer is yes, we have a new measurement method for SR.

The HF-SR multiple mode nonlinear interaction theory is researched based on the basic theory model established. In the multiple interaction mode theory, the modulation depth is affected by electromagnetic wave phase in the nonlinear effect. Before the experiment, a lot of simulation experiments and theoretical research are carried out, including Schumann Resonance global distribution simulation and multi-mode interaction of HF-SR theory etc.. One simpler half wave cross dipole antenna is used to receive the time service signal of China called BPM. And in the demodulation spectrum of BPM, the first 4 order resonance peaks of the SR are obtained successfully, respectively on 7.5Hz, 14Hz, 20Hz and 26Hz.

The electric field distributions and phase variations of the first 3 order peaks of Schumann Resonance in the earth ionosphere cavity are obtained through a series of SR distributed simulation experiments. The result shows that in the same phase region, the phase of SR only depends on time. At the same time all the points have the same vibration phase. Two points have 180 degree difference phase after a phase mutation point.

The actual multi interaction mode effect between RWS and SR is uncertain. It may change with the propagation conditions. The modulation depth can not be increased significantly in the multiple interaction effects of HF wave and SR propagate around the globe. The main reason is the high frequency wave goes through the the phase jump points of Schumann Resonance. The final depth of modulation in the Yampolski experiment is about 0.7-3.5 times to the modulation depth of single interaction.

RWS goes through around the earth. But the modulation depth of RWS and SR nonlinear effect is not significantly far greater than that of 1 jump value because of the path length growth.

Using the RWS signal, greater modulation than short reception, for example, 1 hop, can be obtained. But due to the SR wave distribution in the earth ionosphere cavity, the value is less than the direct summation of each modulation results. That is to say, high frequency electromagnetic wave propagates around the earth for nearly a circle. It is modulation result with SR dose not significantly increase compared with that of the obtained by ionospheric reflection arrive at the receiving station.

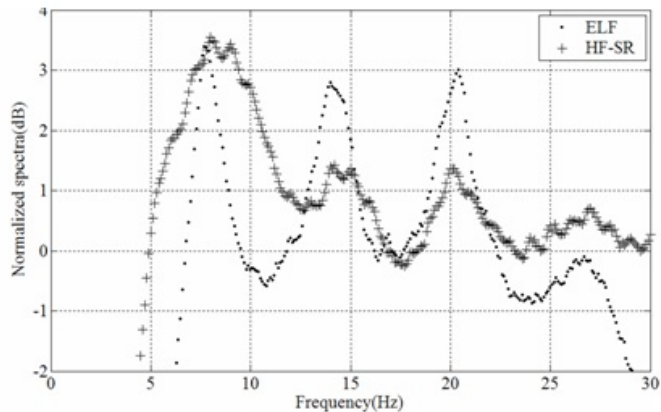
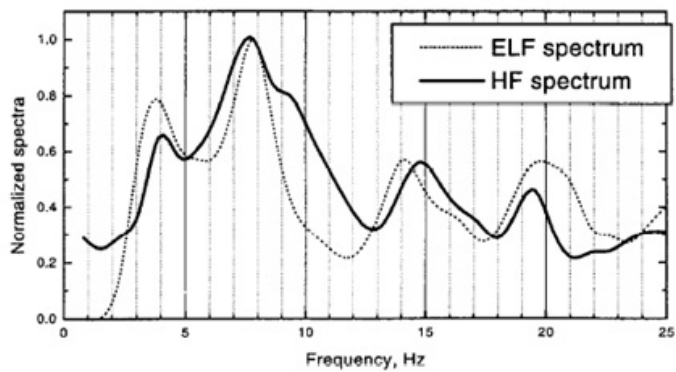
According to the new theory of HF-SR interaction, a receiving station was established. The system receives the BPM time service signals from the National Time Service Center in PuCheng, 1160 km away from the receiver. The carrier frequency is 10 MHz. By demodulating the BPM signal, the first 4 order peaks of SR are obtained. Maybe it is a new way for SR observing.

Keywords: earth ionosphere cavity, Schumann Resonance, nonlinear effect, high frequency wave

HDS28-06

Room:312

Time:May 1 17:30-17:45



## Influence of microtopography in lowland to tsunami disaster of 2011 Tohoku Earthquake

IKARI, Kazuya<sup>1\*</sup> ; NARAMA, Chiyuki<sup>2</sup>

<sup>1</sup>Graduate School of Science & Technology, Niigata University, <sup>2</sup>Faculty of Science, Niigata University

The earthquake (magnitude 9.0) on Mar 11, 2011 in Tohoku, Japan triggered the terrible destructive tsunami, striking the eastern coastal region of Japan. Although residents in valley bottom plain of the Sanriku Coast (ria coast) have a refuge area around hills, residents in Sendai Plain (meander plain of lowland) had to go inland in order to escape tsunami. The lowland such as Sendai Plain is very vulnerable to tsunami. However, Building damages differed among the Sendai Plain. This study evaluated the influence of landform in lowland of Sendai Plain to tsunami disaster.

The Sendai plain is meander plain of lowland (0-3m asl.), including beach ridges and inter-ridge march of ridged beach plain, and natural levees along present and meander scars. Three beach ridges are developed along the coast. Relative height of present beach ridge is 3-5m, and inner two beach ridges are 1-2m.

We classified three damage-categories (flow out, destroy, and remain) to individual buildings in tsunami inundation area of the Sendai Plain, based on interpretation of aerial-photographs on 2011 and Google Earth satellite image 2012. In addition, we made a GIS data of utility pole, flattened tide protection forest, driftwood, tsunami scratch in Sendai Plain, to know flow directions of tsunami and distribution of woods.

Building damages in the Sendai plain show >80% of buildings flowed out within 1km area from the coast. Remaining buildings are located on ridged beaches with 1-2m high. Driftwood and rubble had stopped on the near side of beach ridges and highway embankment. Tsunami flow was concentrated in the inter-ridge march or small stream channels. Around the Abukuma River, buildings under cut slope received tsunami damage, and slip-off slope side was safety. In lowland plain, we clarified microtopography with 1-2m relative height reduced tsunami damages around inland side area (>1km) from the coast.

Keywords: 2011 Tohoku Earthquake, tsunami, Sendai Plain, lowland, microtopography, aerial-photographs

## Eruptive Sequence of Rinjani Caldera, 13th Century, Lombok, Indonesia

FURUKAWA, Ryuta<sup>1\*</sup>; TAKADA, Akira<sup>1</sup>; NASUTION, Asnawir<sup>2</sup>; TAUFIQURROHMAN, Roni<sup>3</sup>

<sup>1</sup>Geological Survey of Japan, AIST, <sup>2</sup>Institute Technology of Bandung, <sup>3</sup>Center for Volcanology and Geological Hazard Mitigation

Rinjani Volcanic Complex located at northern part Lombok Island is centered by a large stratovolcano, Rinjani volcano, which is the volume of 100 km<sup>3</sup> and 3726m high (Nasution et al., 2003). A caldera of 6x8 km in diameter lies western side of the summit formed at mid-13th century (Nasution et al., 2010; Lavigne et al., 2013). Sequence of the caldera forming eruption is reconstructed from original stratigraphy of eruptive deposits and consists of 6 phases with no prominent time interval between them. Phase 1 is a small phreatic eruption produced thin ash fall bed only occurs proximal of the summit. Phase 2 is large plinian eruption dispersed pumice lapilli to western side and extending to adjacent islands. Pumice lapilli become finer and lithic fragments increase upward in the fall bed. Phase 3 is defined by widely extending pyroclastic flow deposit consists of vaguely bedded unsorted ash with subordinating rounded pumice lapilli. Its thickness varies from several to 50 cm especially thickens local topographic depression and eroding underlying pumice fall bed. This deposit extends more than 50 km from the probable source and reached Gili Island isolated by ocean suggesting extremely dilute pyroclastic flow possibly caused by plinian eruption column collapse from high altitude. Phase 4 is unstable plinian eruption implied by graded pumice lapilli bed intercalated by multiple thin ash beds. Phase 5 is characterized by enormous pyroclastic flow effusion resulting thick and massive pumiceous lapilli tuffs extending more than 30 km from the source. Proximally fines depleted lithic breccia including andesite lavas and minor amount of granodiorite are interbedded with massive pumiceous lapilli tuff. Thickly stratified lapilli tuff beds exposes along the coastline suggest the pyroclastic flow caused the secondary explosions and formed littoral cone at the ocean entry. Phase 6 is last plinian eruption dispersed pumice fall of limited extent which is smaller than preceding plinian phases 2 and 4. Petrological analysis shows magma composition changes between phase 3 and 4 suggesting formation of new vent or widening pre-existing vent eventually causes the caldera formation.

Keywords: volcano, caldera, pyroclastic flow, Indonesia, ash, icecore

## Holocene rock avalanche phenomena from the upper Okumatashirodani Basin, Kamikochi Valley, northern Japanese Alps

KARIYA, Yoshihiko<sup>1\*</sup> ; MATSUSHI, Yuki<sup>2</sup> ; HARAYAMA, Satoru<sup>3</sup> ; MATSUZAKI, Hiroyuki<sup>4</sup>

<sup>1</sup>Senshu University, <sup>2</sup>Kyoto University, <sup>3</sup>Shinshu University, <sup>4</sup>University of Tokyo

Hummocks and a minor ridge both of which have been considered to be moraines are present on alluvial fans near the Shinmurabashi Bridge, Tokusawa Area of Kamikochi Valley in the Hida Mountains. A series of geomorphological, lithological, and chronological studies of these landforms and their forming materials revealed that hummocks and a minor ridge were formed by two different rock avalanches that occurred on the steep east face of Kitahotaka-dake north ridge about 3000 m ASL and ran into valley floor near the Shinmurabashi Bridge. A terrestrial cosmogenic nuclide dating method of igneous rocks comprising hummocks and a minor ridge showed that hummocks were formed during 6.0-7.9 <sup>10</sup>Be ka and a ridge was during 0.8-1.1 <sup>10</sup>Be ka.

Keywords: landslide, in-situ terrestrial cosmogenic nuclide dating, Hida Mountains

## Rock failure of welded tuff in Sounkyo valley, Hokkaido, on September 2013

ISHIMARU, Satoshi<sup>1\*</sup> ; TAJIKA, Jun<sup>1</sup> ; WATANABE, Tatsuya<sup>1</sup> ; ISHIKAWA, Isao<sup>2</sup> ; SHIMURA, Kazuo<sup>3</sup>

<sup>1</sup>Geological Survey of Hokkaido, <sup>2</sup>Hokkaido Government, <sup>3</sup>Shin Engineering Consultants

A rock failure occurred at the left valley side of the Ishikari River in Sounkyo, Hokkaido, on 8th September 2013. Although Route 39 runs along the Ishikari River, rocks did not reach on the road, because the road is 170m distance from the collapse slope in the other side of the Ishikari River. However, the rock debris buried a part of the river, and formed a 200m-long flooding area at the upper reach. The type of this rock failure is a rock slide to a debris avalanche with high velocity flow.

Paleogene shale of the Hidaka Supergroup is overlain by Sounkyo welded tuff at the valley wall. Sounkyo welded tuff consists of two facies. The lower is a soft non-welded part, and the upper is a welded part with developed columnar or platy joints. Sounkyo valley has been formed by erosion of the pyroclastic flow deposits (30Ka), Sounkyo welded tuff, from Ohachidaira Caldera by the Ishikari River. In consequence, steep cliffs have developed in the valley. At the collapse point, only the uppermost 30m of the slope is steep cliff, but the lower 140m is about 40 degree. According to air photo interpretation, the surface with gently roughness profile develops on the 40 degree slope. This shows talus deposits as past collapse debris overlie the slope.

The area of the slope failure, erosional and depositional area, is 190m in height, 90-100m in width, and 365m in length. The equivalent coefficient of friction is 0.52. The volume of the collapse is more than 33,000m<sup>3</sup>. Sounkyo welded tuff is exposed on the upper slope with 90m height, and the debris of the collapse covers on the lower slope with 95m height. A debris slump, 45m height and 20m width, is located on the lower center part of the debris slope. A part of the past talus deposits is exposed by this debris slump. The Hidaka Supergroup shale is covered with talus deposits. Springs from the piping holes eroded the gullies in talus, and the talus deposits were wet state at the investigation of two days after the failure.

The debris from the collapse slope was spread in lobe-shapes over the valley flat. Arcuate ridges and troughs, 1-2m high, shaped concentric half circles in the center axes of the main lobe. This suggests flow-type mass movement. The debris is distributed on 130m in length and 120m in width of the valley flat. The most of the debris is grayish white welded tuff, and the pale reddish welded tuff originated from the uppermost slope is distributed around the ridges. Shale of the Hidaka super group is rare. The squeeze of the mixture of the soil deposits, composed of woods and organic matters, and volcanic ash is distributed in front of the ridges and in gaps in the troughs. This was dragged from the base of the moving body of the collapse, and played a role in a flow layer, matrix facies, of debris avalanche. The talus deposits would be fluidized. The debris would run with high velocity at the front part of the depositional area. According to the estimating equation (Sceidegger, 1973), using the equivalent coefficient of friction, the velocity is estimated by 38m/s at the foot of the slope.

The rock failure was occurred by the bellow mechanism. Rock slide was occurred near the boundary, the Hidaka Soupergroup shale and the non-welded part of the tuff, and the upper slope broke down. Ground water concentrates in the permeable layer of the non-welded tuff on the impermeable layer of the shale. Because the pyroclastic flow, the Sounkyo Welded Tuff, buried the former valley slope of the Hidaka Soupergroup shale in 30,000 years ago, the boundary is incline toward the river, and also the structure of the tuff is incline. This rock failure was occurred at the instability slope, which consisted of soft non-welded tuff with concentrated groundwater beneath heavy welded tuff. The columnar joints, the collapse surface, at the uppermost of the slope have opened before the rock failure, because moss grows on the joint surface.

Keywords: rock failure, welded tuff, rock slide, debris avalanche

## Geologic causes of Akatani rockslide induced by heavy rain with typhoon Talas (1112)

NAGATA, Hidehisa<sup>1\*</sup> ; YOKOYAMA, Shunji<sup>2</sup> ; INOKUCHI, Takashi<sup>3</sup> ; KATO, Hironori<sup>4</sup> ; KIMURA, Katsumi<sup>5</sup>

<sup>1</sup>Fu Sui Do co. Ltd., <sup>2</sup>Kochi Univ., <sup>3</sup>NIED, <sup>4</sup>Aratani Civil Eng. Consultants, <sup>5</sup>AIST

Heavy rain by the Typhoon Talas in 2011 triggered many landslides at Kii Peninsula. The Akatani rockslide in Gojo City, Nara Prefecture is one of the largest landslides, which has dimensions of 500 m wide, 1100 m long, about 80-100 m deep, and 10 million cubic meters in volume. Geologic causes of the rockslide were investigated.

Geology of the Akatani rockslide is composed of mudstone and sandstone of the Miyama Complex of the Shimanto Belt. Not only bedding plane, but also fault planes and joint planes formed in various stages are weak planes related to the rockslide. The average attitude of the bedding planes tends to dip steeply northward while varying. However, there are low-angle dip slip faults nearly parallel or daylight to the slope surface. These are considered to be out-of-sequence thrusts, because they obliquely intersect bedding plane and some of them subdivided the Miyama Complex into several tectonic units. The rupture surface is not smooth curved but rough. This was the combined fragile planes including faults subparallel to the slope. It is similar to the other landslides in the Shimanto Belt that simple slide along bedding planes did not occur.

## Development history of sagging around Kanmuriyama Pass, Gifu-Fukui prefecture boundary

KOJIMA, Satoru<sup>1\*</sup> ; NIWA, Ryota<sup>1</sup> ; KANEDA, Heitaro<sup>2</sup> ; IKEDA, Akiko<sup>3</sup> ; NAKAMURA, Toshio<sup>3</sup> ; OHTANI, Tomoyuki<sup>1</sup>

<sup>1</sup>Department of Civil Engineering, Gifu University, <sup>2</sup>Department of Earth Sciences, Chiba University, <sup>3</sup>Center for Chronological Research, Nagoya University

Recently sagging landforms like double ridges and uphill-facing scarps attract attention as precursors of large-scale landslides. Many types of large- and small-scale saggings have been ubiquitously found in the Japanese mountainous regions by the analyses of detailed topographic maps made by LiDAR survey. Their development histories and processes, however, are unclear. We report the results of field and chronological researches on saggings in the Kanmuriyama Pass area, Gifu-Fukui prefecture boundary. Since the lithology and age of sediments accumulated in the linear depression between the double ridges east of the Kanmuriyama Pass were reported in the last meeting, those on the uphill-facing scarps west of the pass will be presented in the meeting this year.

Four rows of uphill-facing scarps parallel to the slope are recognized on the south side of the prefecture boundary ridge about 2 km west of the Kanmuriyama Pass. The sediments accumulated in the linear depressions were collected and analyzed by the hand-auger boring and pit survey. Lithological characteristics of these sediments are common and they are composed of, in descending order, 1) carbonaceous mud/leaf litter mixture, 2) dark gray mud, 3) light gray mud, and 4) orange-color conglomeratic mud. This lithology is also similar to that of the sediments between the double ridges east of the Kanmuriyama Pass. The sediments in the first, second and third depressions from the top include Kikai-Akahoya tephra (K-Ah) about 7.3 ka or have peaks of volcanic glass contents of this tephra. The horizons of the tephra, however, are recognized in the different lithologies; the sedimentary environment about 7.3 ka varied with the depression. The ages of the tephra and the AMS-<sup>14</sup>C ages of wood fragments embedded in the sediments indicate that the sedimentation rates of the dark and light gray mud members are about 0.08 mm/year, and several times slower than those of the upper carbonaceous mud/leaf litter mixture member. The depressions and uphill-facing scarps formed about several tens of thousand years ago on the basis of the estimation of the thickness of sediments and the extrapolation of the sedimentation rate of the mud formations.

Keywords: sagging, landslide, Gifu, Fukui, Kanmuriyama

## Detection of pre movements of landslide or deep collapse using InSAR and LiDAR

KOARAI, Mamoru<sup>1\*</sup> ; NAKANO, Takayuki<sup>1</sup> ; TODA, Kenichiro<sup>2</sup> ; DAIMARU, Hiromu<sup>3</sup>

<sup>1</sup>GSI of Japan, <sup>2</sup>Nagano Prefecture Forestry Reserch Center, <sup>3</sup>Forestry and Forest Products Research Institute

It is possible to detect pre movements of landslide or deep collapse using SAR interferometry technology. As previous studies, there are example of the Shimegake Landslide on the foot of Mt. Gassan, Yamagata Prefecture and the Ohkamizawa Landslide in Higashi-naruse Village, Akita Prefecture. In this research, the usefulness of the monitoring methodology which combined SAR interferometry and LiDAR data will be verified for the monitoring of region where the deep collapse will occurred. This research is supported by the Grants-in-Aid for Scientific Research (No.22500994). The main verification fields are Nagano Prefecture and Shizuoka Prefecture. The used InSAR imageries are analyzed by Geodetic Department, the Geospatial Information Authority of Japan, using the data of PALSAR which is L band SAR of the earth observation satellite "Daichi" (ALOS).

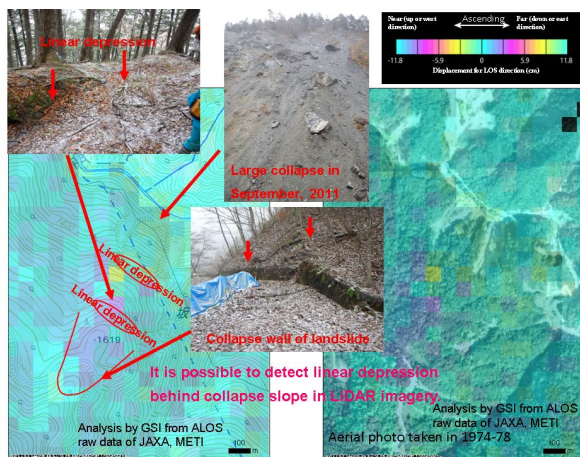
Near the Kuchisakamoto Landslide of Shizuoka Prefecture, a change significant by InSAR imagery in the autumn of 2008 and the autumn of 2009 had occurred, and about 6-7 cm deformation to the LOS direction was observed in one month and a half of 2009. In field survey, the authors checked that the large landslide had occurred between November, 2012 and June, 2013 (Nakano et al., 2013; Koarai et al., 2013).

In west side of Sakamaki hot spring of Nagano Prefecture, about 6-7 cm deformation to the LOS direction was observed in InSAR imagery of one year from 2008 to 2009, and large collapse occurred in September, 2011. In LiDAR data imagery taken before the collapse occurred, it is possible to detect linear depression behind collapse slope.

In this presentation, the authors report many case of pre movement of landslide detected by field survey or LiDAR data in the areas where InSAR imageries show small deformation in Nagano Prefecture.

Fig.1 InSAR imagery of west side of Sakamaki hot spring (2008/07/20-2009/09/07) and sloop deformation detected in field survey

Keywords: deep collapse, landslide, InSAR, LiDAR, Nagano Prefecture



## Prediction and stability evaluation of potential sites of deep-seated catastrophic landslide

CHIGIRA, Masahiro<sup>1\*</sup> ; SAKASHIMA, Toshihiko<sup>2</sup> ; FUNAYAMA, Atsushi<sup>2</sup> ; MINAGAWA, Jun<sup>2</sup> ; SHIBUYA, Kenichi<sup>3</sup>

<sup>1</sup>Disaster Prevention Research Institute, Kyoto University, <sup>2</sup>Pacific Consultants Co. Ltd, <sup>3</sup>Aero Asahi Corporation

Chigira (2009) and Chigira et al. (2013) analyzed geological structures and topographic features of deep-seated catastrophic landslides induced by rainstorms in accretion complexes of the southwest outer belt of Japan, and found that those landslides had been preceded by gravitational slope deformation typified by small scarps along their future crowns, which could be a clue to predict potential sites of catastrophic deep-seated landslide. This paper summarizes the methodology of potential site prediction and stability evaluation of catastrophic landslides, including stratified rocks in addition to broken beds and mixed rocks in accretion complexes.

In order to extract potential sites of catastrophic landslide, we need to judge whether deep-seated gravitational slope deformation may develop to catastrophic failure or not, considering possible structures of gravitational slope deformation on a certain geologic background. We examined the relationships among morphological expression of gravitational slope deformation, geologic body, geological structure, and deformation mechanisms, then took account of upslope and downslope conditions, and finally tried to evaluate the probability of catastrophic failure with the help of our experience of previous catastrophic landslides.

### Irregularly shaped bumpy slope:

This is typically made when incipient sliding zones are being made in a rock body with complex discontinuities like broken beds or mixed rocks. Only this topography does not suggest the high probability of catastrophic failure, but additional eye-brow shaped small scarps and failures in the lower part of a slope may suggest high probability.

### Linear depressions and wrinkles:

Symmetric alignment of linear depressions on both sides of a ridge suggests lateral spreading with the settlement of the ridge top, which does not likely develop to catastrophic failure.

Linear depressions and wrinkles developed on one side of a ridge are made flexural toppling of steeply dipping foliations of bedding or cleavage. This type is self-stabilizing deformation, but when downslope-facing eye-brow scarps are made and lower part of the slope is failed, catastrophic failure likely occur. Ridge-top depressions, when connected to steps and to a hollow on the side margin of a deformed area, catastrophic failure also likely occur.

### Large head scarps or ridge top depressions:

These topographies on an under-dip cataclinal slope suggest buckling deformation, which may be stable when a competent rock layer exists or deformation extent is less, but when the deformation progresses further and lower slope is failed, the probability of catastrophic failure becomes high.

Large head scarps or ridge top depressions on an over-dip cataclinal slope suggest sliding in a strict sense with mature and continuous sliding zones. Such a landslide may continue slow movement without catastrophic failure, but when the foot is cut by failure, it may develop to catastrophic failure.

### References

Chigira, M., 2009. September 2005 rain-induced catastrophic rockslides on slopes affected by deep-seated gravitational deformations, Kyushu, southern Japan. . *Engineering Geology*, 108, 1-15.

Chigira, M., Tsou, C.-Y., Matsushi, Y., Hiraishi, N., Matsuzawa, M., 2013. Topographic precursors and geological structures of deep-seated catastrophic landslides caused by Typhoon Talas. *Geomorphology*, 201, 479-493.

Keywords: deep-seated catastrophic landslide, gravitational slope deformation, site prediction, susceptibility evaluation

## Estimation of the slip-surface of landslide using electromagnetic approaches at Nishiikawa, Japan

YMAZAKI, Tomohiro<sup>1\*</sup> ; HATTORI, Katsumi<sup>1</sup> ; YOSHINO, Chie<sup>1</sup> ; HAN, Peng<sup>1</sup> ; KANEDA, Heitaro<sup>1</sup> ; SAKAI, Hideo<sup>2</sup> ; TSUKADA, Noriko<sup>3</sup> ; TERAJIMA, Tomomi<sup>4</sup> ; SUEMINE, Akira<sup>4</sup>

<sup>1</sup>Graduate school of science, Chiba University, <sup>2</sup>Graduate School of Science and Engineering for Education (Science) , Toyama University, <sup>3</sup>Faculty of Science, Toyama University, <sup>4</sup>The Disaster Prevention Research Institute(DPRI), Kyoto University

Landslide is one of the severe disasters triggered by rainfalls or earthquakes. Recently, landslides tend to increase by global-warming. Therefore, exploration into behavior of landslide becomes more important disaster prevention.

In order to explore landslide's behavior, we verified if there is slip-surface or not using magnetic approaches. In previous research, we had selected a test slope at Nishiikawa, Tokushima and we had performed electrical resistivity exploration and core-sampling. The core-sampling results indicate that there exists the structure which corresponds to slip surface. To verify this result, anisotropy in magnetic susceptibility (AMS) and natural residual magnetization (NRM) of samples that include that structure and periphery of it were measured. AMS result showed that slip-surface region provides the oblate ellipsoid characteristics, which was consistent with the developmental mechanism of slip-surface during sliding. And result of NRM indicated that magnetic minerals in slip-surface region oriented certain direction. This describes that magnetic minerals was able to move in saturated region and then were oriented to direction of earth magnetism.

These studies showed the possibility to identify slip-surface using rock magnetic approach. However, we found necessity of consideration of core-sampling technique to estimate the direction of slip using this approach because samples had rotated during core-sampling.

The details will be provided in the presentation.

Keywords: landslide, anisotropy in magnetic susceptibility, natural residual magnetization

## Dendrochronology of a fossil log from the dammed lake deposit by Dondokosawa rock avalanche, the Southern Japanese Alps

KARIYA, Yoshihiko<sup>1\*</sup> ; MITSUTANI, Takumi<sup>2</sup> ; INOUE, Kimio<sup>3</sup>

<sup>1</sup>Senshu University, <sup>2</sup>Nara National Research Institute for Cultural Properties, <sup>3</sup>Sabo Frontier Foundation

Large-scale rock avalanche deposits (Dondokosawa rock avalanche deposits; DRAD,  $V=1.9 \times 10^7 \text{ m}^3$ ) are present in the east side of Mount Jizo, the Akaishi Range. The age of DRAD has been determined by a <sup>14</sup>C-method as AD780-870 or as AD778-793 (with help of wiggle matching). However, precise age determination of DRAD is further required as the some uncertainties remain in the previous age data. Therefore, we performed dendrochronology of a fossil wood log of Japanese cypress (*Chamaecyparis obtusa*) with 226 tree rings and bark obtained from the dammed lake deposits formed by DRAD. As a result, the fluctuation pattern of tree ring width of the sample log (DDK-A) clearly coincided with the pattern during a period from AD662 to AD887 of the 2705-year-long standard curve (705BC-AD2000) established from some tree ring samples of Japanese cypress. Statistical analysis showed that a degree of agreement between DDK-A's tree ring curve and the standard curve ( $t$ ) is 7.9. Generally, it can be judged that there is high agreement between two tree ring patterns when  $t$ -value is more than 3.5. We also observed cell structures of the outermost tree ring for determining the kill season of DDK-A. The early wood ring was completely formed and the late wood ring was almost invisible. Therefore we concluded that DDK-A was dead in the late summer of AD887.

The old Japanese documents *Nihon-Sandai-Jitsuroku* and *Fuso-Ryakki* described the mega earthquake ( $M$  8-8.5), the *Goki-Shichido* earthquake, in AD887 August. This earthquake was considered to occur along the Suruga and Nankai Troughs off central Japan. Slope movement related to DRAD would be caused by this historical earthquake.

Keywords: dendrochronology, large landslide, Gokishichido earthquake, Akaishi Range

## Occurrence of large landslides in past 40 years and sediment supply in the southern Japanese Alps

NISHII, Ryoko<sup>1\*</sup> ; IMAIZUMI, Fumitoshi<sup>2</sup>

<sup>1</sup>University of Tsukuba, <sup>2</sup>Shizuoka University

Many large landslides are distributed in the southern Japanese Alps which consists of high relief and steep slopes. A lot of sediments deposited in dams suggest that sediments are produced actively in upper streams. To evaluate the sediment supply from landslides, this study addressed the mapping of landslides ( $>10000 \text{ m}^2$ ) in Ooi River and Hayakawa River (total area is  $862 \text{ km}^2$ ) using aerial photographs and orthophotographs in 1970s and 2000s (partly including 2010s). In addition, we computed the volume of sediment supply in several large landslides based on the difference between DEMs from LiDAR data in multiple shooting periods. One hundred eighty landslides were extracted from photographs in 2000s to 2010s. The comparison between the distribution maps of landslides in 1970s and 2000s indicated that an initial large landslide ( $>100000 \text{ m}^2$ ) had not occurred since 1970s. In contrast, some landslides had enlarged gradually. Erosion rate computed from LiDAR data indicated the order of  $10^{-1}$  to  $10^{-2} \text{ m yr}^{-1}$ . Such erosion rate suggests that the bare grounds after landslides are important as sediment supply area.

Keywords: large landslide, sediment supply, aerial photograph, GIS, the Southern Japanese Alps

## Cause and age of the Yabusawa Gravel in the northern foot of Mount Senjo, the Akaishi Range, Japan: a reappraisal

KUROSAWA, Hiroshi<sup>1\*</sup> ; KARIYA, Yoshihiko<sup>2</sup> ; MATSUSHI, Yuki<sup>3</sup> ; MATSUZAKI, Hiroyuki<sup>4</sup>

<sup>1</sup>Graduate School of Senshu University, <sup>2</sup>Senshu University, <sup>3</sup>Kyoto University, <sup>4</sup>University of Tokyo

The Yabusawa gravel (YG) consists of poorly-sorted thick angular clasts of sand stone, mud stone, and hornfels, forming a geomorphic feature like fluvial terraces along Yabusawa River from Mount Senjo. The previous authors had considered that YG was of glaciofluvial or large landslide origin. However, there is no clear consensus as to the origin and age of YG. We therefore carried out new analysis of geology, geomorphology, and geochronology of YG. The following results were obtained. On the outcrop walls of YG, rock clasts clearly exhibit jigsaw crack structures, although specific sedimentary facies reflecting fluvial processes such as lamination and imbrication are not observed at all. A lithotype of rock clasts in YG is almost restricted to single geology at a given outcrop locality. Surficial topography of YG has hummocks and levee-like terrain. Terrestrial cosmogenic nuclide dating of sandstone fragments obtained from three localities apart from each other gave 10.3-8.4 ka, 10.0-8.1 ka, and 9.4-7.6 ka (in <sup>10</sup>Be scale). On the basis of these facts, we concluded that YG was produced by catastrophic rock slide (rock avalanche) in the early Holocene as single event. Although the previous authors stressed degradation of mountain permafrost for landslide occurrence, we invite attention to paleoearthquakes caused by nearby active faults or convergent plate margins as well as early Holocene pluvial climate and long-term gravitational rock deformation. A multidisciplinary study for better understanding of basic factors, onset triggers, kinematic behavior of landslide is further required

Keywords: Shimanto group, Rock avalanche, Terrestrial cosmogenic nuclides, Holocene

## Gravitational rock deformation since the late Pleistocene on the Hounose-dendeiro Ridge, the southern Kanto Mountains

SAWABE, Koichiro<sup>1\*</sup> ; KARIYA, Yoshihiko<sup>2</sup> ; SHIMIZU, Chosei<sup>3</sup>

<sup>1</sup>Graduate School, Senshu University, <sup>2</sup>Senshu University, <sup>3</sup>Komazawa University

We describe the geology and geomorphology related to gravitational rock deformation on the Hounose-dendeiro Ridge(HB), the upper Tama River Basin. HB is a broad ridge line 200 to 300 m wide running from northwest to southeast, and its altitudinal range spans from 1050 m to 1180 m ASL. The bedrock geology of HB is Cretaceous sedimentary rocks of Shimanto Group that generally show NE-SE strike and east dip at 60 to 80 degrees.

Linear depressions and step-like slopes both parallel to HB are present on and around the ridge-top. Depth and length of depressions are usually less than 20 m and several tens to hundreds meters in many cases. Features of valley bulging with downhill-facing scarp and gentle slopes are also found from valley side slopes immediately below ridge-top linear depressions and step-like slopes. In the area of gravitational slope deformation where bulging features occur, rock deformation caused by toppling and buckling can be observed.

We recovered sediment drill cores in the linear depressions on HB (P1 and P2). The bottom of surficial humic soil gave 4.1-4.3 cal ka (P1, -64 cm) and 9.5-9.8 cal ka (P2, -162 cm). Also a vitric ash layer Aira-Tanzawa (30 ka) was found from -153 cm (P1) and -325 cm (P2). In addition, a patch of pumice grain of Ontake-Ina (93 ka) was discovered at -709 cm of P2. These facts indicate that linear depressions as depositional sinks on HB were already formed before 30 ka at P1 and before 93 ka at P2.

Keywords: Shimanto Group, Linear depression, Toppling, Buckling, Tephra, 14C age

## Relief, bell-shape and distortion indexes as critical topography of creep deformation due to mountain gravity

YAGI, Hiroshi<sup>1\*</sup> ; HAYASHI, Kazunari<sup>2</sup> ; IMAIZUMI, Fumitoshi<sup>3</sup> ; SATO, Go<sup>4</sup> ; HIGAKI, Daisuke<sup>5</sup>

<sup>1</sup>Fac. Art, Science & Education, Yamagata University, <sup>2</sup>Okuyama Boring Co.,Ltd., <sup>3</sup>Fac. Agriculture, Shizuoka University, <sup>4</sup>Teikyo-Heisei University, <sup>5</sup>Fac. Agriculture & Life Sciences, Hirosaki University

### 1.Introduction

Double ridges or up-hill facing scarplets distributed on mountain ridge in high relief are known as indicators that mountain bodies are undergoing gravitational creep deformation and as signs of landslide in large scale. However, such micro topographies on ridges in Japan Alps has developed since 30 ka before. That is presumably attributed to one of the para-glacial phenomena. Trench study in Southern Japan Alps clarified that they have intermittently developed in a time scale of 10000 year and the last event, but a slight deformation occurred about 500-600 years ago. It is quite gradual movement. Consequently dense distribution of the up-hill facing scarplets is not always a pre-causious sign of sudden collapse of the mountain body in near future, though the earthquake occurs near the mountains. Other causative factors are required to induce landslide for hazard susceptibility mapping. We analyzed topographic features of mountain around Mt Shichmenzan and Ooyakuzure, which locate along the marginal mountains in Shizuoka Pref, and where huge co-seismic landslides occurred in 17th and 18th century, using DEM of 10m grid scale and more precise scale.

### 2.Topographic feature of mountain collapsed by earthquakes

Mountain ridges around Mt. Shichimenzan and Ooyakuzure show gentle and round and are fringed by distinct break of slopes. Mountain profiles of high contrast between steep lower slope and gentle ridge tops are similar to a bell-shaped mountains of high relief. In another word, the bell-shaped profile is one kind of the concavity in ridge profiles.

### 3.Critical topography of creep deformation

Dense distribution of uphill facing scarplets are observed along the main ridges of the study area by aerial photograph interpretation. However, co-seismic landslides occurred only at Mt. Shichimenzan and Ooyakuzure. We analyzed relief of ridges, considering those of the surrounding slopes and ridge scale over the study area. We call it the relief index. Also we analyzed degree of bell-shape, weighting the area of convex part of the profile. These two indexes are highly scored around Mt. Shichimenzan and Ooyakuzure, but not so high along the main ridge from Mt. Yambushi-toge to Mt Dainichi-toge where the uphill facing scarplets are densely distributed. These are considered as very convenient indexes to know the high susceptibility of landslide induced by earthquake. And distortion index that is calculated ratio of total length of up-hill facing scarplets to a original slope length is also introduced as critical topography of creep deformation due to mountain gravity.

Keywords: gravitational creep, critical topography, relief index, bell-shape index, distortion index, large scale landslide

## Development of Lake Shibire and its geomorphological relationship with landslides in Misaka Mountains, central Japan

SUZUKI, Terumi<sup>1\*</sup> ; KARIYA, Yoshihiko<sup>2</sup> ; KUROSAWA, Hiroshi<sup>1</sup>

<sup>1</sup>Graduate School of Senshu Univ., <sup>2</sup>Senshu Univ.

Geomorphological classification mapping and geological investigation were carried out to reconstruct the development of Lake Shibire (890 m ASL, max depth 9.5 m, perimeter 1.2 km) in Yamanashi Prefecture. Lake Shibire was formed on a closed depression of the hilly mound with antislopes that was produced by landslide on the steep slopes adjacent to the lake. Other smaller landslide bodies were also identified next to Lake Shibire. Lacustrine deposits with plant macro fossils and a thin vitric ash layer (Aira-Tanzawa, 30 cal ka) were discovered from the side slope of a small channel close to Lake Shibire. Radiocarbon age of a plant macro fossil sampled from the bottom of the lacustrine deposits was 47-46 cal ka. The paleo Lake Shibire was likely to consist of independent two or more basins in the late Pleistocene and only one basin has survived to the present-day Lake Shibire. It is also likely that a single basin was decoupled into two or more basins due to occupation of landslide masses caused by secondary landslide activities adjacent to the basins, and only the certain basin linked to the present-day Lake Shibire has endured.

Keywords: landslide, lacustrine deposit, Aira-Tanzawa tephra, 14C dating, late Pleistocene

## Geological implication of the lahar disaster by Typhoon Wipha on October 16, 2013 in Izu Oshima Volcano

KOYAMA, Masato<sup>1\*</sup> ; SUZUKI, Yusuke<sup>2</sup>

<sup>1</sup>CIREN, Shizuoka University, <sup>2</sup>Izu Peninsula Geopark Promotion Council

Heavy rain (over 800mm per 24 hours) triggered by Typhoon Wipha on October 16, 2013, caused many slope failures and associated lahars in the western part of Izu Oshima Volcano, Japan. Tephrostratigraphic study revealed a mechanism of the slope failures and history of similar lahars for the past 700 years. Seven fallout ash or scoria layers, which were ejected during the 7 eruptions since the early 14th century, are distributed in the study area. These tephra layers are interbedded with eolian dust (loess) layers, each of which was deposited during a 10-200 years dormant period. Stratigraphic horizons of the slope failures concentrated at the boundaries between ashes and underlying loess layers. This means that more permeable ash layers were saturated with rainwater and slid down along the upper surface of less permeable loess layers. We newly found that three lahars (Lahar A, B, and C) occurred in historic time. Lahar A and B are correlated to the disaster documents of 1856 (or 1932) and of the late 16th century, respectively. Lahar C overlies directly on the Y5.2 scoria and associated Motomachi Lava and thus occurred in the early-middle 14th century.

Keywords: Izu Oshima, volcano, eruptive history, lahar, Typhoon Wipha (2013), slope failure

## Preliminary report on the landslides, Oct. 2013, Izu-Oshima Volcanic island, central Japan: Shallow landslide, landforms

SUZUKI, Takehiko<sup>1\*</sup> ; TMU GROUP FOR, Izu-oshima typhoon wipha (1326) disaster<sup>1</sup>

<sup>1</sup>Tokyo Metropolitan University

Before dawn of 16th October 2013, the heavy rain associated with Typhoon Wipha (1326) caused landslides disaster in Izu-oshima volcanic island, 120 km south of Tokyo. Many shallow landslides occurred on the west slope of the Younger edifice of Pre-caldera volcano, facing Moto-machi Town. Several reports (e.g. Ministry of Land, Infrastructure, Transport and Tourism; [http://www.mlit.go.jp/river/sabo/h25\\_typhoon26/izuooshimagaiyou131112.pdf](http://www.mlit.go.jp/river/sabo/h25_typhoon26/izuooshimagaiyou131112.pdf)) have suggested that the distribution of the landslides overlap the area of lava flow effused 14 Centuries (AD1338?). For examine this relation between landslides and the geomorphological and geological conditions, we preliminary surveyed shallow landslides, landforms and geology along the Go-jinka Sky Line on the slope of the Younger edifice of Pre-caldera volcano, 7th and 8th of December and 4th to 6th of January. In presentation, we will report results of field survey for shallow landslides, landforms and geology in detail.

Keywords: Izu-Oshima, Typhoon Wipha (1326), Shallow landslide, Fall-out tephra, Lava flow

## Landslides of granite porphyry induced by Typhoon Talas 2011 around Mt. Myoho at Nachikatsuura, Wakayama, Japan

HIRATA, Yasuto<sup>1\*</sup> ; CHIGIRA, Masahiro<sup>2</sup>

<sup>1</sup>Department of Geophysics, Graduate School of Science Kyoto University, <sup>2</sup>Disaster Prevention Research Institute, Kyoto University

Typhoon Talas brought heavy rain in Kii Peninsula, Japan on September 2-5, 2011, causing a large number of rock-avalanches and debris flows in the southeastern part of Kii Peninsula. We mapped the landslide scars on aerial photographs at the scale of 1:20000, made rainfall distribution maps by using the rainfall data analyzed by radar-AMeDAS, and compared position of landslides with rainfall distribution and the geological map by Geological Survey of Japan. The result shows that almost all of the landslides occurred in both over 80 mm/h of rainfall zone and Kumano granite porphyry area. In order to clarify the geological topographical background of the landslides, we also made field investigation around Mt. Myoho at Nachikatsuura, Wakayama Prefecture, where the landslide disaster concentrated.

The field investigation showed that the landslides had different attributes at inside area of granite porphyry mass and at the edge of the mass. Mt. Myoho consists of the Kumano granite porphyry around the top and the Kumano group (sedimentary rock) of Miocene age which occupies at the lower part of surrounding slope and below plain land. Slope is gentle around the top and gets steeper from the surrounding slope break, and eventually becomes gentle again below the boundary between granite porphyry and the Kumano group. The granite porphyry shows typical spheroidal weathering with corestones in the surface layer of gentler slope. The corestones were included in deposits caused by the landslides. Accordingly, landslides within granite porphyry area had scarps at the slope breaks, where weathered and/or reworked material of granite porphyry seemed to have collapsed. At landslides near the boundary between granite porphyry and the Kumano group, the shale of the Kumano group was altered to dark gray clay. Talus deposit of the saprolite and corestones on the clay seemed to have collapsed there.

We estimated volumes of some rock-avalanches around Mt. Myoho to be range from  $10^2$  to  $5 \times 10^5$  cubic meters, and their equivalent friction coefficients were 0.20-0.46 on the basis of positions from the rock-avalanches and following debris flows plotted on topographical maps at the scale of 1:25000. These landslides of granite porphyry were similar to those of granite in Hiroshima Prefecture induced by heavy rain on June 1999 in terms of volume and equivalent friction coefficient. In the case of weathered granite in Hiroshima, however, corestones were formed slightly and it was a different type of landslide that saprolite collapsed and transformed into debris flows.

Keywords: landslides, Typhoon Talas, granite porphyry, Nachi Katsuura

## Interpretation of landslides triggered by 1944 Tonankai earthquake around Owase City using U.S. military aerial photos

SATO, Hiroshi, P.<sup>1\*</sup>

<sup>1</sup>Japan Map Center

Shallow landslides were interpreted around Owase City, Mie Prefecture using U.S. military aerial photographs (1/16,000 in scale) taken on 7 December 1944, just three days after Tonankai earthquake (M7.9). It is thought that some of landslides were triggered by the earthquake. Result of the interpretation will be reported.

Keywords: landslide, slope failure, Tonankai, earthquake, U.S. military, reconnaissance

## Long-traveling conditions for the rock-on-snow landslide: insights from the field and lab evidence

YAMASAKI, Shintaro<sup>1\*</sup> ; KAWAGUCHI, Takayuki<sup>1</sup> ; NAKAMURA, Dai<sup>1</sup> ; YAMASHITA, Satoshi<sup>1</sup> ; SHIRAKAWA, Tatsuo<sup>1</sup> ; HAS, Baator<sup>2</sup>

<sup>1</sup>Kitami Institute of Technology, <sup>2</sup>Asia Air Survey Co., Ltd.

On March 12, 2011, the M 6.6 earthquake hit the typical deep snow area of Niigata and Nagano prefectures. This earthquake (2011 north Nagano Earthquake) induced a lot of landslides, and some of them travelled on snow moving long distance. We are studying that type of landslides which named rock-on-snow landslide by field observations and lab experiments. The rock-on-snow rock avalanche differs from other conventional earthquake-induced landslides because of high mobility, and slash avalanche because water before the event does not drive rocks. Then its high mobility is important to consider earthquake disaster prevention for deep snow area.

The physical properties of snow under the moving mass could affect long-travelling property. We investigated the Tatsunokuchi landslide induced by the earthquake and found temporal liquefaction zone which lay between landsliding mass and autochthonous snow (Yamasaki et al., 2013). The condition of snow getting liquefaction depends on temperature and pressure. Snow also has effect of friction reducing as skiing. However, all rock-on-snow landslides including small rock falls on snow do not travel long-distance, rather most of them stop shorter distance from the origin than normal rock falls. Thus, condition of the long-travelling could be limited. We conducted lab experiments that miniature rock fragments slides on snow slope which tilt angle is 20 degrees, the width is 20 cm and the length is 300 cm, and then we try to understand basic properties of relation between rock and snow and processes during the sliding. The results and our field observations gave us insights to understand larger phenomena.

### Reference

Yamasaki, S. Nagata, H. and Kawaguchi, T., Long-traveling landslides in deep snow conditions induced by the 2011 Nagano Prefecture earthquake, Japan, Landslides, 2013 Online available.

Keywords: landslide, snow, earthquake, avalanche, debris avalanche

## Definition of the database fields for landslide hazard database by NIED

UCHIYAMA, Shoichiro<sup>1\*</sup> ; YAMADA, Ryuji<sup>1</sup> ; ISHIKAWA, Haruna<sup>2</sup> ; SUZUKI, Hinako<sup>1</sup> ; USUDA, Yuichiro<sup>1</sup>

<sup>1</sup>National Research Institute for Earth Science and Disaster Prevention (NIED), <sup>2</sup>Advantechololy Corporation

The history of natural hazard at a certain place is greatly related to the current risk there. It provides indispensable information to the hazard and the risk assessment. The Research Institute for Earth Science and Disaster Prevention (NIED) is building a comprehensive database of natural hazard events over the historical period in Japan, and distributing these information with Web API. Such a hazard event database is, however, no more than an index with a limited amount of information about the reality. Therefore, especially for the large natural hazards that had big social impacts, it is important to provide specific databases classified with types of hazards such as earthquake, volcano, storm, flood, slope, snow and ice disasters. We discuss about the database for slope disasters in particular here.

Keywords: landslide hazard database, database field, definition of fields

## Submarine mass-transport deposits of the Paleogene Muroto Formation in the Kuromi coastal region, Kochi Prefecture

IKAWA, Yu<sup>1</sup> ; TONAI, Satoshi<sup>1\*</sup> ; SHIBATA, Tadahiro<sup>2</sup>

<sup>1</sup>Faculty of Science, Kochi University, <sup>2</sup>Muroto Geopark Promotion Committee

We report stratigraphy and geologic structures of ancient mass-transport deposits exposed as a nearly 2 km continuous outcrop of the Kuromi coastal region, Shikoku Island, Japan to provide detailed information on internal structures of mass-transport deposits and their relationships with encasing sediments. It is allowing important considerations on triggering mechanisms and transport/depositional process of mass-transport deposits.

The mass-transport deposits studied here are in the Upper Eocene to Lower Oligocene Muroto Formation which is a part of the Paleogene Shimanto accretionary complex. The Muroto Formation, about 650 m thick in this area, consists of six lithofacies. These units are thick-bedded mudstone, thin-bedded very fine grained sandstone and mudstone, thin- to medium-bedded fine sandstone and mudstone, thick-bedded sandstone, folded thin-bedded sandstone and mudstone, and chaotic deposits. These sediments are interpreted as a deep-sea channel-levee system with occurrence of submarine landslides.

A field-based study of the Muroto Formation reveals that folded thin-bedded sandstone and mudstone and chaotic deposits are made up of at least two distinct mass-transport deposits, the larger of which reaches thickness of more than 270 m. Fold hinges in these mass-transport deposits are uniformly orientated and parallel to the host bedding. Axial planes in these mass-transport deposits show a girdle-like distribution which are perpendicular to the host bedding. These patterns of fold orientations show that the style of their transport is mainly flow and partly is turbulent flow including broken detrital blocks. These characters show that huge mass-transport deposits may be often formed on plate convergent margins and involved in accretionary prism.

Keywords: submarine mass-transport deposit, accretionary complex, Shimanto belt, Paleogene

## Feature of slump and associated structure observed at Daini-Atsumi knoll, the gas production test site from gas-hydrate

SUZUKI, Kiyofumi<sup>1\*</sup> ; TAKAYAMA, Tokujiro<sup>1</sup> ; SANADA, Yoshinori<sup>2</sup> ; FUJII, Tetsuya<sup>1</sup>

<sup>1</sup>JOGMEC/TRC, <sup>2</sup>Japan Agency for Marine-Earth Science and Technology

The Daini-Atsumi knoll became famous as the first offshore gas production test site from methane hydrate-bearing marine sediments, is one of outer ridges along northeast Nankai trough, near central Japan. Several slumps were found on seismic sections around Daini-Atsumi knoll. Fortunately, several wells had been penetrating slump deposits and logging data were measured. As a result of seismic profile observations, a strong negative-impedance seismic reflector (NISR) was found in the turbidite sequence beneath the slump deposits. A seismic reflector containing the NISR has good continuity with variable reflectivity from a bottom-simulating reflector (BSR) sequence; that is, the NISR does not indicate a slump basement or the boundary of a chaotic unit. Nevertheless, very normal thin-layer turbidites were found at the depth of NISR from LWD measurement and coring, however, fluid data could indicate difference between upper slump unit and beneath turbidites unit. It implies that NISR does not mean pressured fluid but some fluid stagnation.

### Acknowledgement

This research is conducted as a part of MH21 research and the authors would like to express their sincere appreciation to MH21 and the Ministry of Economy, Trade and Industry for disclosure permission for this research.

Keywords: Slump, 3D seismic profile, LWD, Over-consolidate, Gas hydrate, Low impedance

## Role of slump deposits in a high-methane-flux gentle continental slope

MORITA, Sumito<sup>1\*</sup>

<sup>1</sup>AIST-GREEN

A great number of submarine landslide deposits (slump deposits) are known to be buried in Pliocene and the upper formations in northern part of Sanrikuoki Basin (Morita et al., 2011). The slump deposits are mainly made up of imbricated thrust sheets of stacked sedimentary layers which were peeled off from ancient bottom surface. The slump deposits often show dimmed facies as an acoustic characteristic and have dewatering structure from the slip surface, and sometimes have gas chimney at the roof of the slump deposits. These indicate that the slump deposits are strongly related to natural gas in formation water. A key to grasp the nature of the slump deposits is likely in a comparison with a result of previous scientific drilling. Site C9001 is a drill site which was operated by D/V CHIKYU in this survey area (Higuchi et al., 2009). By the result of the expedition, the sedimentary basin is mostly composed of mud and few thin ash and sand layers. The sediments are normal and the parts judged as mass transport deposits (MTD) by visual core description are very limited even in the depth domain interpreted as slump deposits in seismic data. However, methane detected in head space gas and methane hydrate bearing sediments recovery were reported only in the slump deposits domain interpreted in the seismic data. Previous reports with respect to MTD indicate that MTDs generally have the nature as seal where the beds have higher shear strength and density due to compaction. Nevertheless, the nature of the slump deposits in the Sanrikuoki Basin is opposite to those of the other MTDs, and may indicate as if reservoir. The difference of the natures is maybe caused by the environment of very gentle continental slope where the slumping has repeated. There is a hint of it in the fact that slump deposits in the survey area avoided fatal collapse by sliding on the very gentle slope and basically formed the imbrication of block-supported structure.

Keywords: submarine landslide, mass transport deposits, slump, Sanrikuoki Basin, CHIKYU, methane hydrate

## Liquefaction-induced water-film mechanism in submarine slide

KOKUSHO, Takaji<sup>1\*</sup>

<sup>1</sup>Kokusho Takaji

As one of possible mechanisms of seismically triggered submarine slides in cohesionless sandy & gravelly deposits, void redistribution or water film effect seems to be deeply involved (Kokusho, 1999, 2000). In this view, fine soil sublayers sandwiched in coarse grain deposits are considered to play a key role in flow failure. The formation of water films between liquefied sand and overlying lower-permeability seams has been observed under level ground conditions in a number of model tests. Fig. 1 shows a typical example of water film formed beneath a thin silt seam sandwiched in a uniform horizontal sand layer. It has also demonstrated that water film can be generated not only in sands beneath silt seam but also in gravels beneath smaller permeability sands (Kokusho & Kojima 2002). Visit <http://www.civil.chuo-u.ac.jp/lab/doshitu/index.html> for video images of the model tests.

For sloping ground conditions it has been demonstrated, based on model shake table tests, that the water film plays an important role in post-earthquake large lateral flow in liquefied ground. Fig.2 shows typical test results where clean fine sand was rained in water to make saturated sand slope shown in (d) in a transparent soil box (Kokusho 2003). Fig.2(a) indicates a case of a uniform sand model where small flow deformation occurs mostly during shaking. The locations of markers in the model are shown in (d) with the same symbols. If a silt seam shown with chain-dotted arc is sandwiched in the uniform sand, a larger flow deformation above the arc occurs not only during but also after shaking as indicated in (b). These results in (a) and (b) are for the input acceleration of 0.31 G. Interestingly, for weaker input acceleration of 0.18G given to the same model in (c), much larger post-shaking flow than (b) occurs, while only minimal deformation takes place during shaking. In these tests, very thin water film can be observed beneath the silt arc.

A basic question may arise that sand which can be so dilatative if sheared under a low confining stress may absorb ambient excess pore water and hence block the water film development. It can be pointed out, however, based on the comparative observation of the cases with and without a silt seam that a water film formed beneath the seam serves as a shear stress isolator which prevents deeper soils developing shear strain and positive dilatancy (Kokusho, 2000). Consequently, sand can experience large shear strain beneath the silt seam without suffering from the dilatancy effect, whereas it stops moving after the end of shaking if the sand is uniform.

Another shaking table tests has shown that a soil mass slides even on a very gently inclined water film, which breaks at weak points of the overlying sublayer, triggering the boiling failure in the sand above and a mud avalanche of the upper layer (Kokusho 1999, 2000). For video images of these model tests, visit <http://www.civil.chuo-u.ac.jp/lab/doshitu/index.html>.

If water films are formed continuously, they will tremendously reduce the residual strength down to zero if sliding occurs all the way through a continuous water film. Kabasawa and Kokusho (2003) quantified the residual shear resistance exerted during the delayed flow along a water film in the model tests. The result shown in Fig.3 indicates that the residual strength along the water film is almost independent of sand density and other test parameters and remains around 20% that of the uniform sand. Considering that soil deposits are naturally stratified with sandwiched low permeability seams, it seems quite reasonable to identify the water film effect as a major mechanism for seismically induced submarine slides in gently sloped sandy or gravelly sea-bed near coastal areas.

Thus, liquefaction may be highly responsible in earthquake-induced submarine slides, particularly in near-shore sites where the seabed is composed of liquefiable loose sand or gravel.

Keywords: seismic liquefaction, water film, time delay, permeability

## Factors controlling submarine landslide occurrence: Lessons learned from plate-boundary decollement zones

UJIIE, Kohtaro<sup>1\*</sup>

<sup>1</sup>University of Tsukuba

Most submarine slopes are inherently stable. However, once submarine landslide generated, it could induce destruction of seabed infrastructure and tsunamis. The factors controlling submarine landslide occurrence remain poorly understood, mainly because there has been very limited access to slip surface of landslide. Initiation and evolution of plate-boundary decollements in subduction zones may be useful to understand the location of slip surfaces and the slip behavior of submarine landslides. Here, I review decollement processes in subduction zones, which have been revealed from deep ocean drilling in the last 20 years. The decollements develop along (1) weak, smectite-rich layers, (2) the zones of elevated pore pressure, and (3) the mechanical boundary between cemented and non-cemented intervals. These results provide important implications for submarine landslide occurrence. The slip surfaces may localize along an interval of smectite-rich lithology. Such smectite-rich lithology could link to the increased volcanic activity as smectite is commonly derived from alteration of volcanic ash/tuff. The permeability contrast in slope sediments could also play an important role on the development of slip surfaces. The rapid sedimentation of coarse-grained sediments onto fine-grained, argillaceous sediments may cause the generation of elevated pore pressure, which in turn facilitates the onset of submarine landslide. The trap of the hydrate-derived fluid beneath the low permeability sediment may also cause the development of overpressure. The slope sediments may contain the cementation boundary (e.g., opal-A to opal-CT reaction) particularly when geothermal gradient is high. In such case, the submarine landslides may generate along the surface bounding different cementation states.

## Flow dynamics of Nankai Trough submarine landslide inferred from internal deformation using magnetic fabric

KANAMATSU, Toshiya<sup>1\*</sup> ; KAWAMURA, Kiichiro<sup>2</sup> ; KITAMURA, Yujin<sup>3</sup> ; NOVAK, Beth<sup>4</sup> ; STRASSER, Michael<sup>5</sup>

<sup>1</sup>Japan Agency for Marine-Earth Science and Technology, <sup>2</sup>Graduate School of Sciences and Engineers, Yamaguchi University, <sup>3</sup>Department of Earth and Environmental Sciences, Graduate School of Science and Engineering, Kagoshim, <sup>4</sup>Department of Geology Western Washington University, <sup>5</sup>Geological Institute, Seiss Federal Insitute of Technology ETH Zurich

Submarine landslide deposits in one of the most active subduction zone was investigated by Integrated Ocean Drilling Program (IODP) Expedition 333 as "Nankai Trough Submarine Landslides History" (NanTroSLIDE). The expedition recovered a Pleistocene to Holocene sequence of stacked mass-transport deposits (MTDs) within a slope on the footwall of the megasplay fault at Site C0018, Nankai Trough SW Japan (Strasser et al., 2012). A series of MTDs interbedded with coherent intervals were recovered from the upper 190-meter at C0018 site. We present results of detail fabric analysis using drilled succession of buried mass transport deposits in the slope of Nankai Trough in order to investigate rheology of mass transportation in the subduction zone. Despite very limited lithological information of core research, AMS is proved useful tool to identify MTD deformation and recognize depositional process of MTD (Kitamura et al., 2013, Noback et al., 2013).

Magnetic fabric patterns reveal inhomogeneity within each MTD unit indicating a different compaction and shear occurred during flowing and subsequent deposition (MTD2, MTD3, MTD5). Magnetic fabric in upper interval of each unit generally indicates vertical compression. On the other hand lower interval involve magnetic fabrics showing effect of shear. In the largest MTD (MTD6), a distribution of magnetic foliations images tightly folded strata. Using available paleomagnetic data the shear directions are reoriented, and two different directions are obtained in term of MTD flow directions. It is considered that such variation in flow types and directions derived from the results occurred in responding to a change of slope environment controlled by the tectonic evolution of Nankai accretionary wedge. Through such analysis we can improve our understanding for submarine landslide formation in the active margin.

Keywords: submarine landslide, NanTroSLIDE, IODP, Nankai Trough

## Potential tsunamigenic submarine landslides in active margins

KAWAMURA, Kiichiro<sup>1\*</sup> ; JAN SVERRE, Laberg<sup>2</sup> ; KANAMATSU, Toshiya<sup>3</sup>

<sup>1</sup>Yamaguchi Univerisity, <sup>2</sup>University of Tromso, <sup>3</sup>JAMSTEC

A review of modern, historical and submarine landslides from the geological record shows that landslides in active continental margins can generate tsunamis. The tsunamis may damage coastal and seabed infrastructure and so represent an important element of marine geohazards research due to their potentially significant impacts on society. The primary trigger mechanism of tsunamis in this type of setting was thought to be earthquake activity; however, there are also a number of alternative hypotheses regarding the likely initiation mechanism including the generation of submarine landslides. In this paper, we briefly review the geological features and trigger mechanisms of tsunamigenic submarine landslides on active margins. Large tsunamigenic submarine landslides appear to occur mostly on margins characterized by non-accretion. These observations has implications for tsunami warning systems as the Japanese system does not consider the scenario of tsunami excitation by submarine landslides

Keywords: tsunamigenic submarine landslide, tsunami earthquake, tectonic erosion, Japan trench, the 2011 Tohoku-Oki earthquake

## Temporal changes of internal stresses and pore pressures of a large-scale submarine debris flow

OTSUBO, Makoto<sup>1\*</sup> ; NARUSE, Hajime<sup>2</sup> ; MIYAKAWA, Ayumu<sup>1</sup>

<sup>1</sup>Geological Survey of Japan, AIST, <sup>2</sup>Graduate School of Science, Kyoto University

Mass-transport deposits are major components of depositional systems in the deep sea environments. These deposits usually are composed of muddy chaotic deposits, and are expected to conduct as permeability seals over channel deposits. These mass transport deposits appear as transparent layers on seismic data and chaotic intervals in cores (e.g., Weimer, 1991). Regardless of their common occurrence and distinctive geometry, the dynamics of subaqueous mass transport processes (debris flows) are not well known. It is great difficult to observe directly a subaqueous debris flow.

Naruse and Otsubo (2011) documented quantitatively the internal structures of a mass-transport deposit in the Akkeshi Formation, from the middle part of the Cretaceous-Paleocene Nemuro Group, Japan. The paleostress analysis using meso-scale faults (Yamaji, 2000) of a large-scale mass-transport deposit revealed that the flow experienced two different stress fields: (1) a vertical uni-axial compressional stress field with the sigma1-axes oriented normal to the bedding surface (Phase I) and (2) horizontal tri-axial compressional stress fields with the sigma1-axes oriented parallel to paleocurrent direction (Phase II) (Naruse and Otsubo, 2011).

We examined the temporal changes of internal stresses and pore fluid pressures in a submarine mass transport from the relationships between the principal stresses axes and attitude of fault planes in the mass transports deposits in the Akkeshi Formation. We used 22 fault data and stresses of two Phases in a mass transport deposits. We attribute fault variations to the degree of fault overpressure acting on faults to estimate the pore fluid pressure ratio in the submarine mass-transport deposits. The theory can be explained using the Mohr circles. The inferred internal stresses results imply that the stress fields of Phase I are created by a radial spreading of the flow during its downcurrent movement, while the stress fields of Phase II result from compression during deposition on the basin plain (Naruse and Otsubo, 2011). The increase of pore fluid pressure ratio from Phases I to II represents that the pore fluid pressures have been recognized as playing an important role in the occurrence of the faults in Phase II. On the subdivided Phase II, pore fluid pressure ratio increases until Phase IIa and decreases after Phase IIb while sigma-hmax increases during Phase II.

### References:

Naruse, H., and, Otsubo, M. (2011) Heterogeneity of Internal Structures in a Mass-transport Deposit, Upper Cretaceous to Paleocene Akkeshi Formation, Hokkaido Island, Northern Japan. SEPM Special Publication, 96, 279-290.

Weimer, P. (1991) Seismic facies, characteristics and variations in channel evolution, Mississippi Fan (Plio-Pleistocene), Gulf of Mexico, in Weimer, P., and Link, M.H., eds., Seismic Facies and Sedimentary Processes of Submarine Fans and Turbidite Systems, New York, Springer, 323-347.

Yamaji, A. (2000) The multiple inverse method: a new technique to separate stresses from heterogeneous fault-slip data. Journal of Structural Geology, 22, 441-452.

Keywords: stress, pore pressure, meso-scale fault, mass-transport, debris flow, land slide

## CCS-geoengineering: the only one reasonable climate geoengineering technology at present

KOIDE, Hitoshi<sup>1\*</sup>

<sup>1</sup>Climate Change Geosystem

The climate geoengineering is already inevitable to avoid imminent global climate disasters. Even extremely cautious approach is not enough for any grand-scale practices of climate geoengineering as we never understand the complex global climate system exactly. However, modern human beings have unintentionally done the global-scale climate geoengineering that increases the atmospheric CO<sub>2</sub> level with the wide-spread massive burning of fossil fuels.

The CCS-geoengineering in the broad sense includes the CO<sub>2</sub> capture and sequestration, CO<sub>2</sub> capture and CO<sub>2</sub>-EOR/EGR, air capture and sequestration, air capture and CO<sub>2</sub>-EOR/EGR and also underground microbial CO<sub>2</sub> recycling. The CCS-geoengineering only reduces the artificial emission of CO<sub>2</sub> into the atmosphere or suck the excessive CO<sub>2</sub> from the atmosphere. The CCS-geoengineering is a naturally safe geoengineering technology as the CCS-geoengineering restore the atmosphere only toward the natural CO<sub>2</sub> level minimizing untoward effects.

Keywords: geoengineering, CCS, atmosphere, EOR, recycling, global warming

## The influence of measurement methods on evaluation of threshold pressures

KAMEYA, Hiroshi<sup>1</sup> ; ONO, Masaki<sup>1\*</sup>

<sup>1</sup>Oyo Corporation

In site selection process for the geological sequestration of greenhouse gas, threshold pressures should be evaluated as sealing efficiency of a seal layer. Threshold pressure means the minimum gas injection pressure over which constant gas flow will occur through a sealing layer. For evaluating threshold pressure, strictly conditioned tests to reproduce in-situ stress, fluid pressure, temperature and type of injected gas will sometimes be planned. On the contrary, easy evaluation by simple method will sometimes be planned by estimating capillary pressure curves from pore size distributions and surface tensions. The former will provide more strict evaluations of threshold pressures but this process will be limited by using a particular test apparatus. So, researches for comparing the test results from some methods to verify the accuracy of each test have been studied. In the research on CO<sub>2</sub> geological sequestration, three methods are usually used; i.e. (1) threshold pressure test using supercritical CO<sub>2</sub>, (2) threshold pressure test using N<sub>2</sub> gas, (3) threshold pressure estimation from a mercury intrusion test result. In abroad, some researcher report that the results from different methods are consistent considering the surface tensions of relevant fluid system, but others say that the results are inconsistent because of the sample preparation process or anisotropy of samples. Also, there are only few studies in Japan. The authors conducted three kinds of tests using domestic and foreign sedimentary samples (mudstones and sandstones) and examined the consistencies of their results.

Comparing the results using supercritical CO<sub>2</sub> and N<sub>2</sub> gas, the threshold pressures might be consistent considering the surface tensions in relevant fluid systems. However, there are some inconsistencies with the anisotropic young sediments which could not be reused because of their low solidification. On the other hand, the threshold pressures from mercury intrusion tests with estimation are almost equal to or a little lower than those from N<sub>2</sub> threshold pressure tests. This discrepancy may be caused by the anisotropy or shrinkage during drying process.

In Japan, the candidate of seal formation will be thought as not only massive mudstones but also alternated layers of mudstones and sandstones. In latter case, a limit number of strictly conditioned tests should be compensated by sufficient number of lower quality test results. So, the approach in this study will be important in future site selection process.

Keywords: threshold pressure, seal layer, sealing efficiency

## Evaluation of permeability fault related damage zone in sandstone from a viewpoint of microstructure

SATO, Minoru<sup>1\*</sup> ; TAKEMURA, Takato<sup>2</sup> ; TAKAHASHI, Manabu<sup>3</sup> ; ANMA, Ryo<sup>1</sup>

<sup>1</sup>Tsukuba University, <sup>2</sup>Nihon University, <sup>3</sup>National Institute of Advanced Industrial Science and Technology

It is known that strengthened fragmentation is often observed in damage zones along the fault planes. Studying permeability of faults and damage zones is important because they control fluid migration in subsurface environment (e.g. oil migration and reservoir development, carbon dioxide storage, methane hydrate development). Field and laboratory permeability test have shown that permeability within shear bands, fault gouge or cataclasite is lower than of wall rocks (Zhang and Tullis. 1998), and permeability of damage zones is higher than wall rocks (Fowles and Burley. 1994). The authors compared permeabilities of the wall rocks and damaged zones and their relation to the changes in porosity and pore-size distribution obtained by mercury porosimetry.

The sample was chosen from sandstones from the Nichinan Formation. We conducted shear test on cylindrical sample 90mm in diameter and 180mm long to develop damaged zones in the sample. Cylindrical sample of 50mm in diameter and 25mm long were then cored from the 90mm sample, that intersected the shear plane and damages zones at right angle. The permeability tests were conducted on the cored sample using transient pulse method (Brace et al. 1968) at effective confining pressures 5 and 10MPa. We calculated permeability by Hsieh method (Hsieh et al. 1981) that considered the specific storage value of sample and apparatus. Porosity and pore-size distribution were measured using mercury porosimetry on 10mm cube samples taken from 0 to 10mm, 10 to 20mm, 20 to 30mm, 30 to 40mm from the shear plane.

The permeability of the intact wall rock was  $9.40 \times 10^{-9}$  m/s at 5MPa effective confining pressure, and  $2.52 \times 10^{-9}$  m/s at 10MPa. Permeability of damaged zones were  $1.41 \times 10^{-8}$  m/s at 5MPa effective confining pressure, and  $2.70 \times 10^{-9}$  m/s at 10MPa. Porosity of the intact wall rock was 7.9% and the pore size was dominantly  $\sim 0.1$  micro meter. Along the damaged zone, the frequency of 0.1 micro meter pore decreased and that of 0.5 to 10 micro meter pore increased with decreasing distance from the shear plane. On the other hand the porosity of the damaged zones was 5% in average and no clear correlation was observed between the distance from the shear plane and porosity. We suggest that pore structure was affected by micro-fractures or rearrangement of grains from the porosity reduction in the damaged zone samples; nevertheless permeability of the damaged zone samples is higher than that of wall rock samples.

Keywords: permeability, permeability test, mercury porosimetry, pore-size distribution, shear test

## Injection-induced seismicity: insights gained from laboratory AE study using sedimentary rocks

LEI, Xinglin<sup>1\*</sup> ; LI, Xiaying<sup>2</sup> ; LI, Qi<sup>2</sup>

<sup>1</sup>Geological Survey of Japan, AIST, Japan, <sup>2</sup>Institute of Rock and Soil Mechanics, Chinese Academy of Science

Injection-induced seismicity associated with applications, in which fluids are intensively pressed into deep formations such as Enhanced Geothermal System (EGS), fracking shale gas, geological sequence of CO<sub>2</sub>, have attracted growing attentions. Motivated by the desire to better understand the mechanism of damaging events so that they can be avoided or mitigated, we have started an integrated study on rock fracturing and fault reactivation in multiscales. In the present paper, we present some preliminary results of an ongoing experimental study utilizing acoustic emission technique in laboratory. Samples of typical sedimentary rocks collected from Sichuan basin, China, where a number of injection-induced seismic swarms with sizable earthquakes ranging up to M<sub>4</sub>~5 have been observed in some gas/oil reservoirs. Since most injection-induced earthquakes are located in sedimentary formations of a wide range of lithology and depth, the fracturing behaviors of such rocks are thus important. In order to investigate the role of over pressured fluid in triggering fault instability, the authors carried out two rock fracture tests under tri-axial compression in laboratory. Detailed space-time distribution of acoustic emission due to microcracking was used to examine pre-failure damages and failure behaviors. Our experimental results demonstrate that dolomitic limestone, shale, and porous sandstone from the Sichuan basin show both brittle and ductile fracturing behaviors depending on a number of factors, including drainage condition and confining pressure.

Keywords: Acoustic emission (AE), Microfracture, Rock fracture, Injection-induced earthquake, Sedimentary rocks

## Geochemical reproduction of deep water related to Matsushiro earthquake swarm for TOUGH-FLAC simulation

OKUYAMA, Yasuko<sup>1\*</sup> ; FUNATSU, Takahiro<sup>1</sup> ; FUJII, Takashi<sup>1</sup>

<sup>1</sup>Institute for Geo-Resources and Environment, AIST

A technique of fluid flow ? rock mechanics couple simulation is attracting attentions in the research on CO<sub>2</sub> geological storage (CGS) as a promising tool to assess stress conditions in reservoir and caprock associated with CO<sub>2</sub> injection. The assessment is important in CGS to set conditions for sustainable injection that does not cause dynamic responses of underground rock mass such as plastic deformation, minor fracturing, re-activation of small faults and so on. AIST is conducting a study using TOUGH-FLAC simulator developed by LBNL, USA, to numerically simulate the 1965-1967 Matsushiro earthquake swarm as a natural analogue of dynamic leakage of stored CO<sub>2</sub> associated with fault re-activation. The study using natural data was chosen as the basic data on ground motions and recognizable seismicity would never be obtained in actual CGS demonstration sites because the dynamic responses of rock mass must not occur in the demonstration. The objective of this natural analogue study is to customize the simulator applicable to Japanese CGS sites having bedrocks composed of so-called "soft rock".

It is necessary for fluid flow ? rock mechanics coupled simulation to give salinity of formation water in a geologic model as an initial condition. In the case of Matsushiro simulation, the salinity of injected water is also necessary since the Matsushiro earthquake swarm is considered to be caused by a forcible intrusion of saline water beneath the Matsushiro area. The salinity of initial formation water is determined from water geochemistry on several deep wells obtained in the survey during 2010-2011. The salinity of input water is newly estimated based on the similar dataset combined with hydrogen and oxygen isotopic ratios. The hydrogen and oxygen isotopic ratios of well water fall on a line having a gentle slope as compared to the meteoric water line (MWL), a similar relation reported by Yoshida et al. (2002). The extension of this line presents a field of "andesitic water" by Guggenheim (1992). Assuming that the deep water caused the earthquake swarm has isotopic characteristics of the minimum of "andesitic water", the ratio of dilution of the deepest well water was determined from the isotopic ratios of the "andesitic water" and of the shallow ground water on the MWL. The geochemistry of the deep water caused the earthquake swarm was then determined by using the dilution ratio and the compositions of the deepest well water. The salinity of the deep water caused the earthquake swarm is found to be comparable to present sea water. The salinity is about 7 times higher than that assumed in the previous study of TOUGH-FLAC modeling of the Matsushiro earthquake swarm (Cappa et al., 2009). Similarly, the concentration of HCO<sub>3</sub> is estimated by using well water data. The estimated amount of CO<sub>2</sub>-related soluble species indicates that the initial deep water was oversaturated with respect to CO<sub>2</sub> at the postulated temperatures and pressures of Matsushiro simulation.

Keywords: CO<sub>2</sub> geological storage, Matsushiro earthquake swarm, natural analogue, dynamic leakage, TOUGH-FLAC, salinity

## Seismic monitoring at the commercial-scale CO<sub>2</sub> geological storage site, Cranfield, U.S (Part 3)

TAKAGISHI, Makiko<sup>1\*</sup> ; HASHIMOTO, Tsutomu<sup>1</sup> ; HORIKAWA, Shigeo<sup>2</sup> ; KUSUNOSE, Kinichiro<sup>3</sup> ; XUE, Ziqiu<sup>1</sup>

<sup>1</sup>RITE, <sup>2</sup>SuncoH Consultants Co., Ltd., <sup>3</sup>AIST

Public concerns about felt seismic events induced by fluid injection have been raised recently. These felt events have magnitudes of more than  $M_L 3$  and occur in the area where seismicity not active. The induced seismic events were triggered due to the pressure changes at the reservoir. CO<sub>2</sub> geological storage, a kind of the fluid injection activities, is regarded as a key potential technology to mitigate greenhouse gas emission. Since this technology involves long-term and large amount of CO<sub>2</sub> injection, some researchers warn that CO<sub>2</sub> geological storage would trigger felt seismicities at the site. Passive seismic monitoring is conducted at CCS sites around the world since 2000's. A few of the sites reported occurrences of seismic events related to CO<sub>2</sub> injection and these events were unfelt with small magnitudes. To ensure the safety against induced seismicity and obtaining public acceptance, seismic monitoring is necessary for operating CCS project, especially for countries with high seismicity such as Japan.

RITE has performed a long-term seismic monitoring at the commercial-scale CO<sub>2</sub> injection site in the U.S. to elucidate the relation between CO<sub>2</sub> injection and occurrences of seismic events collaborating with Lawrence Berkeley National laboratory (LBNL) and Bureau of Economic Geology, University of Texas at Austin (BEG) since 2011. Seismic monitoring is conducted at the Cranfield oilfield, Mississippi. This oilfield is the CO<sub>2</sub>-EOR field and a million tonnes of CO<sub>2</sub> is annually injected into the Cretaceous sandstone reservoir (porosity 20 ~30%, permeability for 10 ~200mD) at the depth of about 3,100m. A total of more than four million tonnes of CO<sub>2</sub> have stored as of January 2013. We composed a circle seismic monitoring array deploying 6-3component of seismometers at the depth of 100m in a 3km radius.

We have monitored seismicities more than two years now, but we have recorded no seismic events at the Cranfield site. The recorded of vertical components of waveforms were examined by semi-automated processing and visual judgments for the entire monitoring of period, and the triggered signals were all identified as artificial noises, noises due to weather changes such as lightning or strong wind, and distant earthquakes.

In this presentation, we discuss why seismic events were not recorded at the Cranfield site. We estimated minimum detectable magnitudes of our monitoring array by means of theoretical calculations based on discrete wavenumber integration method which concerned geological properties from surface to the reservoir. We confirmed that the array could detect seismic events with more than  $M_w 0.4$  at the hypocentral distance of 3.2 km. We also discuss the question in terms of pressure changes at the reservoir and other studies conducted at the Cranfield site.

**Acknowledgements:** This study was funded by Ministry of Economy, Trade and Industry (METI) as a part of the 'safety evaluation technology development projects carbon dioxide capture and storage'.

**Keywords:** CO<sub>2</sub>geological storage, Seismic monitoring, fluid injection

## Risk Assessment Study of Bio-CCS (2)

TANAKA, Atsuko<sup>1\*</sup> ; SAKAMOTO, Yasuhide<sup>1</sup> ; HIGASHINO, Haruyuki<sup>1</sup> ; SUZUMURA, Masahiro<sup>1</sup> ; KANO, Yuki<sup>1</sup> ; MAYUMI, Daisuke<sup>1</sup> ; YUJI, Nishi<sup>1</sup> ; NAKAO, Shinsuke<sup>1</sup>

<sup>1</sup>National Institute of Advanced Industrial Science and Technology (AIST)

Among in-situ geo-microbes within depleted oil/gas reservoir, there are some species those generate methane gas from residual oil. Mayumi et.al (2013) identified some methanogens in depleted oil reservoir, those generate more methane gas when they are cultivated in higher CO<sub>2</sub> partial pressure environment than in CO<sub>2</sub> poor environment. CO<sub>2</sub> acts as a catalyst in the reaction. If we maintain preferable conditions for methanogenesis archaea during geological CCS, we will be able to abate greenhouse gas emission and produce natural gas as natural energy resource at the same time. We named the technology concept as 'Bio-CCS'. Assuming Bio-CCS site, CO<sub>2</sub> is injected from a well for to abate greenhouse gas emission and cultivate methanogenic geo-microbes, and CH<sub>4</sub> is produced from another well. The procedure is similar to the Enhanced Oil/Gas Recovery (EOR/EGR) operation, but in Bio-CCS, the target is generation and production of methane out of depleted oil/gas reservoir during CO<sub>2</sub> abatement. We are evaluating the basic practicability of Bio-CCS. In our project, while biologists are identifying the most effective cultivating conditions for methanogenic archaea, geologists, environmental scientists and system scientists are evaluating feasibilities of the technology concept. To evaluate total feasibility of Bio-CCS concept, we are estimating: CH<sub>4</sub> generation volume, environmental impact along with life cycle of injection well, and risk-benefit balance of the Bio-CCS. For that purpose, we assumed two conceptual sites of Bio-CCS: One is depleted oil field and the other one is depleted gas field. In our presentation, we will introduce methodologies and interim results of our feasibility study on Bio-CCS.

Keywords: CO<sub>2</sub> Geological Storage, CCS, Methanogenesis, Feasibility study, Risk assessment, Methane gas

## Horizontal wells placement optimization for CO<sub>2</sub> geological storage in confined aquifers subjected to brine recycling

VILCAEZ, Javier<sup>1\*</sup> ; LI, Hualong<sup>1</sup> ; SATO, Kozo<sup>1</sup>

<sup>1</sup>Graduate School of Engineering, The University of Tokyo

Geological storage of CO<sub>2</sub> has potential of mitigating CO<sub>2</sub> emissions into the atmosphere. CO<sub>2</sub> in geological formations can be trapped through solubility, residual, mineral, and structural trapping mechanisms. Of these trapping mechanisms structural trapping is likely to be the least secure because CO<sub>2</sub> accumulated at the cap-rock can potentially leak through pressure-induced fractures in the cap-rock.

In order to maximize the trapping of CO<sub>2</sub> and at the same time prevent the leakage of CO<sub>2</sub>, placement of injection and production wells were optimized in a saline aquifer subjected to brine recycling under the constraint of a fixed maximum bottomhole pressure which corresponds to the breakthrough pressure of the cap-rock. Contrary to previous well placement optimization studies, in this study the target geological formation is a confined saline aquifer, permeability is heterogenous (10 - 100 md), and wells for CO<sub>2</sub> and brine injection are horizontal. TOUGH2-ECO2N and an iterative Latin hypercube sampling optimization method were employed for the multiphase flow and optimization calculations, respectively. Optimization variables included the locations of two CO<sub>2</sub> injection wells and one brine production well, as well as the injection rate of CO<sub>2</sub>. The total volume of the geological model is 20 km × 20 km × 0.1 km which has 4 layers initially containing only brine at a temperature of 40 °C and pressure of 10 MPa at the top layer. Simulations were performed for 30 years of CO<sub>2</sub> injection at rates of 5 - 20 kg/s, and 10 years of brine production and/or recycling. The two injection wells for brine recycling were located above the two CO<sub>2</sub> injection wells.

Optimizations of wells placement were performed for two scenarios: 1) injection of CO<sub>2</sub> without brine recycling, and 2) injection of CO<sub>2</sub> with brine recycling. Our optimization results indicate that placing brine injection wells above CO<sub>2</sub> injection wells in conjunction with equal fractions of brine recycling and CO<sub>2</sub> injection to each well leads to highest amounts of dissolution and residual trapping of CO<sub>2</sub>. The trapping of CO<sub>2</sub> was improved by 5.4% with brine recycling in comparison to the trapping of CO<sub>2</sub> obtained without recycling (13.26 Mt). Although CO<sub>2</sub> was confirmed to be produced along with brine from production wells located near the injection wells, placement of the production well has shown to have little to no affect on the trapping of CO<sub>2</sub> under the given conditions. With regard to the optimal placement of injection wells, 3 and 6 potential areas were clearly identified for scenario 1 and 2, respectively. It is theorized that heterogeneous permeability formations may have multiple local optima; however this is yet to be confirmed.

Keywords: CO<sub>2</sub> geological storage, Well placement, Brine recycling, Optimization

## Reservoir Rocks of CO<sub>2</sub> Micro-Bubble Storage (CMS) and its Dissolution Characteristics

SUZUKI, Kenichirou<sup>1\*</sup> ; MIYOSHI, Satoshi<sup>1</sup> ; HITOMI, Takashi<sup>1</sup> ; OKUZAWA, Koichi<sup>1</sup> ; MIIDA, Hideaki<sup>2</sup> ; YUKI, Noriyuki<sup>2</sup>

<sup>1</sup>Obayashi Corporation, <sup>2</sup>Engineering Advancement Association of Japan (ENAA)

Among many different portfolios in the CCS technology, CO<sub>2</sub> micro-bubble storage (CMS) system that stores CO<sub>2</sub> by injection in the gas phase and dissolution at shallower depths has been proposed. Basic concept of CMS is the replacement of underground water with CO<sub>2</sub> dissolved water. CO<sub>2</sub> is stored safely once it is dissolved and there is low leakage risk because of residual micro-bubbles having little buoyancy forces. CO<sub>2</sub> dissolved in water is weakly acidic and can react with the minerals in the surrounding rocks. It is well-known that acidic solution is neutralized by rocks as it soaks into the ground, however the ability of neutralization is not completely estimated.

In this paper, in order to estimate the ability of rocks to neutralize CO<sub>2</sub> micro-bubble dissolved water, two types of dissolution experiments of rocks were carried out using crushed and column specimens of sedimentary rock such as limestone, sandstone, and tuff. A batch type dissolution experiment in which rock samples were treated with the solution of CO<sub>2</sub> dissolved in pure water using micro-bubble under CO<sub>2</sub> partial pressure 0.0003 atm. And a flow-through type dissolution experiment was carried out using limestone samples for over 40 days in order to investigate the change of pore structure between before and after experiment. From these experimental results, the dissolution rate and the ability of neutralization of reservoir rocks were discussed.

## Dawsonite synthesis/dissolution experiment under the relevant condition of CO<sub>2</sub> underground storage

TAKAYA, Yutaro<sup>1</sup> ; NAKAMURA, Kentaro<sup>2\*</sup> ; KATO, Yasuhiro<sup>1</sup>

<sup>1</sup>Frontier Research center for Energy and Resources (FR CER), Graduate School of Engineering, University of Tokyo, <sup>2</sup>Department of Systems Innovation, Graduate School of Engineering, University of Tokyo

Geochemical trapping is a mechanism for defining the longer-term security of CO<sub>2</sub> underground storage. Especially, mineral trapping improves the storage security by the transformation reaction of injected CO<sub>2</sub> (liquid or supercritical phase) to carbonate minerals.

Recently, several studies based on the computer simulation predicted the formations of dawsonite (NaAlCO<sub>3</sub> (OH)<sub>2</sub>) as an initial phase of mineral trapping and that dawsonite may play important role for the storage security in the early stage of CO<sub>2</sub> storage. However, it has not been reported the formation of dawsonite in the experiments under the relevant condition of the CO<sub>2</sub> underground storage to date and the problem "whether dawsonite will be formed in the CO<sub>2</sub> reservoir and will contribute the improvement of the CO<sub>2</sub> storage security" is still remaining.

In this study, therefore, we conduct the synthesis/dissolution experiments of dawsonite under the CO<sub>2</sub> reservoir condition and discuss the formation/preservation condition of dawsonite. We further discuss the possibility of dawsonite formation in the CO<sub>2</sub> reservoir based on our experimental results.

Keywords: CO<sub>2</sub> underground storage, mineral trapping, dawsonite

## Liquid carbon dioxide storage beneath man-made hydrate-seal layers

OHSUMI, Takashi<sup>1\*</sup> ; SHIDAHARA, Takumi<sup>2</sup>

<sup>1</sup>School of Science, Tokai University, <sup>2</sup>NEWJEC Inc.

The findings by Sakai *et al.* (1990) that carbon dioxide (CO<sub>2</sub>) hydrate occurs on the Okinawa Trough seafloor of 1,335m in depth and at a temperature of 3.8°C stimulated the research on how to isolate the anthropogenic CO<sub>2</sub> from the atmosphere. Various offshore sites under the CO<sub>2</sub>-hydrate stable conditions, *i.e.* above 4.4MPa and below 10°C, are found in the Japan Archipelago. Above all, there are ten or more places where from the coastline the ERD well can make a direct access to the sub-seabed under the CO<sub>2</sub>-hydrate stable conditions (Ohsumi, 2012). Sakai *et al.* postulated that CO<sub>2</sub> hydrate fills in the pore of the sediment right beneath the sea bottom, which can be explained by the fact that the density of CO<sub>2</sub> • nH<sub>2</sub>O as calculated to be 1.07 ~ 1.04 g cm<sup>-3</sup> corresponding to n = 7 ~ 8, is larger than that of the bottom seawater, and hence the even thin hydrate layer functions as a barrier for the underlain fluid (its estimated density is 0.92 g cm<sup>-3</sup>) composed mainly of liquid CO<sub>2</sub> tending to leak to the bottom waters.

Koide *et al.* (1997) pointed out that the formation of CO<sub>2</sub> hydrate in pores and gaps, in rocks and sediments, could almost completely block the migration of fluid. CO<sub>2</sub> that is injected into a deep reservoir would migrate upward into cooler aquifers and eventually form a CO<sub>2</sub> hydrate cap. Numerous engineering studies thereafter were targeted at how such a sealing layer can be created in the CO<sub>2</sub> storage site. It should be noted that CO<sub>2</sub> hydrate exposed to the open bottom water will be dissolved easily even under the low-temperature, high-pressure stable conditions. Nevertheless, in his examination on how underwater pavement operation could realize the CO<sub>2</sub>-hydrate storage beneath seabed, Ohsumi (2012) illustrated that a 1-m thick sediment layer would be enough to serve as an effective barrier. Since the solute CO<sub>2</sub> diffusion in sediment pores between the hydrate layer and the sea-bottom is rate-limiting, the seepage flux of CO<sub>2</sub> would be below 0.1 kgCO<sub>2</sub> m<sup>-2</sup> per year.

There is an offshore steep slope to the Sagami Trough at the north-east coast of the Izu-Oshima Island. A 440-m isobath is near to the shoreline (the nearest point is 1.1 km offshore) and hence due to the fact that the sea bottom temperature will not exceed 10°C throughout the year, the CO<sub>2</sub>-hydrate stable conditions spread over the offshore bottom and its sub-seabed. The offshore geology consists of "old volcano" bodies, several hundred thousand years of age, of which volcanism is probably similar to the present volcano of the Izu-Oshima Island. Hence, we can suppose that it is composed of alternating layers of basalt lava and pyroclastic rocks. When the pores of horizontally permeable layers are filled with CO<sub>2</sub> hydrate, the underlain formations can hold the liquid CO<sub>2</sub> for storage. Ikegawa *et al.* (2012) proposed the injection method of CO<sub>2</sub>-in-water emulsion applicable to the sedimentary layers for the purpose of enhanced recovery of methane hydrate. By their method, while avoiding hydrate blockage in the horizontal pore space flow, as shown in Figure we might be able to create the effective CO<sub>2</sub>-hydrate seal layers with a large area coverage. A horizontal coverage of the supposed storage site could be 5×1 km. When storage layers with 200-m effective thickness are selected, 10% of the effective pore volume ratio for liquid CO<sub>2</sub> storage gives 100 million tCO<sub>2</sub> as an attractive storage potential.

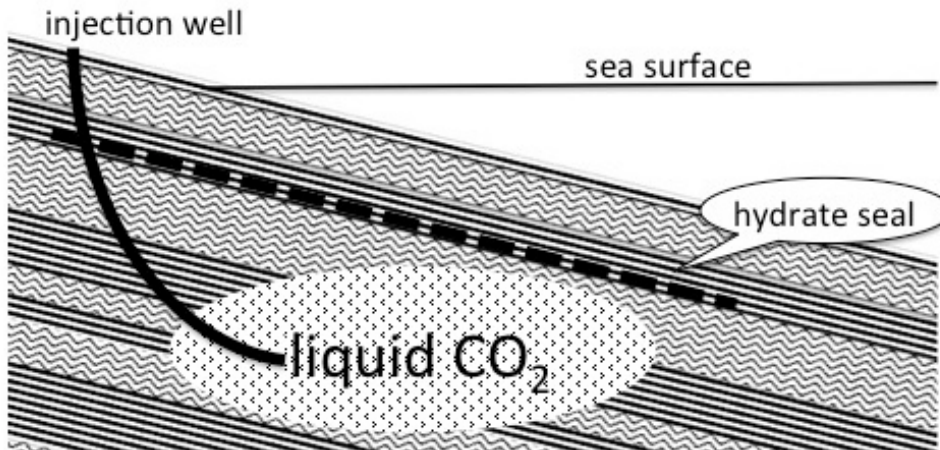
Ikegawa, Y *et al.* (2012) *CRIEPI Report* N11024 (in Japanese with English abstract); Koide *et al.* (1997) *Energy* **22**(2/3) 279-283; Ohsumi, T (2012) The 23rd Ocean Engineering Symposium (in Japanese with English abstract); Ohsumi, T (2013) *2013 Fall meeting Programme and Abstracts* (in Japanese) 152-154; Sakai *et al.* (1990) *Science* **248**, 1093-1096.

Keywords: man-made seal layer, CCS, hydrate seal, Izu-Oshima Island, Extended Reach Drilling, CO<sub>2</sub>-in-water emulsion

HRE31-11

Room:419

Time:May 2 12:15-12:30



## Use of sodium polytungstate as an X-ray contrast agent to reduce beam hardening in hydrogeological experiments

NAKASHIMA, Yoshito<sup>1\*</sup>

<sup>1</sup>AIST

Iodine is conventionally used as a contrast agent in hydrogeological experiments using polychromatic X-ray computed tomography (CT) to monitor multi-phase Darcy flow in porous geological media. Undesirable beam hardening artifacts, however, make the quantitative analysis of the obtained CT images difficult. CT imaging of porous sand packs saturated with iodine and tungsten-bearing aqueous solutions, respectively, was performed using a medical CT scanner. The result (Fig. 1) shows that sodium polytungstate ( $\text{Na}_6\text{H}_2\text{W}_{12}\text{O}_{40}$ ) significantly reduced the beam hardening compared with potassium iodide (KI). This result is due to the location of the K absorption edge of tungsten, which is nearer to the peak of the polychromatic X-ray source spectrum than that of iodine. As sodium polytungstate is chemically stable and less toxic than other heavy element bearing compounds, we recommend it as a promising contrast agent for hydrogeological CT experiments.

### Acknowledgements:

The medical CT experiment was performed under the cooperative research program of Center for Advanced Marine Core Research (CMCR), Kochi University (13B034) with the support of JAMSTEC.

### References:

- Nakashima, Y. and Nakano, T. (2012) *Analytical Sciences*, 28, 1133-1138. <http://dx.doi.org/10.2116/analsci.28.1133>  
Nakashima, Y. (2013) *Journal of Hydrology and Hydromechanics*, 61, 347-351. <http://dx.doi.org/10.2478/johh-2013-0043>  
Nakashima, Y. and Nakano, T. (2014) *Journal of X-Ray Science and Technology*, 22, 91-103. <http://dx.doi.org/10.3233/XST-130411>

Keywords: beam hardening, contrast agent, Darcy flow, porous media, multi-phase flow, relative permeability

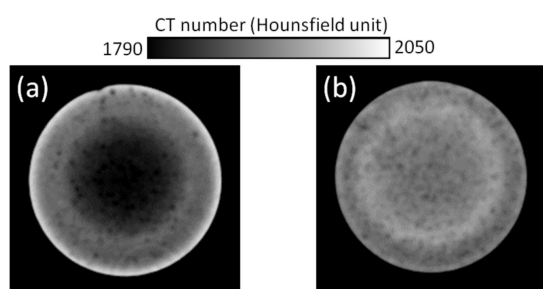


Fig. 1. Two-dimensional CT slices of homogeneous sand pack samples (diameter, 56 mm) saturated with a heavy-element-bearing fluid. Each image dimension is  $210^2$  voxels =  $66^2$  mm<sup>2</sup>. The image for KI 9.16 wt.% (a) shows marked beam hardening compared with  $\text{Na}_6\text{H}_2\text{W}_{12}\text{O}_{40}$  8.80 wt.% (b). Numerous dark spots are small bubbles.

## Gravity monitoring at the Farnsworth CO<sub>2</sub>-EOR site, TX

SUGIHARA, Mituhiko<sup>1\*</sup>; NAWA, Kazunari<sup>1</sup>; SOMA, Nobukazu<sup>1</sup>; ISHIDO, Tsuneo<sup>1</sup>; MIYAKAWA, Ayumu<sup>1</sup>; TANAKA, Akiko<sup>1</sup>; NISHI, Yuji<sup>1</sup>

<sup>1</sup>AIST

Time-lapse gravity measurements with a combination of absolute and relative observation array will reduce uncertainties caused by regional gravity variations. The technique is called hybrid gravity measurement. By adding continuous measurement with a superconducting gravimeter (SG) to the hybrid system we are applying the super-hybrid gravity monitoring at the Farnsworth unit (FWU) in TX along with SWP. We started baseline measurement in January 2013. Using SG and barometric data at FWU, we obtained average gravity-atmosphere admittances. The observed admittances during storms can be far from the mean admittance. We often observed several outstanding responses to atmospheric pressure changes. Comparing with precipitation, soil moisture and atmospheric pressure the residuals were attributed to hydrologic components and/or local atmosphere admittance. Several circular irrigation systems work at FWU. At each system water is pumped from a nearby well to the center of the system. The process will result in the redistribution of mass which may result in gravity signals. Basically the booms rotate to cover the circular field over an approximately three day cycle during agricultural season, however the exact watering pattern varies from field to field. We have tried to monitor the watering effects.

This research is funded and supported by Ministry of Economy, Trade and Industry (METI).

Keywords: Fansworth, CO<sub>2</sub>-EOR, gravity monitoring, superconducting gravimeter

## Analysis of topographical characteristics of flooded areas for constructing simple warning system of pluvial flooding

SATO, Rina<sup>1\*</sup> ; OGUCHI, Takashi<sup>2</sup>

<sup>1</sup>Graduate School of Frontier Science, The University of Tokyo, <sup>2</sup>CSIS, The University of Tokyo

Pluvial flooding is a major disaster in Japanese urban areas. Physical models are often used for assessing pluvial flood risk, but the models are complex. Therefore, this study aims to analyze topographical characteristics of flooded areas in the 23 wards of Tokyo as the basis for constructing a simple warning system. At first, we extracted four factors as topographical characteristics: depression depth, catchment volume, elevation difference and slope using a digital elevation model (DEM) for the whole study area, but there were some problems when the methods were simply applied to the DEM. Accordingly, we extracted the factors only for roads, and then compared the obtained values for flooded and non-flooded areas. According to t-test, there were significant differences between the two types of areas for all factors. However, similar values sometimes occur for these areas, indicating that not only topography but also rainfall and drainage systems should be analyzed in future work.

Keywords: pluvial flooding, topographical characteristics, road, DEM, GIS

## Effect of the definition of a single rainfall event on the rainfall threshold of mass movements

CHEN, Chiwen<sup>1\*</sup> ; OGUCHI, Takashi<sup>1</sup>

<sup>1</sup>Department of Natural Environment Studies, The University of Tokyo

This study analyzes mass movements caused by rainstorm and typhoon events in Taiwan during 2006 to 2012. Data for 263 mass movement events were collected from the reports of the Soil and Water Conservation Bureau of Taiwan, including 172 landslides and 107 debris flows caused by nine frontal rainstorm events and 15 typhoon events. After checking the location of each event, we compiled relevant rainfall data by interpolating data from the surrounding rain gauges. This approach is useful to analyze rainfall conditions for the events and discuss the mechanism of the rainfall-induced mass movements. This study uses two different definitions of a single rainfall event in relation to the triggering of mass movements. One is defined as a period from the time when hourly rainfall becomes greater than 4 mm to the time when the hourly rainfall becomes less than 4 mm for the next six consecutive hours. The other is defined as a period delimited by a non-rainfall period of more than 24 h. These two definitions gave significantly different results concerning the rainfall condition of mass movements. The first definition represents higher rainfall intensity, shorter duration and less cumulative rainfall. The second definition represents lower intensity, longer duration and more cumulative rainfall. We also used the rainfall intensity-duration (*I-D*) relationship from these two definitions to establish two *I-D* thresholds of mass movements in Taiwan. Comparing the thresholds from this study to those for Taiwan and Japan from previous studies, we found that the definition of a single rainfall event and the number of data are two important factors affecting the rainfall threshold of mass movements.

Keywords: mass movements, rainfall event, landslides, debris flows, I-D threshold

## Implementation of Random Forest in landslide susceptibility study, a case study of the Tokamachi area, Niigata, Japan

PAUDEL, Uttam<sup>1\*</sup> ; OGUCHI, Takashi<sup>2</sup>

<sup>1</sup>Graduate School of Frontier Sciences, The University of Tokyo, <sup>2</sup>Center for Spatial Information Science, The University of Tokyo

Random Forest (RF), a bagged trees ensemble, is widely appreciated for its superiority amongst classification algorithms and is popular in various fields of data mining. However, the application of RF in susceptibility analysis of landslide hazard remains very limited. This study highlights the results of such an attempt. The study area was selected on the basis of landslide density distribution. A density map of landslide distribution in Japan was prepared from the landslide inventory provided by the National Research Institute for Earth Science and Disaster Prevention (NIED). The Tokamachi area in Niigata Prefecture has a very high density of events and was thence selected for this study. Seven topographic factors (aspect, curvature, drainage density, elevation, plan curvature, profile curvature, and slope) derived from the 10 m DEM obtained by the Geospatial Information Authority of Japan (GSI) were used for the analysis. The classification data concern 9747 landslide events and 20685 randomly generated instances from the areas with no landslides. Unlike the values of a centroid used in many other studies, each landslide event in the classification data was represented by a mean of values of the respective factors in each landslide feature. Information gain for each factor was also evaluated and it was found that the profile curvature is the most effective factor in classifying landslides in the area, whereas elevation is the least effective. A 10-fold cross validation of the RF model with 200 trees resulted in an 'out of bag error' of 0.1443, an accuracy of 85.87%, and an ROC area of 0.926. These results suggest the suitability of RF in susceptibility analysis, the stability of which can be further strengthened with an increase of factors and the number of trees.

Keywords: Landslide susceptibility, GIS, Machine learning, Random Forest

## Viewshed analysis of the trails in SriPada mountain area in Sri Lanka

SIRIWARDANA, Halgamage malinda<sup>1\*</sup>

<sup>1</sup>University of Tsukuba

Each year about 3 millions of people climb SriPada Mountain. The trail system around SriPada in the Peak Wilderness has been used over centuries in good harmony. According to local people, there used to be 18 trails to reach the top of SriPada Mountain. Some of those trails were rarely used and thus getting vanished over time. This research focuses on analyzing Viewshed and the flow of people along some of the trails.

## Geospatial analysis of deforestation factors in central Cambodia after 2000s

MATSUURA, Toshiya<sup>1\*</sup> ; MIYAMOTO, Asako<sup>1</sup> ; KURASHIMA, Takayuki<sup>1</sup> ; SANO, Makoto<sup>2</sup> ; CHANN, Sopha<sup>3</sup> ; PAK, Chealy<sup>3</sup> ; LENG, Chivin<sup>3</sup>

<sup>1</sup>FFPRI, <sup>2</sup>Forestry Agency, <sup>3</sup>Forestry Administration Cambodia

Reducing emissions from deforestation and forest degradation; and the role of conservation, sustainable management of forests and enhancement of forest carbon stocks in developing countries (REDD-plus) have attracted interest in Southeast Asian countries where deforestation has been a serious issue. To estimate future deforestation, the REDD-plus requires analyses of trends in land cover changes and the effects of various factors including infrastructure development, national policies and natural environment such as topographic conditions. This study analyzed the spatial characteristics and important factors of recent deforestation by taking eastern Kompong Thom, central Cambodia as an example.

We used three periods (i.e., 2002, 2006, 2010) of forest cover maps produced by Cambodian Forestry Administration (FA) and an object-based image analysis map made from Landsat 8 imagery taken in January 2014. We examined three types of geographic factors, namely, (1) distances from roads, rivers/water bodies, settlements, and forest edges (2) terrain features, e.g., gradient and relative slope position generated from 90-m SRTM DEM, and (3) zoning categories such as forest concession, economic land concession (ELC), community forestry and protected forest, in order to clarify the trend and explanatory variables of deforestation. All the spatial data were converted into 90 m resolution raster. A generalized linear model (GLM) with logit link function (i.e., logistic regression) was then used to analyze the effect of each factor on deforestation.

Between 2002 and 2006, deforestation mainly occurred in canceled forest concessions. During the period 2006-2010, this trend of deforestation accelerated particularly in and around the newly designated ELCs for rubber plantation. After 2010, deforestation further increased due to the development of small-scale agriculture by local farmers in addition to the newly designated ELCs. Factors consistently selected during the study periods with negative effects were " forest concession " and " distance from forest edge " . These indicate that deforestation occurred more readily in the canceled forest concessions and closer to forest edges. The magnitude of the effect of " distance from roads " has become smaller, indicating that recent deforestation occurred more in the forest interior. Gradient had a negative effect, highlighting the difficulties in farming on slopes. Community forestry and the protected forest established by the FA from the late 2000s also had negative effects on deforestation, indicating that these zoning have their value for forest conservation.

Keywords: REDD-plus, land use/cover change, generalized linear model, GIS

## ENSEMBLE-CELLULAR AUTOMATA (CA) MODELS FOR IMPROVING FOREST COVER CHANGE SIMULATION

KAMUSOKO, Courage<sup>1\*</sup>

<sup>1</sup>Asia Air Survey Co., Ltd

Reliable spatial simulation models are a prerequisite for understanding temporal and spatial forest cover changes. However, spatial simulation models require accurate transition potential maps, which represent the probability of change from one forest cover class to another. Previous studies have shown that conventional methods such as logistic regression, weights-of-evidence and neural networks fail to adequately model forest cover transition potential. The objectives of this study are to: (1) evaluate the performance of adaboost (AB) and random forests (RF) algorithms for computing transition potential maps, and (2) simulate forest cover changes using the computed transition potential maps and cellular automata (CA) model. Our results show that adaboost-CA and random forest-CA models produced better simulation accuracy than logistic regression/ weights of evidence-CA models. These results provide valuable insights, which can be used to improve transition potential modeling and forest cover change simulation in complex landscapes.

Keywords: Adaboost, Random forests, Cellular automata, Transition potential, Forest cover changes

## Capacity building initiative for satellite data utilization for evaluation of environmental degradation using FOSS4G

IWASAKI, Nobusuke<sup>1\*</sup> ; MORI, Toru<sup>3</sup> ; HESHIKI, Kanetaka<sup>3</sup> ; KAYAMA, Yoichi<sup>4</sup> ; FURUHASHI, Taichi<sup>5</sup> ; MASUMOTO, Shinji<sup>2</sup> ; YONEZAWA, Go<sup>2</sup> ; YOSHIDA, Daisuke<sup>2</sup> ; RAGHAVAN, Venkatesh<sup>2</sup>

<sup>1</sup>National Institute for Agro-Environmental Sciences, <sup>2</sup>Osaka City University, <sup>3</sup>Orkney Inc., <sup>4</sup>Aero Asahi corp., <sup>5</sup>MAPconciierge

Recently, satellite image data become more and more easily accessible. For example, NASA provide MODIS and LANDSAT data as Open Data. ESA will provide Sentinel data free and open access for any user. In addition, GIS data will also become accessible under the influence of the global trend of promoting Open Data. In such circumstance, a demands for utilizing satellite images and GIS also have been growing steadily and widely. But, it is still complicated to get original satellite data and how to deal with it for for the non-specialist, such as public employees.

Under such circumstances, Ministry of Education, Culture, Sports, Science and Technology in Japan (MEXT) has considered the plan of removing the barriers on satellite data usage. From 2009 to 2014, we have taken part in this project, and have strived to overcome this problem through the following three points.

1. Developing the Free & Open Source Software for Geospatial (FOSS4G) tools, such as GRASS, QGIS, GDAL/OGR and Proj.4.
2. Making tutorial about processing and analyzing the satellite data with FOSS4G tools.
3. Constructing the e-learning contents of satellite data usage and conducting outreach activity and capacity building in not only Japan but also developing countries.  
(cf. <http://www.osgeo.jp/foss4g-mext>)

In first three years, main targets of our project were Japanese and novice user. We translate QGIS and GRASS GIS menu and manuals into Japanese and improve such FOSS4G tools to adapt Japanese data format and projection. Also, basic and advanced the tutorials for satellite data utilization were published as e-book and e-learning system including video tutorials.

The software and knowledge base have been rapidly improved by our works. These achievements are anticipated to expand base of satellite data users and to create a new utilization scene for space derived products. One of the effective results from this project was shown in actions against the Tohoku Earthquake in 2011. Many people could collaborate on that software base and offered ortho-image of Tohoku region (i.e. Iwasaki et al. 2011, GISA-Japan).

Based on previous result, we are started next project to develop an evaluation system for environmental degradation based on above GRASS and QGIS. In the project we use Global Map (<http://www.iscgm.org/cgi-bin/fswiki/wiki.cgi>) as a fundamental information for evaluating environment. The project had started from 2102 and focused on natural hazard and environmental degradation, especially in developing countries. We will report the status and progress of the project.

Keywords: FOSS4G, Satellite data, Capacity building

## Assessment of Natural Landscape Resources for Tourism Development in Hangzhou, China

ZHAO, Wenqi<sup>1\*</sup>

<sup>1</sup>University of Tsukuba

This study aims to establish criteria based on various factors and then provide comprehensive assessment to the value of main natural landscape resources in Hangzhou, China. Twenty-two attractions in Hangzhou are selected to be the research objects of this study. Also, eight factors are selected as the criteria of this study, which are general scientific value, rarity, aesthetic value, integrity, scale, popularity, transportation and hotels. The model of Analytic Hierarchy Process(AHP) is utilized in this study to determine the weights of the 8 factors.

In order to collect the root data for determining AHP weights, a questionnaire form was sent out to 12 experts. The other data for measuring the 8 factors are collected from the previous papers, census and reports, the websites and pamphlets of the attractions, Google earth, and also collected by questionnaire survey to the public and doing fieldwork. ArcGIS is a supplementary tool for making evaluation with spatial distribution, especially being used when measuring the factors of transportation and hotels. After evaluating the attractions with abstract scores, rank the scores of the 22 attractions and see the spatial distribution with the map.

Hangzhou's natural landscape resources are mainly categorized into volcanic rock, Karst landform, granite, scenery with hills and waters, waterfall scenery, lakes, wetland and rivers. As the result of the assessment, 9 of the 22 attractions comprehensively have high value, and 10 of them have medium value, and the left 3 have low value. Hangzhou is originally famous for the West Lake, however, after the research it is learnt that the west region of Lin'an city also has abundant natural landscape resources with remarkable value, where should be paid more attention in the future development and preservation. As the suggestion to the future, it is better to construct more nature preserves and Geoparks in Hangzhou.

Keywords: Hangzhou, tourism, natural landscape resources, AHP, evaluation

## Tsunami Vertical Evacuation Sites: A Case Study of Shizuoka City

VOULGARIS, Gerasimos<sup>1\*</sup>

<sup>1</sup>University of Tsukuba, Graduate School of Life and Environmental Sciences

The City of Shizuoka directly faces the Nankai Trough which has given two M8.1 earthquakes in modern history (1944 and 1946), which were tsunamigenic. After the great Tohoku earthquake the Japanese government updated its worst case scenario for a tsunami from the Nankai trough, which is expected to have a maximum run-up of 34m. This study aims to use GIS in order to locate vertical evacuation sites in the City of Shizuoka within the existing urban structure, and to assess their potential in supporting the population for immediate evacuation under an extreme 34m run-up tsunami event. This study is still in its initial phase, however, spatial analysis of the current designated evacuation locations in the city indicates that under extreme circumstances only a very small minority of sites would remain if such an extreme tsunami were to happen. Therefore, there is an apparent need to investigate for new evacuation sites that will be suitable even under a tsunami of great magnitude.

Keywords: Tsunami, Vertical Evacuation, Shizuoka City, GIS

## Spatial Analysis of Urban Accidents; A Case Study of Tehran,Iran

Haji Mirza Aghasi, Niloofar<sup>1\*</sup>

<sup>1</sup>The University of Tsukuba. Spatial Information Science Division

Road accidents may be seen as discrete promote events, localized in space and time. The most important objective of the study was to identify the spatial pattern of urban accidents in Tehran city in order to finding the causes and consequences as well as the temporal and spatial variation of accidents. Based on spatio-temporal data analysis method, this paper aims to analyse traffic accidents data in time and space. The spatial relationship between time of daily activities which generate trips and urban traffic accidents is examined and applied to Tehran for 2010~2011.

The research was based on different primary and secondary data sources, which include locations of accidents and many rich attribute such as date, reason, kind, etc. Questionnaires were distributed to 600 drivers in the study area in order to gather data about drivers' knowledge, beliefs, attitude and behaviours. GIS software was used in this study and different maps were made using GIS Arc view 10.2. Tehran urban accidents point by point data with different attributes was collected from Police Department of Islamic republic of Iran, Tehran. These rich accident data were used as source of information and data analysis. The study considered different factors in urban traffic accidents. These include environmental, human and cultural factors, etc. this study stated that the concentration of educational, commercial and cultural activities that make large number of urban trips and road usage and traffic volume in peak hour and road type are among the main causes of the urban accidents in Tehran city. The spatial distribution and variation of Tehran's urban accidents indicated those accident occurrences are highly concentrated along the residential, primary, and secondary roads as well as dense in highways and freeways. This study also shows the relationship between the occurrences of accidents with peak hours of the day. Highways and freeways are the most dangerous road type in road type variation in Tehran city. And the key reason of accidents in these road types is high speed. High occurrences of urban accidents were caused by culture and behaviour of not only drivers but also all users of the roads. It has been recommended that the improvement of knowledge and culture by education through the public Medias and the rules for offenders must be reissue soon.

Keywords: GIS, Urban Traffic Accidents, Peak time, Road Type

## Historical changes in land price formation factors over 100 years in Kyoto, Japan: comparison of the land price distribu

AOKI, Kazuto<sup>1\*</sup> ; TAKEDA, Koji<sup>2</sup> ; YANO, Keiji<sup>3</sup> ; NAKAYA, Tomoki<sup>3</sup>

<sup>1</sup>Research Center for Disaster Mitigation of Urban Cultural Heritage, Ritsumeikan University, <sup>2</sup>PASCO CORPORATION, <sup>3</sup>Ritsumeikan University

The land price formation factor is an index, which shows the social economy situation of the time.

Although a large number of studies have been made on evaluating land price formation factors which show socio-economic situations, most of the studies have been cross-sectional analysis focusing on specific factors, such as zoning, road width and accessibility to public transportation. Little attention has been paid to historical changes of land price formation in a long-term perspective, mainly because of the lack of historical data representing land price distribution in the past. Fortunately, the Kyoto cadastral map made in 1912 was digitized to create the historical GIS database containing detailed land price information for each land parcel by the GIS research team at Ritsumeikan University. It should be noted that the city has not received large-scale disasters and war damages since the age of the cadastral map. We can thus investigate historical changes of the city without effects of such large-scale disasters. Comparing the current land price distribution with that in early 20th century in the city of Kyoto, we examine historical changes in the geographical factors of land price formations reflecting changes in urban physical and social formations of the city. With the aid of GIS-based mapping and overlay analysis, we mainly argue on the effects of the changes in urban formation on land price distributions over 100 years in the city.

The land price formation factors of quantitative getting are road width and distance from the train station is easy. However, quantitative getting of ambiguous land price formation factor represented by downtown property is difficult. In this study, for the understanding of land price formation factor of 100 years ago, take advantage of old photographs.

Keywords: Kyoto cadastral map, land price formation factor, old map

## Spatio-Temporal Analysis of Bicycle Commuting Behavior in the Greater Tokyo Area Using a Micro-Scale Persontrip Database

GREGER, Konstantin<sup>1\*</sup> ; MURAYAMA, Yuji<sup>1</sup>

<sup>1</sup>University of Tsukuba, Division of Spatial Information Science

Compared to other nations, the share of motorized individual traffic in the daily commuting flows in Japan is rather low. Instead, the share of railway transportation is significantly higher. In addition, this generates feeding traffic from homes and workplaces to and from the stations, which is done mostly on foot or by bike. This holds especially true for highly urbanized areas, such as the Greater Tokyo Metropolitan Area with its 34 million inhabitants, which we use as a study area in this paper.

Here we investigate the role and structure of the use of bicycles in the course of commuting traffic. This paper provides a thorough spatio-temporal analysis of bicycle behavior, since we analyze how bicycles are used in the daily commutes, by whom, and where. We investigate how bicycles are integrated in the commuting process and what spatial factors determine the use of bicycles.

For this paper we employ a massive micro scale person trip database provided by the Center for Spatial Information Science at the University of Tokyo. It contains sociodemographic data about approximately 600,000 sample individuals, as well as information about the purpose of each of their trips, their chosen means of transportation (e.g. car, bus, bike, etc.) and their location in 1-minute steps over all 24 hours of one sample day.

As the scientific discourse about bicycle traffic in Japan is scarce, we hope to be able to contribute by this study and provide valuable insights into this important mode of transportation.

Keywords: bicycle, big data, commuting, gis, japan, tokyo

## Geospatial analysis of land changes in the megacities of Southeast Asia

ESTOQUE, Ronald<sup>1</sup> ; MURAYAMA, Yuji<sup>1\*</sup>

<sup>1</sup>Graduate School of Life and Environmental Sciences, University of Tsukuba, Japan

The advancements of remote sensing and geographic information systems technologies enable us to monitor land changes at various spatial and temporal scales, and analyze the implications of such changes from different perspectives. This study assesses the spatiotemporal patterns of land changes in the megacities of Southeast Asia, namely Bangkok (Thailand), Jakarta (Indonesia) and Manila (the Philippines). The goal is to gain better understanding on the land transformation process in each megacity, which may be useful from the perspective of sustainable landscape and urban planning. Remote sensing data were used to develop land cover maps for the megacities across three epochs, i.e. t1-1990, t2-2000 and t3-2010. A hybrid classification method that integrates pixel-based and object-based techniques was employed in land cover classification. Transition matrices for the two time intervals (t1-t2 and t2-t3) were computed and geospatial tools and techniques were applied in order to reveal the spatiotemporal patterns of land changes in each megacity. The implications of the findings for future landscape and urban planning in relation to the sustainable development of the three megacities are explored.

Keywords: GIS, Remote sensing, Land change, Urbanization, Megacities, Southeast Asia

## Spatial analysis of archaeological sites and landforms in Kayseri, central Turkey using multiscale topographic data

HAYAKAWA, Yuichi S.<sup>1\*</sup> ; OBANAWA, Hiroyuki<sup>2</sup> ; NARUHASHI, Ryutaro<sup>3</sup> ; YOSHIDA, Hidetsugu<sup>4</sup> ; ZAIKI, Masumi<sup>5</sup> ; KONTANI, Ryoichi<sup>6</sup> ; SUDO, Hiroshi<sup>7</sup> ; ODAKA, Takahiro<sup>8</sup> ; YAMAGUCHI, Yuji<sup>9</sup> ; KULAKOGLU, Fikri<sup>10</sup>

<sup>1</sup>Center for Spatial Information Science, The University of Tokyo, <sup>2</sup>Center for Environmental Remote Sensing, Chiba University, <sup>3</sup>Earthquake Research Institute, University of Tokyo, <sup>4</sup>Department of Geography, Meiji University, <sup>5</sup>Faculty of Economics, Seikei University, <sup>6</sup>Notre Dame Seishin University, <sup>7</sup>Okayama Orient Museum, <sup>8</sup>Waseda University, <sup>9</sup>Okayama University, <sup>10</sup>Ankara University

Human habitat and cultural activities had been significantly influenced by natural environments including landforms in the prehistoric periods. Assessment of such relationships between palaeoenvironment and artificial remains is therefore crucial in understanding the historic development. Here we examine the nature-human interactive system in the ancient period of Kayseri region, central Anatolia Highland in Turkey, in terms of spatial analysis of the distribution of landforms and archaeological settlements, targeting mainly the period from B.C. 3000 to A.D.100. We perform geospatial analyses based on several topographic data including topographic maps, satellite-based remote sensing (10 m DEM derived from PRISM sensor images on ALOS), ground-based laser rangefinder measurement with global navigation satellite system (LRF + GNSS) and ground-based structure from motion multi-view stereo photogrammetry (SfM-MVS). The topographic data at different levels of scales provides both regional- and local-scale views of landform conditions, landform classifications, and detailed characteristics of settlements. Certain effects of gradual and sudden changes in palaeoenvironment on human activities are detected, and potential of natural disasters in the study area is also discussed.

Keywords: geoarchaeology, landform classification, digital elevation models, structure from motion

## Estimation of ground displacements by Geomorphic Image Analysis, using multi-temporal LiDAR DEM

MUKOYAMA, Sakae<sup>1\*</sup> ; HOMMA, Shin'ichi<sup>1</sup>

<sup>1</sup>Kokusai Kogyo Co., Ltd.

In the previous study, authors developed the new method which applies the technique of image matching analysis with high resolution DEM over difference times, to estimate the minute ground displacement of less than 1m order quantitatively and easily (Mukoyama et al., 2009 and Mukoyama, 2011). The present study shows the results of subsequent case studies to measure crustal movement, earthquake fault displacements, and the movement of landslides. Additionally we will show the results of comparative verification with some field observations by GNSS stations.

There are two approaches for the calculation of ground displacements from geomorphic point cloud data which is acquirable by temporal high-resolution LiDAR survey. Iterative Closest Point (ICP) is the method for 3D-matching by iterative calculation to find the positions which minimize the difference of coordinate values between paired points in the search area. The other approach is the combined methods of 2D-image measurement for estimation of horizontal component and point cloud calculation for vertical component. These two approaches share common process for finding the best position to minimize the difference between points along the small search window in the temporal data. For this study, we applied the latter approach which is based on the technique of digital image matching analysis using geomorphic image made from grid data of digital elevation model (DEM).

In this method, the existing Particle Image Velocimetry (PIV) algorithm was used for the 2-dimensional image matching. And orthographic slope angle image was used as measurable digital geomorphic image. Although PIV method has been developed generally for fluid analysis, grayscale gradient slope angle image is suitable for PIV analysis as it utilizes the validity of random distribution image of particles in fluid. In order to estimate vertical displacements, the vertical component is available by interpolation of the elevation values of DEM around endpoints of the calculated vector.

In recent study, above-mentioned method was applied to measure ground displacement due to the Great Japan Earthquake in 2011. In the region where liquefaction had damaged the reclaimed land, 10-50cm of lateral displacements were observed in some divided small areas, and seaward deformation of sheet-pile revetment by lateral movement was also observed at the spot on the seaside. After the earthquake, northern part of Japanese Islands moved eastward 6m or less. Verification analysis was conducted in order to compare between the results of Geomorphic Image matching Analysis and GPS observations in the region where temporal LiDAR data and GPS station data was available. Generally both of the results were corresponding with a high correlativity. In the additional study, verification analysis of landslide movement was conducted with GPS observation data; and both of the results were corresponding well with small error range.

The displacement measurement technique by high-definition digital geomorphic image made from high-resolution point cloud survey is effective and simple method, which has the accuracy of about 1/10 pixels or more. It is thought that this method is practicable for measurement of the movement of landslides, earthquake faults, etc.

### References

- Mukoyama, S., Nishimura, T., Asada, N. (2009) JpGU Meeting 2009 Abstract, Y167-004
- Mukoyama, S. (2011) Journal of Mountain Science, Vol. 8, No. 2, pp. 239-245

Keywords: DEM, LiDAR, DEMs of Difference, image matching analysis

## Landslide surface deformation detection by Iwate-Miyagi Nairiku earthquake using 2.5D analysis on SAR interferometry

SATO, Hiroshi, P.<sup>1\*</sup> ; MIYAHARA, Basara<sup>2</sup>

<sup>1</sup>Japan Map Center, <sup>2</sup>Geospatial Information Authority of Japan

We have already reported landslide surface deformation by 2008 Iwate-Miyagi Nairiku earthquake using Synthetic Aperture Radar interferometry (InSAR) images. In this study, to detect the landslide surface deformation quantitatively in the SE area of Mt.Kurikoma, report the result of 2.5D analysis on the images (i.e., combination of the images observed from ascending and descending orbits).

Keywords: SAR, interferometry, earthquake, landslide, 2.5D analysis

## Evaluation of topographic measurements using UAV- and ground-based SfM and TLS: A case study at a rocky coast bench

HAYAKAWA, Yuichi S.<sup>1\*</sup> ; OBANAWA, Hiroyuki<sup>2</sup> ; SAITO, Hitoshi<sup>3</sup>

<sup>1</sup>Center for Spatial Information Science, The University of Tokyo, <sup>2</sup>Center for Environmental Remote Sensing, Chiba University, <sup>3</sup>College of Economics, Kanto Gakuin University

Recent advances in measurement methodologies of high-resolution topographic data, including terrestrial laser scanning (TLS), structure from motion photogrammetry (SfM) on unmanned aerial vehicle (UAV) and ground-based SfM, enabled detailed investigations of land surface morphology in terms of morphometry and processes. Although such advanced methodologies are becoming widely applied in geomorphological studies, the nature of such data including error estimates needs to be carefully assessed when being applied in geomorphological researches. In this study we examine similarities and differences among three methods for the topographic data acquisition at a local scale (~100 m): UAV-SfM, ground-based SfM and TLS. The study site is a coastal bench at Aburatsubo in Miura Peninsula, central Japan, which suffers from intermittent uplift by large earthquakes such as the 1923 Kanto earthquake (M 7.9). UAV-based SfM was performed from higher altitude (ca. 30 m) to lower (ca. 10 m) using a quadcopter on which a digital camera with single-focus lens is mounted. We also used a digital camera mounted on a 4-m long pole for ground-based SfM. TLS measurement was carried out using a short-range scanner from 6 scan positions. Also, coordinates of three benchmarks on ground that are commonly used in all the methods were measured using global navigation satellite system (GNSS) capable of receiving dual radiowaves and post-processing based on carrier-phase correction with an accuracy of centimeters. The comparisons of the point clouds and digital elevation models (DEMs) obtained by three different methods indicate that 1) SfM-based data shows good accuracies in and around, but significant discrepancies outside of the benchmarks, 2) TLS sometimes give significant lack of data in shadow areas, and 3) data quality of SfM partly depends on the altitude of its platform (either UAV and pole). These characteristics we assessed will give insights into the selection of appropriate methodology for different purposes of geomorphological surveys.

Keywords: rocky coast, structure from motion, terrestrial laser scanning, point cloud, digital elevation model, accuracy

## Comparative analysis of knickpoint extraction using semi-automatic and automatic methods

ZAHRA, Tuba<sup>1\*</sup> ; PAUDEL, Uttam<sup>1</sup> ; HAYAKAWA, Yuichi S.<sup>2</sup> ; OGUCHI, Takashi<sup>2</sup>

<sup>1</sup>Graduate School of Frontier Science, The University of Tokyo, <sup>2</sup>Center for Spatial Information Science

Extraction of knickpoints (or knickzones) from a DEM has gained immense significance in studies of fluvial erosion and/or slope failures because of their geomorphological significance. Previously, knickpoint extraction from a DEM included a vector-based semi-automatic, but somewhat tedious and time-consuming data processing because GIS and spreadsheet software were separately used. Raster-based Python scripting, developed in our study and deployed in the form of a toolset, can automate the processes making the extraction of knickpoints automatically, fast and user friendly. Both the methods are based on the assumption that the slope gradient along a bedrock river changes with change in measurement length and any locally steep segment of the riverbed may then be considered a knickpoint. The relative steepness index  $R_d$  or the rate of decrease of gradient along the measurement length is calculated by solving a linear regression equation,  $G_d = ad + b$  where,  $G_d$  ( $\text{m m}^{-1}$ ) is the stream gradient at a point and  $d$  (m) is the measure distance, while  $a$  and  $b$  are coefficients and  $-a$  is regarded as  $R_d$  which means the rate of gradient decrease with increasing  $d$ . In the former method  $G_d$  is measured at the mid-point of a segment of variable length  $d$  along longitudinal stream profiles where;  $G_d = (e_1 - e_2) / d$  where,  $e_1$  and  $e_2$  are elevations at both ends of the segment, thereby analyzing both the upstream and the downstream segments along a stream. The automated Python processing, however, follows a slightly different approach from the one previously used and thus requires a comparative analysis of the two prior to its future use. The methods differ in the calculation of the stream gradient  $G_d$ ; the former employs both the upstream and downstream elevations  $d/2$  apart, whereas the latter uses the elevation at the point and  $d$  downstream. In this study, the Python toolset has been applied to a 10-m DEM of a mountainous region near Mount Ontake in the Northern Japanese Alps. The results were then compared and validated with the previous method. In order to study the fluvial characteristics of the knickpoints, analysis were confined only to the stream locations, the results of which provide insights into morphological developments of the watersheds.

Keywords: automatic extraction, DEM, knickpoints, Python

## Structure from motion and multiview stereo (SfM-MVS) in geomorphometry

UCHIYAMA, Shoichiro<sup>1\*</sup> ; INOUE, Hiroshi<sup>1</sup> ; SUZUKI, Hinako<sup>1</sup>

<sup>1</sup>National Research Institute for Earth Science and Disaster Prevention (NIED)

Software that unifies structure from motion (SfM) and multiview stereo (MVS) is currently in use. Hence, the construction of three-dimensional models and digital elevation models (DEMs) has been readily achieved at low cost using PCs. Both SfM and MVS are technologies developed in the computer vision field. SfM refers to the process of estimating three-dimensional structures from two-dimensional images. MVS generates three-dimensional models as point clouds. Digital camera images or aerial photos are used in the calculations and three-dimensional models are produced. To date, DEMs are derived by conventional photogrammetry or LiDAR. However, photogrammetry requires special software, experience, and extensive manual measurement of ground control points (GCPs); furthermore, LiDAR is expensive. To use SfM/MVS in geomorphometry, data accuracy is an issue as well as the precision of GCPs; issues that have attracted the attention of many researchers. In this study, we discuss three examples of the application of SfM/MVS to geomorphometry.

First, we present the case of a detailed topographic map in Izu-Oshima, Tokyo, where a large-scale slope failure occurred before dawn on October 16, 2013, owing to the heavy rains of Wipha typhoon. To obtain a detailed DEM of the damaged slope, we took vertical photographs by UAV and generated a DEM by using SfM/MVS. As a result, we produced a topographic map with a 0.5 m contour interval. The topography was well reproduced and well compared to the LiDAR map with a resolution of 5 m provided by the Geographical Survey Institute.

Second, we created a topographic map using a vertical movie taken by UAV and SfM/MVS processing. A movie has few total pixels per picture compared with a still picture. A 4K-resolution movie has approximately 8 million pixels, whereas a high-definition (HD) movie has approximately 2 million. Moreover, because of lens distortion corrections when a wide-angle lens is used, the pixels that can be used in the calculations decrease. However, there is noise owing to compression compared with a still picture. Thus, the results are not as good as time-lapse photography using still pictures. UAV has also the risk of crashing, thus, it is wise not to use expensive equipment. Cheap cameras without time-lapse function are also available for SfM/MVS. Moreover, old video data can be used to obtain DEMs.

Finally, third, we obtained DEMs from scanning aerial photos. In Japan, the aerial photo archives are currently exceeding 1 million sheets. Therefore, if accurate DEMs are obtained from aerial photos, comparisons are possible and changes over time can be identified. We examined color aerial photographs taken in 1978 and 2012 at downstream area of Nakama River, Iriomote island, Okinawa Prefecture. The aerial photos comprised scans of 23-cm one-side analog photographs (1978) and digital aviation camera data (2012). The data were scanned at a resolution of approximately 1,270 dpi and the total number of pixels per image was approximately 120 million pixels. The resolution of the digital aviation camera photographs was 9,920 x 14,430 pixels. We also processed them by using SfM/MVS and we obtained DEMs with ground resolution of 0.3 m. We used the processed photographs to evaluate the vegetation damage caused by the 2006 and 2007 typhoons.

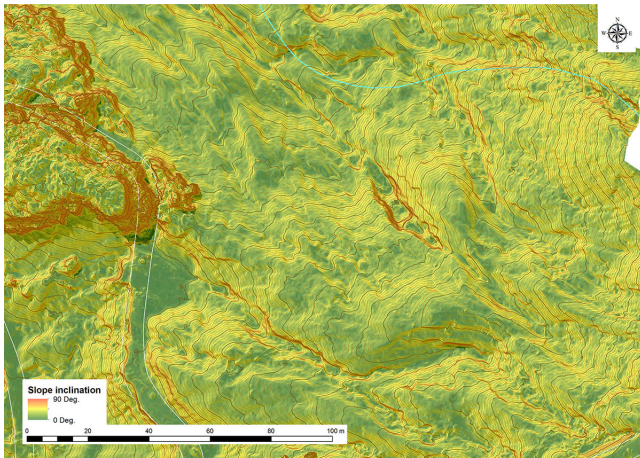
We show that SfM/MVS can be used in geomorphometry taking advantage of archived records. We anticipate that this methodology will be used more in the future.

Keywords: Structure from Motion (SfM), multi-view stereo (MVS), geomorphometry, topographic map, movie, aerial photograph

HTT08-P01

Room:Poster

Time:April 29 18:15-19:30



## Terrestrial laser scanning approach on quantification of weathering depth of sandstone blocks in a coastal environment

AOKI, Hisashi<sup>2</sup> ; HAYAKAWA, Yuichi S.<sup>1\*</sup>

<sup>1</sup>Faculty of Business Administration, Daito Bunka University, <sup>2</sup>Center for Spatial Information Science, The University of Tokyo

Weathering in a coastal environment often causes degradation of artificial constructions if they are composed of weathering-prone materials including natural rocks and cements. Conservations of the vulnerability of such construction materials to weathering processes are thus important for their maintenance. Point to point, or cross-sectional measurements using scale bars have often been effective in describing the degree of weathering of such materials. However, accurate measurements of the amount of weathering in terms of areas and volumes have not often been performed due to the limitation in the measurement method for detailed, three-dimensional surface morphology. Here we demonstrate terrestrial laser scanning to describe three-dimensional surficial morphology of a weathered material: sandstone blocks used for masonry piers of bridge on a shore platform at Aoshima, Miyazaki in western Japan. The blocks have suffered from salt weathering above the sea level since the construction of the bridge in 1951. Weathering-induced depressions of sandstone blocks well develop in the spray zone. Our approach revealed sub-centimeter scale morphology of the block surfaces, as well as weathering depths and volumes of each block. Spatial distribution of the amount of weathering was also examined with regard to the sea level and the rock surface hardness. Continuous measurement of such detailed morphology will be necessary to clarify the contemporary rates of weathering therein.

Keywords: Weathering, Sandstone, TLS, Rock strength

## Simple technique of PM<sub>2.5</sub> measurement in Higashi-Hiroshima city using a portable particle counter

OSHIME, Azusa<sup>1\*</sup> ; SAKUNO, Yuji<sup>2</sup>

<sup>1</sup>Graduate School of Engineering, Hiroshima University, <sup>2</sup>Institute of Engineering, Hiroshima University

In recent years, we are anxious about the trans-boundary air pollution by PM<sub>2.5</sub>. Therefore the development of various measurement, monitoring methods is demanded. It was begun the full-time monitoring in Hiroshima from FY.2012. It is only ten places at the end of May, 2013 to measure PM<sub>2.5</sub> among 39 places of atmosphere measurement station in the prefecture. In addition, because there is not the PM<sub>2.5</sub> measurement station in Higashi-Hiroshima city that population continues increasing, we did not understand the situation of PM<sub>2.5</sub>. Therefore, in this study, a technique to measure PM<sub>2.5</sub> with a relatively cheap portable particle counter (PPC) was considered. At first each particle size (the number of each particle more than diameter 0.3, 0.5, 0.7, 1.0, 2.0, 5.0 $\mu$ m) included in the atmosphere was measured using PPC (KR-12A, RION Ltd.) near Inokuchi Elementary School station (34.37268 degrees N, 132.38475 degrees E) that was one of the observation stations of Atmospheric Environmental Regional Observation System (AEROS) in order to estimate PM<sub>2.5</sub> from PPC. All 11 data set measured was used on May 25, June 8, June 22, August 3. The number of the particles less than 2.5 $\mu$ m (C<sub>2.5</sub>) was calculated by the relationship between cumulative particle number (CPN) and particle size. After having aspirated the atmosphere of 1L per 1 measurement, CPN of each particle size is measured by the scattering intensity of the semiconductor laser at 790nm. On the other hand, CPN for 195 days from March, 2013 to April, 2014 were observed to check PM<sub>2.5</sub> in Higashi-Hiroshima. On the other hand, CPN were measured for 195 days (only on weekdays) from March, 2013 to April, 2014 to check PM<sub>2.5</sub> in the city. Statistically high correlation was observed the relationship between CPN (total count of all particle size) and the in-situ PM<sub>2.5</sub> in Inokuchi station. The measurement limit of PM<sub>2.5</sub> and the estimation error (RMSE) were 4.1-12.8 $\mu$ g/m<sup>3</sup>. The environmental standards of PM<sub>2.5</sub> in our country are 35 $\mu$ g/m<sup>3</sup> by one-day average now. Therefore, the measurement limit by this method is judged to be a value quite lower than these standard values. This simple technique can be used enough as how for it to be careful of PM<sub>2.5</sub> at least. Moreover, as a result of creating the time series variation diagram of PM<sub>2.5</sub> in Higashi-Hiroshima using this observation method, the percentage which exceeds environmental standards in Higashi-Hiroshima was about 16%. Moreover, the season when the probability which exceeds the standard is the highest was in August.

Keywords: PM<sub>2.5</sub>, atmosphere, monitoring, particle counter

## Examination of the green space index by using CO<sub>2</sub> concentration at Ibaraki prefecture

ISHII, Kenta<sup>1\*</sup> ; IMAI, Yukako<sup>2</sup> ; KANZAWA, Masanori<sup>3</sup> ; KUWAHARA, Yuji<sup>4</sup>

<sup>1</sup>Department of Urban and Civil Engineering, Ibaraki University, <sup>2</sup>Graduate School of Science and Engineering, Ibaraki University, <sup>3</sup>U-DOM co., Ltd., <sup>4</sup>Center for Water Environment Studies, Ibaraki University

The objective of this study is to propose the correction method and evaluation index of CO<sub>2</sub> concentration data which is observed in human living sphere, Ibaraki prefecture. Since, sensor drift arises in the process of long-term continuous duty, it is important to correct the process by using standard reference gas. However, sensor drift times are different in each sensor and installation location, so, it is conducted the laboratory experiment and observation data analysis to grasp the action of CO<sub>2</sub> sensor. The results of this study were as follows: 1) It was proposed that the correction method for observation data which is combined linear transformation. 2) It was verified of the correction effect focused on the time variation and spatial distribution of CO<sub>2</sub> concentration.

Keywords: CO<sub>2</sub> concentration, fixed point observation, living environment sphere, the green space index

## Estimation for water surface temperature distribution in Lake Shinji and Lake Nakaumi using Landsat-8 TIRS data

SAKUNO, Yuji<sup>1\*</sup>

<sup>1</sup>Institute of Engineering, Hiroshima University

Lake Shinji and Lake Nakaumi are brackish water lakes with the rich biological resources represented by *Corbicula japonica*. However, the abrupt increase of blue-green algae or the spontaneous expand of aquatic macrophytes are anxious about the influence on such a biological resources of the lake in recent years. Therefore, various monitoring methodology for the elucidation of those generating mechanisms is examined. The satellite remote sensing is expected as a leading monitoring tool. Especially water temperature is important as most fundamental physical parameter. On the other hand, the Landsat-8 in the field of satellite remote sensing on February 11, 2013 was launched by NASA/USGS. This satellite has been continuing observation with 16 diurnal periodicity. The thermal infrared sensor (spatial resolution of 100 m) called TIRS (Thermal Infrared Sensor) with the multiple-spectrum sensor at visible and near- infrared bands with a spatial resolution of 30 m called OLI is carried in this satellite. Since high quantization (12 bits) and 2 band of TIR are realized as compared with conventional Landsat-7, more highly precise WT distribution estimation is expected. So, in this paper, to develop the surface water temperature (SWT) estimation by MCSST (Multi Channel Sea Surface Temperature) algorithm in these lakes using TIRS sensor and the accuracy was checked. Moreover, the SWT distribution characteristic in these lakes was considered using the proposed algorithm. The satellite data used is ten scenes from April to December, 2013. The Landsat-8 TIRS Level 1 product data was downloaded through the Internet site "Earth Explorer." The average value of 3x3 pixels of Band10 (10.6 - 11.2  $\mu\text{m}$ ) and Band11 (11.5 - 12.5  $\mu\text{m}$ ) in these lakes was extracted from the obtained satellite data. The data was changed into brightness temperature (BT). On the other hand, the SWT data at 1.0 meters under water was obtained from the Water Information System of Ministry of Land, Infrastructure and Transport. Moreover, MCSST (Multi Channel Sea Surface Temperature) which can reduce the air effect using two bands at thermal infrared for WST estimation from TIRS data was adopted. 19 datasets in the center of these lakes were used for development of MCSST. Three datasets acquired to the Yonago Bay were used for validation. WST estimation accuracy is expressed by average (bias) and standard deviation (error) of the residual substance of in-situ WST and satellite estimation WST. The WST accuracy using the single band algorithm of TIRS Band 10 and Band 11 was [bias: 1.3 oC, error: 1.7 oC] and [bias: 0.9 oC and error: 2.4 oC], respectively. On the other hand, the WST accuracy by the MC method was calculated with [bias: 1.3 oC, error: 0.6 oC]. The WST difference of the 3 data validated in Yonago Bay was an average of 1oC. Noise Equivalent Differential Temperature (NE $\Delta$ T) of TIRS sensor, The estimation accuracy of NOAA AVHRR in Mutsu Bay using the MCSST method is considered that this result is an appropriate numerical value from their being 0.4K (= 0.4 oC) (Irons et al, 2012) and about 0.5 $\pm$ 0.2oC, respectively. The WST map in these lakes was created using the proposed MCSST type. As for the WST in Lake Shinji lake in this period, it was checked through every year from these figures that a surface water temperature difference is about 3-5oC in the range of 5-30oC. Moreover, in the mouth of a river of Hii River and Shintate River which are located in the Shinji Kosai shore especially in a summer, the low-wash temperature pattern resulting from inflow of river water was observed.

Keywords: satellite, remote sensing, water temperature, lake

## Feasibility Study for the Estimation of the Chlorophyll-a Using ASTER Data in an Eutrophic Lake, Sri Lanka

DAHANAYAKA, D.d.g.l.<sup>1\*</sup> ; TONOOKA, Hideyuki<sup>1</sup> ; WIJEYARATNE, M.j.s.<sup>2</sup> ; MINATO, Atsushi<sup>1</sup> ; OZAWA, Satoru<sup>1</sup>

<sup>1</sup>Graduate School of Science & Engineering, Ibaraki University, <sup>2</sup>Department of Zoology, University of Kelaniya

The objective of this study is to evaluate the performance of the previously proposed band ratio approach in estimating Chl-a in Bolgoda Lake, Sri Lanka as a representative example of Case II waters. Lake is located at western province in an area with lot of industries and also with some agricultural activities. Considerable amount of industrial effluents are discharged into it. Illegal filling and also encroachment has occurred in the recent past. This study focused on to determine the trends in eutrophication via Chl-a changes during the recent past, make predictions and recommend mitigatory measures and suggest precautionary measures to restore the environment. From March to December 2013, water samples at 5 points of Lake were collected once per month parallel to ASTER overpass and Chl-a of each sample was measured using a laboratory spectrophotometer. Cloud-free ASTER scenes acquired over Lake under clear sky conditions were selected during 2000 to 2013 for Chl-a estimation and trend analysis. All the ASTER images were atmospherically corrected using FLAASH and in-situ Chl-a data on Lake were regressively analyzed with atmospherically corrected three ASTER VNIR band ratios such as B1/B2 of the same date. Finally, the regression equation of the band ratio with highest correlation (B1/B2;  $R^2 = 0.78$ ) was used to develop algorithm for generation of 15-m resolution Chl-a distribution maps using atmospherically corrected time series satellite imageries in day by day basis. This method applied for ASTER band 1/2 ratio due to Chl-a is positively correlated with the green band reflectance and negatively correlated with the red band reflectance. Therefore, the reflectance ratio of green and red bands becomes a robust parameter to estimate the Chl-a content. According to the ASTER based Chl-a distribution maps it is clearly evident that eutrophication of the Bolgoda Lake has been gradually increased from 2005-2011. Further, results showed that there were significant eutrophic conditions throughout the year 2013 in several parts of the Lake and considerable spatial heterogeneity with higher concentrations being recorded water stagnant areas and in water adjacent to freshwater outlets. It is clear that Bolgoda Lake is apparently a disposal site of various discharges of factories in addition to poor drainage and sewage systems present in this area. Highly unplanned urbanization and absolutely lack of adequate waste disposal management facilities in industries close to Lake have resulted in pollution of water. If the present trend of waste disposal and unplanned urbanization continue, they would create enormous environmental problems in future. Results of the present study showed that information from satellite remote sensing can play a useful role in determining the changes in Chl-a related to eutrophication in Bolgoda Lake and in the development of time series Chl-a distribution maps. Such information is important for the future predictions, development and management of this area as well as in the conservation of biodiversity. Therefore we recommend incorporation with this technique for routine monitoring of water quality using multi satellite data such as ASTER in inland water bodies like Bolgoda Lake in the future.

Keywords: Chlorophyll-a, Remote Sensing, ASTER, Sri Lanka, Bolgoda Lake

## Study on the information visualization aimed at maintenance and utilization of local resources

ISHIUCHI, Teppei<sup>1\*</sup>

<sup>1</sup>Akashi National College of Technology

In recent years, the problems of loss of sense of community and increase of indifferent residents, dilution of human relationships in the neighborhood, by dilution of a sense of belonging to the community, such as the moral decline is happening at local areas. Therefore, It become difficult for precisely corresponds to such changes alone to public administration ? driven. Target area of this study is Akashi city. This area has many rich rural environment and ponds, wooded area, waterway as remnant of village forest. And half of the residents of the town Uozumi-cho are a migrant.

In these areas, in order to promote community development befitting UOZUMI town, on an understanding of the digging up the history and culture of various regions, it is possible to stare life in the current region is important in the future. And, it is leading to a chance to foster protect the charm of a familiar town to residents themselves living in the town. Further, in order to form a hometown, it is necessary to dig the local resources, reaffirming residents share a town appeal. In this study, we dug up local resources existing in Uozumi-cho, and visualized as maps using the GPS positioning system. Finally, in order to convey to posterity the presence of valuable community resources, this study is proposed that the residents to re-recognize the appeal of the region by using a map.

Keywords: local resources, hometown, GPS, visualization

## Examination of land cover change region presumption method by using coherence value

SEKINE, Daiki<sup>1\*</sup> ; YUKI, Sohei<sup>2</sup> ; KUWAHARA, Yuji<sup>3</sup>

<sup>1</sup>Department of Urban and Civil Engineering, Ibaraki University, <sup>2</sup>Graduate School of Science and Engineering, Ibaraki University, <sup>3</sup>Center for Water Environment Studies, Ibaraki University

In recent years, many natural disasters have occurred because of abnormal climate. In a time like this, use of satellite data is advantageous to observation of the disaster region for a wide area. However, in order that photo sensor data may tend to be subject to the influence of atmospheric, synthetic opening data attracts attention. And, this research examined coherence data among the information generated from the Synthetic Aperture Radar data. The results of the research are as follows: 1)The coherence value of a vegetation region is low. This result is expressing that the growth environment of vegetation differs for every year. 2)The coherence value of a city area is high.

Keywords: land cover change, SAR, coherence value, land cover classification map, PALSAR

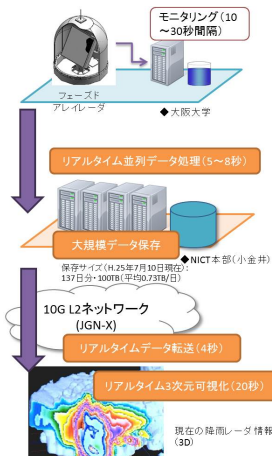
## A Technique for High-performance Data Processing of Satellite Observation Data via NICT Science Cloud

MURATA, Ken T.<sup>1\*</sup> ; KASAI, Yasuko<sup>1</sup> ; SATO, Shinsuke<sup>1</sup> ; ISHII, Shoken<sup>1</sup> ; WATANABE, Hidenobu<sup>1</sup> ; UKAWA, Kentaro<sup>2</sup> ; MURANAGA, Kazuya<sup>2</sup> ; YUTAKA, Suzuki<sup>2</sup> ; YAMAMOTO, Kazunori<sup>1</sup> ; TATEBE, Osamu<sup>3</sup> ; TANAKA, Masahiro<sup>3</sup> ; KIMURA, Eizen<sup>4</sup>

<sup>1</sup>Natl. Inst. of Info. and Communications Technology, <sup>2</sup>Systems Engineering Consultants Co., LTD., <sup>3</sup>University of Tsukuba, <sup>4</sup>Ehime University

It is said that data-intensive/data-centric science is the fourth paradigm of science after observation/experiment, theory and computer simulation. The NICT science cloud is one of the cloud systems for scientists who are going to carry out their research works for their big-data science. The science cloud is not for simple uses: Many functions are expected to the science cloud; such as data standardization, data collection and crawling, large and distributed data storage system, security and reliability, database and meta-database, data stewardship, long-term data preservation, data rescue and preservation, data mining, parallel processing, data publication and provision, semantic web, 3D and 4D visualization, out-reach and in-reach, and capacity buildings.

The present talk is focused on the topics of applications of the NICT Science Cloud to environment sensing research works. There are three applications to be introduced: (1) real-time data processing and visualization of 3D Doppler radar, (2) GOSAT CH4 data processing for global mapping, and (3) high-performance simulation of the ISOSIM-L (Integrated Satellite Observation SIMulator for a spaceborne coherent Doppler lidar) for wind measurement from space. These three projects are started and carried out in the NICT. With help of the NICT Science Cloud, they show progressive development to either larger-scale studies or more practical uses.



## Investigation of geographical feature and vegetation using for planting plan of the coastal zone at Tuvalu

KUWAHARA, Yuji<sup>1\*</sup> ; SATO, Daisaku<sup>2</sup> ; HIROMUNE, Yokoki<sup>3</sup> ; FUJITA, Masafumi<sup>4</sup>

<sup>1</sup>Center for Water Environment Studies, Ibaraki University, <sup>2</sup>Dept. of Architectural, Civil and Environmental Engineering, Tokyo Denki University, <sup>3</sup>Dept. of Urban and Civil Engineering, Ibaraki University, <sup>4</sup>Dept. of Urban and Civil Engineering, Ibaraki University

The objective of this study is to investigate the geographical feature of coastal vegetation growing in Funafuti Atoll, Tuvalu. In order to maintain the living environment of the South Pacific islands countries, sea-level rise is a serious problem. Thus, in this study, analyzed was the relation of land cover of shoreline area and hinterland by using aerial photograph (1984) and satellite image (2004). Then, geographical feature conditions of the coastal vegetation growing under natural condition were surveyed, and it was found that the coastal vegetation was growing in the altitude between 1.1m - 2.2m at Fongafale-island, Funafuti atoll.

## Factor analysis and vegetation change in China Inner Mongolia through Satellite Remote Sensing

BUHE, Baoyin<sup>1\*</sup> ; KONDOH, Akihiko<sup>1</sup>

<sup>1</sup>Center for Environmental Remote Sensing, Chiba University

In this study, the spatial and temporal vegetation cover change of the Inner Mongolia Autonomous Region was analyzed by using the time series satellite SPOT VEGETATION dataset from 1999 to 2012. The vegetation change trend was analyzed by the Normalized Difference Vegetation Index (NDVI), and the result was estimated by the Mann-Kendall rank statistic method. Annual maximum vegetation biomass can respond well with maximum NDVI change trend and annual vegetation product approximately similar with total amount of NDVI trend. Vegetation index has closely correlation with annual precipitation. The results revealed that the vegetation status of Inner Mongolia was affected significantly by the precipitation. Due to the benefit of return farmland to grassland and forestry policy such as forestation, cultivation of the arable land and increase the irrigation area, the vegetation in the southeast and middle south of Inner Mongolia significantly increased. In the northeast of Inner Mongolia, due to the global warming and wetland development the forestry growing period become longer that exactly reflect the vegetation cover increasing phenomenon . The vegetation distributed in middle-west of Inner Mongolia has decreasing trend and desert area was continuously extending within 14 years.

Keywords: Inner Mongolia, Desertification, Vegetation change, Mann-Kendall rank statistic, SPOT VEGETATION

## Study on the Spatial Analysis of River Flooding in the Amur River Basin

YOU, Qin<sup>1\*</sup> ; KONDOH, Akihiko<sup>2</sup> ; HARADA, Ippei<sup>3</sup>

<sup>1</sup>Graduate School of Science, Chiba University, <sup>2</sup>Center for Environmental Remote Sensing, Chiba University, <sup>3</sup>GIS Laboratory, Tokyo University of Information Sciences

Amur River is flowing through the border of China and Russia, and pour into the sea of Okhotsk. There are three plains in the Amur River basin, China famous commercialized food producing area of the Sanjiang Plain and the Songneng Plain are two of them. In order to develop the arable land in recent years, the land cover change and destroyed natural environment made the floods to be easily happened which be concerned. On the other hand, the drainage area of Amur River is 2.05 millions km<sup>2</sup>, it is a problem for satellite observation in spatial, and for extracting the flood information when there are clouds in the sky, the microwave image is used, but it will be expensive in the area of Amur River basin. So the analysis of river flooding will be the challenge. In this study, in order to understand the flooded situation of the Amur River basin, we used high temporal resolution satellite image to extract the two big floods of 1998 and 2013 by the spectral absorption characteristics of the water. We understood that there are different courses in twice flooded, and at the downstream of Amur River where is well to flooding, because of the wetland be changed and topography relief bring about drain off water difficulty.

Keywords: Near-infrared, MODIS, AVHRR, SRTM, Spectrum Character

## A preliminary study on using MODIS NDVI time series for monitoring abandoned farmlands in mountainous areas

SAKUMA, Asahi<sup>1\*</sup> ; SHIMAZAKI, Hiroto<sup>1</sup>

<sup>1</sup>Kisarazu National College of Technology

This study preliminary evaluated the feasibility of Normalized Difference Vegetation Index (NDVI) time series for monitoring abandoned farmlands in mountainous areas in Chiba prefecture. NDVI time series was derived from 8-day composite of MODIS Surface-Reflectance Product (MOD09) for the period from 2003 to 2013. The noise component in NDVI time series, which was induced mainly by cloud contamination and atmospheric variability, was reduced with the method based on Savitzky-Golay filter. The refined NDVI time series was then decomposed into trend, seasonal, and remainder components. A simple linear regression model was fitted to the trend component of each pixel, and model parameters (i.e., intercept and slope) estimated were considered to be candidate features to find the occurrence of abandoned farmlands in the pixel area. This idea was based on the assumption that (1) overall NDVI in mountainous areas would be higher than that in other areas because of relatively-dense vegetation; and that (2) NDVI in specific seasons would have differences between farmlands and abandoned farmlands due to the effect of cropping activity. Classification performance was measured with the area under the receiver operating characteristic (ROC) curve (AUC). The results showed that the model parameters were poor (AUC=0.6) in terms of classification performance. Further efforts are needed to evaluate the feasibility of NDVI time series for detecting abandoned farmlands in mountainous areas.

## Visual Surveillance of Natural Geography by means of UAV

HASEGAWA, Hitoshi<sup>1\*</sup> ; ISOGAI, Tatsuhiro<sup>1</sup> ; ONO, Isamu<sup>1</sup>

<sup>1</sup>Kokushikan University

Unmanned aerial vehicle (UAV) systems can lead to major advances in physical geography. We have obtained a high-resolution digital aerial photographs using UAV (Unmanned Aerial Vehicle). UAV can make an automatic flight under the GPS control and take aerial photographs repeatedly with the same flight route. In this study, UAV was flying at 50 to 100m altitude. We have taken aerial photographs at coral reefs ,mangrove forests and the trench site of active fault. The high-resolution aerial photographs, a detailed classification map could be created, and it would also allow the extraction of dynamical topographic and vegetation development temporal changes.

Keywords: UAV, High-resolution digital aerial Pjotograh, Proximal Remote Sensing Method

## The acquisition of geospatial information by small UAV

TANAKA, Kei<sup>1\*</sup> ; KONDOH, Akihiko<sup>2</sup>

<sup>1</sup>Japan Map Center, <sup>2</sup>Center for Environmental Remote Sensing, Chiba University

The recent advances of MEMS devices(GPS, gyro and acceleration sensor) has made possible low-cost and miniaturization. Thereby, multi-copter mounted with these sensors have appeared. That it requires a high level of technology and knowledge in the handling of RC traditional helicopter, beginners to steer is difficult. To enable even beginners to get easily geospatial information of high-resolution by multicopter.

In this study, we examined method of acquiring geospatial information(orthophoto, DSM, NDVI, and temperature distribution) by using small UAV.

Keywords: UAV (Unmanned Aerial Vehicle), SfM (Structure from Motion), DSM, orthophoto, NDVI, temperature distribution

## UAV application and possibility for disaster prevention.

SAITOU, Osamu<sup>1\*</sup> ; KUWAHARA, Yuji<sup>1</sup>

<sup>1</sup>Center for Disaster Prevention and Security, IBARAKI University

Videos of the tsunami taken from the airplane conveyed the horror of the recent great disaster which attacked the various places in eastern Japan, the Great East Japan Earthquake of 2011. Numerous engineers and researchers were shocked by the images. Moreover, many real-time movies and images of this disaster exist. Especially in the past several years, other disasters caused by extreme weather because of our changing climate, such as heavy typhoons, rain cataracts, flurries, and tornadoes, also cause widespread destruction. When these disasters or earthquakes occur, rapid situational assessment is crucially important, but it is difficult because transportation systems including roads and railways often shut down under those circumstances. Therefore, a monitoring system that provides information immediately when a disaster occurs is required. When a disaster occurs, monitoring from an airplane or satellite is effective but such systems are not easy to use. This study examines the possibility of disaster monitoring systems using uncrewed aerial vehicles (UAV).

Keywords: UAV, sensor network, sensor, disaster prevention

## Proximity air measurement of the radiation by unmanned small helicopter

KAJIWARA, Koji<sup>1\*</sup> ; HONDA, Yoshiaki<sup>1</sup>

<sup>1</sup>Center for Environmental Remote Sensing, Chiba Univ.

The decontamination work of the radioactive material which dispersed in the accident of Fukushima nuclear power plant accompanying the Great East Japan Earthquake, is continuing to residential area, cultivated land, etc.

However, the still high dose is measured in the forest region.

It is a question whether safety can be guaranteed or not, even if it performs the roof of a house or building, and decontamination of only soil, when a forest is in living environment.

The radiation measuring instrument which enabled it to adjust the distance to the target for measurement with the winch attached to the small unmanned helicopter in this research is used, the dose of a tree crown from the position close to about 100m has been measured, and it was shown that field dose measurement in the forest is possible.

Moreover, even if it was the decontaminated place, it checked that a space dose in case it approaches and a forest exists changed with altitudes.

Keywords: UAV, Radiation Measurement, Forest Canopy

## Generating three-dimensional models by a software that unifies SfM and multiview stereo (MVS)

UCHIYAMA, Shoichiro<sup>1\*</sup>

<sup>1</sup>National Research Institute for Earth Science and Disaster Prevention (NIED)

In recent years, the software which unified Structure from Motion (SfM) and multi-view stereo (MVS) was developed. By this, construction of three-dimensional models and its Digital elevation models (DEMs) can be achieved with PC at easy and low cost. This paper shows a method for generating three-dimensional models by using with a SfM-MVS software and images captured by a handheld camera or an UAV's.

Keywords: structure from motion (SfM), three-dimensional model, digital surface model (DSM), unmanned aerial vehicle (UAV), geomorphometry, image acquisition for calculation

## Safety measures for multicopter aerial photo survey

INOUE, Hiroshi<sup>1\*</sup> ; UCHIYAMA, Shoichiro<sup>1</sup> ; SUZUKI, Hinako<sup>1</sup>

<sup>1</sup>National Research Institute for Earth Science and Disaster Prevention(NIED)

Low-altitude aerial photographing using multicopters, radio-controlled multi-rotor helicopters, became easy for everybody because of their recent technical advancement and price declines of the equipment. The technology will become popular rapidly as one of the methodologies of field surveys. Multicopters, however, can crash into the ground. We have experienced crash or near-crash accidents through our surveys and test flights in the past. The causes are sometimes a simple pilot error, loss of a propeller, unexpected strong wind, and out of battery, and are sometimes unclear, like GPS signal loss and barometer error, and their combinations. The crashes could have made serious injuries if the multicopters hit humans judging from the damage to the equipment we experienced.

The measures we take are careful pre-examination of the flight plan, making propeller guards, knowing battery capacity-flight time characteristics, monitoring battery voltage during the flight, regular maintenance of the batteries, pre-flight equipment checks, acceleration and compass calibrations, communication between the pilot and copilot, full utilization of autonomous flight, training of manual control for emergency, and following the safety check list.

Multicopter survey could cause problems to the society if accidents occur often as the result of popularization. If the usage becomes too strictly regulated, we may limit or even lose the large potential of applying the multicopter technology to our field survey. We therefore need to establish the safety measures to be obeyed, and share experiences of accidents for wider recognition of its potential danger, clarify individual causes, in order to strengthen the measures. Compliance to the aviation and wireless communication laws and regulations are indisputable. We also have to buy an insurance to compensate the possible damage caused by an accident.



## Mapping active faults by using small unmanned aerial vehicle and structure from motion: a case study on Midori fault

UCHIYAMA, Shoichiro<sup>1\*</sup> ; NAKATA, Takashi<sup>2</sup> ; INOUE, Hiroshi<sup>1</sup> ; KUMAHARA, Yasuhiro<sup>2</sup> ; SUGITA, Satoru<sup>3</sup> ; GOTO, Hideaki<sup>2</sup> ; IZUTSU, Jun<sup>3</sup> ; FUKUI, Hiromichi<sup>3</sup> ; SUZUKI, Hinako<sup>1</sup> ; TANIGUCHI, Kaoru<sup>4</sup>

<sup>1</sup>National Research Institute for Earth Science and Disaster Prevention, <sup>2</sup>Hiroshima University, <sup>3</sup>Chubu University, <sup>4</sup>National Institute of Advanced Industrial Science and Technology

We photographed the geomorphometry of the Midori fault scarp formed by the 1891 Nobi earthquake in Motosu city, Gifu Prefecture (Japan) by using a multirotor radio control helicopter as a small unmanned aerial vehicle (sUAV), and we analysed these images. A digital surface model (DSM) of 0.09 m mesh and an orthophoto with a resolution of 0.03 m were generated from these images by PhotoScan software produced by structure from motion (SfM). A topographic map with 1 m interval contours and a cross-section profile were processed using a DSM produced by ArcGIS. We expect that the new technology will be applied to tectonic landform survey and geomorphology research. In addition, our results should help to ensure flight safety and compliance with the law.

Keywords: structure from motion (SfM), small unmanned aerial vehicle (sUAV), digital surface model (DSM), orthophoto, geomorphometry, midori fault scarp



## Generating an orthophoto from SfM calculation with the low-quality air photographs taken in the 1964 Niigata earthquake

SUZUKI, Hinako<sup>1\*</sup> ; UCHIYAMA, Shoichiro<sup>1</sup>

<sup>1</sup>National Research Institute for Earth Science and Disaster Prevention (NIED)

This study shows that generating the orthophoto from low quality aerial photographs using structure from motion (SfM). National Research Institute for Earth Science and Disaster Prevention (NIED) is archiving a lot of old aerial photographs and its original roll films. However, some films are deteriorating. One of them is the 1964 Niigata earthquake's film. This deteriorated photographs were taken 50 years ago, nevertheless, the result of SfM calculating were sufficient quality and generated orthophoto with 0.2 m resolution. As a result, low quality aerial photographs are available to utilize for SfM.

Keywords: structure from motion (SfM), low quality aerial photograph, 1964 Niigata earthquake, ground control point (GCP), orthophoto



## Mapping of the fault scarp formed during the 2013 Bohol earthquake by small UAV

NAKATA, Takashi<sup>1\*</sup> ; INOUE, Hiroshi<sup>2</sup> ; CAHULOGAN, Mabee<sup>3</sup> ; RIVERA, Danikko<sup>3</sup> ; LIM, Robjunelieaaa<sup>3</sup> ; POGAY, Cathy<sup>3</sup>

<sup>1</sup>Hiroshima University Professor Emeritus, <sup>2</sup>NIED, <sup>3</sup>PHIVOLCS

A 5km-long surface fault rupture appeared during 2013 Bohol earthquake (M 7.1) in the Philippine. We took low-altitude air-photos of the ruptures using a small UAV, and made 3D images and contour maps by SfM software. This survey method is a low-cost, easy and effective method for mapping for quick respond field work for unexpected large earthquake damage especially in remote areas in under developing countries.

Keywords: UAV, SfM photogrammetry, earthquake fault, 2013 Bohol earthquake

## Multicopter Aerial Photo Survey of Building Damages by 2013 Bohol Earthquake in the Philippines

INOUE, Hiroshi<sup>1\*</sup> ; HANAZATO, Toshikazu<sup>2</sup> ; IMAI, Hiroshi<sup>1</sup> ; MELOSANTOS, Arnold<sup>3</sup> ; ALCONES, Ponzch<sup>3</sup> ; SORIANO, Karl vincent<sup>3</sup>

<sup>1</sup>National Research Institute for Earth Science and Disaster Prevention(NIED), <sup>2</sup>Mie University, <sup>3</sup>Philippine Institute for Volcanology and Seismology(PHIVOLCS)

We demonstrate the effectiveness of multicopter aerial photographing for recording earthquake damages of low to medium-rise buildings. M7.2 shallow inland earthquake occurred on Bohol Island in the Philippines on October 15, 2013, which caused thousands of building damages and more than 200 casualties in the western part of the island. Post- earthquake surveys by PHIVOLCS showed the maximum earthquake intensity in Tagbilaran city near the epicentral area was VII in Philippines Earthquake Intensity Scale, which is equivalent to VI in JMA intensity scale. We visited the island three weeks after the earthquake, to make the damage survey focusing on church buildings using a multicopter. We also carried out aerial photogrammetric survey of the surface rupture of the earthquake fault and the coastal uplift(Nakata et al., JpGU 2014) and the landslide damage of chocolate hill, a distinguishing morphology on the island.

A number of stone masonry churches founded in the 16th century in the Spanish colony times were damaged by the earthquake. The existing building of Baclayon Church, which was constructed in 1727 and known as the oldest church in the Philippines, lost the upper half of the bell tower and the whole front wall of the cathedral. Loboc Church and the adjoined museum in the Loboc city lost most of the side walls except their lower part. Maribojoc Church in the west and Clarin Church in the north of the island collapsed completely. Notable damages are also on non-structural masonry walls confined by RC columns and beams of public buildings, such as Sagbayan city hall and Tubigon city hall.

We used a small and easy-to-fly multicopter named DJI Phantom and a high-resolution and compact digital camera GoPro Hero3 Black Edition for the aerial photographing. We attached the camera facing obliquely down and manually controlled the copter in GPS stabilized mode. We used a FPV (First Person's View) system FatShark Telepoter V3 for watching the camera view. Photos were taken continuously in 2 seconds interval, while the copter was flying around the subjects. We limited the duration of each flight to five minutes and attached propeller guards to the rotors in order to reduce the possible dangers by crash as much as possible because people's activities in the areas around the churches were normal. We had no accident during the survey. We found that FPV is very useful in building damage survey because it can reduce the risk to crash to the building when taking photos, while it is difficult to know the distance from the copter to the subject in manual control from the ground.

The left figure shows the multicopter aerial photos of the damaged Baclayon Church. We can observe the fracture surfaces of the upper structure and its inside which are invisible from the ground. Aerial photographing using multicopter right after an earthquake is an efficient tool to easily get full picture of the damage even when approaching from the ground around a building is difficult. We then processed about 50 aerial photos using an SfM (Structure from Motion) software PhotoScan to reconstruct the 3-D model of the bell tower as shown in the right figure. The techniques enable modeling fractures of buildings and their analyses. The 3-D models are also valuable as digital architectural remains of disasters. Aerial photogrammetry using multicopter and SfM is easier than 3-D measurement using laser scanner. Creating a miniature of damaged building from the digital model using 3-D printer will also be useful for planning repairs and earthquake resistant design of buildings.

HTT33-P04

Room:Poster

Time:May 2 16:15-17:30



## Production of vegetation/landcover and dose rate maps by small helicopter and UAV

KONDOH, Akihiko<sup>1\*</sup> ; HONDA, Yoshiaki<sup>1</sup> ; KAJIWARA, Koji<sup>1</sup> ; NORO, Naoki<sup>2</sup> ; TAKARA, Yohei<sup>2</sup> ; ANDO, Fuminori<sup>2</sup> ; FUJIMORI, Takahiro<sup>2</sup> ; NONAMI, Kenzo<sup>3</sup> ; YAMAGUCHI, Hidetoshi<sup>4</sup>

<sup>1</sup>Center for Environmental Remote Sensing, Chiba University, <sup>2</sup>EBA JAPAN CO.,LTD., <sup>3</sup>Graduate School of Engineering, Chiba University, <sup>4</sup>SWR CO.,LTD.

The most essential and important information for restoration of the area contaminated by radioactive materials is dose rate and landcover map. The map should cover the SATOYAMA watershed with several hundreds to several kilometers scale, because the life in mountain village depend on water and material cycles in SATOYAMA watersheds and mode of deposition is strongly affected by vegetation type such as deciduous broad-leaved or evergreen coniferous forests. However, large scale maps on present vegetation and dose rate distribution are not available at present, so our team attempts to create vegetation/landcover map and dose rate distribution map by using UAV(Unmanned Aerial Vehicle).

Manned helicopter (Robinson R44), radio controlled gasoline engined helicopter (YAMAHA/RMAX), and radio controlled electric multicopter (Minisurveyer MS-06L) are used as platform of dose rate measuring system. Dose rate is measured by radiation detector module (C12137-01, Hamamatsu Photonics) controlled by small laptop computer.

Hyperspectral camera (NH-7, Eba-Japan Co.,Ltd.) and video camera are installed on manned and unmanned helicopter to map precise vegetation and landcover map. In hyperspectral camera operation, both pushbroom and still images are taken. Motion video is captured to get still images, and mosaicked to ortho-areal photo.

Field campaign are carried out two times during August and November in 2013, and various photographing modes three-dimensional dose rate mapping, and dose rate on various landcover such as forest canopy are attempted.

The campaign reveals the feasibility of low-cost, on-demand photographing and dose rate survey buy using UAV. Next subject is implementation to the actual scene. We plan to continue dose rate survey in Yamakiya district, Kawamata Town in Fukushima Prefecture.

Keywords: nuclear disaster, dose rate measurement, UAV, hyperspectral camera, Yamakiya District, FUKUSHIMA

## Airborne LiDAR bathymetry survey in Japanese Pacific coast in 2013

MATSUNAGA, Tsuneo<sup>1</sup> ; ISHIGURO, Satoshi<sup>1\*</sup> ; YAMANO, Hiroya<sup>1</sup> ; OGUMA, Hiroyuki<sup>1</sup>

<sup>1</sup>National Institute for Environmental Studies

In 2013, Airborne lidar bathymetry survey in Japanese Pacific coast was planned and partially conducted at several selected-sites.

The objective of this survey is to acquire detailed bathymetry data in Japanese Pacific coast which are important for Tsunami simulation as well as monitoring of coastal environment and ecosystem heavily damaged by the Great East Japan Earthquake occurred in March 2011.

An airborne lidar bathymetry system, Fugro LADS Mk. III, was brought to Japan for the first time in October 2012. Data acquisition flights over several coastal areas in Hokkaido, Tohoku, Mie, and Tokushima were conducted in November and December, 2012, and remaining areas in Tohoku and Izu were conducted in September and October, 2013. Obtained data are currently being calibrated and evaluated.

In this presentation, the outline of the survey including instrument specifications, mapping areas, and the survey schedule as well as lidar data acquired will be presented.

Keywords: Airborne LiDAR

## Identification of sidewalk steepness from LIDAR data for Tsukuba University campus bicycle riders

MURAYAMA, Yuji<sup>1</sup> ; LWIN, Koko<sup>1</sup> ; ZHOU, Yifei<sup>1\*</sup>

<sup>1</sup>Graduate School of Life and Environmental Sciences, University of Tsukuba

### (1) Motivation

Bicycles are the most prominent travelling mode in many universities. Measurement of safety factors for sidewalk bicycle riders is essential for university authorities in order to concern public safety and to improve campus facility management information system. Information of sidewalk steepness is useful for daily bicycle riders inside the university campus in order to prevent unnecessary accidents while they are riding, especially at night.

### (2) Data and Methods

In this study, we used very fine scale Light Detection And Ranging LIDAR data to identify the sidewalk steepness by integrating with Smart Field Data Collection System\* and deliver the information through Campus Web-GIS.

### (3) Results

Based on our study, LIDAR data are much promising to detect sidewalk steepness in open spaces. However, the accuracy was reduced in some areas where the sidewalk covered with trees and bridges. Intensive field investigations are required to correct them. We built a *Smart Field Data Collection System* to correct and modify the results by using Android smart phone application.

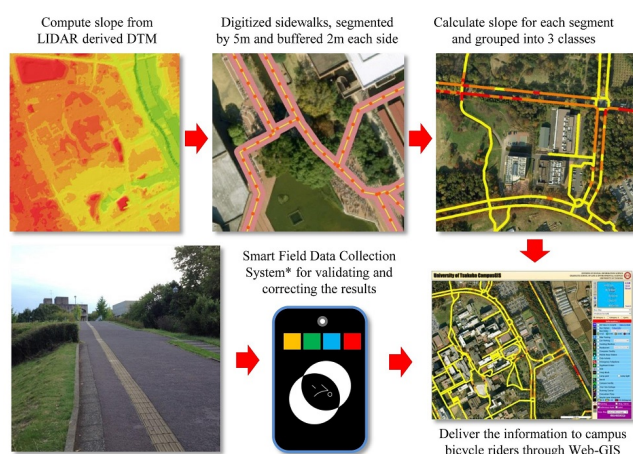
### (4) Prospect

Identification of sidewalk steepness from LIDAR data is cost and time effective. Additional user friendly real-time Web-based GIS field data collection system to collect, store and modify the results by multiple users is a great benefit for data validating purposes.

### (5) References

Yuji Murayama and Ko Ko Lwin, (2013). Smart Data Collection and Real-time Digital Cartography, IGU Kyoto Regional Conference 2013, August 4-9, Kyoto, Japan.

Keywords: Lidar, fieldwork, campusGIS



## The Buffer Zone Model of Natural Conservation Area

TANKA, Kazunari<sup>1\*</sup> ; YOSHIKAWA, Shin<sup>1</sup>

<sup>1</sup>Osaka Institute of Technology

### 1. Introduction

In the Kii mountainous region in the south Kinki area, there are preserved beautiful forest and river. However, the area faces problems of sustaining local industries as number of successors was declining due to the decrease of birthrate which is the major problem of Japanese society. Especially the decline of population and competitiveness of local industries are serious problems.

The 'Sacred Sites and Pilgrimage Routes in the Kii Mountain Range' are registered under the World Heritage Site in July 2004. This is the second example of linear type World Heritage Site. The first Site was the 'Camino de Santiago', which means the 'Way of St. James' in northern Spain.

The buffer zone of the 'Sacred Sites and Pilgrimage Routes in the Kii Mountain Range' is set as fifty meters from the center of the trails for both sides. This fifty meters' buffer zone was set without theory in terms of conservation of the environment around the World Heritage registered area.

The core area of the 'Camino de Santiago' is linear type as well. It connects cultural monuments, cathedrals and beautiful nature sites in Spain and in France. The buffer zones of the area was set for thirty meters from the center of the trails for both sides. However, if considering the visibility of the Pyrenees mountainous areas, wider area should be covered as buffer zone. As there are no standard criteria for the buffer zone setting that the study aims to develop GIS, which can determine the appropriate buffer zone.

### 2. Purpose of Report

In this report, we tried two studies; one was to survey the visibility of forest with plants laser measurement device. Secondly, the study achieved the method to describe the forest model in digital format. As for the further step, we will analyze the relationship between the result of the survey and the model. Based on the data we obtained, we will try to make a model to set buffer zone for conservation area.

### 3. Analysis

The analyzed area of this report is Koyasan Cyoichi-michi trail in the 'Sacred Sites and Pilgrimage Routes in the Kii Mountain Range' World Heritage Site. We surveyed several points using 3D laser scanner. The points were determined based on the pre-survey by photo and conventional measured. The points we surveyed differ such as vegetation and geographical conditions. The typical vegetation was the cluster of plants of cryptomeria. On an average within the seventeen meters there were many obstacles, which disturb visibility (24.7%).

We also analyzed to application of the survey results to a model plantation area for the comparison. The artificial plantation model is created from the typical trunks of trees with locations and even distances, which make the model to be quantitative.

We set the viewpoint surface every one meters. We estimated that the visible area and invisible area can be determined by setting lines between human visions and trees within. It showed the difference between visible area and invisible area. The percentage of the transitivity of visibility is calculated based on the above results.

The model is set based on periodical growth of plants. The previous study indicated that statistically cryptomeria of forty to sixty years old is majority of plantation. We calculated the distances of transitivity (an average distance) based on the visible-invisible analysis using GIS system. Finally, we verified the results (photographs) at the actual sites.

### 4. Conclusion

The study found out the possibility of the method that make the model of the buffer zone related with real space. The model we established in this study can expect statistically reliable results from simple survey method and objective data. The study will fine-tune results in applying the detailed data. Simultaneously, we aim to develop criteria based on the differences of the part of trees, as well as other natural environment.

Keywords: buffer zone, world heritage, Sacred Sites and Pilgrimage Routes in the Kii Mountain Range, GIS

## Effects of the buffer models in the estimation of the spatial SPM distribution at the sky of the Yokohama city

YAMAKAWA, Junji<sup>1\*</sup>

<sup>1</sup>Graduate School of Natural Science and Technology, Okayama University

In the estimation of the SPM distribution on successive region of interest from the concentrations observed at the observatories located in various places, the kriging method (Matheron, 1973) has been frequently employed. At the case, the universal kriging with auxiliary maps is used for minimize the variance of the estimation. In this study, two types of the auxiliary maps were used in the universal kriging estimation of the SPM concentration distribution. One of the map was a terrain map based on the DEM, and the other map is a buffer map generated from the buffer model based on the buffer distance from the coastline. However, if the region of interest is a wide area that includes a sea part and the land part, and if the observed values of SPM concentration at sea part have not been obtained, the validity of the estimated SPM distribution by the universal kriging may be affected by the used buffer models. Therefore, the effect of the buffer maps in the estimation of the SPM spatial distribution by a universal kriging was investigated in this study.

The SPM concentration data used in this study were published by the National Institute for Environmental Studies. The DEM data was extracted from the digital elevation models that have been published from the Geographical Survey Institute used with the FGDV application. The buffer model were created by the GIS applications based on the coastline data extracted from 1:200,000 Japan seamless geological map that was published from the Geological Survey of Japan. The coordinate projection method of all data were converted to Japan datum 2000 (JGD2000) to minimize the occurrence of error due to the difference of the projection method in geospatial computing. In the representation and geospatial statistical analysis of the data, the R language and its geospatial packages and, the Google earth and FOSS4G were used.

In this study, the observation points of the SPM concentration were present only on the land area and not present on the sea part. Moreover, the altitude of the sea part were all zero in the DEM data. Therefore, in the prediction by the universal kriging at the sea part, even if the variance of the prediction is small, the accuracy of the prediction may be lost at the relatively large buffer distances. So, some care may be required when the predicted distributions are used.

Keywords: GIS, Kriging, R-Language, FOSS4G, Google earth, JPGIS-GML-DEM

## Investigation of indoor positioning technology focused on signboard in railway station

SHIMIZU, Tomohiro<sup>1\*</sup> ; YOSHIKAWA, Shin<sup>2</sup>

<sup>1</sup>Graduate School of Eng., OIT, <sup>2</sup>Faculty of Eng., OIT

The acquisition of the outdoor location information has become convenient and precise by the appearance and development of the satellite positioning technology. Recently, it has been more high precise positioning on a centimeter level by the launch of the quasi-zenith satellite in 2010. So, the various services utilizing the location information have been produced. In this way, the location information has become more important and essential as a kind of social infrastructures. Under such circumstances, the acquisition of location information in the indoor environment where the satellite radio wave cannot reach has been regarded important as a next step.

In this study, the authors are going to investigate an indoor positioning estimation technology focused on the railway station. In the railway station, the various needs, such as the advancement of amenities, the facilitation of pedestrian movement, the universal design associated with an aging society, the creation of a compact space appropriate for the population decline society and so on, have been required. In particular, the development of the railway station with multiple functions like business has been recently promoted in the metropolitan areas. So, the spatial structure of the railway station has been complicate because it has been required to play various daily roles for urban residents. And the precise acquisition of location information is more important in the indoor environment like the railway station which has much complexity in recent years. Therefore, the authors are going to investigate an indoor positioning estimation technology in the railway station space. Especially, the authors pay their attention to the signboards of important information indicating "positional relations of the space" in the railway station.

First of all, the authors built the database of the sign system and the floor maps to estimate the indoor location. The authors built it with three-dimensional information including the display height in addition to the plane information by extracting the signboard from the photograph. Also, they built the attribute information like the size and direction of sign boards, and the type and number of pictograms in the database. So, they tried to estimate an indoor location by using the photograph. Actually, they extracted signboards in the photograph by using the image processing technology. After that, the rough location where the signboards were taken in photos can be grasped by matching the attribute information. It is necessary to set an area in each signboard. In this study, the authors set up "the effective visual field range" of signboard, because they assumed to take a photograph when the signboard is confirmed. Finally, they are going to estimate a detailed indoor location by using photogrammetry technology. For the purpose, it is necessary to orient the already known three points with coordinates. Therefore, in this study, the detailed location is estimated by using three-dimensional coordinates on four corners of the signboard in the database. This study could obtain certain results as an indoor positioning technology through the investigation of "the extraction of a signboard from the photograph", "the estimation of the area from effective visual field range" and "the estimation of the point location by photogrammetry technology".

In future, it is necessary to make an effort for the improvement of accuracy related to the technology used in this study. In addition, the authors have to build the system that can automatically estimate an indoor position from the photograph.

Keywords: railway station space, railway signboards, indoor positioning, image processing

## Handling non-aggregated person trip data with Web-GIS

MURAYAMA, Yuji<sup>1\*</sup> ; LWIN, Koko<sup>1</sup> ; GREGER, Konstantin<sup>1</sup> ; ESTOQUE, Ronald<sup>1</sup> ; KUBO, Takafumi<sup>1</sup>

<sup>1</sup>Yuji Murayama

Understanding of human mobility from spatial perspective is important for urban transport planners, human geographers, social scientists and other spatial information users. Advances in geospatial data collection methods and communication devices, we can nowadays collect, store and integrate large amounts of data with GPS and GIS technologies, including mobile phone log data, real-time weather information, person flow data etc. However, handling of these Spatial Big Data require computational power and considerable period of time. Extraction of information from these Spatial Big Data is also challenging for end users in terms of time consuming and requires knowledge on spatial data handling and processing. Here we construct a Web-GIS to extract, visualize and analyze the Person Trip Survey (PTS) data by providing common GIS analytical functions to novice to expert users in timely manner.

Keywords: GIS, person trip, big data, spatial analysis, WebGIS, visualization

## The Process of Growth and Cityscape Transition in Modern Osaka

NISHIMOTO, Takahiro<sup>1\*</sup> ; YOSHIKAWA, Shin<sup>2</sup> ; TANAKA, Kazunari<sup>2</sup>

<sup>1</sup>NEWJEC Inc., <sup>2</sup>Faculty of Eng.,OIT

Most of big cities in modern Japan had been growing up remarkably with modernization from the Meiji period. Especially, the structure of space has been changing dramatically throughout a revival development in the post-war and in the high economic growth period. As the result, it have been become difficult to see the cityscapes of the past which built up with the modernization. However, in recent years after the arrangement of urban infrastructure settled down, the community development or a tourism using the historical environment have been carried out, and the interest in history has been increasing. In other words, to keep the historical environment has been increasing importance as property of city. On the other hand, GIS becomes more familiar to us by geospatial information technology spreads rapidly in recent years, in the middle of a highly information-oriented society. Especially, the utilization GIS is effective for the historical research, because it can process long-term spatiotemporal information like transition analysis.

Osaka was prosperous as the Aqua Metropolis in Edo period, and has become the modern city crowded with public transport and high-rise buildings in Kansai area at present. In this study, the authors are trying to investigate the historical transition in Osaka with modernization by using geospatial information technology. And they are going to recognize again the existence of characteristics in urban space which formed and disappeared with modernization, and to aim at reconstructing the historical environment.

It becomes necessary to arrange the long-term change efficiently in the study of urban transition. Therefore the authors decided to use the topographical map for six terms in this study from the middle of Meiji period when the modernization began. The authors make the spatial data which the street and the wetlands from this topographical map. And they constructed the urban transition database by using both these data and the database which was already built the river and the railway in our laboratory. As a result of expressed urban transition, the authors grasped that Yodo River which was the most catchment area in the present was formed with repairing Nakatsu River in the late Meiji period. And, the Dohjima canal was dug in Umeda from the early Meiji until before the war, the authors thought that this area was different urban space from present day. Paying attention to the street, the right bank area of the old Yodo River focusing Umeda has been becoming earlier urbanization than the other areas. At the same time, the reconstruction of buildings in the built-up area repeated with modernization, and the authors found the possibility that a changing of the scene was taking place close to the old Yodo River. From these results, the authors direct their attention to Umeda and the old Yodo River basin, and tried to simulate of the cityscape transition using the three-dimensional models in this study.

A terrain model is important for constructing urban model. In this study, the terrain was created 140 kilometers square using digital elevation model (DEM) data based a knowledge of the precedent study. The features are created as landmarks and general houses using CAD/CG. The authors selected Osaka station of Umeda and the mint of the old Yodo River basin for landmarks. These are reconstructed in great detail basing historical materials. As a results of the simulation, the authors could visualized the landscape transition in Umeda and the old Yodo River basin with modernization.

As the result of this study, the authors clarified the historical transition in the part of Osaka by using GIS and CAD/CG. At the same time, they reconstructed the historical environment as property of Osaka. In the near future, they are going to construct the animation of the transition of Osaka for the communication tool by using created spatial data. And it is necessary for three-dimension models to improve the accuracy.

Keywords: modernization, cityscape transition, Umeda, old-Yodo River

## Landscape analysis of daimyo garden using photograph information

ONO, Yoichi<sup>1\*</sup> ; YOSHIKAWA, Shin<sup>2</sup> ; TANKA, Kazunari<sup>2</sup>

<sup>1</sup>FUKKEN CO., LTD., <sup>2</sup>Faculty of Engineering, Osaka Institute of Technology

In recent years, social media in the information technology have been developed remarkably. The scenes at sightseeing are photographed, and the photos are accumulated as the personal spatio-temporal information in a non-structured state on the Internet. In this study, the authors analyze the landscape phenomenon by using personal photographs, the photos are accumulated on the Internet in daimyo gardens.

Specifically, they take photograph images and spatio-temporal information on site and they pay their attention to the both sides of the space and time, and analyze the data on using GIS. At first, they choose the case study area from daimyo gardens where many tourists visit at present. Then, they pay their attention to the flickr is a photograph community site, and they make a photograph information database and grasp the scene phenomenon by using it.

Among other things, the three famous gardens in Japan are Kairakuen, Kenrokuen, and Korakuen. And Riturin-park is a beautiful garden as well as the three famous gardens. In addition, there are sightseeing spots that many people visit at present. Then, they collected spatio-temporal information and photograph images taken by the visitors in the four gardens by using the flickr API. As a result, Kenrokuen was selected as the case study garden for analysis.

At first, they utilize the Exif information contained in the photographic image data. This metadata is the information of the camera itself, and various information including the F-number and the focus distance are recorded with the positioning data. The Exif information is the index recorded at the time of the photography. In this study, the authors grasp visual characteristics of Kenrokuen by using the focus distance and a photography direction.

Based on the positional information, they plotted the focus distance on GIS with conversion into the 35mm film camera. As a result, they were able to grasp the characteristic in the garden. First of all, around the Ume grove, an angle of view range is narrow and people look the fixed scenes. People watched the buds and the flowers of the plum closely. The second is around the Kotoji-torou area. This area is an angle of view range is wide, and photography is carried out of showed, using the plural focus distances.

Then, the analysis was focused on the photographic images, The photography position is not usually fixed and shows a variety of distribution for one object. Therefore, the authors grasp each viewpoint field by a directional distribution analysis. In this analysis, the point cloud are photography positions, so the standard deviation ellipse created by the analysis is regard as the photography viewpoint field.

First of all, they classify the photographs and create the photography viewpoint fields. As a result, it was revealed that the place, where plural viewpoints fields were overlapped, while people went round the gardens. So, in the sequence around the garden, the people do not watch an object in turn, and it is thought that the features were seen under the complicate influence. In addition, as they investigate the relationship between the subject and the viewpoint field individually, they found several characteristics from the positional relationship between the object and the shape of the standard deviation ellipse. So, they classified photography viewpoint field based on the analysis and grasped viewpoint field with four different characteristics. They grasp on landscape phenomenon in viewpoint field at minute time, and they were similar to expression of the camera work.

In this study, the authors grasped visual characteristics of the case study area by using the Exif information. In addition, they grasp each viewpoint field for every photography object, and was able to model the viewpoint field.

Keywords: daimyo garden, landscape, photograph information

## Spatial pattern of agriculture using GIS and small area statistics

MORIMOTO, Takehiro<sup>1\*</sup>

<sup>1</sup>University of Tsukuba

The author used small area statistics of agriculture and composed grid square statistics to make spatial pattern of agriculture in the Kanto District of Japan using GIS. The grid square statistics is suitable for analyses in combination with other ready-made social and environmental grid-square statistics.

## GIS analysis of Australian urban social geography by using Census Table Builder Data designated by ABS

TSUTSUMI, Jun<sup>1\*</sup>

<sup>1</sup>Graduate School of Life and Environmental Sciences, University of Tsukuba

A body of literature about multi-cultural aspects in Australia can be found in the fields of international politics, international relations and Australian history as well as Australian geography. Diverse origins of immigrants had a great impact on the changing structure of metropolitan areas in Australia. Based on some previous studies, non-English speaking immigrants, e.g. Greek and Italian in the 1960s, tended to live in the suburbs located 10-15 km apart from the Melbourne metropolitan core. These suburban areas were relatively “ less convenient area ” in terms of public transportation, but newly developed area supported strongly by motorization. New university, huge industrial parks, distribution centres and relocated suburban offices have been established in these newly developed areas. Immigrants in 1960s could only find affordable houses in these “ new suburbs, ” resulted in the expansion of the metropolitan area.

After 1990s and later, Australian cities are strongly affected by a “ surge ” of immigrants from Asian countries. They tended to live in the existed Asian communities located at the peripheries of the metropolitan area, much farther than “ new suburbs. ” Footscray in the west, Glen Waverley in the east and Springvale in the southeastern suburbs are typical examples of those communities.

In this paper, I focused on the changing structure of Sydney and Melbourne metropolitan areas in terms of diverse origins of immigrants. A GIS-based mapping with “ table-builder data ” distributed by Australian Bureau of Statistics was used to identify the process. This paper not only provides a methodological innovation but also a new and practical contribution to urban-social process studies.

Keywords: GIS, Australia, Urban area, Sydney, Melbourne, metropolitan area

## Land use change in the Loess Plateau of North-Shaanxi and East-Gansu Province, China

HARA, Yuta<sup>1\*</sup>

<sup>1</sup>GSGES, Kyoto Univ.

The Loess Plateau in China has some problems about erosion, desertification and economical problems. Erosion has a major influence on agriculture, forestry and grazing, because it cut the cropland and ruin the ecosystem (Matsunaga 2013, Saito 2008a).

From the end of 1990s, the Conversion of cropland to forest and grassland, namely the afforestation project to steep slope, started by the Chinese government for deal with these problems. However, these are not only the fruits (Saito 2008b). The reason, the Loess Plateau has diversity about the environment and humanity due to extensive.

From 2000, there are many investigations about the Land use change in the Loess Plateau. They made the quantitative spread about the green land clear caused by the Conversion of cropland to forest and grassland in China. However the quantitative land use change in the wide area of the Loess Plateau is unknown, because the study areas of the investigations are each basin of the Yellow River. Their compared years are deferent. The compared years are 2 after 1980s.

This study cleared the land use change by remote sensing in North-Shaanxi and East-Gansu Province of the Loess Plateau. In addition, I made the division map based on the change of forest and grassland. Used satellite photos are Landsat/MSS, TM. I did supervised classification by Maximum likelihood estimation. Moreover I did logical disjunction operation using the ArcGIS.

The following results were obtained : 1. There are conflicting differences to changes of the forest in Huanglong Mountains and Ziwu Mountains. 2. There are differences about more than one degree of desertification in the adjacent area of Mu Us desert. 3. Since 1990s, there are conflicting differences to changes about desertification in the hilly-gullied loess region as administrative boundary of Gansu and Shaanxi province. Moreover I estimated the first factor due to local differences using the SRTM.

Keywords: the Loess Plateau, land use change, Landsat, ArcGIS

HTT34-P02

Room:Poster

Time:April 28 18:15-19:30

## Miniature LiDAR DEM data smoothing techniques and effects

KAMIHARA, Noriya<sup>1\*</sup> ; SATOU, Takeharu<sup>2</sup>

<sup>1</sup>Eight-Japan Engineering Consaltants Inc., <sup>2</sup>Okayama University of Science, Faculty of Biosphere-Geosphere Science

Miniature LiDAR DEM data smoothing techniques and effects

Keywords: LiDAR DEM, Mass Mouvement, Laplacian, Convex

## Review of development of AMS in the past 30 years and future perspective

NAKAMURA, Toshio<sup>1\*</sup>

<sup>1</sup>Center for Chronological Research, Nagoya University

One of the main aims of Quaternary research is to understand global environmental changes of the past and to predict the expected changes in the near future. To pursue this aim, high-resolution age estimation is particularly important. Dating methods so far used for Quaternary research can be classified into five categories: (1) age estimation based on the decay procedure of cosmogenic radioisotopes such as radiocarbon ( $^{14}\text{C}$ ) and  $^{10}\text{Be}$ , U-series nuclides and a K-Ar pair; (2) age estimation by cumulative dose from natural nuclear radiation and cosmic rays such as TL, OSL, ESR, FT dating methods; (3) age estimation with geological or geochemical evidences of prehistoric events such as paleomagnetic reversals or excursions, oxygen stable-isotope-ratio variations, tephra stratigraphy; (4) age estimation with paleontological records of prehistoric events such as diatom, pollen, nanno-plankton and shellfish assemblages, as well as semi-global fluctuations of tree ring width; (5) age estimation based on archeological evidences. These dating methods are selectively applied dependent on the characters of geological and archeological events to be analyzed. Among the radio-isotopic dating methods,  $^{14}\text{C}$  dating is most frequently used because of its applicability to many different types of Quaternary samples, as well as age range covered by this method (a few hundred to 50,000 yr BP).

Developments of accelerator mass spectrometry (AMS) have triggered a wide area of application in radiocarbon ( $^{14}\text{C}$ ) dating. The AMS system requires only 1mg of carbon in precise determination of  $^{14}\text{C}/^{12}\text{C}$  and  $^{13}\text{C}/^{12}\text{C}$  isotope ratios, and this advantage has broadened the applicability of  $^{14}\text{C}$  measurements. Nowadays, AMS contributes to almost all kinds of research that utilize  $^{14}\text{C}$  dating in archeology, cultural property science, geology, and those that employ  $^{14}\text{C}$  tracer in environmental sciences, medical sciences and even forensic studies.

For example, a Tandem AMS system dedicated to  $^{14}\text{C}$  measurement was installed at Nagoya University, and its routine operation for  $^{14}\text{C}$  measurement was started in 1983 for the first time in Japan. In 1996, another AMS system (HVE-Model-4130-AMS) was purchased and has been used for high precision  $^{14}\text{C}$  measurements. By 30 minutes measurement of carbon isotopes repeated for consecutive three days for a sample, one-sigma uncertainty of  $\pm 17$  to  $\pm 30$  years is achieved. A reproducibility test for 2000-year-old archeological samples yielded a fluctuation error as small as  $\pm 11$  years. We also have evaluated accuracy in our  $^{14}\text{C}$  measurements by participating in international  $^{14}\text{C}$  inter-comparison tests, and confirmed that our  $^{14}\text{C}$  results were quite consistent with the consensus values by all the participants. After the critical tests, we are sure that our AMS system can be applicable to historical samples that require high precision as well as high accuracy  $^{14}\text{C}$  measurements.

Quite frequent applications of  $^{14}\text{C}$  dating with AMS to the Quaternary samples in the last bidecade are promoted by the following reasons: (1) a very small amount of carbon (about 1mg of carbon for the final target preparation) is required; (2) uncertainties of  $^{14}\text{C}$  ages are from  $\pm 17$  to  $\pm 30$  yr, mainly owing to the  $^{14}\text{C}$  counting statistics; (3) calibration of  $^{14}\text{C}$  age to the calendar age scale become quite popular, for  $^{14}\text{C}$  ages up to 50,000 cal BP; (4) marine reservoir effect on  $^{14}\text{C}$  age has been recognized and investigated recently, and a realistic correction for the effect is becoming possible partly.

Along with  $^{14}\text{C}$ , other cosmogenic radioisotopes such as  $^{10}\text{Be}$ ,  $^{26}\text{Al}$ ,  $^{36}\text{Cl}$ ,  $^{129}\text{I}$  are also measured with AMS systems. We briefly describe history of development of domestic AMS groups as well as worldwide AMS groups, along with the research fields of AMS applications and future perspective.

Keywords: accelerator mass spectrometry, cosmogenic nuclides, radionuclide, age measurement, ion nuclide separation, ion particle counting

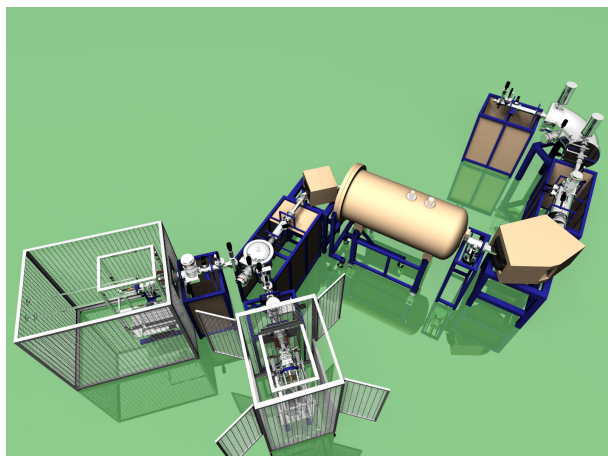
## Present status of YU-AMS

TOKANAI, Fuyuki<sup>1\*</sup>

<sup>1</sup>Center for YU-AMS

Yamagata University (YU) installed an AMS (YU-AMS) system in the Kaminoyama Research Institute to meet the requirement of <sup>14</sup>C AMS for microdosing and medical studies as well as that of radiocarbon dating in the same facility. An automated graphitization line was also installed in the same research institute for sample preparation. This AMS system is the first AMS system installed in a university in north Japan (Tohoku-Hokkaido region). The facility also provides radiocarbon dating for samples from other universities, institutes and public organizations. Currently, we are planning to install a second new ion source and an automated graphitization line until March in 2014. In this paper, we describe the status of the YU-AMS system.

Keywords: AMS, microdose



## Development of isobar suppression system using Laser in Accelerator mass spectrometry

MIYAKE, Yasuto<sup>1\*</sup>; MATSUZAKI, Hiroyuki<sup>1</sup>; HASEGAWA, Shuichi<sup>2</sup>

<sup>1</sup>Department of Nuclear Engineering and Management, School of Engineering, The University of Tokyo, <sup>2</sup>Nuclear Professional School, The University of Tokyo

For Accelerator mass spectrometry (AMS), isobar separation is quite important to improve measurement accuracy and the background. In order to suppress isobar interference, gas-filled magnet or gas counter have been conventionally used [1,2]. Nuclides of interest are separated from isobars by interaction between ions and materials in these devices.

In the 1980s, Berkovits et al. tried to remove stable isobars before acceleration with laser light[3]. In this method, the difference of the electron affinity (EA) was utilized for isobar suppression. If the EA of the nuclide of interest is higher than the EA of the isobar nuclide, only negative isobar can be selectively neutralized by photodetachment with photons of energy, which is higher than the EA of isobar nuclide but lower than the EA of the nuclide of interest. Consequently, only nuclide of interest can be injected into the accelerator and isobar suppression can be effectively achieved. However, due to the limited laser performance, the laser-ion interaction time was too short to suppress isobar sufficiently at that time. Therefore, this technique has not been in practical use yet.

Recently, as laser improved in quality and the way to increase the laser-ion interaction time effectively was proposed, development of isobar suppression system is going on. For example, Liu et al. developed the RFQ ion cooler to slow ions [4]. This apparatus is filled with a buff gas and ions collide with gas molecules, which results in the deceleration of ions and the long interaction time. This photodetachment system can remove isobar interference in AMS measurements for nuclides, such as Cl-36 (EA=3.62eV) with S-36 (EA=2.08eV), Ni-59 (EA=1.156eV) with Co-59 (EA=0.661eV) [4]. Furthermore, even if the EA of the nuclide of interest is lower than the EA of the isobar nuclide, photodetachment could be useful by converting the nuclides into the molecular ions and reversing these electron affinities.

In order to make laser interact with ion beams effectively, the ion beam optics including the devices like the ion cooler should be optimized. This device will be installed after the electrostatic deflector or after the injection magnet in the beam line. In this study, as a preliminary step, optimization of the ion beam optics including some components to decelerate ion will be discussed.

[1] H. Matsuzaki, Journal of the Vacuum Society of Japan, Volume 50, Issue 7, 467-474 (2008).

[2] T. Aze, H. Matsuzaki, H. Matsumura, H. Nagai, M. Fujimura, M. Noguchi, Y. Hongo. and Y. Yokoyama, Nucl. Instr. Meth. **B259**, 144-148 (2007).

[3] D. Berkovits, E.Boaretto, G. Hollos, W. Kutschera, R. Naaman, M. Paul, and Z. Vager, Nucl. Instr. Meth. **A281**, 663 (1989).

[4] Y. Liu, P. Andersson, J.R. Beene, O.Forstner, A. Galindo-Uribarri et al., Rev. Sci. Instr. **83**, 02A711 (2012).

Keywords: AMS, isobar, laser, photodetachment

## Development of C14-free laboratory animals.

KOBAYASHI, Koichi<sup>1\*</sup> ; AMS, Dating group<sup>1</sup>

<sup>1</sup>Paleo Labo Co.,Ltd.

In the early stage of pharmaceutical researches, <sup>14</sup>C labeled chemicals with very high radioactivity are administrated to laboratory animals to study pharmacokinetics. However, when <sup>14</sup>C/<sup>12</sup>C of the laboratory animals could be reduced, the radioactivity level of the chemicals is expected to be reduced lower. Also when <sup>14</sup>C-free (DC ; denoted as dead carbon) laboratory animals were developed, the radioactivity level for the study is expected to be reduced down by five orders of magnitude or lower by using AMS technique. That means that we need not the <sup>14</sup>C labeled chemicals but natural level chemicals for the study of pharmacokinetics. In this case, it is also expected that we can be free from the hazardous high radioactivity and from the strictly regulated troublesome laboratory to handle the high level radioactive materials.

In Dec. 2010, we started the project to produce <sup>14</sup>C-free lives as feed for the <sup>14</sup>C-free laboratory animals. This is a preliminary report on the project, and parts of the investigation were already reported at 13th Japanese Symposium on AMS (Kobayashi et al., 2011). Here will be also introduced some recent studies.

When lives were cultivated in DC surroundings they grow up inevitably to be DC lives. For example, photosynthetic lives like vegetables or some kinds of microbes with chloroplast like euglena (midorimushi ; in Japanese) can easily be DC lives when they were cultivated in DC surroundings.

For the first step, we cultivated some plants and euglena using <sup>14</sup>C free water set in a glove box that was filled with artificial air (N<sub>2</sub>, O<sub>2</sub> and dead carbon CO<sub>2</sub> with proper concentration) irradiating with some artificial lights. <sup>14</sup>C concentrations in the plants and the microbes were measured by AMS. Since the modern carbon (natural carbon) CO<sub>2</sub> could not be perfectly removed from the air and the water and air tightness of the glove box system was also not perfect, the percentages of dead carbon to modern carbon (DC ratio) in the samples could not be higher than about 80 %.(Kobayashi et al., 2011a ; Kobayashi et al., 2011b)

While investigating the cause of the imperfect DC ratio, we got 96% DC Euglena by using a little different way. That is to use a small glass bowl with an airtight lid, in which were set CO<sub>2</sub> tablets, a small amount of chemical fertilizer and Euglena. From outside of the bowl, fluorescent lamps irradiated adequate amount of light to them. One or two months later, the euglena was carefully collected on glass filters in a glove box filled with DC air. <sup>14</sup>C/<sup>12</sup>C of the euglena was measured by AMS and the <sup>14</sup>C concentration was 3.71±0.02 pMC (percent Modern Carbon) which leads to DC ratio as 96% (Kobayashi et.al., 2012).

In order to make sure that mice really eat the euglena tablets, we fed the mice with euglena tablets which were mixed with chlorella powder by 20%. The tablet is on the market for people as a health food. After three months feeding on three mice, there were no large differences compared to the other three mice which were fed by ordinary food for comparison. The experiment concluded that mice will grow up healthy by eating the euglena tablet.

Those two above data show the possibility to realize the DC animals.

Recently, we have started to extend the project to realize for business, supported by a grant.

### References:

Kobayashi, K. et al. (2011a), Production of <sup>14</sup>C-free plants and animals (in Japanese) ; Kobayashi, K. et al. (2011b), Production of <sup>14</sup>C-free plants and animals ; Kobayashi, K. et al. (2012), Production of dead carbon lives (in Japanese)

Keywords: Pharmacokinetics by AMS, C14-free lives, Euglena

## <sup>14</sup>C measurement of the Southern Japanese tree by the AMS method for high-precision radiocarbon calibration

HAKOZAKI, Masataka<sup>1\*</sup> ; NAKAMURA, Toshio<sup>1</sup>

<sup>1</sup>Center for Chronological Research, Nagoya University

Radiocarbon (<sup>14</sup>C) dating method has contributed to the age determination of samples of the past 50,000 years in geology and archaeology. However, since <sup>14</sup>C date is not in agreement with the calendar year, the calibration using a dataset which consists of <sup>14</sup>C data of calendar year known samples is required for it. Moreover, since there is regional difference of <sup>14</sup>C concentration in the atmosphere (regional <sup>14</sup>C offset; Hogg et al. 2002), in order to be high-precision calibration, the dataset for each area needs to be established.

The Center for Chronological Research (CCR), Nagoya University has measured <sup>14</sup>C data of tree-rings of a Yaku cedar from the Southern Japan, in order to establish a calibration dataset for Japan. Previous measurement has shown that the cedar shows <sup>14</sup>C date older than global standard calibration dataset IntCal13 (Reimer et al. 2013) in various times for the past 2000 years (Nakamura et al. 2013). This report shows the measurement result of the tree-rings formed in the 5th century.

Sample is a Japanese cedar from Yaku Island, Kagoshima prefecture (sample code: Yaku\_A). Dendrochronological analysis with a master-chronology (Kimura unpublished) has carried out, and the calendar year of this sample is known. After exfoliating the annual rings of AD434-502 of a sample in one year respectively, only even-numbered years was measured (n = 35). The tandemron AMS II of CCR was used for this measurement. Measuring only even-numbered years in order to understand a whole tendency previously, it also measures the samples of odd-numbered years in the future.

Thirty five <sup>14</sup>C dates of tree-ring samples showed that it will be older than IntCal13 for an average of  $28 \pm 22$  years, a maximum of  $76 \pm 21$  years (in AD488). These <sup>14</sup>C dates were mostly located in the middle of IntCal13 and SHCal13 (the calibration dataset for the Southern Hemisphere; Hogg et al. 2013).

Since Yaku Island touch the northernmost end of the Intertropical Convergence Zone in a summer, it is thought that the Southern Hemisphere atmosphere with regularly low <sup>14</sup>C concentration is easy to be supplied (Nakamura et al. 2012). This measurement result might suggest that <sup>14</sup>C concentration in the atmosphere of the Japanese neighborhood fell in the 5th century, and the atmospheric supply from the Southern Hemisphere may have become strong. Sakamoto et al. (2013) measured the tree-ring samples in the 5th to 6th century of the Japanese cedar from Nagano Prefecture Central Japan, and they has reported that the data is older than a IntCal13. Our result harmonizes with the measurement result of the trees from Nagano, and this time can consider a possibility that the influence of the Southern Hemisphere atmosphere had reached to central Japan. From now on, the tree-rings of Yaku cedar in formed the 6th century will measure, and it will compare with the result of Sakamoto et al. (2013).

Keywords: radiocarbon calibration, regional <sup>14</sup>C offset, Southern Japan, tree-ring, Yaku cedar

## C-14 dating and geochemical analyses of the tsunami sediments in continuous soil deposits from Tohoku area, Japan

WATANABE, Takahiro<sup>1\*</sup> ; HOSODA, Norihiro<sup>1</sup> ; TSUCHIYA, Noriyoshi<sup>1</sup> ; NAKAMURA, Toshio<sup>2</sup> ; YAMASAKI, Shin-ichi<sup>1</sup> ; NARA, Fumiko<sup>1</sup>

<sup>1</sup>Graduate School of Environmental Studies, Tohoku University, <sup>2</sup>Center for Chronological Research, Nagoya University

Past tsunami sediments preserved in continuous soil and lake sediments are crucial and unique clues to reconstruct the past tsunami invasion area. Generally, the tsunami sediments originated from sea floor, sandy beach and/or coastal land soils containing gravels, sands, muds, shells and microfossils. In particular, muddy tsunami sediments should be found to detect the limit of tsunami invasion areas, because relative small particles move to more inland area with tsunami in comparison with sand deposits. Additionally, dating of tsunami sediments is indispensable to refer for historical disaster events. Therefore, we have to make age models of continuous soil deposits with tsunami sediments and new techniques for detection of invisible muddy tsunami sediment in strata. In this study, we performed the nine radiocarbon measurements of plant residues in continuous soil deposits as well as geochemical characteristics of tsunami sediments. 2m-continuous soil deposits were taken by the handy geoslicer (Fukkenn co. ltd.) from the Pacific coast of Tohoku area in northeast Japan. The samples were composed of cultivated surface soils, peaty clay, silt and sub-rounded medium sands. The sandy deposits were found between the peaty clay layers. To show the sedimentary ages of sandy deposits, plant residues were taken from the sandy and peaty clay layers in the continuous soil sediments. The plant residues were washed with ultra pure water using ultra sonic cleaner to remove soil particles containing relative old carbon. Then, the samples were treated sequentially with 1.2M-HCl, 1.2M-NaOH and 1.2M-HCl at 60 degrees of Celsius for 3 hours. After neutralization and freeze-drying, the samples were combusted in evacuated quartz tubes. Then, the purified carbon dioxide was reduced to graphite using Hydrogen gas with iron catalysts. Radiocarbon measurements were performed by the Tandem AMS system (Model-4130, HVEE) in Center for Chronological Research, Nagoya University. Total organic carbon contents of the plant residues were from 45.9 to 54.5 wt.% (50.4 wt.% in average) and stable carbon isotope ratios of the plant residues ranged between -26.7 and -30.1 permil (vs. PDB), which consist with those of modern terrestrial C3 plants. As a result of this study, part of the calibrated ages of plant residues taken from just above the sandy tsunami sediments was about 1000-1300 cal BP, and these ages were agreed well with those of the Jogan earthquake and tsunami in the Sendai plain.

Keywords: Radiocarbon dating, Tsunami deposits, Jogan tsunami, Geochemistry, EDXRF

## AMS radiocarbon dating of tephra layers on Adak Island, central Aleutian

OKUNO, Mitsuru<sup>1\*</sup> ; NAKAMURA, Toshio<sup>2</sup>

<sup>1</sup>Fac. Sci., Fukuoka Univ., <sup>2</sup>CCR, Nagoya Univ.

The Holocene tephra layers distribute on Adak Island located in the central part of the Aleutian Islands. Radiocarbon (<sup>14</sup>C) age determination of charcoal fragments in the soil layer has been performed. Moreover, tephra is intercalated with sand layer of dune. Since sand dune has high depositional rate and low contamination of organic matter, a possibility of polluted charcoal sample from below and above tephra is low. Thus reliable age was able to be obtained by the AMS method to these small samples. We report those results.

Keywords: Adak Island, Holocene, tephra, radiocarbon date

## Radiocarbon dating of stalagmites from the Ryugashi Cave, Shizuoka

KATO, Tomomi<sup>1</sup> ; MINAMI, Masayo<sup>2\*</sup> ; HORIKAWA, Keiji<sup>3</sup> ; NAKAMURA, Toshio<sup>2</sup>

<sup>1</sup>Graduate School of Environmental Studies, Nagoya University, <sup>2</sup>Center for Chronological Research, Nagoya University, <sup>3</sup>Graduate School of Science and Engineering for Research, University of Toyama

Stalagmites are cave deposits precipitated from drip water. Drip water consists of carbon derived from soil CO<sub>2</sub>, which has atmospheric <sup>14</sup>C values in isotopic equilibrium with atmosphere, and carbonate-dissolved CO<sub>2</sub>, which has <sup>14</sup>C-free (dead) carbon through interaction with cave host bedrock. As a result, drip water contains a percentage of dead carbon, which will make the <sup>14</sup>C ages of the stalagmite older. Therefore, a correction of the dead carbon fraction is needed for <sup>14</sup>C dating of stalagmites. In recent years, young stalagmites of 10-20 ka have been <sup>14</sup>C dated by comparing the <sup>14</sup>C on samples of known calendar age with the tree ring record of atmospheric <sup>14</sup>C during a period of overlap (Hoffmann *et al.*, 2010; Southon *et al.*, 2012). This procedure involves the implicit assumption that dead carbon fraction in stalagmite remained constant through its growth time. In this study, therefore, we examined dead carbon fraction in two stalagmites from the Ryugashi Cave in Hamamatsu, Shizuoka by investigating seasonal variation in <sup>14</sup>C concentrations of drip water coupled with soil CO<sub>2</sub>, atmospheric CO<sub>2</sub>, and host limestone, in order to reveal possibility of accurate and precise <sup>14</sup>C dating on stalagmite in Japan.

The drip water samples showed <sup>14</sup>C of 1130 BP to 980 BP and  $\delta^{13}\text{C}$  of -10.1 ‰ to -9.1 ‰, which are lower in fall and winter, and higher in spring and summer, and have the annual means of <sup>14</sup>C of 1025±140 BP and  $\delta^{13}\text{C}$  of -9.4±0.4 ‰. The RYGS12 stalagmite of 7 cm in length showed 945±30 BP at its top and 2150±40 BP at its bottom, and had a growth rate of about 60  $\mu\text{m}/\text{yr}$ . The calibrated age of RYGS12 was estimated by comparing the <sup>14</sup>C with the IntCal13 calibration curve, resulting that the stalagmite had a constant dead carbon fraction through its growth time and gives <sup>14</sup>C ages of 1050 years older than the true age. The carbon isotopic fractionation between drip water and stalagmite was negligible. The results indicate that high-resolution <sup>14</sup>C measurement can be performed on stalagmites in the Ryugashi Cave.

The RYGS12 sample showed rapid decrease of  $\delta^{13}\text{C}$  from -8.3 ‰ to -11.8 ‰ at around AD1450. The decrease suggests an increase of soil input to the stalagmite, since soil CO<sub>2</sub> has low  $\delta^{13}\text{C}$  of -22.0 ‰. It is reported that there was a great earthquake of magnitude 8.6 (Meio earthquake) accompanied by a catastrophic tsunami in this study area in AD1498. Therefore, the  $\delta^{13}\text{C}$  decrease might be caused by the Meio earthquake. In the presentation, we will present <sup>14</sup>C result on another stalagmite sample RYG08 of 30 cm in length.

Keywords: stalagmite, radiocarbon age, carbon isotope ratio, oxygen isotope ratio

## 14C-based source apportionment of carbonaceous component in PM2.5 in Nagoya city

IKEMORI, Fumikazu<sup>1\*</sup>; YAMAGAMI, Makiko<sup>2</sup>; HONJYO, Koji<sup>3</sup>; NAKAMURA, Toshio<sup>4</sup>

<sup>1</sup>Graduate School of Environmental Studies, Nagoya University, Nagoya City Institute for Environmental, <sup>2</sup>Nagoya University, Nagoya City Institute for Environmental, <sup>3</sup>Graduate School of Environmental Studies, Nagoya University, <sup>4</sup>Center for Chronological Research, Nagoya University

The measurement of radiocarbon (<sup>14</sup>C) has been used to estimate the relative contributions of fossil and contemporary carbon sources in particulate matter throughout the world. In this study, we use <sup>14</sup>C to provide quantitative estimates of carbon origin sources in Nagoya in April 2003 to March 2004. pMC and OC/EC showed similar seasonal variations and high values (range 39.8 to 68.4, 1.0 to 2.0; average 53.4, 1.5, respectively) in May and early June, whereas the values of pMC stayed relatively low values (range 28.3 to 41.9, 0.7 to 1.2; average 34.2, 1.0, respectively) after middle June. To estimate the source region of high pMC values, backward air mass trajectories were calculated during the sampling period in April to June. The air mass appeared to have passed through eastern Siberia when the pMC values showed high values in May and early June which also showed high values of OC/EC ratio and OC concentrations. In 2003, many researchers reported the influence of large forest burning in Siberia. This large forest burning occurred in spring to summer. The smoke from this forest burning had reached to Korea, Japan, and North America. The influences from the Siberian forest fires had an important implication for air quality over East Asian region. We conclude that high pMC values measured in spring are originated from large forest fires in Siberia and transported long distance.

Keywords: atmospheric aerosol, PM2.5, radiocarbon

## Decadal change in bomb-produced radiocarbon in the Pacific Ocean revealed by WHP repeat hydrography

KUMAMOTO, Yuichiro<sup>1\*</sup> ; MURATA, Akihiko<sup>1</sup> ; KAWANO, Takeshi<sup>1</sup>

<sup>1</sup>Japan Agency for Marine-Earth Science Technology

Radiocarbon produced by nuclear weapon tests is one of ideal tracers for the air-sea gas exchange and ocean circulation. In the 2000s, radiocarbon in dissolved inorganic carbon was measured during revisit cruises along the WOCE (World Ocean Circulation Experiment) lines of P01 (47N approx., 2007), P03 (24N approx. 2005), P06 (32S approx., 2003), P10 (149E approx., 2005), P13N (165E approx., 2011), P14N/C (179E approx., 2007), P17N (135W approx., 2001), and P21 (17S approx., 2009) conducted in the 1990s in the Pacific Ocean. Comparison of radiocarbon data from the 1990s and 2000s revealed decadal changes of radiocarbon concentration in the thermocline, most of which were due to temporal changes in the bomb-produced radiocarbon. Vertical profiles and vertical-integrated inventories of the bomb radiocarbon in the subarctic and equatorial regions have not changed significantly. In the subtropical regions, radiocarbon decreased in upper thermocline from surface to about 500-m depth. In contrast, radiocarbon increased in lower thermocline from about 500-m to 1500-m depths. In the southern and northeastern subtropical regions, the two opposing directions in radiocarbon change resulted in small temporal changes of the total inventory of the bomb radiocarbon. On the other hand, the water column inventory significantly decreased in the northwestern subtropical region because the radiocarbon decrease in the upper thermocline was larger than the radiocarbon increase in the lower one. These decadal changes are primarily due to the meridional transport of the bomb radiocarbon from high latitude into temperate zone. The decrease in the vertical-integrated radiocarbon in the northwestern subtropical region implies that the turnover time of the thermocline circulation in the region is faster than those in the other subtropical regions in the Pacific Ocean. In addition the loss of the bomb-radiocarbon in the North Pacific Ocean could be explained by its transformation to the Indian Ocean via Indonesian Through Flow. This work was partially supported by Japan Society for the Promotion of Science (JSPS) KAKENHI Grant Number 18310017 and the Common-Use Facility Program of JAEA (2007A-F03, 2007B-F05, 2008A-F02, 2009A-F05, 2010A-F06, and 2011A-F04).

Keywords: bomb-produced radiocarbon, Pacific Ocean, ocean circulation

## Study on property of soil organic matter decomposition by global warming using radiocarbon

ARAMAKI, Takafumi<sup>1\*</sup> ; LIANG, Naishen<sup>1</sup> ; TERAMOTO, Munemasa<sup>1</sup> ; TOMITA, Ayako<sup>1</sup>

<sup>1</sup>National Institute for Environmental Studies

Current research indicates that future atmospheric CO<sub>2</sub> concentration may be increased more than predicted value by furthering of soil organic matter decomposition due to global warming. The information on soil organic matter decomposition property in long-term warmer environment has not yet been obtained. We have carried out artificial soil warming experiment in six forest sites having different vegetation in Japan for long time. We planned vertical <sup>14</sup>C measurement of soil core at an even-green Japanese oak forest in Setonaikai region (Higashi-Hiroshima). A soil core was collected from both the soil warming and the control plot in December 2011, and was cut into 1cm layers in laboratory. Each sample was hydrolyzed with 1N HCl overnight to remove inorganic carbon in the sample, and then was analyzed particulate organic carbon (POC) and organic nitrogen (PON) by an elemental analyzer. For <sup>14</sup>C analysis by an accelerator mass spectrometer (AMS), soil samples adjusted to a weight of approximately 3mg-C were first converted to CO<sub>2</sub> gases by combustion with CuO and Ag foil at 900 °C, and then purified cryogenically in a vacuum line. The CO<sub>2</sub> gas samples were reduced to graphite with H<sub>2</sub> gas over Fe powder. The <sup>14</sup>C/<sup>12</sup>C ratios of the sample graphite were measured at the Tandem AMS Facility in the Mutsu Office of the Japan Atomic Energy Agency. The <sup>14</sup>C results are expressed as Δ<sup>14</sup>C. The typical analytical error of the Δ<sup>14</sup>C values was about ± 4 ‰ based on the 1σ value of the counting statistics.

Both of POC and PON weight percent in the soil were high above 3cm depth and decreased sharply with depth from 5cm to 15cm. Both of POC and PON of the soil warming plot were 20-30% lower than those of the control plot irrespective of depth above 15cm depth. The result indicates that the soil warming experiment was encouraged the microbial decomposition of soil organic matter up to comparatively deep layer. The Δ<sup>14</sup>C profile of the warming plot was unique with a maximum (220 ‰) at 5cm depth, although the Δ<sup>14</sup>C of the control plot was approximately constant from surface to 10cm depth. In terms of Δ<sup>14</sup>C vertical profile above 10cm depth, although the Δ<sup>14</sup>C of the warming plot above the 3cm depth having POC >15 wt% were lower than those of the control plot, the Δ<sup>14</sup>C of the warming plot below the 3cm depth were obviously higher than those of the control plot. The results indicate that microbes selectively decomposed young POC at surface layer and old POC at intermediate layer by the soil warming experiment.

Keywords: soil carbon, radiocarbon, global warming, organic matter decomposition, forest soil

## Cosmogenic $^{36}\text{Cl}/^{10}\text{Be}$ ratio in the Antarctic ice core during the last deglaciation and early Holocene

SASA, Kimikazu<sup>1\*</sup> ; KUROSUMI, Kazuna<sup>1</sup> ; SUEKI, Keisuke<sup>1</sup> ; TAKAHASHI, Tsutomu<sup>1</sup> ; MATSUSHI, Yuki<sup>2</sup> ; TOSAKI, Yuki<sup>3</sup> ; HORIUUCHI, Kazuho<sup>4</sup> ; UCHIDA, Tomoko<sup>5</sup> ; MATSUZAKI, Hiroyuki<sup>6</sup> ; MOTOYAMA, Hideaki<sup>7</sup>

<sup>1</sup>University of Tsukuba, <sup>2</sup>Kyoto University, <sup>3</sup>National Institute of Advanced Industrial Science and Technology, <sup>4</sup>Hirosaki University, <sup>5</sup>Tohoku University, <sup>6</sup>The University of Tokyo, <sup>7</sup>National Institute of Polar Research

$^{36}\text{Cl}$  is cosmogenic nuclide (half-life:301 kyr) produced mainly by a reaction of  $^{40}\text{Ar}(p, n\alpha)^{36}\text{Cl}$  in the upper atmosphere. Cosmogenic nuclides fall on the Earth's surface at a rate depending on the nuclide production rates and hence reflecting the cosmic ray intensity. Therefore we can reconstruct fluctuations of cosmic ray intensity, by determining the past  $^{36}\text{Cl}$  depositional flux. Such fluctuations of cosmic ray intensity may indicate paleo solar activity and/or variations in the Earth's geomagnetic field.

In this presentation, we report the results of cosmogenic  $^{36}\text{Cl}$  measurements during 10.55 - 18.42 kyr b2k in the ice core drilled at the Dome Fuji station, Antarctica (Motoyama et al., 2007).  $^{36}\text{Cl}$  in the ice was measured with the accelerator mass spectrometry (AMS) system at the University of Tsukuba (Sasa et al., 2010). The results show that  $^{36}\text{Cl}$  conc. is  $0.21 - 1.80 \times 10^4$  atoms  $\text{g}^{-1}$  and  $^{36}\text{Cl}$  flux is  $0.54 - 3.25 \times 10^4$  atoms  $\text{cm}^{-2} \text{yr}^{-1}$ . The variation of  $^{36}\text{Cl}$  flux in early Holocene shows similar fluctuations of  $^{10}\text{Be}$  flux in the same ice core.  $^{36}\text{Cl}/^{10}\text{Be}$  is constant at  $0.10 \pm 0.01$  in early Holocene. This means that this value can be used for radioactive age dating of the old ice core.  $^{36}\text{Cl}/^{10}\text{Be}$  varies in the last deglaciation. It suggests that the decrease in  $^{36}\text{Cl}/^{10}\text{Be}$  ratio is linked to climate change.

Keywords:  $^{36}\text{Cl}/^{10}\text{Be}$ , Cosmogenic nuclide, Accelerator Mass Spectrometry, Radiometric age determination, Ice core

## Correlation between the concentrations of cosmogenic Be-7, Be-10 in atmosphere and solar activities.

YAMAGATA, Takeyasu<sup>1\*</sup> ; NARAZAKI, Yukinori<sup>2</sup> ; NAGAI, Hisao<sup>1</sup> ; MATSUZAKI, Hiroyuki<sup>3</sup>

<sup>1</sup>Collage of Humanities and Sciences, Nihon University, <sup>2</sup>Fukuoka Institute of Health and Environmental Science, <sup>3</sup>School of Engineering, the University of Tokyo

The concentrations of <sup>7</sup>Be and <sup>10</sup>Be were investigated at Dazaifu, Fukuoka (1998-2002), Hachijo-Island (2002-2005) and Tokyo (2002-2008) during 1998 to 2008. The seasonal variations were same each year; high concentrations and high isotopic ratios of <sup>10</sup>Be/<sup>7</sup>Be that was caused by strong stratosphere-troposphere exchange (STE) were appeared in February to June, and various concentrations but constant <sup>10</sup>Be/<sup>7</sup>Be by vertical convection in troposphere were appeared in July to December. The concentrations were reconstructed by the box model formula. The parameters of the mean residence time and STE intensities, and period, were constant. The amplitudes of production rate were higher than the amplitude of cosmic ray neutron flux observed at Moscow near earth's surface by a factor of 4. Since the neutron flux amplitude at polar region that was little influenced by geomagnetic field was only 10% higher than Moscow, the high amplitudes of production rate were assumed that caused by changing of energy spectrum of galactic cosmic ray.

Keywords: Accelerator mass spectrometry, Cosmogenic nuclide, atmosphere, aerosol

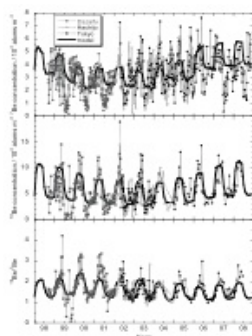


Fig. 1 The decadal variations of <sup>7</sup>Be, <sup>10</sup>Be concentration and <sup>10</sup>Be/<sup>7</sup>Be in the atmosphere in Dazaifu, Hachijo-Island and Tokyo during 1998 to 2008.

## Distributions of radionuclides Cl-36 and I-129 in surface soils before Fukushima accident

SUEKI, Keisuke<sup>1\*</sup>; KITAGAWA, Jun-ichi<sup>2</sup>; SASA, Kimikazu<sup>1</sup>; TAKAHASHI, Tsutomu<sup>1</sup>; MATSUKURA, Masumi<sup>1</sup>; KINOSHITA, Norikazu<sup>3</sup>; TOSAKI, Yuki<sup>4</sup>; MATSUSHI, Yuki<sup>5</sup>; MATSUZAKI, Hiroyuki<sup>6</sup>

<sup>1</sup>University of Tsukuba, <sup>2</sup>High energy accelerator research organization, <sup>3</sup>Shimizu corporation, <sup>4</sup>The National Institute of Advanced Industrial Science and Technology, <sup>5</sup>Kyoto University, <sup>6</sup>The University of Tokyo

The long-lived radionuclides <sup>36</sup>Cl and <sup>129</sup>I are generated by the nuclear tests or interaction with cosmic rays. They have descended to ground or sea level surface, and they have remained ground surface afterward. We have measured amount of <sup>36</sup>Cl and <sup>129</sup>I by accelerator mass spectrometry (AMS) before nuclear accident at the Fukushima No. 1 nuclear power plant.

We have collected surface soil samples from the Sea of Japan to the Pacific Ocean at the equal-latitude cross-sectional areas (37° 20' N - 37° 30' N) in the south Tohoku, Japan. Inorganic chlorine in soil developed an improved leaching process that uses diluted HNO<sub>3</sub> as an extractant, activated carbon to remove organic matters without decomposition, and H<sub>2</sub>O<sub>2</sub> to remove residual organic matters. After leaching from soils, the AgCl samples for AMS-target made from the obtained solutions at ordinary treatment. Isotopic ratios of <sup>36</sup>Cl/Cl were determined by AMS at Tandem Accelerator Complex, University of Tsukuba. Preparation of Iodine-129 target was following ordinary method. Isotopic ratios of <sup>129</sup>I/I were determined by accelerator mass spectrometry (AMS) at MALT, the University of Tokyo. Moreover, we determined <sup>137</sup>Cs concentrations by gamma spectroscopy and LOI (loss on ignition used by an electric furnace) which related to the amount of the organic matter in soil.

We obtained the distributions of radionuclides <sup>36</sup>Cl and <sup>129</sup>I in surface soils. The measured <sup>36</sup>Cl/Cl ratios of 34 surface soil samples which were about 0-10 cm in depth from 6 sites at the equal-latitude cross-sectional areas were between  $0.1 \times 10^{-13}$  and  $4.1 \times 10^{-13}$ . It was shown that the <sup>36</sup>Cl/Cl ratios are lower at both sea sides. The concentrations of <sup>129</sup>I and <sup>129</sup>I/I ratios in surface soil (0-10 cm) at 28 points were determined to be 0.18 - 1.13 mBq/kg and  $4.3 \times 10^{-9}$  -  $11.7 \times 10^{-9}$ , respectively.

The depth profiles of <sup>36</sup>Cl/Cl, <sup>129</sup>I and <sup>137</sup>Cs were examined that the difference of distribution. The concentrations are higher at close surface in each nuclide. The results of <sup>36</sup>Cl/Cl profiles in soil cores up to 1 m long suggested that bomb-produced <sup>36</sup>Cl remains in uppermost sections, typically for ~20 cm deep, in undisturbed soil layers. The observed close correlation between organic matter content and <sup>36</sup>Cl/Cl ratio implies that presence of biological activity contributes the retention of fallout <sup>36</sup>Cl in the surface zone. The concentration of <sup>129</sup>I is shown the highest in uppermost surface. It is thought that the influence of global fallout has been received until now. In both nuclides, a constant amount exists in deeper than 30 cm. The concentrations of <sup>137</sup>Cs are not detection in deeper than 40 cm. It is showed that <sup>137</sup>Cs was lower mobility in soils. Therefore, the sampling soils were not a disturbance.

Keywords: AMS, Cl-36, I-129, soil

## Geoscience studies using by AMS at JAEA-AMS-TONO in the Tono Geoscience Center of the Japan Atomic Energy Agency

KOKUBU, Yoko<sup>1\*</sup> ; MATSUBARA, Akihiro<sup>1</sup> ; HANAKI, Tatsumi<sup>1</sup> ; YASUE, Ken-ichi<sup>2</sup> ; UMEDA, Koji<sup>2</sup>

<sup>1</sup>Tono Geoscience Center, Japan Atomic Energy Agency, <sup>2</sup>Geological Isolation Research and Department Directorate

The JAEA-AMS-TONO facility was established in 1997 at the Tono Geoscience Center, Japan Atomic Energy Agency (JAEA). Our AMS system is a versatile system based on a 5MV tandem Pelletron type accelerator (National Electrostatic Corporation, US) and has been made available for <sup>14</sup>C-, <sup>10</sup>Be- and <sup>26</sup>Al-AMSs. These multi-nuclide AMSs have been mainly applied to neotectonics and hydrogeology, in support of our research on geosphere stability applicable to the long-term isolation of high-level radioactive waste. Furthermore, the <sup>14</sup>C- and <sup>10</sup>Be-AMSs are used for geoscience, environmental science and archaeology by researchers of universities and other institutes under the JAEA's common-use facility program.

Major contribution of radiocarbon (<sup>14</sup>C) dating through our <sup>14</sup>C-AMS to geoscience studies are as follows. Yasue *et al.* identified fault displacement and stratigraphic correlation of black soils based on <sup>14</sup>C ages (presented in this conference). They conducted <sup>14</sup>C dating of the black soil collected from a trench wall of the Atera Fault, Gifu. The results of <sup>14</sup>C date show that the soil age varies from 4,000 to 2,000 y with depth of the sampling points and the soil was deposited at approximately constant rate. Imaizumi *et al.* (2006) estimated the faulting age based on <sup>14</sup>C dating of soils at the Senya Fault in the Toen Fault Zone, Yokote Basin, Akita. It was found that the ages range between 1000 - 1300 y, indicating that the Senya Fault was caused by the Rikuu Earthquake in the year of 1896. Sasaki *et al.* (2006) studied local climate change in an inland basin. Pollen records and <sup>14</sup>C ages of sediments in Ohkute Basin, Gifu were used to reconstruct past climate change. The results suggested that the local climate has been warmer for the last 10000 yBP.

Since the fiscal year of 2013, the <sup>10</sup>Be-AMS has been routinely measured and used to study long-term erosion rates of weathered granitic soil surfaces using cosmogenic <sup>10</sup>Be depth profile under the joint research program with the National Institute of Advanced Industrial Science and Technology (AIST). Recently, we have started development of <sup>26</sup>Al-AMS. The system tuning and test measurement have been carried out for routine measurement. The development has so far done well and the routine measurements of the <sup>26</sup>Al-AMS will be started in near future. The <sup>10</sup>Be- and <sup>26</sup>Al-AMSs will be used to estimate the exposure age of basement rocks as well as the sedimentation rate and the assessment of volcanoclastic material ejected during volcanic eruptions.

Keywords: AMS, Dating, C-14, Be-10, Al-26

## Radiocarbon dating of charcoal by the ABOX-SC method

TOMIYAMA, Shinji<sup>1\*</sup>; MINAMI, Masayo<sup>2</sup>; NAKAMURA, Toshio<sup>2</sup>

<sup>1</sup>Department of Earth and Environmental Sciences, Graduate School of Environmental Studies, Nagoya Uni, <sup>2</sup>Center for Chronological Research, Nagoya University

Charcoal is one of the most important samples for radiocarbon dating. It is necessary to remove contaminants from charcoal sample to obtain the reliable date. ABA (acid-base-acid) method is usually used for chemical pretreatment of charcoal: First, a sample is treated with HCl to remove carbonate contaminant. Next, the sample is treated with NaOH to remove organic contaminants derived from soil during burial. After then, the sample is treated with HCl again to remove absorbed atmospheric carbon dioxide during NaOH treatment. The residue is combusted with CuO at 850°C and graphitized to be <sup>14</sup>C-dated.

However, the ABA treatment often cannot completely remove contaminants from poorly-preserved and/or old charcoals (>about 30 ka). Bird et al. (1999) showed that the ABOX-SC (acid-base-oxidation stepped combustion) method removes organic contaminants more efficiently than the ABA treatment. The age of the charcoal sample treated with the ABOX-SC was reported to be older than that of the charcoal sample treated with the ABA (Brock et al., 2010).

The ABOX-SC method consists of 3 step chemical pretreatments: HCl and NaOH treatments followed by K<sub>2</sub>Cr<sub>2</sub>O<sub>7</sub>-H<sub>2</sub>SO<sub>4</sub> treatment in a sealed tube at 60°C for 20 hr (Brock et al., 2010). The mixed solution of K<sub>2</sub>Cr<sub>2</sub>O<sub>7</sub> and H<sub>2</sub>SO<sub>4</sub> removes organic contaminants effectively from charcoal samples, and can extract carbon fraction of oxidation resistant elemental carbon, OREC, which is resistant to oxidation and is less affected by contamination during burial (Bird et al., 1999). After the ABOX chemical treatment, the OREC is heated at 630°C with CuO for 2 hr to remove atmospheric CO<sub>2</sub> contaminants adsorbed during sample treatment and contaminants remained after the ABOX treatment. Finally, the residue of OREC is oxidized completely into CO<sub>2</sub> at 850°C for 1 hr, and the CO<sub>2</sub> is graphitized to be <sup>14</sup>C-dated.

In this study, we apply the ABOX-SC method to some charcoal samples of known age to measure <sup>14</sup>C ages. The charcoal samples, which were excavated from Tang-e Sikan cave in Arsanjan city, Iran, have been dated at about 40 ka and 26 ka by the ABA method, and are considered to be attributed to Upper Paleolithic period. In this study, we confirm the age difference of Paleolithic charcoal samples by the two pretreatment methods of ABA and ABOX-SC.

Keywords: Radiocarbon, Charcoal, ABOX-SC method

## AMS radiocarbon dating of Japanese tree rings for regional calibration curve

SAKAMOTO, Minoru<sup>1\*</sup> ; OZAKI, Hiromasa<sup>2</sup> ; IMAMURA, Mineo<sup>1</sup>

<sup>1</sup>National Museum of Japanese History / The Graduate School for Advanced Studies, <sup>2</sup>The University Museum, The University of Tokyo

Calibration of radiocarbon data can be achieved by comparison of measured radiocarbon age of samples with known calendar age. Tree rings that determined by dendrochronology are one of the important data set for calibration. IntCal13 calibration curve was launched mainly based on trees grown in the northern high latitude. These rings were sampled in ten years each at once to cancel the variation of solar activity, and to obtain sufficient sample size for conventional radiocarbon measurement as well. AMS radiocarbon dating can measure less than 1mg of carbon efficiently and is capable of date annual tree rings. Recent advance in accuracy of AMS radiocarbon measurement reveals that the resolution of IntCal may be insufficient for precise calibration. In particular, regional effect on the calibration curve had turned out to be a major problem. AMS radiocarbon dating of Japanese tree rings with actual age has been carried out to accomplish Japanese regional calibration curve. Tree ring preserves atmospheric <sup>14</sup>C concentration at that time, therefore the offset between radiocarbon age of Japanese tree ring and IntCal should indicate the inhomogeneity in the northern hemisphere.

Keywords: radiocarbon dating, tree ring, calibrated age, atmospheric inventory, regional effect

## Radiocarbon dating of archeological remains related with the 13th century Mongol Invasion to Japan

NAKAMURA, Toshio<sup>1\*</sup>

<sup>1</sup>Center for Chronological Research, Nagoya University

The shallow sea floor off Takashima, Matsuura, Nagasaki Prefecture, has been investigated archeologically as a potential site where many Mongolian warships exist under the sea sediments. It is historically recorded that more than 4000 Mongolian warships were destroyed by a typhoon during the Mongol invasion to Japan in 1281. The underwater investigations have been performed since 1980, and a lot of archeological remains related with the invasion have been collected there. In 2006, we were allowed to get some archeological remains for 14C dating with AMS. The samples were fragments of palm-bark ropes, lacquer products, bamboo ropes and charred rice. 14C ages for the samples were all consistent with the age of Mongol invasion in 1281.

Recently a body of submerged wrecks most probably originated from Mongolian warship has been discovered in the 1m-deep horizon of the sea sediment off Takashima. During the survey of the new warship, shell samples were collected near the ship. Some shells were recognized to be hull-fouling species, which may have grown up on the bottom of Mongolian warship and preserved along with the broken ship in the sea sediment. We have conducted 14C dating for some shell samples and found out that shells belong to hull-fouling species showed 14C ages consistent with the time of Mongol Invasion. Some other shells not belonging to hull-fouling species showed younger or older dates as compared with the time of Mongol invasion.

Keywords: AMS 14C dating, historical remains, remains from submerged wrecks, Mongol invasion, shell of hull-fouling species

## AMS radiocarbon dating of peaty layers in Kimotsuki lowland, southern Kyushu

FUJIKI, Toshiyuki<sup>1</sup> ; OKUNO, Mitsuru<sup>1\*</sup> ; NAKAMURA, Toshio<sup>2</sup> ; MORIWAKI, Hiroshi<sup>3</sup>

<sup>1</sup>ACRIFIS-EHAI, Fukuoka Univ., <sup>2</sup>CCR, Nagoya Univ., <sup>3</sup>Fac. Law, Econ. Human., Kagoshima Univ.

Since the middle Holocene, peaty layers have accumulated on the Kimotsuki lowland in south Kyushu, Japan. They can be applied radiocarbon (<sup>14</sup>C) wiggle-matching for establishing high-resolution chronology. Moreover, several tephra intercalated with the peat bed which originated from Kaimondake, Sakurajima, and the Kirishima volcanoes, and they can certify the reproducibility of <sup>14</sup>C dates. On the other hand, the age of the tephra by them can be determined correctly. We present here the results of AMS <sup>14</sup>C dating on the core sample, and report the age of each tephra determined from these dates.

Keywords: Kimotsuki lowland, peaty layer, tephra, radiocarbon date

## Offset in radiocarbon ages between shell and plant pairs in the Holocene sediments around the Korea

NAKANISHI, Toshimichi<sup>1\*</sup> ; HONG, Wan<sup>1</sup> ; SUNG, Kisuk<sup>1</sup> ; SUNG, Kilho<sup>1</sup> ; NAKASHIMA, Rei<sup>2</sup>

<sup>1</sup>KIGAM, <sup>2</sup>AIST

Since 2009, a research project to evaluate the marine reservoir effects of the coastal sites of Korea has been progressed by KIGAM. Estimating the reservoir effect of this area is difficult because age-known marine samples obtained before AD 1950 are rare. In order to solve this problem, 61 sediment cores were collected with 1 m intervals by a percussion drilling tool from 52 coastal sites in the southern area of the Korean Peninsula. These drilling sites were roughly preselected by the interpretation of modern air photos of internet map services provided by the websites such as Daum and Google. Topographic maps in 1918-1926 with 1/50000 scale and old air photos were also used for the site selection. The length of each core was less than 5 m and the total length was 132 m. Based on analysis of lithology and mollusk assemblages, we selected marine shell and terrestrial plant pairs from same horizons. These samples were cleaned by physical and chemical pretreatments, and reduced by automatic graphitization system in KIGAM. The radiocarbon ages of the samples were measured by the AMS facility of KIGAM. This presentation will report about spatial and historical variation of radiocarbon marine reservoir effect around Korea.

Keywords: Radiocarbon dating, Marine reservoir effect, Coastal sediments, Korea

## Estimation for the growth rate of benthic biotic communities in Antarctic lakes

TANABE, Yukiko<sup>1\*</sup> ; UCHIDA, Masaki<sup>2</sup> ; KONDO, Miyuki<sup>3</sup> ; UCHIDA, Masao<sup>3</sup>

<sup>1</sup>Waseda Institute for Advanced Study, Waseda University, <sup>2</sup>National Institute of Polar Research, <sup>3</sup>National Institute for Environmental Studies

Antarctica is an ice continent. It has one of the most extreme environments for life in the world. There are very little ice-free regions with life in it, so these regions are sometimes called polar oasis within the polar desert. The ice-free regions are scattered along the coastal regions and around mountainous peaks (Nunataks) in continental Antarctica or concentrated in Antarctic Peninsula in maritime Antarctica. The biota is simple due to lack of remarkable organisms at the top of food webs, and primary producers such as cyanobacteria, algae, lichens, mosses, heterotrophic microorganisms and metazoans dominate the sparse communities. A remarkable diversity of lakes exists in Antarctica, ranging from hypersaline with nearly 10 times the conductivity of seawater, to brackish and freshwater, sub-glacial, permanently ice-covered and seasonally ice-covered lakes. These lakes are unproductive with typical photosynthetic levels of 0.5 — 30  $\mu\text{g-C/L/day}$  from phytoplankton. Phytoplankton cannot bloom and hardly survives in the water column during the best light-available summer around the Syowa region. This results from low annual levels of photosynthetically active radiation and ice cover that attenuate light into the water column or photo-inhibit photosynthetic systems due to continuous low temperatures and the lack of any significant input of inorganic nutrients. Despite such severe situations, one of the most productive ecosystems in continental Antarctica is found in freshwater lakes, where benthic microbes form thick mats, and aquatic mosses can flourish on the lakebeds of the Syowa region. These lakes were exposed by glacial retreat after the Last Glacial Maximum. The benthic mats consist of almost organisms, dominantly cyanobacteria, algae, and mosses in the lakes, because there are a little inorganic particles and organic matters inflow to the lakes from the water catchment, and as pointed out above, almost no phytoplankton in the water column. This negligible level of any sedimentation and turbulence situation is specific to Antarctica, which is suitable to estimate the growth rate of benthic biotic communities in fine-scale. We collected sediment cores from 17 freshwater lakes in Sôya Coast on the south area of Syowa station, continental Antarctica during January-February in 2009 — 2010. The core samples were vertically sliced in each 1 cm as soon as possible after sampling in the field hut, and transported to Japan at -20 °C. Then, we analyzed the samples by using an AMS (accelerator mass spectrometry), and estimated the growth rate of the benthic biotic mats in each Antarctic lake.

Keywords: sediment, AMS, lakes, Antarctic, growth rate

## Black SOM dynamics during reforestation of Japanese grassland

IIMURA, Yasuo<sup>1\*</sup> ; UCHIDA, Masao<sup>2</sup> ; KONDO, Miyuki<sup>2</sup>

<sup>1</sup>School of Environmental Science, The University of Shiga Prefecture, <sup>2</sup>National Institute for Environmental Studies (NIES)

The dynamics of the polyaromatic structures of black humic acids (HAs), which are presumably derived from charred materials, are of significant interest for the global carbon cycle. However, the details of those dynamics are not yet well understood. We investigated differences in the degree of darkness (A600/C values), isotopic ratios ( $\delta^{13}\text{C}$ ,  $\delta^{15}\text{N}$ , and  $\Delta^{14}\text{C}$  values), and  $^{13}\text{C}$  NMR spectra of size-separated black HAs extracted from Japanese volcanic ash soils in order to estimate the variations in the polyaromatic structures of black HAs during ca. 100 years of natural reforestation of Japanese pampas grassland. For several hundred years, all the study sites were managed similarly as grassland by burning. Subsequently, their management differed: at site G (*Miscanthus sinensis*: C4 plant), maintenance as of the time of this study was still performed by mowing, while at sites P (*Pinus densiflora*: C3 plant) and Q (*Quercus crispula*: C3 plant), maintenance was discontinued ca. 30 and 100 years ago, respectively. Thus, the sites range from grassland (site G) to coniferous forest (site P) to broad-leaved forest (site Q). For all HA size fractions at all sites, we found that  $\delta^{13}\text{C}$  values correlate positively with  $\delta^{15}\text{N}$  values, although the gradients are much lower for fractions of small to medium molecular size than for fractions of medium to large molecular size (denoted as lower-size and higher-size fractions, respectively). Overall, for the lower-size fractions, the contribution ratio of C4-plant-derived carbon shows a significant positive correlation with A600/C values and a negative correlation with  $\Delta^{14}\text{C}$  values, and their aromatic characteristics are greater than those of higher-size fractions within the same black HA. Furthermore, the relative proportion of lower-size fractions decreases with reforestation, especially from site P to Q. The  $\delta^{13}\text{C}$  values for all size fractions are similar for sites G and P, but are relatively low for site Q. The aryl C contents of the lower-size fractions are lower and the O-alkyl C contents and the aliphaticity (alkyl C:O-alkyl ratio) are clearly higher for sites P and Q than for site G. These results strongly suggest that stimulation of HA biodegradation might be achievable by continuous input of new plant litter during reforestation, even for lower-size HA polyaromatic structures, despite the fact that lower-size HAs biodegrade more slowly than higher-size HAs.

Keywords: land use, reforestation, soil organic matter,  $^{14}\text{C}$

## Potential sink of soil organic carbon in a Japanese cool-temperate forest based on bomb radiocarbon based residence time

KONDO, Miyuki<sup>1\*</sup>; UCHIDA, Masao<sup>1</sup>; OHTSUKA, Toshiyuki<sup>2</sup>; MURAYAMA, Shohei<sup>4</sup>; SHIRATO, Yasuhito<sup>3</sup>; SHIBATA, Yasuyuki<sup>1</sup>

<sup>1</sup>National Institute for Environmental Studies, <sup>2</sup>Gifu University, <sup>3</sup>National Institute for Agro-Environmental Studies, <sup>4</sup>Environmental Management Technology

Functional roles of SOC pool for carbon dynamic remains almost unknown. In this study, residence time (RT) based on carbon and radiocarbon (<sup>14</sup>C) inventories, was investigated in a Japanese temperate forest (Takayama) under Asian Monsoon climate, and the potential of soil carbon sequestration were also investigated. Soil organic matter was divided to two fractions as low density humified material (LOM) and high density mineral-associated material (HOM). Our results were thoroughly compared with those in a temperate forest (Harvard forest) conducted using a similar approach [Gaudinski et al., 2002]. The LOM was the major part of the SOC (76%) and its contribution was higher even in the deep layer. <sup>14</sup>C contents of LOM in surface layer were similar to those of atmospheric CO<sub>2</sub> and roots, whereas those in deep layer are significantly low (<sup>14</sup>C < -200 per mil) as well as HOM fractions, although LOM fraction seems to consist of labile carbon. RTs for low density fractions as derived from their radiocarbon content are 53 ± 330 yrs BP in surface layer and 1760 ± 2780 years BP. Storage of SOC in our site was larger, irrespective of depths and differed considerably from that in Harvard forest. We also measured soil <sup>14</sup>CO<sub>2</sub> profile to determine the rate of CO<sub>2</sub> production from heterotrophic respiration of two SOM fractions. The <sup>14</sup>C values of soil CO<sub>2</sub> profile was constant down to 75 cm depth, which were close to those of atmospheric CO<sub>2</sub> and fine roots, suggesting that most of soil CO<sub>2</sub> is derived from recent photosynthetic fixed C. These results indicate that this forest might be higher sequestering soil carbon as low density fractions semi-permanently, which is also concerned about instability of near future climate change.

## Source diagnosis of PAHs using compound class specific $^{14}\text{C}$ analysis and Monte Carlo source apportionment at Kolkata canal

KUMATA, Hidetoshi<sup>1\*</sup>; UCHIDA, Masao<sup>2</sup>; KONDO, Miyuki<sup>2</sup>; SHIBATA, Yasuyuki<sup>2</sup>; SAHA, Mahua<sup>3</sup>; TAKADA, Hideshige<sup>3</sup>

<sup>1</sup>Tokyo Univ Pharm Life Sci, <sup>2</sup>NIES, <sup>3</sup>Tokyo Univ Agri Technol

Atmospheric polycyclic aromatic hydrocarbons (PAHs) originate mostly from incomplete combustion of carbon-based fuels. PAHs account for most (35-82%) of the total mutagenic activity of ambient aerosols. Reduction of air pollution by PAHs is essential for an effective air quality control, which requires reliable source apportionment. It has been reported that atmospheric pollution by PAHs in Indian megacities, such as Kolkata, Mumbai and Chennai, is comparable to the highest levels across the globe and Kolkata air exhibit the highest level among them. Also, our previous survey revealed that sediments from Kolkata city canals have the highest PAHs concentrations (i.e.,  $15.9 \pm 11.6 \mu\text{g}$  of  $\sum 14$ -parent PAHs/g dw, n=12) among the 174 surface sediments from 8 tropical Asian countries.<sup>1</sup> Examining methylated-to parental PAHs ratios of three homologous series and C30-hopane/ $\sum$ PAHs ratios both in sediment samples and in probable source materials, the high level sedimentary PAHs were ascribed to those emitted from combustion sources. However, relative importances of combustion sources were not solved. The present study aimed to apportion sources of combustion to PAHs in highly contaminated sediments from Kolkata, India by using combined approaches of CCSRA technique, molecular fingerprinting and Monte Carlo source apportionment.

Furthermore, three- and four ring PAHs (MW178, 192, 202) in leftover extracts were harvested on PCGC and analyzed for  $^{14}\text{C}$  on AMS at NIES-TERRA, NIES (Tsukuba, Japan). PAHs isolated from Kolkata canal sediments showed mostly fossil carbon isotopic signatures, i.e.,  $^{14}\text{C}$  signal of PAHs with MW178, 202 and those with MW228 were  $10.6 \pm 0.1$ ,  $5.9 \pm 0.4$ ,  $7.6 \pm 0.5$  pMC (KKNC),  $8.4 \pm 0.5$ ,  $8.3 \pm 0.4$ ,  $8.5 \pm 0.3$  pMC (KKSC). By using source end-members of MW202 and MW276 isomer pair ratios, Monte Carlo source apportionment<sup>2</sup> revealed that most of fossil-PAHs were derived from coal combustion, i.e., relative contributions (median) from coal and petroleum combustions were 50% and 11% in KKNC and 13% and 56% in KKSC.

1. Saha M. *et al.*, *Mar. Pollut. Bull.*, **2009**, 58 (2), 189-200
2. Sheesley R.J. *et al.*, *Atmos. Environ.*, **2011**, 45(23), 3874-3881

Keywords: compound class specific radio carbon analysis, PAHs, monte carlo simulation, molecular fingerprinting, source apportionment

## Accurate age estimation using $^{14}\text{C}$ in human teeth enamel.

KUNITA, Keisuke<sup>1\*</sup> ; NAKAMURA, Toshio<sup>2</sup>

<sup>1</sup>Graduate School of Environmental Studies, Nagoya University, <sup>2</sup>Center for Chronological Reserch, Nagoya University

Radiocarbon ( $^{14}\text{C}$ ) concentration in the atmosphere showed a stable value until 1955. However, as a result of the nuclear bomb testing, modern  $^{14}\text{C}$  concentration in the atmosphere dramatically increased during late 1950s and early 1960s. These bomb-produced  $^{14}\text{C}$  is then oxidized to form  $\text{CO}_2$ , and incorporated into plants by photosynthesis. Then, by eating plants or animals fed by these plants, the  $^{14}\text{C}$  concentration in human body reflects the  $^{14}\text{C}$  value of atmospheric  $\text{CO}_2$  at a certain time. Recent studies insisted that these  $^{14}\text{C}$  can play important role for forensic analysis, especially age estimation using  $^{14}\text{C}$  in human teeth enamel.

Teeth enamel is such a harder part of the human body that they are hardly destroyed by a natural process. And, the most important is, there is no turnover of enamel after its formation has completed. Although there are previous works which estimate the birth year of individuals by using  $^{14}\text{C}$  concentration in enamel, their samples are teeth from Swedish, Scottish and American people, and study areas are mainly at high latitudes of the northern hemisphere. The precision of age estimation using teeth enamel is determined by enamel formation time of teeth and atmospheric  $^{14}\text{C}$  concentration in a certain area at a certain year. It is known that teeth formation time of Japanese is different from that of Caucasian. It has been found that  $^{14}\text{C}$  concentration in the atmosphere indicates 5 different zones according to different peak  $^{14}\text{C}$  concentration of the nuclear bomb testing. These zones are named NH zone1, NH zone2, NH zone3, SH zone3 and SH zone1-2 from north to south. The boundary between NH zone1 and NH zone2 is Ferrel cell - Hadley cell boundary. It is nearly located at 35 °N. So it means that previous works mainly focused on NH zone1 samples, not NH zone2 samples. One of NH zone2 samples, teeth enamels of Japanese have not studied sufficiently. The aim of this study is to clarify whether age estimation using teeth enamels of Japanese can determine the precise year of birth of individuals and to discuss the mechanism of carbon fixation of enamels or other parts of the teeth.

7 of 44 collected tooth samples have been analyzed. They are 5 third molars and 2 second molars. The year of birth of each individual is 1943, 1946, 1951, 1951, 1951 for third molars, and 1933 and 1959 for second molars. In order to get the estimated year of birth, a model age for enamel completion of Japanese was subtracted from the year given by the  $^{14}\text{C}$  analysis of samples. The result shows that age estimation using teeth of Japanese gives precise age determination. Needless to say, taking account of the degree of individual variation and possibility of differences in local environment or in diet is important, however, this result seems to be uninfluenced by those effects. Larger number of, more and more various parts of teeth (for example, first molars, anteriors, such as early-completed teeth.) have to be analyzed.

To determine whether an individual is born before or after the peak of atmospheric  $^{14}\text{C}$  concentration (in 1964, in NH zone2), root of teeth have to be analyzed. Since root completion age is some years after enamel completion age, it can be easily found that the sample age is whether rising or falling part of the atmospheric  $^{14}\text{C}$  curve. We now are preparing for analysis of  $^{14}\text{C}$  of root dentine collagen and root inorganic matter. Their results will give more compelling data, now discover what is waiting for you!!

Keywords: human tooth, enamel,  $^{14}\text{C}$ , forensic science, nuclear bomb testing, age estimation

## Observations of atmospheric radiocarbon in carbon dioxide at Hateruma Island and Cape Ochi-ishi, Japan

TERAO, Yukio<sup>1\*</sup> ; MUKAI, Hitoshi<sup>1</sup>

<sup>1</sup>Center for Global Environmental Research, National Institute for Environmental Studies

Atmospheric radiocarbon in carbon dioxide ( $^{14}\text{CO}_2$ ) is a powerful tracer for understanding of carbon cycles, e.g. oceanic and biospheric  $\text{CO}_2$  exchanges and  $\text{CO}_2$  emissions from fossil fuel combustion. Observation sites for radiocarbon concentrations,  $\Delta^{14}\text{C}$ , are not many enough to evaluate the global and regional carbon flux. We present an analysis of trends, interannual variability (IAV) and seasonal cycle of  $^{14}\text{CO}_2$  in background air from July 2004 to December 2012 at two NIES/CGER monitoring stations; Hateruma Island (HAT; latitude 24.06N, longitude 123.81E) and Cape Ochi-ishi (COI; latitude 43.16N, longitude 145.50E). The air samples were collected in 2 L Pyrex glass flasks. The sampling frequency was monthly.  $\text{CO}_2$  was extracted from the whole air at NIES and  $\text{CO}_2$  samples were converted to graphite and analyzed ratios of  $^{14}\text{C}/^{12}\text{C}$  by accelerator mass spectrometry (AMS, National Electrostatics Corp., 1.5SDH) at Paleo Labo Co., Ltd., Japan. Analytical precision in  $\Delta^{14}\text{C}$  determined from statistical uncertainty (number of  $^{14}\text{C}$  counts) was  $\pm 1.7\text{-}2.0\text{‰}$  for most samples. The repeatability of measurements using modern reference air was  $\pm 1.9\text{‰}$ . A decreasing trend in  $\Delta^{14}\text{C}$  was  $-5\text{‰ yr}^{-1}$  in average but large IAV was observed at both stations: large decreases in 2007-2008 and in 2010-2011 ( $-8$  to  $-9\text{‰ yr}^{-1}$ ) and almost zero decrease in 2009. We also observed clear seasonal cycle of  $\Delta^{14}\text{C}$ . The peak-to-peak amplitudes in the seasonal cycle determined from the smooth curve fits were  $7\text{‰}$  at both stations and the maximum of  $\Delta^{14}\text{C}$  appeared in July and the minimum in January at HAT, and the maximum in September and the minimum in May at COI. The differences in phase of  $\Delta^{14}\text{C}$  seasonal cycle between HAT and COI suggested that the atmospheric  $\Delta^{14}\text{C}$  at COI was influenced by  $\text{CO}_2$  emitted from terrestrial biosphere.

## Radiocarbon based source apportioning of PM<sub>2.5</sub> carbonaceous aerosols at Cape Hedo, Okinawa and Fukue island, Japan

UCHIDA, Masao<sup>1</sup> ; KONDO, Miyuki<sup>1\*</sup> ; KANEYASU, Naoki<sup>2</sup> ; ARAKAKI, Takemitsu<sup>3</sup> ; HANDA, Daishi<sup>3</sup> ; KUMATA, Hidetoshi<sup>4</sup>

<sup>1</sup>National Institute for Environmental Studies, <sup>2</sup>National Institute of Advanced Industrial Science and Technology, <sup>3</sup>University of Ryukyus, <sup>4</sup>Tokyo University of Pharmacy and Life Sciences

Radiocarbon (<sup>14</sup>C) analysis of the carbonaceous aerosol allows an apportionment of fossil and non-fossil sources of air-borne particulate matter (PM). A chemical separation of total carbon (TC) into its sub-fractions organic carbon (OC) and elemental carbon (EC) refines this powerful technique, as OC and EC originate from different sources and undergo different processes in the atmosphere. Although <sup>14</sup>C analysis of TC, EC and OC has recently gained increasing attention, Nowadays gigantic brownish haze from various burning and combustion processes is also blanketing India and surrounding land and oceans during the winter season. In China and surrounding countries, same kind of atmospheric pollution are widely observed and occurred as well. Additionally this soot-laden Brown Cloud is affecting South and East Asian climate as much or more than carbon dioxide and cause hundreds of thousands of premature deaths annually, yet its sources have been poorly understood. In this study, we investigated the contribution of continent derived aerosol to Japan. Aerosol samples with diameter of 2.5µm were collected at Fukue island, one of Goto islands and at the Cape Hedo is located at the northern end of Okinawa Island. The <sup>14</sup>C contents of EC of PM<sub>2.5</sub> aerosols collected from October, 2009 and May, 2010 including the Kosa event in Cape Hedo and Fukue were measured. The <sup>14</sup>C content represents in the unit of pMC. Results of EC-<sup>14</sup>C in both sites were 25-30pMC in Cape Hedo and 18-44pMC in Fukue, respectively. These results mean that relative apportionments of biomass burning and fossil fuel were 25-30% and 18-44% in Cape Hedo and 25-35% and 65-75% in Fukue, respectively. The observed variations of pMC in Cape Hedo during February and March were relatively smaller than those of Fukue, which was more than 20%. According to back trajectory analysis in this duration, because ca. 70% of air mass in both sites was derived from the continent. The aerosols particulate matter to be transferred to Cape Hedo from continent would be relatively smaller than those to Fukue. Our data of EC-<sup>14</sup>C obtained during the Kosa event showed the relatively higher contribution of biomass burning sources in Fukue although these interpretation need to consider variation of the magnitude and concentration of EC in both sites. In further study we need to investigate details of the source of EC during this period.

Keywords: Radiocarbon, PM<sub>2.5</sub>, aerosol, source apportioning

## Study on monitoring of volcanic activity using $^{129}\text{I} / ^{127}\text{I}$ ratios in crater lake and hot spring at Zao volcano

MATSUNAKA, Tetsuya<sup>1\*</sup>; SASA, Kimikazu<sup>1</sup>; SUEKI, Keisuke<sup>1</sup>; SHIBAYAMA, Nao<sup>1</sup>; TAKAHASHI, Tsutomu<sup>1</sup>; MATSUMURA, Masumi<sup>1</sup>; SATOU, Yukihiro<sup>1</sup>; MATSUZAKI, Hiroyuki<sup>2</sup>; GOTO, Akio<sup>3</sup>; WATANABE, Takahiro<sup>3</sup>; TSUCHIYA, Noriyoshi<sup>3</sup>; HIRANO, Nobuo<sup>3</sup>; KIZAKI, Akihisa<sup>3</sup>

<sup>1</sup>University of Tsukuba, <sup>2</sup>The University of Tokyo, <sup>3</sup>Tohoku University

Volcanic tremors and mountain gradient changes have been detected at Zao volcano in Miyagi and Yamagata since January 2013, volcanic activity began to intensify although Zao volcano will not erupt immediately<sup>[1]</sup>. Since the water quality of crater lake are correlating with volcanism changes<sup>[2][3]</sup>, basic water quality of crater lake and hot spring at Zao volcano have been studied by the group of Tohoku University from September 2013. As a part of this project, we are trying to monitor the volcanic activity using  $^{129}\text{I} / ^{127}\text{I}$  ratios (atomic ratio of radioiodine and stable iodine) in crater lake and hot spring of Zao volcano.

Natural  $^{129}\text{I}$  (half-life: 15.7 million year) are produced by nuclear spallation reaction of  $^{129}\text{Xe}$  with cosmic ray in the atmosphere and spontaneous fission of  $^{238}\text{U}$  in the geological layer. In the ocean, steady-state  $^{129}\text{I} / ^{127}\text{I}$  ratio of the seawater is estimated to be  $1.5 \times 10^{-12}$ <sup>[4]</sup>. Sunken iodine by the ocean plate having lower  $^{129}\text{I} / ^{127}\text{I}$  ratio (older  $^{129}\text{I}$  age) compared to the steady-state ratio of seawater, are supplied to the atmosphere mainly via magmatic activity. In general,  $^{129}\text{I} / ^{127}\text{I}$  ratio in hot spring water and brine water are used as indicator of origin and behavior of iodine in the water<sup>[5][6]</sup>.  $^{129}\text{I} / ^{127}\text{I}$  ratio of hydrothermal at Zao volcano are considered to become lower by the supply of chronologically-old iodine in terms of global iodine cycle.

In September 2013, water samples of 2 L were collected from the surface of crater lake (Okama, diameter: 350 m, maximum depth: 35 m) located at 1,560 m in elevation and hot spring (Kamoshika Hot Spring) located at 1,230 m in elevation in the eastern side of Zao volcano. Water temperature and pH were measured on site. After water samples were filtered by 0.2  $\mu\text{m}$  filter,  $^{129}\text{I} / ^{127}\text{I}$  ratio were measured for the isotopic diluted water samples by adding carrier ( $^{127}\text{I}$  standard) at MALT, The University of Tokyo.  $^{127}\text{I}$  concentrations were measured by ICP-MS, and original  $^{129}\text{I} / ^{127}\text{I}$  ratio of water samples were estimated.

Water temperature and pH were 10.2 °C and 3.3 at Okama; 40.0 °C and 3.3 - 4.0 at Kamoshika Hot Spring.  $^{129}\text{I} / ^{127}\text{I}$  ratios of Okama and Kamoshika Hot Spring were respectively, estimated to be  $(1.5 \pm 0.4) \times 10^{-9}$  and  $(0.78 \pm 0.2) \times 10^{-9}$ , 500 - 1000 times higher than the steady-state ratio of sea water ( $1.5 \times 10^{-12}$ )<sup>[4]</sup>. Since  $^{129}\text{I} / ^{127}\text{I}$  ratio of anthropogenic metric water were over  $9.0 \times 10^{-12}$ <sup>[7]</sup>, surface water of Okama and Kamoshika Hot Spring water were very likely to be strong affected by the meteoric water including anthropogenic  $^{129}\text{I}$ . For the monitoring of volcanic activity using  $^{129}\text{I} / ^{127}\text{I}$  ratio, it is necessary to decide the site as few anthropogenic  $^{129}\text{I}$  as possible through the measuring of  $^{129}\text{I} / ^{127}\text{I}$  ratio of the Okama bottom water and some hot spring around Zao volcano. Continuous water quality survey of 1 - 2 times for Okama and 1 time per 1 - 2 months for hot springs are planned from June to November of this year.

- [1] Japan Meteorological Agency (2013) Monthly Volcanic Activity Report.
- [2] Ohba et al. (2000) Journal of Volcanology and Geothermal Research, 97, 329-346.
- [3] Ohba et al. (2008) Journal of Volcanology and Geothermal Research, 178, 131-144.
- [4] Moran et al. (1998) Chemical Geology, 152, 193-203.
- [5] Snyder and Fehn (2002) Geochimica et Cosmochimica Acta, 66, 3827-3838.
- [6] Muramatsu et al. (2001) Earth and Planetary Science Letter, 192, 583-593.
- [7] Tomaru et al. (2007) Applied Geochemistry, 22, 676-691.

Keywords: Zao volcano, volcanic activity, crater lake, hot spring,  $^{129}\text{I} / ^{127}\text{I}$ , AMS

## Speciation analysis of the Fukushima accident derived I-129 in the soil using sequential extraction method

HONDA, Maki<sup>1\*</sup> ; MATSUZAKI, Hiroyuki<sup>2</sup> ; SAITOU, Takumi<sup>3</sup> ; NAGAI, Hisao<sup>4</sup>

<sup>1</sup>Graduate School of Integrated Basic Sciences, Nihon University, <sup>2</sup>Department of Nuclear Engineering and Management, School of Engineering, The University of Tokyo, <sup>3</sup>Nuclear Professional School, School of Engineering, The University of Tokyo, <sup>4</sup>College of Humanities and Sciences, Nihon University

In previous study, we investigated the depth profile of the accident derived <sup>129</sup>I ( $T_{1/2} = 1.57 \times 10^7$  y) and downward migration speed in soils of near field of Fukushima Dai-ichi Nuclear Power Plant (FDNPP), including crop fields and man-made fields. <sup>129</sup>I in soil was measured by AMS and stable iodine (<sup>127</sup>I) was measured by ICP-MS at MALT (Micro Analysis Laboratory, Tandem accelerator), The University of Tokyo. It was found that <sup>129</sup>I was concentrated near surface but distributed deeper compared with <sup>137</sup>Cs ( $T_{1/2} = 30$  y). From the estimation of relaxation length using depth profiles, the FDNPP derived <sup>129</sup>I move 0.6 cm/y downward and <sup>137</sup>Cs 0.3 cm/y for it. It was also found that <sup>129</sup>I seems to move downward more quickly than <sup>137</sup>Cs.

To investigate the adsorption mechanism and the elemental process of migration of the accident derived <sup>129</sup>I in soil, it is important to know what kind of component the <sup>129</sup>I combines with.

Recent studies on the X-ray absorption fine structure (XAFS), especially near edge structure (XANES), reported that the stable iodine (<sup>127</sup>I) in soil existed as an organic component<sup>[1]</sup>. However, it had not yet been proved that it was also the case with the accident derived <sup>129</sup>I because it had been incorporated in the soil system only recently and the abundance of <sup>129</sup>I in soil was more than 8 orders of magnitude smaller than sub-ppm level stable iodine (<sup>127</sup>I).

In this study a progressive sequential extraction method including the dialysis was newly developed to obtain only the iodine sticking to the soil organic component. The advantage of sequential extraction over other method is that stable iodine can be quantified by direct analysis of the fraction and <sup>129</sup>I can be quantified by AMS method of the fraction added with carrier. The fraction of the organic component for <sup>127</sup>I and <sup>129</sup>I can be evaluated respectively by comparing with the other fraction and/or with the total concentration obtained by the bulk analysis (e.g. by the pyrohydrolysis).

Repeatability is 20% for the water soluble, oxides and organic fraction, 10% for Exchangeable fraction and 50% Residue (mainly minerals).

The results show that 60% of the total <sup>129</sup>I are associated with oxides and 30% associated with organic matter in crop field soil. The former, the oxides bond iodine, it takes a form of iodate ( $\text{IO}_3^-$ ) absorbed in amorphous oxides, especially goethite or delta- $\text{MnO}_2$ . They are formation of monodentate mononuclear outer-sphere species and bidentate, binuclear inner-sphere species<sup>[2]</sup>. The latter iodine are linked to organic carbon directly by a covalent bond.

[1] Y. S. Shimamoto et al., 2011, *Environ. Sci. Technol.*, **45**, pp2086-2092

[2] T. Nagata et al., 2010, *Geochim. Cosmochim. Acta.*, **74**, pp6000-6013

## Relationship between progress of borehole investigations and the geometric data of fractures at the crystalline rocks

ISHIBASHI, Masayuki<sup>1\*</sup> ; SASAO, Eiji<sup>1</sup> ; NAKAJIMA, Makoto<sup>2</sup> ; ATSUMI, Hiroyuki<sup>2</sup> ; ONOE, Hironori<sup>1</sup> ; SAEGUSA, Hiromitsu<sup>1</sup> ; KAWABATA, Junichi<sup>2</sup> ; MASUMOTO, Kazuhiko<sup>2</sup> ; SENO, Shoji<sup>2</sup> ; IWANO, Keita<sup>2</sup>

<sup>1</sup>Japan Atomic Energy Agency, <sup>2</sup>Kajima Corporation Technical Research Institute Rock Mechanics and Hydrogeology Group

In order to evaluate deep geological environment for geological disposal of high level radioactive waste (HLW) and underground storage of liquefied petroleum gas, understanding of the geometry of water conducting features such as fractures is essential. Geometric data of fractures are obtained by borehole investigations. But, methodology to understand the geometry of fractures has not been established in terms of planning borehole investigation such as number and total length of boreholes. Thus, relationship between progress of borehole investigation and increase of the geometric data of fractures is studied.

In this study, discrete fracture network models with the size of 100×100×100m cube were used as virtual fractured rock mass, and virtual boreholes were drilled in the virtual rock mass. Five boreholes with the length of 100m each were located in four directions. One dimensional fracture intensity (as the number of fractures per unit length; P10) of virtual boreholes is calculated. The P10 is depending on the relationships borehole directions and fracture orientations. In addition, The P10 is become constant at each direction of borehole as investigations progressed.

These results suggest that in order to obtain the geometric data of fracture, the borehole investigation should be planned in consideration of distribution of the fracture orientations.

Keywords: Borehole investigation, DFN model, Methodology, Fracture intensity

## Characterization of the fracture zone on the basis of fracture spacing, case study at the Toki granite, central Japan

SASAO, Eiji<sup>1\*</sup> ; ISHIBASHI, Masayuki<sup>1</sup>

<sup>1</sup>Japan Atomic Energy Agency

In order to evaluate deep geological environment for geological disposal of high level radioactive waste, understanding of the geometry of water conducting features such as fractures is essential. The fracture zones have been divided based on the fracture intensity that has been obtained deep boreholes. But fracture intensity could be changeable in different portion of the rock body. The method to divide the fracture zones based on fracture spacing is studied. In this study, cumulative frequency curve of fracture spacing based on fifteen deep borehole with the total length of ca.12,000 meters was used. Cumulative frequency curve shows that half of fracture spacing is lower than 1m. Thus, fracture could exist in fracture zones. The fractures with the dip of middle to high angle are needed to divide into fracture zones based on the fracture spacing. In the future, we will establish the methodology to divides the fracture zones coupled with spatial distribution of fracture spaces.

Keywords: fracture zone, fracture spacing, Toki granite

## Examination of realistic conceptual model of near-field process in HLW repository

YOSHIDA, Hidekazu<sup>1\*</sup> ; KOJIMA, Keiji<sup>2</sup> ; OONISHI, Yuzo<sup>3</sup> ; TOCHIYAMA, Osamu<sup>4</sup> ; NISHIGAKI, Makoto<sup>5</sup> ; TOSAKA, Hiroyuki<sup>6</sup> ; SUGIHARA, Kozo<sup>7</sup> ; OGATA, Nobuhisa<sup>7</sup>

<sup>1</sup>Nagoya University, <sup>2</sup>Geospace Labo, <sup>3</sup>Kansai University, <sup>4</sup>Nuclear Safety Research Association, <sup>5</sup>Okayama University, <sup>6</sup>University of Tokyo, <sup>7</sup>Japan Atomic Energy Agency

Since 2000, data of deep underground has been accumulated through the URLs in-situ studies and related underground investigation. Based on these data, here we show the result on the examination of realistic conceptual model of near-field process in HLW repository.

Keywords: Geological Disposal of Radioactive Waste, Near filed processes

## An approach to establish information basis of Weathered zone for the Safety Assessment to HLW Disposal over long-term.

SHIMEMOTO, Hidenori<sup>1\*</sup> ; WAKASUGI, Keiichiro<sup>2</sup> ; SHIBATA, Masahiro<sup>2</sup> ; YAMAGUCHI, Masaaki<sup>2</sup>

<sup>1</sup>Japan Atomic Energy Agency (\*Present position: Mitsubishi Materials Techno Corporation), <sup>2</sup>Japan Atomic Energy Agency

The consideration of evolution on geological environment is required in the safety assessment of geological disposal for the high level radioactive waste (HLW). The HLW repository can be expected to come close to ground surface assuming a continuous uplift and erosion for a long-term period. Therefore, the consideration of shallow zone (weathered zone) environment is also required. Since the geological condition in the near-surface underground is different from that in the deep underground due to weathering, the basic information and understanding for the near-surface condition are essential for the scenario development. Therefore, information regarding weathered zone is surveyed and arranged based on available literatures.

As a result, 37 data of depth (thickness) of weathered zone were extracted. Then the data distribution and these characteristics for the thickness of weathered zone were discussed. In order to understand the formation process of weathered zone, the relation between weathered zone and landform was also discussed and categorized into four patterns. The key factors which account for the patterns are also analyzed in a qualitative manner.

Regarding the geological property/condition in the weathered zone, although information on hydraulic and chemical conditions are very limited, information on tensile strength and porosity are available.

For the sake of condition setting for near-surface underground in the long-term safety assessment, continuous research and development for the characterization on weathered zone are important.

Keywords: HLW, Long-term, Safety Assessment, Weathered Zone, Landform, Geological Environmental Conditions

## A Bayesian approach to assess the probability of concealed active faults existing using helium isotope ratios

MARTIN, Andrew<sup>1\*</sup>; ISHIMARU, Tsuneari<sup>2</sup>; UMEDA, Koji<sup>2</sup>; ASAMORI, Koichi<sup>2</sup>

<sup>1</sup>NAGRA, <sup>2</sup>Tono Geoscience Center, JAEA

In Japan, numerous studies have been carried out to assess the stability of the geological environment including in particular, the spatio-temporal distribution of active faulting in the context of site selection of a radioactive waste repository and/or assessing the safety of current nuclear facilities etc. One key concern is the existence of active faults that do not show any surface rupture.

High He-3/He-4 ratios which tend to be found in volcanic regions have also been measured in non-volcanic regions. This has been attributed to degassing from the mantle with faults potentially acting as conduits (e.g., Kennedy et al., 1997). Studies carried out in the western Tottori district have shown the potential of using He-3/He-4 ratios as a means of providing indirect evidence of the existence of source fault(s) that caused the 6 Oct 2000 Tottori earthquake (Mw 6.8), but which had no apparent surface indication prior to the earthquake (Umeda and Ninomiya, 2009).

Here we introduce a new technique based on Bayesian inference in an effort to quantify this theory. In the Bayesian paradigm, we make *a priori* assumptions based on the tectonic setting of the study area as a starting point. 'Known' active faults are divided into equal distant fault segments. The *a priori* assumption here is that 'unknown' fault segments do not exist far from 'known' fault segments. It is also assumed that the probability of 'unknown' faults existing decreases with distance from the 'known' faults.

2D *a priori* probability distributions of unknown fault(s) existing are then calculated using kernel functions (Martin et al., 2003) centered over the known fault segments. A Cauchy probability density function (PDF) is assigned here conservatively as the *a priori* distribution in the first step so that probability is never zero.

In the second step, the method developed by Martin et al. (2004, 2012), is adapted to remap He-3/He-4 ratios into a PDF, called a likelihood function based on Kolmogorov-Smirnov statistical tests. The *a priori* PDF from the first step above is then combined with the likelihood PDF using Bayes's rule to produce a *a posteriori* PDF.

Carrying out the calculation using data from before the Tottori 2000 earthquake, the *a posteriori* 2D probability maps showed increased probability of unknown active fault(s) existing in the region above the source zone of the 2000 earthquake. Thus, in the case of the Tottori region, the *a posteriori* probabilities corroborate the theory that faults could be acting as conduits for mantle helium.

The potential of the methodology to incorporate other information such as gravity and crustal strain rates will also be presented and discussed.

### References

- Kennedy et al. (1997), Mantle fluids in the San Andreas fault system, California, *Science*, 278, 1278-1281.  
Martin et al., (2003) *Acta Geophys.* 51, 271-289  
Martin et al. (2004) *J. Geophys. Res.*, 109, B10208, doi:10.1029/2004JB003201.  
Umeda, K. and Ninomiya, A. (2009) *Geochem. Geophys. Geosys.*, 10, Q08010, doi:10.1029/2009GC002501.  
Martin A. J., Umeda K. and Ishimaru T. (2012) *InTech Pub.*, doi:10.5772/51859

Keywords: Active fault, Bayesian, Helium isotope ratio

## An active shear zone, southwest Japan: electromagnetic geophysics and noble gas geochemistry

UMEDA, Koji<sup>1\*</sup> ; ASAMORI, Koichi<sup>1</sup> ; MAKUUCHI, Ayumu<sup>1</sup> ; KOBORI, Kazuo<sup>1</sup>

<sup>1</sup>Japan Atomic Energy Agency

In 1997, the Kagoshima earthquake doublet with two  $M_w \sim 6$  strike-slip events struck 5 km and 48 days apart in southwest Japan, where an E-W trending discontinuity along 32 degree N latitude in GPS velocities across southern Kyushu Island is clearly defined, indicating a highly active left-lateral shear zone. However, there was no obvious pre-faulting indication at surface (active fault) in relation to the shear zone. Three-dimensional inversion of magnetotelluric sounding data observed in the source region of the earthquake doublet reveals a near-vertical conductive zone with a width of 20 km, extending down to the base of the crust and perhaps into the upper mantle. The prominent conductor corresponds to the western edge of the active shear zone. Elevated  $^3\text{He}/^4\text{He}$  ratios of groundwaters sampled around the seismic source region suggest the emission of mantle-derived helium from the electrical conductor. The geophysical and geochemical observations provide significant evidence that the invasion of mantle fluids into the crust, driven by upwelling asthenosphere from the Okinawa trough, triggers off the notable left-lateral shear zone in the present-day subduction system. In addition, the conductive fluids enhance stress concentration in the seismogenic layers leading to mechanical failure of strong asperities, resulting in the occurrence of the 1997 earthquake doublet.

Keywords: 1997 Kagoshima earthquake doublet, active shear zone, magnetotelluric sounding, helium isotope

## Predominant process for transport of radiocaesium released by the TEPCO's Fukushima Daiichi Nuclear Power Plant Accident

NIIZATO, Tadafumi<sup>1\*</sup> ; ISHII, Yasuo<sup>1</sup> ; ABE, Hironobu<sup>1</sup> ; WATANABE, Takayoshi<sup>1</sup> ; SASAKI, Yoshito<sup>1</sup>

<sup>1</sup>Fukushima Environmental Safety Center, Japan Atomic Energy Agency

Understanding the environmental dynamics of the radiocaesium (particularly Cs-134 and 137) released from the Fukushima Daiichi Nuclear Power Plant provides the firm foundation for a remediation of the Fukushima environment because it is the main radionuclide to radiological dose within the contaminated area. One of the main sources of radiocaesium under the current situation is a mountain forest, where the decontamination work has not been carried out as yet. Therefore, transport process, flux and chemical form of the radiocaesium flowing from the mountain forest are crucial issues for an evaluation of a radiation exposure, taking into a dynamics behavior of radiocaesium from the highest contaminated mountain forests down through the river to eventual deposition in the sea. This paper discusses the predominant process of the radiocaesium transport in the mountainous region, Fukushima, Japan.

The four investigation areas, which have different characteristics of vegetation, geomorphology and soil type, were selected in the Abukuma Mountain, eastern part of Fukushima. The soil samples were obtained from ridge, slope, and valley bottom in the areas by soil sampler and scraper plate to the depth about 40 cm and 20 cm, respectively. The observation plots, which have an area of 40 to 60 m<sup>2</sup>, for a monitoring of surface runoff and soil loss are also installed. The concentration of radiocaesium in the uppermost soil horizon is related to the geomorphological aspects, that is, the concentration trends to be higher in the depositional area than in the erosional area. Additionally, the radiocaesium concentration of solid phases (soil particles and fragmented organic materials) including in surface runoff is one to two orders of magnitude greater than that of a liquid phase (running water).

Therefore, predominant process of the radiocaesium transport is the surface runoff accompanied with a detachment of soil particles from the mountain slope.

Keywords: radiocaesium, environmental dynamics, mountain forest, nuclear accident, Fukushima

## Current State of the additional geological surveys of crush zones at the fast breeder prototype reactor "Monju" site

ISHIMARU, Tsuneari<sup>1\*</sup> ; SHIMADA, Koji<sup>1</sup> ; SASAKI, Akimichi<sup>1</sup> ; TANAKA, Yukumo<sup>1</sup> ; MIYAZAKI, Masashi<sup>1</sup> ; YASUE, Ken-ichi<sup>1</sup> ; NIWA, Masakazu<sup>1</sup> ; SUEOKA, Shigeru<sup>1</sup> ; UMEDA, Koji<sup>1</sup> ; IKEDA, Makinori<sup>1</sup>

<sup>1</sup>Japan Atomic Energy Agency (JAEA)

**Background:** In the fast breeder prototype reactor Monju of the Japan Atomic Energy Agency (JAEA), a report of the additional geological survey regarding the crushed zones at the Monju site was submitted to the Nuclear Regulation Authority (NRA) on April 30, 2013. The NRA instructed to develop a further additional research plan on September 25. Accordingly, JAEA compiled and submitted the plan on October 3, followed by a "preliminary report" on November 29, and a "complete report" in March 2014.

**Overview of additional research:** The instructions from the NRA of September 25, 2013 were as follows:

1. to implement the dating of materials within the crushed zones, to research the displacement markers, and to understand their formation age, etc., in order to enhance understanding of the activity of crushed zones at the Monju site in the bedrock of the site investigation area; 2. to investigate the distribution of the fracture zones, the relationship of the sediment layer, and the depositional age of the sediment layer (14C dating, tephra analysis, etc.) for data expansion of the extended portion of the L-2 lineament located near the Monju site; and 3. to implement marine seismic surveys in the coastal sea area and geographical and geological surveys of the coast, etc., in order to understand the geological structure and activities of the coastal seabed in the extended portion of the Shiraki-nyuu active fault and the L-2 lineament.

JAEA developed a research plan in response to these instructions and conducted the stripping investigation over an expanded area, the additional detailed geographical and geological surveys around the mountains/terrace boundary, and the marine seismic surveys in the coastal waters.

**Summary of findings:** The basement rock of the northern Tsuruga peninsula where the Monju site is located is composed of the Late Cretaceous-Paleogene granite known as the Kojyaku granite. In the on-site investigation, the stripping area was extended in the northern direction of the longest fracture zone in the reactor building foundation rock. The fracture zones were grouped into 2 systems called  $\alpha$ -system and  $\beta$ -system. We examined the cross-cutting relationships and displacements of the fracture zones and confirmed that the  $\alpha$ -system was formed after the  $\beta$ -system. The  $\alpha$ -system fracture zones are left-lateral faults that have mesh-like clay veinlets, and the width of the  $\alpha$ -system fracture zones is several centimeters. The K-Ar ages of the basalt dyke displaced by the  $\alpha$ -system fracture zones were about 19Ma. In addition, U-Pb and FT dating of apatite and zircon separated from the fracture zone materials and granite were conducted to reconstruct their thermal histories. The investigation results so far obtained were similar to the survey results of April 30, 2013, offering no clear evidence that the on-site crushed zones are of an active fault. It can be considered that these crushed zones are small-scale older (pre-Quaternary?) geological structures formed under the hydrothermal environment of the deep part before exposure of the granitic body. On the detailed geographical and geological surveys around mountainous/terrace boundary, no fracture zone along the strike of the boundary was observed. From the C-14 dating and tephra analysis of the depositional layer covering the granite, the distribution of sediments from about 40,000-50,000 years ago was confirmed in a few outcrops. The marine seismic surveys in the coastal waters were performed in conjunction with the bathymetric survey in December 2013. Currently, the data are being analyzed.

**Upcoming:** In order to further enhance the reliability of the investigation results and accumulate further data related to on-site geology and the underground, voluntary investigations are being conducted on a continuous basis. In addition, a basic study is also being carried out on the evaluation method of the activity of the fault zone not applicable to the overburden strata method.

Keywords: fast breeder reactor Monju, survey of crush zone, Kojyaku granite, Nuclear Regulation Authority

## The linearity of geographical features and a planation surface along the seashore around the fast breeder reactor Monju

SASAKI, Akimichi<sup>1\*</sup> ; YASUE, Ken-ichi<sup>1</sup> ; SHIMADA, Koji<sup>1</sup> ; TATEISHI, Ryo<sup>2</sup> ; ISHIMARU, Tsuneari<sup>1</sup> ; TANAKA, Yukumo<sup>1</sup>

<sup>1</sup>Japan Atomic Energy Agency, <sup>2</sup>OYO Corporation

We have not only conducted a survey of crush zones near the reactor building in the fast breeder prototype reactor Monju site but also carried out geographical investigations such as terrace classification and lineament investigation around the site. This presentation reports the results of the geographical and geological survey on the linearity of geographical features and a planation surface along the seashore around the site.

### 1. An investigation into the linearity of the mountain/terrace boundary

It is estimated that the lineament of the NW-NNW direction, also called the L-2 lineament, exists to the south of the Monju site. Geographical and geological surveys by JAEA suggest that this lineament is highly likely to be a structural landform. The mountain/terrace boundary to the north of this lineament extends in a straight line-like form in the NW direction. During an expert meeting of the Nuclear Regulation Authority, it was suggested that an active fault might exist along this boundary. It was in response to this suggestion that we carried out the geographical and geological survey.

**Geographical investigation:** We carried out a terrace classification, field survey, and analysis of the survey data for regions around the mountain/terrace boundary. The mountain slope directly faces the sea; the slope of the present stream bed and terrace surfaces is comparatively steep in the investigation area. In the topographical map before artificial change, we can recognize that the stream makes the loosely curved dissected topography without winding greatly and that the mountain/terrace boundary is loosely curved similarly.

**Geological survey:** Outcrop investigation was conducted on the mountain/terrace boundary by paying attention to the existence of crush zones and the development style of the joints. In addition, we also estimated the age of the sedimentary layers.

The results clearly indicate that the joints are progressing mainly in the NW or the NE direction, and the comparatively hard granite is also distributed. Moreover, although crush zones were observed in some outcrops near the mountain/terrace boundary, we could not detect crush zones that continue in the same direction as the mountain/terrace boundary. In the outcrop near the northwestern end of the mountain/terrace boundary, it was observed that the covering layer, which was deposited after about 40,000-50,000 years ago and covers a crush zone, is not displaced.

The results of the above-mentioned geographical and geological survey suggest that the linearity of the mountain/terrace boundary has not originated from fault displacement.

### 2. An investigation into the linear coastline and planation surface along the seashore

A linear coastline extending in the NE direction can be seen around the Monju site. In addition, a planation surface is observed in parts along the seashore. We performed a geographical and geological survey to determine the origin of such a geographical feature and whether such a planation surface could exist elsewhere.

**Geographical investigation:** While carrying out the air photograph interpretation, the contour line maps and topographic profiles were created using a digital elevation map created from aviation laser survey data. As a result, except for one place which is present at an altitude of about 5 m, a geographical feature that can be recognized as a comparatively flat field was not observed.

**Geological survey:** We carried out an outcrop investigation that paid attention to the development of joints and searched for evidence that suggested the upheaval of land. The results suggest that the direction of the coastline and the direction of developing joints are similar. Moreover, we could not observe the remains of living things which suggest the possible upheaval of land.

**Keywords:** fast breeder reactor Monju, survey of crush zone, lineament

## On the turn determination of crush zone activity, a lesson from granitic basement rock holding the fast breeder reactor

SHIMADA, Koji<sup>1\*</sup> ; TATEISHI, Ryo<sup>2</sup> ; ISHIMARU, Tsuneari<sup>1</sup> ; SASAKI, Akimichi<sup>1</sup> ; TANAKA, Yukumo<sup>1</sup> ; MIYAZAKI, Masashi<sup>1</sup> ; YASUE, Ken-ichi<sup>1</sup> ; NIWA, Masakazu<sup>1</sup> ; SUEOKA, Shigeru<sup>1</sup> ; UMEDA, Koji<sup>1</sup> ; IKEDA, Makinori<sup>1</sup>

<sup>1</sup>Japan Atomic Energy Agency, <sup>2</sup>OYO Co.

Activity evaluation of crush zones encountered in basement rock is an issue of the seismic safety assessment of nuclear plant and geological isolation of radioactive wastes. The selection of crush zone of which has been evaluated should be defined as the latest one by means of turn determination of crush zone activity based on stratigraphic or structural geological method. A lesson from granitic basement rock (Kojaku granite) holding the fast breeder reactor "Monju" is presented. The Kojaku Granite form the oval Tsuruga peninsula (ca. 8km in width) on the southeastern coast of the Sea of Japan and the age is  $68.5 \pm 0.7$ Ma (Zircon U-Pb age).

### 1. Stratigraphy-oriented turn determination of crush zone activity.

#### (1.1) Turn determination using cover sediments

The age determination of undeformed cover sediments indicates the activity of crush zone older than the sediments. In the case of crush zones observed at separate outcrop, deformation of the same strata can be utilized for the turn determination.

Trenching evidence (with tephra chronological analyses) of the active Shiraki-Nyu fault near the Monju site indicate repeated activity after ca. 30ky strata (including AT-tephra). On the other hand, crush zones in the Monju site affect no deformation on the strata of identical age observed during the site construction. These data indicate the last movement of the latter is older than the active fault, and no movement in sympathy with the active faulting repeatedly during, at least, ca. 30ky.

#### (1.2) Turn determination using dyke, mineral and clay vein ("Dyke", hear after)

Undeformed dykes intersecting crush zones indicate that the movements of crush zones are older than the dyke formation. Age determination of the dyke constrain the latest age of the crush zone activity.

Excavation survey of basement rocks at the Monju site shows a basaltic dyke (ca. 19Ma, Plagioclase K-Ar age) cut by the crush zone (crush zone alpha-3 and alpha-4) indicate that the movements of these crush zones are later than the dyke formation.

### 2. Structural-oriented turn determination of crush zone activity

Intersecting relationship between crush zones indicate which of them is the latest one at least locally. This rule can be hold in the case of conjugate set, although they suggest the contemporaneous development in one tectonic stage. Conjugate relations should be judged from traditional Griffith-Coulomb failure criterion as well as the Maximum effective moment criterion<sup>(1)</sup>. Despite of the development of remarkable clay rich zone, cross cutting crush zone with meso- and microstructures developed under the higher temperature and pressure indicate the movement of the clay rich zone is older.

Excavation survey of basement rocks at the Monju site shows conjugate like development of the crush zone beta and younger alpha-3 with 50-55 degrees between them. The crush zone beta is composed of clay rich vein. Along the crush zone alpha-3, dragged sigmoidal quartz veins, dragged biotite along shear layers and preferred orientation of quartzo-felspathic lenses composed of foliated cataclasite with P-Y-R<sub>1</sub> fabric are observed. These ductile features suggest that relatively higher temperature and pressure during the development of crush zone alpha-3. Hence, the crush zone beta is old structure.

These stratigraphic and structural evidences for the turn determination indicate that the activity of crush zone alpha-3 is the object of the evaluation.

(1)Zheng et al., 2004, Journal of Structural Geology, 26, 271-285.

Keywords: fast breeder reactor Monju, survey of crush zone, Kojaku granite

## Depth-dependent coseismic groundwater level changes by seismic ground motion of the 1999 Chi-Chi earthquake, Tiwan

HIGA, Mayumi<sup>1\*</sup>; NAKAMURA, Mamoru<sup>2</sup>; KOIZUMI, Naoji<sup>3</sup>; LAI, Wen-chi<sup>4</sup>

<sup>1</sup>Faculty of Science and Graduate School of Engineering and Science, University of the Ryukyus, <sup>2</sup>Faculty of Science, University of the Ryukyus, <sup>3</sup>Geological Survey of Japan, National Institute of Advanced Industrial Science and Technology, <sup>4</sup>Disaster Prevention Research Center, National Cheng Kung University, Taiwan

The coseismic water level change (Cw) has been reported (Montgomery and Manga, 2003; Koizumi, 2013). One of the causes of the Cw is crustal displacement (static strain change and vertical displacement etc.), and seismic ground motion (dynamic volumetric strain change and hydraulic conductivity change etc.) (Lee *et al.*, 2002; Lai *et al.*, 2004; Wang *et al.*, 2001). The static strain change has been assumed as one of the main factor of the water level change from the comparison of water level change with static strain change in the earthquakes. However, the relation between water level change and static strain change doesn't correspond clearly. Although the dynamic strain change by the ground motion would be more effective to the cause of Cw, the effect has not been known yet.

The Chi-Chi earthquake (Mw7.6) occurred in central Taiwan at 1:47 (local time) on September 21, 1999. The earthquake was the largest event which occurred recently in the inland of Taiwan. Since the both networks of strong motion seismometer (Lee *et al.*, 1999) and water level monitoring system (Koizumi, 2001) are distributed densely around the source fault of the Chi-Chi earthquake, good seismic waveform and the data of Cw has been obtained.

For the previous study of Cw in the Chi-Chi earthquake, Wang *et al.* (2003) has been analyzed the relationship between Cw and seismic ground motion from the point of view of liquefaction at the shallow groundwater in the alluvial plain part. They showed that there is correlation between the spectrum velocity or acceleration and water level. However, they did not account much for the effects of the permeability or other characteristics in each aquifer although they analyzed the Cw of all wells at once. Since the hydrogeological conditions effects to the occurrence of liquefaction similar to the effect of ground motion, the effect for the hydrogeological conditions, that is the geological characteristics and permeability of aquifer in confined aquifer or unconfined aquifer, must be investigated.

We divided the aquifer to similar hydrogeological categories and examined the Cw response by the ground motion in each aquifer. We put target groundwater of two aquifer, the shallow aquifer 1 (unconfined aquifer) and underlying aquifer 2 (confined aquifer), and investigated whether there are the different character in those. I measured the degree of Cw. Therefore the wells observed Cw were 84 wells, fall wells were 14 wells in these wells. I used the observation wells with water level rises in the alluvial plain part, because the mechanism of water level change for water level fall is different. We investigated the relationship spectral response of seismic wave and groundwater level change, because spectral response can read the effect to the ground in comparison spectrum of normal. We calculated the response of Cw against the frequency of 1 Hz (high-frequency) and 0.1 Hz (low-frequency) to evaluate the groundwater level change as a function of frequency. We calculated the acceleration, velocity, and displacement spectral response of vertical, horizontal, and 3 components from acceleration waveform data. I investigated the correlation coefficient between spectrum and Cw in each aquifer. The result frequency band in those show different response was obtained. Correlation between the response spectrum and water level change in the high-frequency side (1 Hz) was higher in the aquifer considered unconfined aquifer, but the correlation in low-frequency side (0.1 Hz) was higher in the aquifer considered confined aquifer. In common to both aquifer, correlation between hydraulic conductivity and water level change showed strong positive correlation.

Keywords: Groundwater level changes, The 1999 Chi-Chi earthquake, Taiwan, Seismic ground motion

## Occurrence of faults and water conducting features at 350m gallery of the Horonobe URL project

HAYANO, Akira<sup>1\*</sup> ; MATSUOKA, Toshiyuki<sup>1</sup> ; ISHII, Eiichi<sup>1</sup>

<sup>1</sup>Japan Atomic Energy Agency

In the Horonobe Underground Research Laboratory Project, methodology development for the investigation of geological structure in sedimentary rocks has been carried out through construction of underground facility. As part of the methodology development, hydrogeological models have been constructed and the geological structure associated with water-conducting features (WCFs) has been conceptualized on the basis of the surface-based investigations including geophysical survey, outcrop observation and borehole investigation. The horizontal gallery named ' 350m gallery ' and having approximately 740m long in total has been excavated at a depth of 350m below the surface by January 2014. This study presents the predictive distribution of geological structures contributing to WCFs in 350m gallery based on the surface-based investigations and the characteristics of geological structures observed in 350m gallery.

Keywords: Hydrogeological model, Fault, Water-conducting feature

## Permeability variation in Toki granite and its relationships with crack structure and alteration processes

KUBO, Taiki<sup>1\*</sup> ; MATSUDA, Norihiro<sup>1</sup> ; KASHIWAYA, Kouki<sup>1</sup> ; KOIKE, Katsuaki<sup>1</sup>

<sup>1</sup>Kyoto University

Understanding of physical and chemical properties of rock mass is essential to implement the geological disposal of the high level nuclear waste. Especially, extraction of highly permeable zone that acts as channel of fluid flow is required. In this study, permeability measurements of Toki granite were carried out to reveal the permeability variation in rock mass and to understand factors causing that. Image analysis was applied to disc-like specimens and thin sections of the granite, for quantitative characterization of crack structure. Additionally, fluorescent X-ray analysis (XRF) was carried out to obtain elemental compositions of granite cores showing various degrees of alteration and to consider the relationship of the permeability with the alteration degree.

Permeability was measured using the gas permeameter. The samples are cores collected from about 1 kilometer depth range boreholes in Tono area (Mizunami, Gifu, Japan) drilling by Japan Atomic Energy Agency (JAEA). Over 40 granite cores were sampled at 25-meter intervals ranging from 100 to 1000 meters depth to measure the permeability. Permeability was larger in the altered and fault zones. In addition, the anisotropy was appeared around the fault part and the permeability was enhanced along E-W direction. This direction is consistent with the fault strike, and thus the anisotropy of the permeability was presumably caused by the cracks developed in the fault movement.

Next, the crack structures were quantitatively characterized using an image analysis and compared with the permeability data to clarify their relationship. The specimens were impregnated with fluorescent resin and images were acquired to characterize the mesocrack structure using a fluorescent scanner equipped with ultraviolet ray source. Additionally, thin sections were made from the specimens and microphotographs for characterizing microcracks were taken with a stereomicroscope. Cracks were extracted from these images and length and direction of each crack were determined by the image analysis, following segmentation of crossing cracks. Positive correlation was observed between the permeability and cumulative crack length. These results suggest that cracks cause the permeability anisotropy and microcrack can be a factor controlling the permeability.

XRF was carried out to examine relationships between the permeability and the alteration processes of Toki granite. Positive correlations were recognized between the permeability and Ca concentration in the cores. Hydrothermal alteration of Toki granite is considered to follow three steps, 1) chloritization of biotite, 2) illitization of plagioclase, and 3) precipitation of calcite (Nishimoto and Yoshida, 2010). Considering that precipitation containing Ca is formed in the illitization of plagioclase, strong hydrothermal alteration presumably occurred in the altered and fractured zones that show relatively high Ca concentration. It implies that these zones were highly permeable as forming flow paths of hot water in the past. Although the fault-zone core had high permeability, its Ca concentration was relatively low. Fault movement caused development of fault gouge in addition to fracturing of granite. Permeability was enhanced by the fracturing, but the impermeable fault gouge occurred in the fault interfered circulation of hot water and addition of Ca precipitation.

These results suggest that fractured zone accompanying densely distributed microcracks and altered zone can be groundwater flow paths. Distribution of the highly permeable zones is essential to understand the hydrogeological structure.

Acknowledgement: We would like to express our sincere thanks to the co-researchers of Japan Atomic Energy Agency for their supports and many constructive comments for this study.

### References

Nishimoto, S., Yoshida, H. (2010): Hydrothermal alteration of deep fractured granite: Effects of dissolution and precipitation, *Lithos*, vol. 115, pp. 153-162.

Keywords: fracture system, permeability, microcrack, altered zone, hydrogeological structure, Toki granite

## The relation between imaging of soil structure with GPR and depth profile of radioactive cesium

WATANABE, Takayoshi<sup>1\*</sup> ; MITACHI, Katsuaki<sup>1</sup> ; ABE, Hironobu<sup>1</sup> ; NIIZATO, Tadafumi<sup>1</sup>

<sup>1</sup>Japan Atomic Energy Agency

Radionuclides such as radioactive cesium, now the main radiological contributor, were released in the environment by the Fukushima Dai-ichi nuclear power plant accident. The government and local governments have proceeded with decontamination plans to reduce dose rate in living spheres. But most areas of forests have been still contaminated. Japan Atomic Energy Agency initiated a project entitled 'Long-Term Assessment of Transport of Radioactive Contaminant in the Environment of Fukushima' (F-TRACE project) in November 2012. Main objective of this project is to implement a comprehensive system for predicting radioactive cesium transport in the future and the impact of various countermeasures by understanding transport of radioactive cesium from forests to living spheres and the sea through rivers and dams.

To understand radioactive cesium transport in forest, we have conducted forest investigation at Ogi district, Kawauchi Village and Yamakiya district, Kawamata Town, Fukushima Prefecture since December 2012. As a part of the investigation, we carried out geophysical exploration of soil structure with ground penetrating radar (GPR) with 100MHz and 500MHz radio wave.

In this presentation, we report correlation between imaging of soil structure obtained by GPR survey and depth profile of radioactive cesium in soil.

Keywords: ground penetrating radar, depth profile of radioactive cesium, F-TRACE project

## Current situation and improvement of methylene blue adsorption testing method for bentonite

HORIUCHI, Yu<sup>1\*</sup> ; MIYOSHI, Youko<sup>1</sup> ; TAKAGI, Tetsuichi<sup>1</sup>

<sup>1</sup>Geological Survey of Japan

Large amount of bentonite will be required as shielding material for radioactive waste disposal from nuclear power plant and contaminated soil management of Fukushima disaster. The testing methods of bentonite performances are important in terms of the safety of the disposal facility. Methylene blue (MB) adsorption test, which has generally been used for determining either cation exchange capacities (CEC) or surface areas of bentonite, is one of the important testing methods. However, current testing method of MB adsorption is different for each company and it is difficult to compare the performance of bentonite products. Since the current standard testing methods, which are developed by JBAS in the 1970s, are obsolete already, it is necessary to renew the standard testing methods. Therefore, we are planning to propose new standard testing methods for bentonite as JIS, based on this study.

In this study, we interviewed 13 companies and conducted questionnaire about the details of the current MB adsorption testing method. As the result, 10 companies are currently doing MB adsorption test. Of the 10 companies, MB adsorption test based on conventional JBAS method is conducted in eight companies. In addition, four companies are using their own methods, such as colorimetric method which is not defined in the JBAS, including 2 companies using compound of JBAS and colorimetric methods. The tests based on conventional JBAS methods have variation among companies in terms of determining the end point, reagents and sample preparations. Short testing time and simple decision of end point were raised by several companies, as the reasons for using their own methods such as colorimetric method.

As consider in result of interview, the method which aims to propose in this study is required of eliminating the ambiguity of the conventional method, minimal use of consumables, and streamlining for time saving. At the same time, sufficient accuracy is required with this method for ensuring safety in waste disposal. In future, it needs to consider time of reaching adsorption equilibrium, and dispersion and adsorption properties of bentonite by different localities and conditions.

Keywords: bentonite

## The sedimentary process and distribution of tsunami deposits in coastal lakes: a flume experiment

YAMAGUCHI, Naofumi<sup>1\*</sup> ; SEKIGUCHI, Tomohiro<sup>2</sup>

<sup>1</sup>Center for Water Environment Studies, Ibaraki University, <sup>2</sup>Center for Research in Isotopes and Environmental Dynamics, University of Tsukuba

A series of flume experiments were performed to examine the sedimentary process and distribution of tsunami deposits in coastal lakes. In the experimental program, a fixed slope of 1/20 and terrestrial area including a pool as a coastal lake were installed, and tsunami-like solitary wave was generated. The tsunami flow transported sediments from a sand bed placed on the slope, and deposited them on the terrestrial area. When the tsunami flow irrupted into the pool, hydraulic jump was occurred. In the area where the hydraulic jump made turbulence, little sediment deposited. Thus, the distribution of the tsunami deposits in the pool did not always show the thinning-landward trend in the present experimental series. The dependence of the amount of sediments on magnitude of tsunami waves was more pronounced in the pool than the land area.

Keywords: tsunami deposit, flume experiment, coastal lake

## Variations of terrigenous organic carbon content in flood and slope failure sediments

OMURA, Akiko<sup>1\*</sup>; IKEHARA, Ken<sup>2</sup>; KATAYAMA, Hajime<sup>2</sup>; USAMI, Kazuko<sup>2</sup>; IRINO, Tomohisa<sup>3</sup>; KUWAE, Michinobu<sup>4</sup>; ASHI, Juichiro<sup>5</sup>

<sup>1</sup>JSPS Research Fellow, Univ.Tokyo, <sup>2</sup>IGG, AIST, <sup>3</sup>Hokkaido Univ., <sup>4</sup>Ehime Univ., <sup>5</sup>Univ. Tokyo

In this study, we analyzed the stable organic carbon isotope of sea floor sediments, which were deposited by the modern large floods with typhoon and the slope failure with earthquakes. Stratigraphic variations of terrigenous organic carbon content in the flood sediments were different from those of slope failure sediments.

Sediment cores KH-11-9-FB12 and FB14 were corrected from the deep-sea floor off the Kumano River mouth, which is located on the Kii Peninsula. The sediment cores contain flood-induced sediments by large typhoon in September, 2011, the largest 20<sup>th</sup> century typhoon, and the large 19<sup>th</sup> century Totsukawa flood (Ikehara et al., 2012). These flood-induced sediments have high terrigenous organic carbon content. The base of turbidite, which include wood fragments, has highest peak of terrigenous organic carbon content. On the other hand, terrigenous organic carbon content of the lower part of turbidite mud are lower than those of the middle and upper parts of turbidite mud. The stratigraphic variations of terrigenous organic carbon content is not recognized in the middle and upper parts of turbidite mud.

Sediment cores 95A and 104A were corrected from the shallow depression on shelf off the Saru River mouth, Hokkaido, in 2007. These cores contain the sediments by the severe flood with typhoon in August, 2003. The shallow depression on shelf, which is thought to be the old river path during lowstand of the last glacial age, was suitable for preservation of the flood-induced sediments (Katayama et al., 2007). The lower part of the turbidite mud has low terrigenous organic carbon content and the middle and upper parts have high terrigenous organic carbon content. The stratigraphic variations of terrigenous organic carbon content is not recognized in the middle and upper parts of turbidite mud. The turbidite mud off the Saru River mouth have same characteristics as those off the Kumano River mouth. These results suggest that the lower part of flood-induced sediments were formed by erosion and deposition of sea-floor sediments during the early stage of flood. The middle and upper parts were considered to be formed by continuous supply and deposition of terrigenous materials from river mouth during the flood.

The sediment core BP09-6 was corrected from the Beppu Bay. The sediment core contains the slope failure sediments by the large earthquake in 1596 (Keicho-Bungo earthquake; Kuwae et al., 2013). The slope failure sediments are characterized by upward decreasing of terrigenous organic carbon. This result suggests that the turbidity currents were caused by collapse of delta slope sediments, which contain both terrigenous and marine organic materials.

Stratigraphic variations of terrigenous organic carbon content might be important information, when we investigate the records of paleo natural disasters with sea-floor sediments.

### References

Ikehara, K. et al., 2012, Unique 210-Pb and 137-Cs profiles in marine sediment cores containing recent event deposits off Kumano and Sanriku Japan. *2012 Annual Meeting of Geological Society of America*.

Katayama, H. et al., 2007, Distribution of surface sediments after the 2003 flood on the shelf off Hidaka, southern Hokkaido. *Bull. Geol. Surv. Japan*, 58, 189-199.

Kuwae, M. et al., 2013, Stratigraphy and wiggle-matching-based age-depth model of late Holocene marine sediments in Beppu Bay, southwest Japan. *Journal of Asian Earth Science*, 69, 133-148.

Keywords: turbidite mud, hemipelagites, organic carbon, natural disasters

## Quartzose sand and kaolinite-dominated mud derived from felsic plutonic rocks in intense weathering condition

YOSHIDA, Kohki<sup>1\*</sup> ; HATANO, Nozomi<sup>1</sup> ; MORI, Saori<sup>1</sup> ; IRIE, Shiori<sup>2</sup> ; ADACHI, Yoshiko<sup>3</sup>

<sup>1</sup>Shinshu University, <sup>2</sup>Inpex Cooperation, <sup>3</sup>Center for Transdisciplinary Research, Niigata University

In the Upper Miocene - Early Pliocene time, Japanese island had a warm and subtropical climate. The mineralogical and chemical compositions of sand and mud of the Upper Miocene Tokiguchi Porcelain Clay and the Early Pliocene in the Kobiwako Group were examined for sedimentary petrography and geochemistry to clarify the influence of the warm climatic condition on sediment composition. Both sediments are considered to have been produced from felsic crystalline basement provenance. These sediments are characterized by the deposition in warm and humid climate on the basis of plant and diatom fossils.

The humid tropical climate produced quartz rich sand and kaolinite rich mud. The Upper Miocene sediments indicate that mafic silicates and feldspars were destroyed so that the sand ranges from arkoses with plagioclase rich sand to subarkoses with dominant of K-feldspar. The Upper Miocene mud show kaolinitic clay mineral composition and aluminous chemical composition. In contrast, the Pliocene sand is arkosic to litharenitic with abundant of feldspars and accessory minerals. In the Pliocene mud, an increase in the relative abundance of smectite accompanies the breakdown of volcanic fragments and volcanic glass is detected.

The intense weathering, rare earth elements (REE) are concentrated in mud. The Miocene sand shows the REE concentration less than one of PAAS level, whereas the Miocene mud display similar level of concentration in PAAS. In many samples, the REE concentration is mostly by biotite and zircon evidenced by HREE concentration.

The intense weathering condition, such as high temperature with humidity, affects the sand and mud compositions with selective destruction of minerals and newly formation of clay minerals. The relative increase of HREE, which is mainly housed in durable minerals, and mineral assemblage of sand and mud probably provide quantitative estimation of weathering degree for the sediments derived from felsic plutonic rocks.

Keywords: Miocene, sand composition, mud composition, REE composition, weathering

## Depositional environment of the recent Yangtze Delta sediment deduced from the natural gamma-ray spectroscopy of YD13-G2

IRINO, Tomohisa<sup>1\*</sup>; WANG, Ke<sup>1</sup>; SAITO, Keita<sup>2</sup>; TADA, Ryuji<sup>2</sup>; SUZUKI, Yoshiaki<sup>2</sup>; KUBOKI, Yui<sup>2</sup>; SUGISAKI, Saiko<sup>2</sup>; ZHENG, Hongbo<sup>3</sup>

<sup>1</sup>Hokkaido University, <sup>2</sup>University of Tokyo, <sup>3</sup>Nanjing Normal University

The Yangtze River has transported approximately 500 mt/yr of sediments which formed a well-developed tide-dominated delta on its mouth during the Holocene high-stand. Sediment transport is dominant in rainy summer season or during flooding events, and the 40% is deposited in the estuary and the remaining sediments are transported offshore by tide forming a submerged delta or re-transported southward during stormy winter season. Due to these seasonally contrasted and event driven feature of sedimentation, spatial distribution of the accretion and erosion of the delta body is highly heterogeneous.

The Holocene subaqueous delta sediment has been also used as good sediment archives of the history of the Yangtze discharge and flooding due to its high sedimentation rate and good coverage of the Late Holocene. We also performed drilling of the delta sediment and collected two ~30 m drilling cores and four gravity cores in order to reconstruct the flooding history and the associated change in the detrital provenance. The drilled site (YD-13) is located on clayey bottom with the water depth of 40 m. The top 10 m of the sediment core consists of homogeneous clay with rare sand patches, which could be formed during the Holocene high stand. One of the gravity core (YD13-G2) recovers the 140 cm of surface sediments, and we decided to examine the natural gamma-ray spectrum and stacking pattern of this gravity core at 1 cm resolution in order to stationarity of sedimentation.

Since Cs-137 was not detected from the YD13-G2 sediment, even the surface material was judged to be older than 1950. Pb-210 is detected from the top 50 cm interval, which suggests the near-surface sediments were deposited during these ~100 yrs. However, the vertical profile of Pb-210 shows highly variable from zero to 25 Bq/kg with zigzag shape, which suggests repeated intercalation of old materials. Th-234 / K-40 and Ac-228 / K-40 ratios varies consistently suggesting some varieties in the provenance or grain size. Further examination is necessary to resolve potential event sedimentation and the apparent age of the related sediments.

Keywords: Yangtze Delta, Depositional environment, natural gamma-ray spectroscopy

## Provenance changes of Yangtze Delta core sediments and their implications for precipitation changes during the Holocene

WANG, Ke<sup>1\*</sup> ; TADA, Ryuji<sup>2</sup> ; IRINO, Tomohisa<sup>1</sup> ; ZHENG, Hongbo<sup>3</sup> ; SUGISAKI, Saiko<sup>2</sup> ; SAITO, Keita<sup>2</sup> ; KUBOKI, Yui<sup>2</sup>

<sup>1</sup>Hokkaido Univ., <sup>2</sup>Univ. of Tokyo, <sup>3</sup>Nanjing Normal Univ.

Understanding the complex evolution of the natural environment in response to changes in climatic boundary conditions is a major challenge. Changes in frequency and magnitude of flooding of the Yangtze in association with the variations in East Asian Summer Monsoon (EASM) precipitation during the Holocene is one of such examples. The Yangtze River catchment is particularly sensitive to periodic flooding and droughts caused by temporal and spatial variations in the seasonal precipitation regime.

As a joint research project with Nanjing Normal University, we conducted Yangtze Delta drilling to reconstruct temporal and spatial changes in precipitation within the Yangtze River drainage during the Holocene. Core YD13-1 (31°02' 59.9250" N, 122°50'00.2538" E) was recovered from Yangtze subaqueous delta at a water depth of 37 m, its penetration depth is 39.5 m, and probably covering the entire Holocene. The project focus on decadal/centennial-scale variability of river discharge and its provenance in the lower Yangtze reaches, deltaic system and East China Sea (ECS). It includes the study of the reconstruction of the flood history, the variability of fresh-water input and redistribution of Yangtze-derived sediments and Holocene floodplain development in these areas.

A new tool that use of electron spin resonance (ESR) signal intensity of the E1' center and the crystallinity index (CI) of quartz is introduced to characterize the provenance of the Yangtze River Delta sediments, which were derived from various parts of the Yangtze River drainage, and its temporal changes that should have reflected the spatio-temporal changes in precipitation and flooding. The result will contribute to a more accurate understanding of the changes in spatial precipitation pattern associated with rapid climatic changes, of evolution of the lower Yangtze river-delta-shelf system, and of the environmental and climatic conditions under which the process took place. Our previous research result from the mudbelt core in ECS suggests possible scenarios for the response of the Yangtze catchment to the changes in monsoon intensity and extreme events. New analytical result of the provenance proxy for core sediments from Yangtze River Delta will be presented and possible scenario will be discussed.

## Estimating mixing ratio of the sediments from tributaries in the sediments from Yangtze River mouth

SAITO, Keita<sup>1\*</sup> ; TADA, Ryuji<sup>1</sup> ; ZHENG, Hongbo<sup>2</sup> ; IRINO, Tomohisa<sup>3</sup> ; CHAO, Luo<sup>4</sup> ; MENG YING, He<sup>4</sup> ; WANG, Ke<sup>3</sup> ; SUZUKI, Yoshiaki<sup>1</sup>

<sup>1</sup>EPS, Univ. of Tokyo, <sup>2</sup>Nanjing Normal University, <sup>3</sup>Hokkaido University, <sup>4</sup>Nanjing University

Yangtze river is the largest river in eastern Asia. The rain front is accompanied with the development of summer monsoon, and moves within the Yangtze drainage, bringing heavy rain. Thus, the spatial fluctuation is also important for understanding the behavior of summer monsoon.

A paleoclimate record is needed for reconstructing the distribution of precipitation before metrological record. In Yangtze, over 95% of yielded sediment is suspended particle matter (SPM). The precipitation in drainage is proportional to water discharge, and water discharge is also proportional to suspended sediment concentration.

In this study, as a basis for reconstructing the past distribution of rain in Yangtze drainage, 1) analyze the ESR (Electron Spin Resonance) signal intensity of each tributary, 2) confirm that ESR values can explain the mixture of sediments in the mainstream, 3) discussing how large flood can be detected as a change of ESR values in the river mouth.

The sediments from major tributaries of Yangtze shows different ESR values each other. Using ESR values of each tributary as end members, the modern ESR value at rivermouth is estimated. The estimated value is consistent with the analyzed ESR value of sediments near rivermouth. So, ESR signal intensity can be used for estimating mixture of sediments.

We also calculated how large ESR value at rivermouth can change on the assumption that the flood occurs in specific tributaries. As a result, the flood can be detected as the change of ESR value at rivermouth when the sediment yield increases 5 times than usual.

## Evaluation of chemical weathering and sediment flux for several drainages within the Yangtze River basin

KUBOKI, Yui<sup>1\*</sup> ; LUO, Chao<sup>3</sup> ; TADA, Ryuji<sup>1</sup> ; SAITO, Keita<sup>1</sup> ; ZHENG, Hongbo<sup>2</sup> ; IRINO, Tomohisa<sup>4</sup> ; HE, Mengying<sup>3</sup> ; WANG, Ke<sup>4</sup> ; SUZUKI, Yoshiaki<sup>1</sup>

<sup>1</sup>Department of Earth and Planetary Science, The University of Tokyo, <sup>2</sup>Nanjing Normal University, <sup>3</sup>Nanjing University, <sup>4</sup>Graduate School of Environmental Science, Hokkaido University

Chemical weathering is closely coupled with erosion and driving landscape evolution. Silicate weathering plays a major role of fixing atmospheric CO<sub>2</sub> in the carbon cycle in time scales longer than 10<sup>5</sup> years. Therefore, quantitative estimation of chemical weathering rate and evaluation of its controlling factors are critical to understand its role on landscape evolution and controlling the carbon cycle on a long time scale. Researches on evaluating controlling factors of the weathering rates have been conducted using various methods and on various temporal and spatial scales, including theoretical approaches based on mineral dissolution experiments, empirical approaches based on analyses of river water, suspended material and sediments, and numerical modeling approaches to synthesize these data. Although empirical formulations of the chemical weathering and physical erosion rates specific to a certain river have been presented, processes of weathering and erosion should be considered together both from physical and chemical aspects in order to obtain more generalized formulas. Besides, in order to reconstruct the past processes of chemical weathering and erosion from the knowledge of the present processes, it is necessary to establish methods for reconstructing chemical vs physical weathering processes by using sediments which are the end products of weathering and erosion.

Toward the objective above, this study aims to explore the present processes of chemical weathering and erosion in the Yangtze River drainage as an example. Yangtze River is the longest river in Asia with the great water discharge and sediment flux. Hence, the river's role on material cycle on Earth's surface is significant. In addition, water and meteorological data are accumulated for long time period by many gauging stations and meteorological stations in the basin.

Mineral and chemical compositions of suspended particles and sediments as well as chemical composition of dissolved matter are analyzed for water samples and river bank sediments obtained from Yangtze River and its tributaries in the summer of 2011. Using these results, together with river discharge data and dissolved/suspended load concentrations, the fluxes for each element are calculated, and then the inputs from each watershed are obtained. Then, the relative contribution between chemical weathering and physical erosion is estimated. The calculation revealed that chemical weathering rate increases downstream but the relative contribution between chemical weathering and physical erosion in the uppermost part is the maximum in the upper, erosional part. In the lower, depositional part, dissolved carbonate is diluted after the main stream has merged with Poyang Lake, and then increased again toward the river mouth. The processes of chemical weathering and physical erosion in each watershed and their possible controlling factors will be discussed.

## Underwater topographic survey for inaccessible water areas, and its applications to submarine and sublake landslides

YAMASAKI, Shintaro<sup>1\*</sup>

<sup>1</sup>Kitami Institute of Technology

Landslides, volcanoes, active faults and other hazard related topographies exist on the sea floor or lake bottoms. It is important to investigate them for assessing future hazard potential. But investigations for these underwater topographies are not so easy because it needs quite high cost, and its heavy weight equipment also requires a ship big enough to hold it. These days, dramatically advanced leisure-use fish finders enable us to investigate underwater topographic survey from shallow to several hundred meters deep. These fish finders are low cost and light weight, so can be equipped on inflatable rafts that is accessible into ultra shallow area of 0.5 - 20 m deep that is usually inaccessible for usual scientific research vessels. Thus the investigating method using the fish finder and an inflatable raft is more versatile than other technical ways. Some advanced fish finders have a side-scan sonar system that obtains 2D image of acoustic reflections, and it can identify bottom materials and underwater structures. Now we are trying to apply for studying submarine and sublake landslides in water areas that have not been surveyed. This presentation shows successful examples of our conducted investigations for the sublake landslides in Lake Kussharo and the 1923 Nebukawa landslide that a part of the landslide dived into the sea. These results have contributed the innovative discussion in generation of tsunamis on the lake, and revealed unknown submarine ruins that landslide devastated.

Keywords: fish finder, submarine landslide, underwater landslide, bathymetric survey, side-scan sonar

## Development of a monitoring system of bathymetric change and related sediment transport using optic fiber cables

YOSHIKAWA, Shuro<sup>1\*</sup> ; SAKAGUCHI, Hide<sup>1</sup> ; AKUTAGAWA, Shinichi<sup>2</sup> ; MACHIJIMA, Yuichi<sup>3</sup> ; YUE, Zhao<sup>3</sup>

<sup>1</sup>JAMSTEC, <sup>2</sup>Kobe University, <sup>3</sup>LAZOC Inc.

A development of monitoring system is important for understanding more detailed process of the bathymetric change and sediment transport. At the nearshore zone, to monitor the nearshore features such as sand ripple migration, and the sediment suspension processes, optical back-scatter sensors (Downing et al., 1981), rotary sidescan sonar system (Traykovski et al., 1999), and sand ripple profiler (Masselink et al., 2007) were developed and used. Those systems can provide the very high-resolution morphological change and transportation, but not suitable for investigation of large-scale sediment erosion and deposition generated by high-energy waves in the surf zone. Where change in water depth is large (e.g. more than 1 m) in short span, the systems will be destroyed, lost, or submerged.

In the present study, we developed a new instrumentation for the monitoring of bathymetric change and related sediment transport in the high-energy shallow marine environment using optic fiber cables. The system consists mainly of four components: (1) an array of optical sediment sensors (OSSs); (2) a support structure (steel pipes); (3) an electronics unit that transmit and receive the LED through the optic fiber cables; and (4) a digital data acquisition system. The OSSs are mounted in a vertical steel pipe, 2 m long; and the spacing between the sensors is 10 cm. The steel pipe with OSSs was embedded to the seafloor at two places beneath a pier (427 m long) of Hazaki Oceanographical Research Station (HORS) owned by the Port and Airport Research Institute (PARI) at Sudahama Coast facing the Pacific Ocean, Japan. Both the electronics unit and the data acquisition system were installed in an observation room on the pier. In addition, those points of measurement are aligned perpendicular to the coastline in water depth approx. 4-5 m. Since active sediment transport that creates and deforms the longshore bar have been observed in this area (e.g., Kuriyama, 2010), detailed process of change in the cross section will be acquired by the present systems. In this presentation, we will show the system and data, and discuss those availability and future plan.

**Acknowledgment:** We would like to thank Dr. Satoshi Nakamura and Mr. Masayuki Banno belonging to the PARI for understanding and support of using the HORS, and MIKUNIYA Construction Co., Ltd. for installation work of the pipes. We wish to express our deep gratitude to the above-mentioned individuals and organizations.

**Keywords:** monitoring system, bathymetric change, sediment transport, optic fiber cable

---

HCG37-10

Room:421

Time:April 30 16:45-17:00

## New insight of tsunami excitation mechanism and its recordable evidence in deep-sea

KAWAMURA, Kiichiro<sup>1\*</sup>

<sup>1</sup>Yamaguchi University

Not yet

Keywords: Japan trench, 2011 Tohoku-Oki earthquake, Tsunami, Earthquake, Sediments, Submersible

## Deposition and preservation of fine-grained turbidites around the Japanese islands

IKEHARA, Ken<sup>1\*</sup> ; USAMI, Kazuko<sup>1</sup> ; NISHIDA, Naohisa<sup>1</sup>

<sup>1</sup>Geological Survey of Japan, AIST

We will report the sedimentological characteristics of fine-grained turbidites occurred around the Japanese islands such as off Sanriku, off Kumano, Suruga Bay, Beppu Bay, Japan Trench and off Hidaka. Some of these are thought to be formed in relation to the slope failures by the earthquake-ground shaking. Sometimes, subaqueous debris flow deposits were observed below the fine-grained turbidites. Agitation of the shelf floor by the tsunami waves is another mechanism to create the fine-grained turbidites. Third mechanism is the hyperpycnal flows related to the flood events. Preservation potential of the fine-grained turbidites will be discussed based on the repeated surveys of surface sediments off Sanriku region after the 2011 Tohoku-oki earthquake and its related tsunami. Based on these observation, we will discuss on the depositional processes of the fine-grained turbidites and preferable setting to preserve them as the geological records.

Keywords: turbidite, earthquake, tsunami, preservation potential, sedimentary structure, depositional process

## Comparison between the Tidal Zone Deposits and the Terrace Deposits Emerged in the 1703 and 1923 Kanto Earthquakes

KIM, Haeng yoong<sup>1\*</sup> ; MANNEN, Kazutaka<sup>1</sup> ; SASAGE, Kazuo<sup>2</sup> ; KUMAKI, Yohta<sup>3</sup> ; MATSUHIMA, Yoshiaki<sup>4</sup>

<sup>1</sup>Hot Springs Reserch Institute of Kanagwa Prefecture, <sup>2</sup>PASCO, <sup>3</sup>Senshu University, <sup>4</sup>Kangawa Prefecture Museum of Natural History

Recurrent giant earthquakes at the plate boundary along the Sagami Trough have been considered as one of the greatest thread of the Tokyo Metropolitan area. At the southwestern tip of the Miura Peninsula, in south of Tokyo, the tide gauge station records the coseismic uplift amount of 1.4 m and the interseismic subsidence amount of 0.3 m in and after 1923 earthquake, respectively. It is effective to reveal evidences of the past coseismic uplift to know the future earthquake.

Wave-cut benches which emerged in 1923 are widely distributed along the rocky coast. Higher wave-cut benches, good indicators of coseismic uplift prior to 1923, are also recognizable. It is, however, often difficult to spatially compare one another due to the erosion.

We investigated the distribution of the tidal-flat deposits and the 1923 wave-cut benches at two small bays in the southwestern and southern parts of the Peninsula. The aggradation of the coastline associated with the 1923 uplift was identified by the comparison between the 1:25,000 topographic maps before and after the 1923 earthquake. Observations of outcrops and drilling cores at the 1923-formed marine terrace showed that the tidal-flat deposits consist of shelly sand and gravels. The elevation of tidal-flat deposits indicates the coseismic uplift in 1923 and the interseismic subsidence after 1923. The uplift amount was estimated approximately 0.9 m and 2.1 m at the southwestern and southern parts of the Miura Peninsula, respectively. The uplift amount inferred from the tidal-flat deposits is concordant with that inferred by the wave-cut benches.

Keywords: Kanto Earthquake, Paleo-earthquake Record, Terrace Deposits, Tidal-flat Deposits

## The paleosols and topography of sedimentary basin relationships in the upper Miocene Clay deposit, central Japan

HATANO, Nozomi<sup>1\*</sup> ; YOSHIDA, Kohki<sup>2</sup>

<sup>1</sup>Division of Science and Technology, Graduate School of Shinshu University, <sup>2</sup>Department of Geology, Faculty of Science, Shinshu University

The Tokiguchi Porcelain Clay Formation is fluvial deposit distributed in central Japan in middle to late Miocene period. The sedimentary facies analyses were carried out in this formation. Those studies, however, were insufficient to reconstruct fluvial environment, because the fluvial deposit essentially have been bounded by short hiatuses due to sub-aerial erosion and paleo-surface formation. In this study, therefore, we focused on paleosols so as to reconstruct the weathering environment during the hiatuses. In general, paleosol formation in the fluvial sediments also depends on the supply of detritus and drainage conditions. Consequently it is very useful to research paleosol features for reconstruction of the topography in the small sedimentary basin where Tokiguchi Porcelain Clay Formation was deposited.

The clay-dominated sediments, which are interpreted to have been deposited in small sedimentary basin within a radius of 2 kilometers, were examined in two mines, Hishiya and Nakayama mines, across Toki and Tajimi Cities in Gifu Prefecture. The sediments in Hishiya mine shows the deposition in proximal area of the sedimentary basin, whereas those in Nakayama mine displays the facies formed in marginal area of the basin. On the sedimentary facies analysis, 13 facies are recognized in the formation. The sedimentary facies associations indicate the deposition mainly in backswamp environment with minor channel incision. Furthermore the coarse-grained sediments which were deposited as channel-bar and levee deposits intercalating debris flow deposits, with high accumulation rate, were particularly deposited in the marginal area of the basin. In contrast, the fine-grained sediments which were deposited with low accumulation rate in lakes and swamps, were particularly distributed in the proximal area of the basin. For this result, the fluvial system with lakes and swamps was developed near mountain slope side. In the whole are of the basin, approximately 20 paleosol horizons were founded in the lake and swamp deposits within a thickness of approximately 30 meters. In the proximal of the basin, these paleosol horizons range sparser. These paleosol horizons, with various pedogenic features, such as root with approximately 150 centimeters length and trunk traces with approximately 50 centimeters wide, pedogenic concretions, ped structures and microfabric of clay minerals, are formed thickly and developed clearly. In addition to, abundant siderite nodules covered with bright clay are present in lake deposit in the proximal area of the basin.

As a result the characteristics of the sedimentary facies could depend on the sedimentation rate depending on variation of the distance from the rim of the sedimentary basin. Besides the characteristics of the paleosol features could be affected by the drainage conditions due to morphological variation related to the location in the sedimentary basin. The characteristics of the sedimentary facies and paleosol features, however, suggest the large change of water level in the whole sedimentary basin. Concretely the redox condition had shifted from reductive condition in lakes or swamps to oxic condition in bushy grounds. The plausible cause for this change of redox condition in the sedimentary basin could be responsible for water-level change which was frequently occurred by damming of rivers formed from debris flow deposition.

Keywords: paleosols, Miocene, terrestrial environment, Tokiguchi Porcelain Clay Formation, sedimentary facies analysis

## Applications of a method to detect varved sediments

SASAKI, Hana<sup>1</sup> ; ISHIHARA, Yoshiro<sup>1\*</sup> ; SAITO-KATO, Megumi<sup>2</sup> ; KOMATSUBARA, Junko<sup>3</sup>

<sup>1</sup>Fukuoka University, <sup>2</sup>National Museum of Nature and Science, <sup>3</sup>Geological Survey of Japan / AIST

Studies of lacustrine deposits, especially on varved sediments, have further clarified the high-resolution record of paleoenvironments. Varved sediments are very useful for these studies because they are expected to contain annual records of depositional environments. In order to obtain annual records such as annual thickness, color tones, and chemical compositions, at the very least, it is necessary to detect the boundaries of annual bands. In addition, the detection and measurements should be reproducible.

Methods to measure boundaries of varved sediments are divided into two main categories: (1) measurement by visual judgment and (2) measurement by image analyses. The latter method uses photographs of the sediment, soft-X ray images, element maps, and so on. In order to detect boundaries, a threshold value, wavelet analysis, and wave analyses of the gray value of images have been previously used. While the visual judgment method has the disadvantages of human error and criteria, the image analysis method also has limitations as follows: one threshold value cannot be used for all locations in successive images; this method is dependent on the resolution of images, and it is affected by noise in the image-values.

In this study, we used a new method to detect the boundaries of banded deposits using the following procedure: (1) smooth the images, (2) calculate the inclination of "gray-value map" of the images, (3) calculate a mid-value in one wavelength of the "gray-value wave" in the map, and (4) detect a boundary as a point of the maximum inclination around the mid-value. The result obtained using this method shows well-defined "boundary map" of the bounded deposits, similar to the result obtained by visual judgment. Using this method, internal information, such as the transmittance value of soft-X ray in a lamina, can also be digitized like a lamina thickness. Since a time-series of lamina thickness and internal information of the lamina can be calculated based on this method, lamina-by-lamina facies analysis, such as that performed for detection of flood deposits, can be employed in studying varved deposits automatically and quickly.

Keywords: varved sediments, image analysis, time-series, soft-X ray, diatomite

## Depositional cycle and flood and slope-failure events in an 8,000-yr varve of Pleistocene Hiruzenbara Formation, Japan

SASAKI, Hana<sup>1\*</sup> ; ISHIHARA, Yoshiro<sup>1</sup> ; SAITO-KATO, Megumi<sup>2</sup> ; NARUSE, Hajime<sup>3</sup>

<sup>1</sup>Fukuoka University, <sup>2</sup>National Museum of Nature and Science, <sup>3</sup>Kyoto University

Paleoenvironmental changes can be reconstructed from varve deposits. The Middle Pleistocene Hiruzenbara Formation, which is distributed in the Hiruzen Highland, Maniwa city, Okayama Prefecture in Japan, is composed of mostly pure lacustrine diatomite that contains finely-laminated varves. From these varves, researchers have found decadal-scale depositional cycles that are thought to correspond to solar activities (Ishihara and Miyata, 1999), and intercalated flood- and slope-failure events have been detected. However, the relationship between the solar cycles and hydrogeological events remains unclear. In the present study, we sampled the finely laminated varves in the Hiruzenbara Formation, and obtained an 8,000-yr time-series of varve-thickness, gray-values for each lamina, variance of the gray-values, and deposits of flood- and slope-failure events using image analysis methods. Wavelet analysis and a fast Fourier transform (FFT) were applied to these time-series data to evaluate event-cyclicities.

In the time-series of varve-thickness, a long-term cyclicity of 1,000 - 2,000 yr was recognized. The upper parts of varves were light-green in color, and these were likely deposited during the winter season. Clear increases in thicknesses of the light-green parts were observed from the lower to upper parts of the analyzed section. Results from frequency analyses using the FFT and wavelet analysis of the time-series of varve-thickness data suggest that periods of 8 to 12 yr, 20 yr, and 30 to 35 yr dominate in this region. These periods were also found by Ishihara and Miyata (1999) and Masuda et al. (2004) in other sections of the formation. The periods in varves of 8 - 12 yr and around 20 yr correspond to solar activity, and a 35-yr periodicity of lake environmental change has been reported previously. In this study, however, these periods were not stable in the analyzed section, which is similar to the results obtained by Ishihara and Miyata (1999) and Masuda et al.(2004) who measured varve-thickness using a microscope.

One hundred-forty seven flood deposits were identified in the 8,000-yr record. Portions of the high-frequency parts and low-frequency parts were repeated in the analyzed section. Mean thickness of the flood beds was around 2 mm. Thirty-three deposits from slope failures were found in the section. These deposits were rare in the upper and lower most parts of the section, but were dominant in the lower part. There was no repetition of domination for the deposits that were observed during the flood events. Mean thickness of the slope-failure deposits was around 5.5 mm.

In the sections where flood deposits dominated, the mean varve-thickness tended to thinner without exception. In the upper part of the analyzed section, which lacked flood event signatures, the mean varve-thickness was generally greater. These trends suggest that climate conditions and the frequency of flood events might have affected the productivity of diatoms (thickness of the lamina). In addition, the periods detected by frequency analyses were not clear in the flood-deposit dominated sections. Results showing that dominations of slope-failure deposits were not related to the varve-thickness and the gray-values suggest that the slope-failure events were influenced by local phenomena related to lake development.

Keywords: Banded diatomite, Varve, Image analysis, flood deposit, slope-failure deposit, Solar activity

## Subsidence and a change of depositional environment by the 1662 Hyuganada earthquake in southern Miyazaki Plain

IKUTA, Masafumi<sup>1\*</sup> ; SATO, Yoshiki<sup>1</sup> ; NIWA, Masakazu<sup>1</sup> ; KAMATAKI, Takanobu<sup>2</sup> ; KUROSAWA, Hideki<sup>3</sup> ; TAKATORI, Ryoichi<sup>4</sup>

<sup>1</sup>Japan Atomic Energy Agency, <sup>2</sup>Akita University, <sup>3</sup>OYO Corporation, <sup>4</sup>Chi-ken Sogo Consultants Co.,Ltd.

The Miyazaki Plain, southern Kyushu Island, have been damaged repeatedly by a number of great earthquakes (measured or estimated to be >M7-8) occurred in not only the Nankai trough but also the Hyuganada coastal region. A total of six great earthquakes happened in the Hyuganada coastal region in the range of AD1909 to 1984. Historical documents indicate such great earthquakes had also occurred in AD1662, 1769 and 1899. Furthermore, the great earthquakes in the Nankai trough, such as the 1707 Hoei Nankai earthquake and the 1946 Showa-Nankai earthquake, had also attacked the plain with terrible tsunamis (Usami *et al.*, 2013).

Recently, the Nankai trough has received extensive attention as hypocenter of great earthquake attacking the Miyazaki Plain, because the Central Disaster Management Council (2012) proposed a new source model of the earthquakes including the Hyuganada coastal region. On the other hand, previous geological and seismological studies about past Hyuganada earthquakes are much less than the Nankai trough despite of their high seismic activity indicated by historical documents.

For example, historical documents shows that the 1662 Hyuganada earthquake brought about serious social and natural damages to the plain (Hatori, 1985). Especially, around the estuaries of the Oyodo-gawa River and the Kaeda-gawa River in southern area of the plain, the tsunami with about 4-5 m height and ~1 m subsidence occurred. This coseismic subsidence made a coastal lagoon around the estuarine area of the Kaeda-gawa River (Shimayama region). After buried by riverine debris, this lagoon was reclaimed and became paddy fields (Miyazaki-city, 1978).

The purpose of our study is to clarify depositional changes around the Shimayama region including coseismic geomorphological change. A multiple geological borings were carried out in the study area. Depositional environments were reconstructed inferred from paleontological, geochemical analyses. Depositional ages of core sediments were estimated by radiocarbon ages. The surface geology was divided into four layers mainly (layer A, B, C and D) in ascending order. The layer A was composed of alternate layers of grayish sand and silt with many angular pumices and organic materials. The layer B consisted of alternate layers of gray or grayish brown mud and sand including numerous well-preserved molluscan fossils. The bottom of the layer B, which covered the layer A above ~1.5 m T.P. with 10 to 40 cm thick, was black or dark gray muddy fine sand with bioturbation including rip-up clasts, shell fragments and volcanic rocks with >1 mm diameter. The layer C was composed of gray silt with several thin layers of fine to medium sand and plant fragments. The layer D consisted of silt to fine sand layers and surface cultivated sediments with ~20 cm thick overlying them.

Result of some analyses showed their quantitative differences corresponding to depositional facies. The main diatom components of the lower part of the layer A was fresh water benthic species such as *Cymbella turgidula* and *Gomphonema parvulum*, and the upper was few diatom fossil. On the other hand, the layer B showed abundance of brackish to marine water species such as *Cocconeis scutellum* and *Thalassionema nitzschioides*. In addition, absorbed water analysis of the core sediments showed that K, Ca, Na, Mg and SO<sub>4</sub><sup>2-</sup> concentration, which are rich in sea water, were few in the layer A but increased drastically at the bottom of the layer B. And grain size and molluscan fossils species were also different between the layer A and B.

These results indicate that depositional environment changed drastically from fresh water marsh or shallow pond to tidal or inner bay. Depositional ages of the layer A, B and C were estimated from radiocarbon ages to be AD1445 to 1595, AD1549 to 1771 and AD1651 to 1771 respectively and suggest that the depositional environment between the layer A and B correlate to crustal deformation by the 1662 Hyuganada earthquake.

Keywords: Hyuganada earthquake, Miyazaki Plain, depositional environment

## Selected organisms for systems of life-support in closed bio-ecosystem, and the chemical circulation

TOMITA-YOKOTANI, Kaori<sup>1\*</sup>

<sup>1</sup>University of Tsukuba

Living organisms on the earth have been evolved since its origin a long time ago. They equip several important functions affecting each other. Knowledge on those functions and interaction of the ecology is essential for secure design of a closed-ecosystem with limited number of living species under the harsh environments, such as space and deep sea or desert. The important elements related to the closed bio-ecosystem have to be discussed among the researchers, having each specialized field. Here, we will discuss the detail of species of several selected organisms for the closed bio-ecosystems and its chemical circulation.

Keywords: chemical circulation, closed bio-ecosystems

## Dry heat tolerance of the dry colony in *Nostoc* sp. HK-01 for useful usage in closed bio-ecosystems

KIMURA, Shunta<sup>1\*</sup> ; KATO, Hiroshi<sup>2</sup> ; SATO, Seigo<sup>1</sup> ; TOMITA-YOKOTANI, Kaori<sup>1</sup>

<sup>1</sup>University of Tsukuba, <sup>2</sup>Mie University

Closed bio-ecosystem as an artificial design requires the high flexibility and versatility system. As one of elements for all of introduced organisms, heat tolerance is important one such closed environment. *Nostoc* sp. HK-01 is one of terrestrial cyanobacterium having a high dry tolerance and it has several ability, photosynthesis, nitrogen fixation and usefulness as a food, it is thought that it can be used for bio-chemical circulation in a closed ecosystem, including space. Besides, a study on each tolerance predicted at the time of introduction to a closed bio-ecosystem is necessary. Therefore, as one of the tolerance that are intended to space environment, dry heat ( 100 °C, 10 h ) tolerance of dry colony in *Nostoc* sp. HK-01 has been investigated, but the detail function of them has not yet been elucidated. We focused on the extracellular polysaccharides ( EPS ) having the various tolerance, desiccation, low temperature, NaCl, and heavy particle beam. We will consider the function and useful usage of this cyanobacterium in closed bio-ecosystems after the consideration of the results of contribution of the possibility that EPS improves dry heat tolerance under a dry condition.

Keywords: bio-chemical circulation, closed bio-ecosystem, cyanobacteria, dry heat tolerance, extracellular polysaccharides, *Nostoc* sp. HK-01

## Utilization of the terrestrial cyanobacteria

KATOH, Hiroshi<sup>1\*</sup> ; YOKOSHIMA, Mika<sup>2</sup> ; KIMURA, Shunnta<sup>2</sup> ; FURUKAWA, Jun<sup>2</sup> ; TOMITA-YOKOTANI, Kaori<sup>2</sup> ; YAMAGUCHI, Yuji<sup>3</sup> ; TAKENAKA, Hiroyuki<sup>3</sup>

<sup>1</sup>Mie University, <sup>2</sup>University of Tsukuba, <sup>3</sup>MicroAlgae Corporation

The terrestrial, N<sub>2</sub> -fixing cyanobacterium, *Nostoc commune* has expected to utilize for agriculture, food and terraforming cause of its extracellular polysaccharide, desiccation tolerance and nitrogen fixation. Previously, the first author indicated that desiccation related genes were analyzed and the suggested that the genes were related to nitrogen fixation and metabolisms in *Nostoc(Anabaena)* sp. PCC 7120. In this report, we suggest possibility of agriculture, using the cyanobacterium. Further, we also found radioactive compounds accumulated *Nostoc commune* (cyanobacterium) in Fukushima, Japan after nuclear accident. Thus, it is investigated to remove radioactive compounds from soil by the cyanobacterium and showed to accumulate radioactive compounds using the cyanobacterium. We will discuss utilization of terrestrial cyanobacteria under closed environment.

Keywords: desiccation, terrestrial cyanobacteria, bioremediation, agriculture, decontamination

## Evaluation of functional components in selected organisms as food after cooking in closed bio-ecosystem

KIMURA, Yasuko<sup>1\*</sup> ; KATOH, Hiroshi<sup>2</sup> ; CHIDA, Yukari<sup>3</sup> ; NITSU, Fumie<sup>3</sup> ; SATO, Seigo<sup>3</sup> ; TOMITA-YOKOTANI, Kaori<sup>3</sup>

<sup>1</sup>Jumonji University, <sup>2</sup>Mie University, <sup>3</sup>University of Tsukuba

We have been studying life-support in closed bio-ecosystem to provide food and oxygen for the habitation area in the sever environment. To select the species of organisms is very important matter because it is difficult to use all the species of creature for the system. We have been proposing the several species of organism as the candidate species. In this time, we have selected and show terrestrial cyanobacteria and tree that have a possibility as high contributed materials for the induction into the closed systems. Here, we will discuss about the changes of the functional components produced from each materials, after their cooking.

Keywords: Cyanobacteria, tree plant, food, closed bio-ecosystem

## Study of Closed Life Support System for Manned Space Exploration

SAKURAI, Masato<sup>1\*</sup>

<sup>1</sup>JAXA

To further advance manned space exploration, a critical issue that must be addressed is recycling of resources, especially air revitalization and water reclamation. Japan is already a leader in terrestrial environmental technologies, and aims to apply this know-how to develop air and water recycling technologies for space applications. To support proposed post-ISS missions such as manned lunar or asteroid exploration and an Earth-Moon Lagrange point (EML1) space station, JAXA is developing an air revitalization system for an on-orbit demonstration on the International Space Station (ISS) early in the extended ISS operation period (2015-2020). The requirements for this technical demonstrator have been investigated and its specifications established. Regenerative life support functions include oxygen recovery from carbon dioxide using a combination of CO<sub>2</sub> reduction by a Sabatier process and O<sub>2</sub> generation by electrolysis. Each air and water re-vitalization subsystem is planned to be transported to the ISS separately by H-II Transfer Vehicle (HTV) launches in the Water Electrolysis This paper presents the air re-vitalization system developed by JAXA, and gives details of water electrolysis in microgravity.

A technical issue with space electrolysis systems is that gas-liquid separation is fundamentally different in a microgravity environment to its behavior in a gravity field. It is supposed that the electrode surface will become covered with generated gas. In microgravity, the gas will have to be removed using forced convection. A water/gas separator will be used to separate gas and water.

**Keywords:** Life Support System, Manned Space Expolaration, Air Re-vitalization, Microgravity, Closed System, Water Electrolysis

## Human body and oxygen

SHIMIZU, Tsuyoshi<sup>1\*</sup>

<sup>1</sup>Shimizu Institute of Space Physiology, Suwa Maternity Clinic Hospital

We found recently that a mild hyperbaric condition with a mild hyper oxygen-concentration ,which was maintained in the special container called as Ishihara's original oxygen capsule, was effective to treat infertility women patients. This result did let us realize again an importance of oxygen for cells and tissues of human body . In space development effects of microgravity, space radiation and other various environmental factors have been extensively

investigated and discussed, however we should also remember again that oxygen is the basic component to support our body in the space environment as well as on the earth. In this presentation I will summarize over again the meaning of presence of oxygen related to human body for future space development.

Keywords: oxygen, human body, space environment

## Growth of *Hydrobryum puncticulatum*(*Yakushimakawagoromo*) may be blocked by the increase of *Melosira varians* in Isso River

KITABUCHI, Hiroyuki<sup>1\*</sup> ; NAGAFUCHI, Osamu<sup>1</sup> ; NAKAZAWA, Koyomi<sup>1</sup> ; YOKOTA, Kuriko<sup>2</sup> ; TETUKA, Kenshi<sup>3</sup> ; AYUKAWA, Kazuyasu<sup>4</sup> ; TANABE, Masahiro<sup>5</sup>

<sup>1</sup>The University of Shiga Prefecture, <sup>2</sup>Toyohashi University of Technology, <sup>3</sup>Yakutane-goyou Research Group, <sup>4</sup>Environmental System Co., Ltd, <sup>5</sup>Nikkaki Bios Co., Ltd

*Hydrobryum puncticulatum* (*Yakushimakawagoromo*), the national monument and endangered species are making their habitat only in Isso river of Yakushima. For the first time in our observation, the bloom of *Melosira varians* which is periphyton of diatom was observed to be covered over the *H.puncticulatum* from 2011. This impact for the *H.puncticulatum* is a serious concern. The purpose of this study is to clarify the cause of bloom of *M.varians*. We examined the annual variability of dissolved nutrient concentration which was most accessible to *M.varians*. As a result, there was no increase in concentration of NO<sub>3</sub>-N, SiO<sub>2</sub>-Si from 2009 to 2013. In addition, PO<sub>4</sub>-P was much lower concentration(0.003±0.001 mg/ l). Therefore, we assumed that there was no relationship between the bloom of *M.varians* and dissolved nutrient concentration in Isso river. Meanwhile, the floating mud which was deposited in the bottom of the river has been continued during dry-spell. Tachibana et al (1986) reported that an algae can intake the suspended nutrient same as dissolved nutrient. It suggests that the *M.varians* and *H.puncticulatum* can take suspended nutrient.

Keywords: *Hydrobryum puncticulatum*, periphyton, Yakushima, nutrient

## Environmental response in bacteria to an applied magnetic field

ABE, Makoto<sup>1\*</sup> ; YAMANA, Masao<sup>2</sup> ; ABE, Tomoko<sup>2</sup>

<sup>1</sup>Graduate School of Science and Engineering, Graduate School of Tokyo Denki University, <sup>2</sup>School of Science and Engineering, Tokyo Denki University

Metabolic changes in living cells under various magnetic fields should be considered in closed-ecology on planets.

Magnetic fields may induce multiple effects in biological systems, including change in DNA replication or RNA transcription and modification of ion and protein flow across membranes. In recent years, influences of various electromagnetic fields on cell and organisms have been investigated by many researchers. However, the detailed mechanisms in the effects of magnetic field on organisms are still controversial.

In this study, we had focused on influences of the magnetic field on environmental microbes. Some bacteria susceptible to the applied magnetic field were isolated from the soil. To investigate expression changes of intracellular proteins involved in regulating cell growth by the applied magnetic field, cellular proteins in the bacteria cultured under the applied magnetic field were analyzed by SDS-polyacrylamide gel electrophoresis.

Keywords: Magnetic field, Bacteria, Growth curve

## Useful utilization in closed bio-ecosystems of *Nostoc* sp. HK-01 having the tolerance of gamma-ray

AJIOKA, Reiko<sup>1\*</sup> ; KIMURA, Shunta<sup>1</sup> ; KATOH, Hiroshi<sup>2</sup> ; SATO, Seigo<sup>1</sup> ; TOMITA-YOKOTANI, Kaori<sup>1</sup>

<sup>1</sup>University of Tsukuba, <sup>2</sup>Mie University

Photosynthetic organisms contribute to the circulation of oxygen or carbon dioxide and utilization of foods as a induced organism in closed bio-ecosystems. A terrestrial cyanobacterium, *Nostoc* sp HK-01, having a high drought tolerance, photosynthetic organism, is one of candidate organisms that can be introduced into the closed environment. It has a possibility that HK-01 has also a high gamma-ray tolerance in according to the results from several reports related to the interaction of drought tolerance and gamma-ray tolerance. Here, we will show the several influences on the growth of HK-01 after the exposure of gamma-ray in the dry colony.

Keywords: closed bio-system, cyanobacteria, gamma-ray tolerance, *Nostoc* sp. HK-01, photosynthetic organism